

DOCTORAL THESIS

CARVACROL ENCAPSULATION
BY ELECTROSPINNING OR SOLVENT CASTING
TO OBTAIN
BIODEGRADABLE MULTILAYER ACTIVE FILMS
FOR FOOD PACKAGING APPLICATIONS



UNIVERSITAT POLITÈCNICA DE VALÈNCIA

Instituto Universitario de Ingeniería de Alimentos para el Desarrollo

:

Alina Tampau

Supervisors:

Amparo Chiralt Boix
Chelo González-Martínez

Valencia, Enero 2020



UNIVERSITAT
POLITÈCNICA
DE VALÈNCIA

Dra. Amparo Chiralt Boix, Catedrática de Universidad, perteneciente al Departamento de Tecnología de Alimentos de la Universitat Politècnica de València.

Dra. Chelo González Martínez, Catedrática de Universidad, perteneciente al Departamento de Tecnología de Alimentos de la Universitat Politècnica de València.

Hacen constar que:

La memoria titulada **“CARVACROL ENCAPSULATION BY ELECTROSPINNING OR SOLVENT CASTING TO OBTAIN BIODEGRADABLE MULTILAYER ACTIVE FILMS FOR FOOD PACKAGING APPLICATIONS”** que presenta **D^a Alina Tampau** para optar al grado de Doctor por la Universitat Politècnica de València, ha sido realizada en el Instituto de Ingeniería de Alimentos para el Desarrollo (IIAD – UPV) bajo su dirección y que reúne las condiciones para ser defendida por su autora.

Valencia, Enero 2020

Fdo. Amparo Chiralt Boix

Fdo. Chelo González Martínez

To my husband Perry

and my son Dragomir.

ACKNOWLEDGEMENTS

My deepest thanks and gratitude go to my directors, **Amparo** and **Chelo**, for granting me the unique opportunity to enhance my education through this doctoral contract. **Amparo**, it has been a privilege to receive your guidance; your energy and passion permeate through all layers of life, not just the investigative work. Thank you for this extraordinary learning experience that has not only rounded my academic training, but has also enriched me personally through all the amazing people I have met in your investigative group during this period. Thank you **Chelo**, for your support and encouragement. You always had your door open for me whenever I had questions or needed guidance in my work. I have been truly fortunate to learn from you.

Professor **António Vicente**, I am grateful to you for receiving me in your research group at University of Minho, Braga. I have been very touched by the way your team made me feel so accepted, providing academic support for my work and also introducing me to Portuguese culture. Thank you **Ricardo** and **Paula** for your collaboration during those three months. I made good friends in Braga.

I am grateful to my lab colleagues at IIAD. You have all shared with me either laughter or advice, and on many occasions “el café con leche” in the morning: **Amalia, Caro, Cristina, Emma, Eva, Ramón, Raquel**. Thank you **Carolina**, our savy technician, you have given me so much more than just professional support. **Cristina**, many thanks for your friendship and support, it has meant a lot. **Emma**, your kindness and energy is something I really valued during my time at the IIAD lab. Don’t ever change. Cara **Martina**, it was so nice to have met you, even if it was just for a few months.

My dear **Mayra, Sofia** and **Johana**, you have been the “cherry on the top” of this whole experience. Thank you for all the positive energy you have given me through these years, I have enjoyed all our moments together. I will cherish your friendship forever.

To **my father**, thank you for all your teachings and guidance through the years. They have shaped me into the person I am today. Life took you away too soon from me, but you are always present in everything I do.

And last but not least, **Perry**, you have been my most valuable support during this journey. I am truly blessed to have you by my side. I could not have done it without you.

ABSTRACT

The massive use of synthetic plastics and their environmental impact makes necessary the search for biodegradable alternatives for food packaging. Likewise, the need to increase the shelf life of food has aroused great interest in the development of active materials (antimicrobial and antioxidant) that maintain food quality and safety for longer periods of time through the use of compounds of natural origin, safe for the consumer. In this sense, the development of active biodegradable materials for food packaging is both a major imperative and challenge for the food industry today.

In the present Doctoral Thesis, the encapsulation of carvacrol has been studied by means of the electrospinning or casting of different polymeric solutions with carvacrol. Biodegradable polymers with different polarities (thermoplastic starch: TPS, poly(vinyl-alcohol): PVA, poly-(ϵ -caprolactone): PCL or poly(lactic acid): PLA) dissolved in the appropriate solvent have been used to obtain active layers. These have been combined with other polymers with complementary properties, to obtain active laminates suitable for food packaging. The laminates combined polar polymers (TPS or PVA) and non-polar polyesters (PCL or PLA) incorporating carvacrol in one of the layers. The release kinetics of the active ingredient was evaluated, as well as the antimicrobial action of the materials obtained. The laminates were characterized in their functionality as a packaging material (barrier, mechanical or optical properties), as well as in their structure and thermal behaviour.

Encapsulation studies revealed a higher encapsulating potential of carvacrol for non-polar polymers (PCL and PLA), although PVA also showed a good affinity with the active compound. The PVA matrix showed a higher retention of carvacrol by electrospinning of its aqueous solutions than by casting, without the need for addition of surfactants such as Tween 85. For the encapsulation in PLA, binary mixtures of solvents suitable for food contact (ethyl acetate and DMSO) were used. A higher encapsulation efficiency of PLA was obtained in the materials produced by casting than by electrospinning.

The carvacrol release kinetics of PCL fibres explained the higher antibacterial effect against *Escherichia coli* and the lower antilisterial effect. The release ratio of the active ingredient increased when the polarity of the food simulants decreased, showing a complete release in non-polar systems and only up to 75% in aqueous systems that would require a higher proportion of the active ingredient in the packaging material to enhance its effectiveness.

The combination of TPS films with carvacrol loaded PCL fibres resulted in materials with improved water vapour permeabilities, compared to starch films, with no relevant effects on the other functional properties. When the laminates were tested *in vitro* against Gram (+) and Gram (-) strains, they showed a similar antibacterial effect to that of PCL fibres with carvacrol, but delayed in time. Disintegration-biodegradation studies of PCL-starch laminates revealed that carvacrol films affected the activity of the compost inoculum, slightly decreasing the biodegradability of the laminates, but reaching similar disintegration values (75-80%) to the carvacrol-free samples.

PLA and PVA laminates were also obtained by casting aqueous PVA solutions with carvacrol. The surface of PLA was submitted to aminolization in order to improve the extensibility of the aqueous solutions. Despite the increase in the polar component of the PLA surface energy and its improved wettability with PVA solutions, these bilayers did not show significant improvement in mechanical and barrier properties over the PLA monolayers.

RESUMEN

El uso masivo de plásticos sintéticos y su impacto medioambiental obliga a buscar alternativas biodegradables para el envasado de los alimentos, etapa necesaria para su adecuada conservación. Así mismo, la necesidad de incrementar la vida útil de los alimentos ha despertado gran interés en el desarrollo de materiales activos (antimicrobianos y antioxidantes) que mantengan su calidad y seguridad por más tiempo, mediante el uso de compuestos de origen natural, seguros para el consumidor. En este sentido, el desarrollo de materiales biodegradables activos para el envasado de alimentos constituye hoy en día un reto importante para la industria alimentaria.

En la presente Tesis Doctoral, se ha estudiado la encapsulación de carvacrol mediante el electroestirado o extensión y secado de diferentes disoluciones poliméricas con carvacrol. Se han utilizado polímeros biodegradables portadores de diferente polaridad (almidón termoplástico: TPS, polivinil-alcohol: PVA, policaprolactona: PCL o ácido poliláctico: PLA) disueltos en el solvente adecuado, con el fin de obtener capas activas. Estas capas se han combinado con otras de polímeros con propiedades complementarias, para obtener laminados activos adecuados para el envasado de alimentos. Los laminados combinaron polímeros polares (TPS o PVA) y poliésteres no polares (PCL o PLA) incorporando el carvacrol en una de las capas. Se evaluó la cinética de liberación del activo, así como la acción antimicrobiana de los materiales obtenidos. Los laminados se caracterizaron en su funcionalidad como material de envase (propiedades de barrera, mecánicas u ópticas), así como en su estructura y comportamiento térmico.

Los estudios de encapsulación revelaron un mayor potencial encapsulante del carvacrol para los polímeros no polares (PCL y PLA), aunque el PVA mostró también una buena afinidad con el compuesto activo. La matriz de PVA mostró una mayor retención de carvacrol mediante electroestirado de sus disoluciones acuosas que por extensión y secado, sin necesidad de adición de tensoactivos como el Tween 85. Para la encapsulación en PLA, se usaron mezclas binarias de solventes aptos para contacto con los alimentos (acetato de etilo y DMSO). En este caso, se obtuvo una mayor eficiencia encapsulante del PLA en los materiales obtenidos por extensión y secado que en los electroestirados.

La cinética de liberación del carvacrol de las fibras de PCL explicó el mayor efecto antibacteriano contra *Escherichia coli*, y el escaso efecto antilisteria. La velocidad de

liberación del activo aumentó cuando disminuyó la polaridad de los simulantes alimentarios, mostrando una liberación completa en los sistemas apolares, pero solo hasta un 75% en los sistemas acuosos, que requerirían una mayor proporción del activo en el envase para potenciar su efectividad.

La combinación de láminas de TPS con fibras de PCL cargadas con carvacrol dio lugar a materiales con una permeabilidad al vapor de agua mejorada, en comparación con los films de almidón, sin efectos relevantes sobre las otras propiedades funcionales estudiadas. Cuando los laminados se probaron *in vitro* contra cepas Gram (+) y Gram (-) mostraron un efecto antibacteriano similar al de las fibras de PCL con carvacrol, pero retrasado en el tiempo. Los estudios de desintegración-biodegradación de los laminados almidón-PCL revelaron que las películas con carvacrol afectaron la actividad del inóculo del compost, disminuyendo ligeramente la biodegradabilidad de las películas, pero alcanzando valores de desintegración similares (75-80%) a las muestras libres de carvacrol.

Se obtuvieron también laminados de PLA y PVA mediante la extensión y secado de disoluciones acuosas de PVA con carvacrol. La superficie del PLA fue sometida a aminolización a fin de mejorar la extensibilidad de las disoluciones acuosas. A pesar del incremento de la componente polar de la energía superficial del PLA y su mejorada humectabilidad con las soluciones de PVA, estas bicapas no mostraron una mejora significativa en las propiedades mecánicas y de barrera respecto a las monocapas de PLA.

RESUM

L'ús massiu de plàstics sintètics i el seu impacte mediambiental obliga a buscar alternatives biodegradables per a l'envasament dels aliments necessari per a la seua conservació. Així mateix, la necessitat d'incrementar la vida útil dels aliments ha despertat gran interès en el desenvolupament de materials actius (antimicrobians i antioxidants) que mantinguen la seua qualitat i seguretat per més temps, per mitjà de l'ús de compostos d'origen natural, segurs per al consumidor. En este sentit, el desenvolupament de materials biodegradables actius per a l'envasament d'aliments constituïx un repte important per a la indústria alimentària.

En la present Tesi Doctoral, s'ha estudiat l'encapsulació de carvacrol per mitjà de l'electroestirat o extensió i assecat de diferents dissolucions polimèriques amb carvacrol. S'han utilitzat polímers biodegradables portadors de diferent polaritat (midó termoplàstic: TPS, polivinil-alcohol: PVA, policaprolactona: PCL o àcid polilàctic: PLA) dissolts en el solvent adequat, a fi d'obtindre capes actives. Estes s'han combinat amb altres de polímers amb propietats complementàries, per a obtindre laminats actius adequats per a l'envasament d'aliments. Els laminats van combinar polímers polars (TPS o PVA) i polièsters no polars (PCL o PLA) incorporant el carvacrol en una de les capes. Es va avaluar la cinètica d'alliberament de l'actiu, així com l'acció antimicrobiana dels materials obtinguts. Els laminats es van caracteritzar en la seua funcionalitat com a material d'envàs (propietats de barrera, mecàniques o òptiques), així com en la seua estructura i comportament tèrmic.

Els estudis d'encapsulació van revelar un major potencial encapsulant del carvacrol per als polímers no polars (PCL i PLA), encara que el PVA va mostrar també una bona afinitat amb el compost actiu. La matriu de PVA va mostrar una major retenció de carvacrol per mitjà d'electroestirat de les seues dissolucions aquoses que per extensió i assecat, sense necessitat d'addició de tensioactius com el Tween 85. Per a l'encapsulació en PLA, es van usar mesclades binàries de solvents aptes per a contacte amb els aliments (acetat d'etil i DMSO). Es va obtindre una major eficiència encapsulant del PLA en els materials obtinguts per extensió i assecat que en els electroestirats. La cinètica d'alliberament del carvacrol de les fibres de PCL va explicar el major efecte antibacterià contra *Escherichia coli*, i l'escàs efecte antilisteria. La velocitat d'alliberament de l'actiu va augmentar quan va disminuir la polaritat dels simulants alimentaris, mostrant un alliberament complet en els sistemes no

polars, però només fins a un 75% en els sistemes aquosos, que requeririen una major proporció de l'actiu en l'envàs per a potenciar la seua efectivitat.

La combinació de làmines de TPS amb fibres de PCL carregades amb carvacrol va donar lloc a materials amb una permeabilitat al vapor d'aigua millorada, en comparació amb els films de midó, sense efectes rellevants sobre les altres propietats funcionals. Quan els laminats es van provar *in vitro* contra ceps Gram (+) i Gram (-) van mostrar un efecte antibacterià semblant al de les fibres de PCL amb carvacrol, però retardat en el temps. Els estudis de desintegració-biodegradació dels laminats midó-PCL van revelar que les pel·lícules amb carvacrol van afectar l'activitat de l'inocule del compost, disminuint lleugerament la biodegradabilitat, però aconseguint valors de desintegració semblants (75-80%) a les mostres lliures de carvacrol.

Es van obtindre també laminats de PLA i PVA per mitjà de l'extensió i assecat de dissolucions aquoses de PVA amb carvacrol. La superfície del PLA va ser sotmesa a aminolització a fi de millorar l'extensibilitat de les dissolucions aquoses. A pesar de l'increment de la component polar de l'energia superficial del PLA i la seua millorada mullabilitat amb les solucions de PVA, estes bicapes no van mostrar una millora significativa en les propietats mecàniques i de barrera respecte a les monocapes de PLA.

PREFACE

DISSERTATION OUTLINE

This Doctoral Thesis is organized into five sections: **Introduction**, **Objectives**, **Chapters** that include the obtained results, **General Discussion** and **Conclusions**.

The **Introduction** section focuses on the use of bioplastics in the food packaging field, highlighting the use of biodegradable or compostable materials such as starch, poly(lactic acid) and poly(vinyl alcohol) and the development of multilayer assemblies (with polymer sheets with complementary properties) that can act as carriers for active substances - specifically, substances that provide antimicrobial or antioxidant properties to the packaging materials. Emphasis has been placed on carvacrol, the active compound used in the present study. Encapsulation through electrospinning has also been analysed. Next, the **Objectives** section presents the general and specific objectives of this Thesis.

The obtained results are organized into two main blocks in the **Chapters** section (**Chapter I** and **II**), with each block divided into three article-style sections (scientific publications), each structured into: abstract, introduction, materials and methods, results and discussion, conclusions, and references.

Chapter I deals with the comparative study of carvacrol encapsulation by electrospinning in polar and non-polar matrices and the selection of the best encapsulating matrix for the development of starch-based multilayers. Thus, **Chapter I.1**, entitled "*Carvacrol encapsulation in starch or PCL based matrices by electrospinning*", compares the carvacrol retention potential of two systems (starch-NaCas and PCL) by means of the electrospinning. The characterisation of the electrospun solutions (particle size, rheological behaviour, ζ -potential, conductivity, surface tension) and the obtained materials (microstructure and encapsulation efficiency) is carried out. Based on the results of this study, the PCL is selected as a better CA carrier and used for the following study (**Chapter I.2**) entitled "*Release kinetics and antimicrobial properties of carvacrol encapsulated in electrospun poly-(ϵ -caprolactone) nanofibres. Application in starch multilayer films.*" This article deals with the characterization of the obtained CA-loaded PCL fibrous mats in terms of the CA release kinetics in different polarity food simulants and their antimicrobial effect on G(+) and G(-) bacteria. The materials obtained by inclusion of the active mats between sheets of TPS are also characterised as to their functional properties relevant for the food packaging purpose. The last study in this chapter, **Chapter I.3**, entitled "*Biodegradation of thermoplastic starch*

films containing electrospun poly-(ϵ -caprolactone) encapsulating carvacrol” deals with the disintegration-biodegradation behaviour of the developed TPS-PCL multilayers, analysing the influence of carvacrol on this pattern.

Chapter II presents the development of the second group of active materials, based on combination of PLA and PVA. Firstly, the CA encapsulation capacity of both polymers are studied. Thus, **Chapter II.1**, named “*Poly(vinyl alcohol)-based materials encapsulating carvacrol obtained by solvent casting and electrospinning*” deals with the comparison study between the encapsulation efficiency of solvent casting and electrospinning of CA-carrying PVA aqueous solutions. Liquid formulations are characterised as to their particle size, rheological behaviour, ζ -potential and conductivity, while the microstructure, encapsulating efficiency and thermal behaviour of solid encapsulating materials are also analysed.

Chapter II.2, labelled “*Poly(lactic acid) based materials encapsulating carvacrol obtained by solvent casting and electrospinning*” identifies different food contact binary solvent systems for PLA to act as CA carrier while comparing the polymer capability to retain the active compound when submitted to solvent casting or electrospinning. The electrospinning parameters are fitted for each system and the characterisation of the encapsulating matrices is carried out as to their microstructure, encapsulation efficiency and thermal behaviour. Finally, **Chapter II.3**, entitled “*Enhancement of PLA-PVA surface adhesion in bilayer assemblies by PLA aminolization*”, analyses initially the improvement of PLA wettability with PVA aqueous solution by surface aminolization; then, the PLA-PVA bilayers obtained by coating the activated PLA with carvacrol-loaded PVA solutions are characterised as to their functional properties as food packaging materials.

The **General Discussion** section analyses from a global perspective the most relevant results obtained from the two main blocks (Chapter I and Chapter II) and draws a comparison between the encapsulation efficiency of the different polymers/techniques used for the two kinds of developed multilayers.

Finally, the **Conclusions** section presents the most relevant findings of this Doctoral Thesis.

DISSEMINATION OF RESULTS

INTERNATIONAL JOURNALS JCR

Published

Research article: “**Carvacrol encapsulation in starch or PCL based matrices by electrospinning**”. Alina Tampau; Chelo González-Martínez; Amparo Chiralt. *Journal of Food Engineering* (2017), 214, 245-256

Research article: “**Release kinetics and antimicrobial properties of carvacrol encapsulated in electrospun poly-(ϵ -caprolactone) nanofibres. Application in starch multilayer films**”. Alina Tampau; Chelo González-Martínez; Amparo Chiralt. *Food Hydrocolloids* (2018), 79, 158-169.

Submitted

Research article: “**Poly(vinyl alcohol)-based materials encapsulating carvacrol obtained by solvent casting and electrospinning**”. Alina Tampau; Chelo González-Martínez; Amparo Chiralt. *Reactive and Functional Polymers*.

Research article: “**Poly(lactic acid) based materials encapsulating carvacrol obtained by solvent casting and electrospinning**”. Alina Tampau; Chelo González-Martínez; Amparo Chiralt. *Journal of Food Science*.

Research article: “**Biodegradability and disintegration of multilayer starch films with electrospun PCL fibres encapsulating carvacrol**”. Alina Tampau; Chelo González-Martínez; Amparo Chiralt. *Polymer Degradation & Stability - BIOPOL Special Issue*.

Research article: “**Enhancement of PLA-PVA surface adhesion in bilayer assemblies by PLA aminolization**”. Alina Tampau; Chelo González-Martínez; Antonio Vicente; Amparo Chiralt. *Food and Bioprocess Technology*.

COMMUNICATIONS IN INTERNATIONAL CONGRESSES

Poster: **“Carvacrol encapsulation by electrospinning in polymer matrices”**. International Conference on Nanotechnology Applications. NANOTEC 2016. Valencia, Spain (2016).

Poster: **“Multilayer active starch films with electrospun PCL encapsulating carvacrol”**. Alina Tampau; Chelo González-Martínez; Amparo Chiralt. International Conferences in Food Innovation. Food Innova 2017. Cesena, Italy (2017).

Poster: **“Release kinetics and antimicrobial properties of carvacrol encapsulated in electrospun PCL nanofibres”**. Alina Tampau; Chelo González-Martínez; Amparo Chiralt. The 6th International Conference on Biobased and Biodegradable Polymers. BIOPOL 2017. Mons, Belgium (2017).

Poster: **“Biodegradation of thermoplastic starch films containing electrospun poly- ϵ -caprolactone encapsulating carvacrol”**. Alina Tampau; Chelo González-Martínez; Amparo Chiralt. The 7th International Conference on Biodegradable Polymers and Sustainable Composites. BIOPOL 2019. Stockholm, Sweden (2019).

COMMUNICATION IN SCIENTIFIC EVENTS

Oral communication: **“Encapsulación de compuestos activos mediante electrospinning para su incorporación en materiales de envase alimentarios”**. Alina Tampau; Chelo González-Martínez; Amparo Chiralt. IV encuentro de estudiantes de doctorado de la UPV, Valencia, Spain (2017).

PREDOCTORAL STAYS AT FOREIGN INSTITUTIONS

Departamento de Engenharia Biológica, Universidade do Minho, Campus de Gualtar (Braga, Portugal). From September 10th, 2018 to December 14th, 2018; under the supervision of Professor António Augusto Vicente.

TABLE OF CONTENTS

LIST OF ACRONYMS.....	27
INTRODUCTION	29
1. Biodegradable active materials for food packaging	31
2. Active packaging materials	36
3. Use of electrospinning to develop active films	42
3.1. Description of the technique	42
3.2. Encapsulation of active compounds by electrospinning and development of multilayer active films.....	44
4. References.....	54
OBJECTIVES	63
CHAPTERS	65
1.1 Carvacrol encapsulation in starch or PCL based matrices by electrospinning	69
Abstract.....	71
1. Introduction	72
2. Materials and methods.....	75
2.1. Raw materials and reagents	75
2.2. Preparation of formulations.....	75
2.3. Characterization of the initial solution/dispersion properties	76
2.4. Electrospinning process.....	77
2.5. Characterization of electrospun products	78
2.5.1. Nanostructure of electrospun material	78
2.5.2. Encapsulating efficiency of CA	78
2.6. Statistical analysis	79
3. Results and discussion	79
3.1. Properties of the carvacrol liquid formulations	79

3.2. Characterization of the electrospun product	87
3.3. CA encapsulation efficiency.....	90
4. Conclusions	94
5. Acknowledgments.....	95
6. References	95

1.2 Release kinetics and antimicrobial properties of carvacrol encapsulated in electrospun poly-(ϵ-caprolactone) nanofibres. Application in starch multilayer films.	101
Abstract.....	103
1. Introduction	104
2. Materials and methods.....	106
2.1. Materials and reagents	106
2.2. Obtaining and characterizing the electrospun fibre of CA-loaded PCL	106
2.3. Release kinetics of CA in different food simulants	107
2.3.1 CA release mathematical modelling	108
2.3.2. Prediction of CA antimicrobial effect based on the release study	109
2.4. Incorporation of PCL fibres in multilayer starch films	109
2.5. Thermal analysis.....	110
2.6. Antimicrobial properties	111
2.7. Statistical analysis	111
3. Results and discussion	112
3.1. Electrospun fibre layers of CA loaded PCL.....	112
3.2. Release kinetics of CA from PCL fibres in different food simulants	114
3.3. Antibacterial properties of the CA loaded fibres.....	118
3.4 Multilayer starch films with electrospun PLC fibres with and without CA	121
4. Conclusions	129
5. Acknowledgements.....	130
6. References	130

I.3 Biodegradation of thermoplastic starch films containing electrospun poly-(ϵ-caprolactone) encapsulating carvacrol	137
Abstract.....	139
1. Introduction	140
2. Materials and experimental design	141
2.1. Materials	141
2.2. Films preparation	142
2.3. Samples characterization	142
2.4. Compost and synthetic solid residue (SSR)	143
2.5. Disintegration test.....	144
2.6. Biodegradation test.....	144
2.7. Statistical analysis	145
3. Results.....	146
3.1. Properties of multilayer films.....	146
3.2. Compost characteristics	146
3.3. Disintegration test	148
3.4. Biodegradation test.....	153
4. Conclusions	156
5. Acknowledgements.....	157
6. References	157

II.1 Poly(vinyl alcohol)-based materials encapsulating carvacrol obtained by solvent casting and electrospinning 163

Abstract.....	165
1. Introduction	166
2. Materials and methods.....	168
2.1. Materials and reagents	168
2.2. Preparation of the liquid formulations	168
2.3. Obtaining the dry encapsulating material.....	169

2.4. Characterization of the liquid systems	170
2.4.1. Particle size distribution	170
2.4.2. Rheological behaviour	170
2.4.3. Conductivity, surface tension and ζ potential	170
2.5. Characterization of the solid material.....	171
2.5.1. Microstructure	171
2.5.2. Encapsulation efficiency	171
2.5.3. Thermogravimetric analysis (TGA) and differential scanning calorimetry (DSC)	171
2.6. Statistical analysis	172
3. Results and discussion	172
3.1. Properties of the liquid systems	172
3.2. Characterization of the solid material.....	176
4. Conclusions	186
5. Acknowledgements.....	186
6. References	186

II.2. Poly(lactic acid) based materials encapsulating carvacrol obtained by solvent casting and electrospinning	193
Abstract.....	195
Practical Application	195
1. Introduction	196
2. Materials and Methods.....	198
2.1. Materials	198
2.2. Obtaining the CA encapsulating matrices.....	198
2.3. Characterization of the obtained materials	199
2.3.1. Microstructure	199
2.3.2. CA encapsulating efficiency	199
2.3.3. Thermal analysis	200
2.4. Statistical analysis	200
3. Results and Discussion.....	201

3.1. Solvent system screening.....	201
3.2. Microstructure of the ES matrices.....	204
3.3. Carvacrol encapsulating efficiency	204
3.4. Thermal analysis.....	206
4. Conclusions	213
5. Acknowledgments.....	213
6. References	213

II.3 Enhancement of PLA-PVA surface adhesion in bilayer assemblies by PLA

aminolization.....	217
Abstract.....	219
1. Introduction	220
2. Materials and methods.....	223
2.1. Materials	223
2.2. Mono- and bi- layer preparation.....	223
2.4. Surface microstructure.....	227
2.5. Analysis of functional properties of bilayer films	227
2.6. Thermogravimetric analysis (TGA) and differential scanning calorimetry (DSC) ...	228
2.7. Statistical analysis	229
3. Results and Discussion.....	229
3.1. Changes in the PLA surface induced by aminolization	229
Wettability of PLA with PVA liquid systems	233
3.2. Functional properties of PLA-PVA bilayer films	235
3.3. Thermal behaviour as affected by the aminolization treatment.....	239
4. Conclusions	244
5. Acknowledgements.....	244
6. References	244
GENERAL DISCUSSION	251
CONCLUSIONS	263

LIST OF ACRONYMS

B%:	Biodegradability	MIC:	Minimum Inhibitory Concentration
B _{max} :	Percentage of biodegradation at infinite time	n:	Diffusional exponent of Korsmeyer-Peppas model
CA:	Carvacrol	NaCas:	Sodium caseinate
CS:	Corn starch	OP:	Oxygen permeability
D:	Distance spinneret tip-collector	PLA:	Poly (lactic acid)
D ₈₄ (%):	Disintegration after 84 days	PVA:	Poly (vinyl alcohol)
DS:	Dry solids	RH:	Relative humidity
DSC:	Differential scanning calorimetry	SSE:	Sum of Squared Errors
DTGA:	Thermal weight loss derivate	SSR:	Synthetic solid residue
ε:	Elongation at break	ST:	Surface tension
EM:	Elastic Modulus	T _g :	Glass transition temperature
EO:	Essential oil	TGA:	thermogravimetric analysis
ES:	Electrospinning	T _i :	Internal transmittance
FESEM:	Field Emission Scanning Electron Microscopy	T _m :	Melting temperature
FR:	Flowrate	T _o :	Onset temperature from TGA
G(-):	Gram negative	T _p :	Peak Temperature from TGA
G(+):	Gram positive	T85:	Tween 85 (polyoxyethylene sorbitan trioleate)
GAA:	Glacial acetic acid	TPS:	Thermoplastic starch
Gly:	Glycerol	TS:	Tensile Strength
k:	Rate constant of Korsmeyer-Peppas model	UV-VIS:	UltraViolet-Visible Spectroscopy
k ₁ :	Kinetic constant of Peleg model	V:	Applied electrospinning voltage
k ₂ :	Constant of the Peleg model	VS:	Volatile solids
M _∞ :	Amount of active compound released at equilibrium	WVP:	Water vapour permeability
MCC:	Microcrystalline cellulose	ΔH _c :	Crystallization enthalpy
		ΔH _m :	Melting enthalpy

INTRODUCTION

1. Biodegradable active materials for food packaging

Food packaging in its traditional concept is intended to contain, protect and safely transport the foodstuffs. To achieve its purpose, it needs to be made from materials as inert as possible, such as glass, plastics, cardboard, or coated metal, for the purposes of avoiding any alteration in the sensory characteristics of the content it is transporting. Of these materials, petro-chemically derived plastics are by far the most widely used, due to their good water and gas barrier properties, flexibility, durability, lightweight and attractive production cost. Their wide usage creates a demand in Europe alone of 51.2 million tonnes of generated plastics per annum, from which 39.7% is destined for packaging (Plastic the Facts 2018 report). In 2016, the postconsumer plastic packaging waste was up to 16.7 million tonnes of which 40.8% were recycled, with a significant percentage (20.4%) still ending up in landfills. One of the major drawbacks of the landfill plastics is that there is no recovery of the materials used to generate them, while the by-products of their breakdown (constitutional monomers, plasticizers, etc.) pose the risk of soil and groundwater contamination (Hopewell et al. 2009; Teuten et al. 2009). Increasing consumer awareness of these environmental concerns, combined with demands for fresher, higher quality foodstuffs, free of synthetic chemicals, are influencing the current food packaging technologies.

In order to address the environmental impact of packaging materials, the bioplastics family has emerged as a viable alternative to the non-degradable petroleum-derived materials, having similar properties to the latter but a smaller carbon footprint, improved functionalities (in some cases) and better end-of-life waste management. Figure 1 presents a classification of the plastics, adapted from the European Bioplastics and Food Packaging Forum (both pages accessed in September 2019). Under the term bioplastics, three material categories are included, based on their origin and biodegradability potential: biodegradable bio-based plastics, biodegradable fossil-fuel based plastics and non-degradable bio-based materials. Predictions regarding the global production of bioplastics are pointing to a growth from 2.11 million tonnes in 2018 (of which 43 % are biodegradable) (Figure 2) to approximately 2.62 million tonnes by 2023. (European Bioplastics, Nova Institute, 2018). Many factors contribute to bioplastic biodegradation. Some are related to its inherent chemical structure (chain length, crystallinity degree, molecular complexity), while others are strictly dependent on the environment in which this degradation takes place (pH, temperature, moisture,

oxygen content, microorganism population and diversity). Typically, polymers presenting a less complex formula, a shorter chain, and less crystallinity are more sensitive to the microbiological breakdown process (Emadian et al. 2017). Table 1 presents the biodegradability potential of some of these materials. Of the biodegradable bioplastics, starch blends and PLA are the more available in the market plastics.

bio-based (from renewable sources)		
non degradable	Bioplastics	biodegradable
	<ul style="list-style-type: none"> • biobased poly(ethylene) (PE) • biobased poly(ethylene terephthalate) (PET) • biobased polyamides (PA) • biobased poly(trimethylene terephthalate) (PTT) 	
	Bioplastics	
	<ul style="list-style-type: none"> • polysaccharides • proteins • lipids • polyesters: poly(lactic acid) (PLA), polyhydroxyalkanoate (PHA), poly(butylene succinate) (PBS) 	
	Conventional plastics	
	<ul style="list-style-type: none"> • polyethylene (PE) • polypropylene (PP) • polyethylene terephthalate (PET) 	
	Bioplastics	
	<ul style="list-style-type: none"> • Poly(butylene adipate-co-terephthalate) (PBAT) • poly-(ε-caprolactone) (PCL) • poly(vinyl-alcohol) (PVA) 	
fossil-fuel based		

Figure 1. Classification of plastics (sourced from European Bioplastics, 2019)

Despite their environmentally-friendly nature, the use of biopolymer-based materials has been restricted at industrial level, due to their cost and the need to adequate their mechanical and barrier properties (Ortega-Toro et al. 2017). Then, these properties need to be improved and adapted to address the food packaging requirements. Therefore, many studies have been carried out to overcome these limitations and bring the functionalities of certain bioplastics as close as possible to those offered by the petrochemical-derived materials. In this sense, extensive work has been focused on starch and poly(lactic acid), due to their availability and competitive production cost (Muller et al. 2017a).

Table 1. Environmental degradability of the bioplastics, adapted from Emadian et al. (2017)

Bio-plastics	Environment		
	compost	soil	seawater
Poly(lactic acid) (PLA)	+	-	-
Polyhydroxyalkanoate (PHA)	+	+	+
Polycaprolactone (PCL)	+	<i>not specified</i>	-
Polybutylene succinate (PBS)	+	-	<i>not specified</i>
Polyamides-based (Nylon 4)	+	+	<i>not specified</i>
Starch-based	+	<i>not conclusive</i>	+
Cellulose-based	+	<i>not specified</i>	<i>not specified</i>

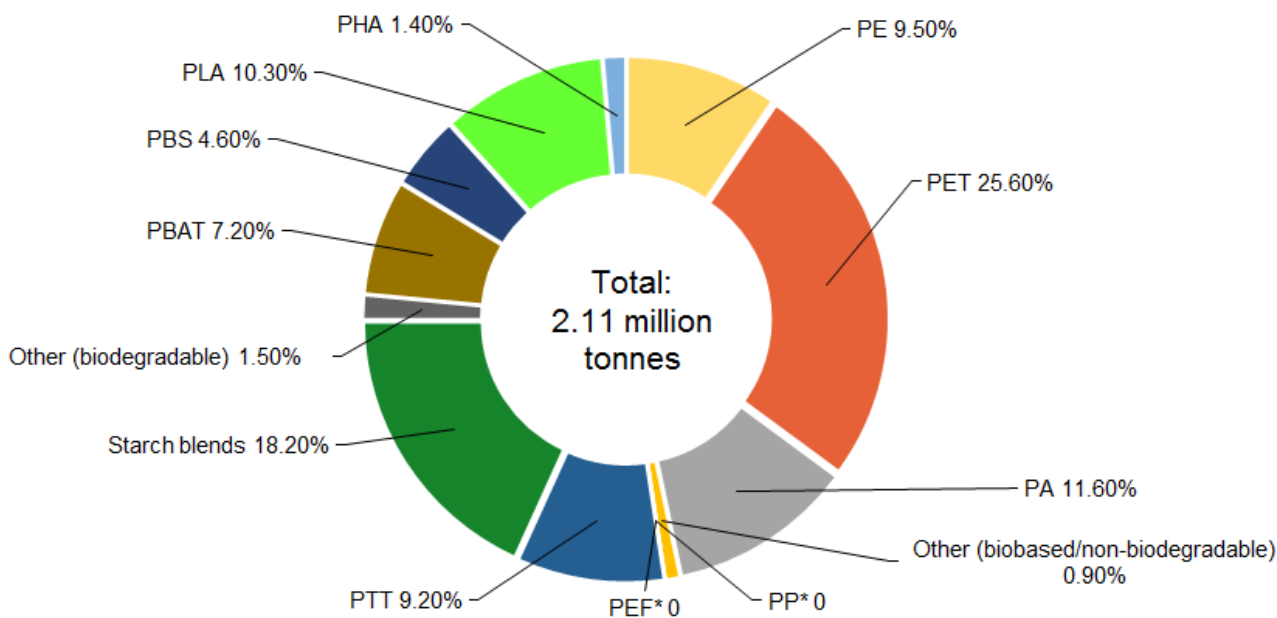


Figure 2. Global production capacities of bioplastics in tonnes, by material type (source: European Bioplastics, Nova Institute, 2018). * *Bio-based PP and PEF are currently being developed and they are predicted to be available commercially in 2023.*

Some characteristics of the bioplastics used in the present study are described below.

STARCH

Starch is the most commonly-studied polysaccharide, found abundantly in many plants (such as cereals, tubers, legumes), where it acts as energy storage. Starch has attracted great interest for food packaging applications due to its versatility as regards processed, either by casting, or thermoplastic processing, such as extrusion and compression or injection moulding (Collazo et al. 2018). Starch is a homo-polysaccharide, whose chemical structure is made up of two macro-components, amylose and amylopectin, both composed of monomers of α -glucose. While amylose is a linear polymer, formed mainly (~99%) by α -(1, 4) bonds between the monomers, amylopectin presents a highly branched structure, where the main chain of α -(1, 4) linked glucose molecules presents lateral α -(1, 6) ramifications, spaced every 20-30 glucose units. The assembling of these two fractions leads to the starch granules being formed in concentric rings, with semi-crystalline and amorphous layers (Thakur et al. 2019). Film formation with starch requires the disruption of the granules through gelatinization, which occurs in the presence of plasticizers, such as water or polyols, and thermal and/or mechanical treatments to obtain thermoplastic starch (Fang et al., 2005). The functional properties of the starch films are closely related to the proportion and physical organization of the amylose and amylopectin within the granules, differing from one botanical source to another (Thakur et al. 2019). Starch forms homogenous, transparent cast films (Collazo et al. 2018), with good extensibility and oxygen barrier properties (López et al. 2013). However, the presence of the hydroxyl groups in its structure gives these films a highly hydrophilic nature, limiting their range of use to low moisture foodstuffs. Different strategies, such as blending with other polymers or lipids, have been used to improve the starch functionality for packaging uses (Ortega-Toro et al. 2017).

PLA

Poly(lactic acid) (PLA) is one of the most promising bioplastics with which to replace conventional fossil-fuel derived polymers for packaging applications. Due to the industrial advances and rising demand, the PLA production cost is becoming increasingly competitive with that of the traditional polymers. PLA is a linear aliphatic polyester, obtained industrially through lactide open ring polymerization or by the condensation-polymerization of the lactic acid monomer (Armentano et al. 2009; Ahmed and Varshney, 2011). Its building block, the lactic acid, is obtained through an environmentally-friendly process of the microbial fermentation of renewable plant sources, rich in starch (corn, cassava, potato) or

fermentable sugars (sugar cane or beet) (Armentano et al., 2009). As a result of chirality, the lactic acid can present two isomers: L(+) and D(-) lactic acid. As such, when these monomers become dimerized into the cyclic lactide and later polymerized, three diastereoisomeric forms of polylactide can be generated: poly(L), poly(D) and poly(DL)lactide (Ahmed and Varshney, 2011; Muller et al. 2017a). Both L(+) and D(-) forms present crystallinity with a melting point from 130 °C to 180 °C, whereas the atactic meso-lactide (LD) is amorphous, with a glass transition temperature in the range of 50-80 °C (Auras et al. 2004).

PLA displays very attractive qualities: biodegradability, biocompatibility, good thermal processability, high mechanical strength and resistance, smooth appearance, UV resistance, low flammability and toxicity (www.plasticsinsight.com/resin-intelligence/resin-prices/polylactic-acid/#bioplastics). Safety assessments have reported limited migration levels of polymeric components into the food this material is in contact with. The studies have shown there is no threat to human health as these migrants are expected to be metabolized to lactic acid, reaching levels far below to those to which lactic acid as a food additive amounts to (Conn et al. 1994). Encouraging reports such as this have earned PLA the status of approved for food contact by the Food and Drug Administration (FDA). Therefore, PLA is already enjoying some foodstuffs packaging applications on the market such as bottled water, juices, yoghurts (Stonyfield Farm (U.S.) and Danone (Germany)) (www.greenerpackage.com) and short shelf-life containers, cups, lamination films and blister packages (Ahmed and Varshney, 2011).

PVA

Poly(vinyl alcohol) (PVA) is a synthetically obtained, fully biodegradable polymer available for applications in the market since its introduction in the early 1930s. It has found many applications, such as: transdermal patches, skin substitute for burnt derma, rapid dry jellies for skin treatments, controlled and sustained release formulations, ophthalmic solutions for medical purposes; resins, lacquers, coatings for commercial purposes, and food-contact approved additive and packaging. (DeMerlis and Schoneker, 2003; Peixoto et al. 2006).

PVA is obtained through the catalysed hydrolysis of polyvinyl acetate and PVA with different chemical and physical characteristics can be yielded depending on the degree of hydrolysis (total or partial) and the chain length (polymerization degree) (DeMerlis and Schoneker, 2003). Due to its chemical resistance to acids and good oxygen barrier properties, PVA has

already been studied as packaging or coating material (Peixoto et al. 2006; Tian et al. 2017). Owing to its hydrophilic and water soluble nature, PVA exhibits excellent film-forming properties through the casting of its aqueous solutions (Cano et al. 2015). Its cast films are transparent, highly adhesive to surfaces, and exhibit attractive mechanical properties (high tensile strength and flexibility) which are highly dependent on the films' moisture and plasticizer contents (Cano et al. 2015).

However, thermoplastic processing (such as compression moulding, extrusion blowing and melt spinning) is quite challenging given that PVA's melting point is very close to its decomposition temperature. This has been mitigated through the addition of plasticizers (such as glycerol (Cano et al., 2015) or an amido-containing compound (Chen et al. 2013)), which reduce the melting temperature and allow for thermal processing.

2. Active packaging materials

To address the quality concerns raised by consumers, innovative strategies have arisen in the form of "active packaging" seeking to extend the shelf-life and increase the quality of the packaged products, by interacting with them or the atmosphere inside the packaging (Regulation (EC) No. 450/2009, EU, 2009; Fuciños et al. 2016). Some "active packaging" approaches aim to scavenge oxygen, carbon dioxide or ethylene, control and sustain the release of antioxidant or antimicrobial compounds, deliver aroma molecules or adsorb off-flavours (Jamshidian et al. 2010). There are different ways in which these strategies can be applied to the packaging materials (COST actinpak). One way consists of inserting it as a separate item (e.g. sachets with silica gel or reduced iron) (Rooney, 1995) inside the packaging. Another approach is to use a naturally active packaging material (e.g. chitosan with proven antimicrobial properties) or to activate an inert carrier material. This activation can be achieved by blending the active compounds with the polymer mass or applying them only onto its surface. The application of the active packaging material to the food system can vary, depending on the type of food with its specific characteristics (susceptible to oxidant or microbial attack, moisture content, presentation in the package) and desired effect (antimicrobial, antioxidant, aroma enhancing, molecule scavenging). As such, there are "coatings" and "films". The "coatings" are applied directly to the surface of the foodstuff, where the drying occurs (e.g. coating of fresh-cut fruits), whereas "films" are standalone sheets created before application to the food and can be placed as wrappers, separation

laminas (Ribeiro-Santos et al. 2017) or adhered to the surface of the packaging transporting the product. This last option of “films” offers the opportunity of creating multi-layered materials where matrices, carrying or not active compounds, with different complementary properties can be assembled in a laminate structure, conferring combined protective functionalities to the final material.

In line with the consumer demand for a reduction in the use of food additives from chemical synthesis, interest in natural alternatives has grown in the past decades (Bakkali et al. 2008; Carcho et al. 2015). Many of these alternatives are plant essential oils (EO) and extracts, which are able to exert antimicrobial and/or antioxidative functions, thus addressing two major food spoilage concerns. These properties are owed to certain compounds, of terpenoid or phenolic nature, which have been identified and studied in depth (Burt, 2004; Bassolé and Juliani, 2012; Dhifi et al. 2016). Despite their benefits, most of these naturally-derived active compounds present drawbacks, such as a high degree of volatility, degradability (when exposed to oxygen, heat and/or light) and a marked sensory impact (including altering food taste). Thus, incorporating them into suitable polymeric matrices would serve the double purpose of obtaining active packaging materials, while protecting the active molecules until their controlled release to exert the desired effect. One of the most active compounds of essential oils is carvacrol, whose main characteristics are described below and which was used in the present study to obtain active packaging materials.

Carvacrol is a naturally occurring monoterpenoid found in the essential oil of some aromatic herbs: oregano (*Origanum vulgare*), thyme (*Thymus vulgaris L.*), and marjoram (*Origanum majorana*) (DeVicenzi et al. 2004; Burt, 2004). Its active properties make it one of the most widely-studied plant-derived compounds (Lopez-Mata et al. 2013; Higuera et al. 2014). The carvacrol molecule has a phenolic structure that plays a critical role in its antimicrobial activity, reported to be one of the strongest (Ben Arfa et al. 2006). Ultee et al. (2002) reported that the particular structure created by the hydroxyl group in close proximity to the delocalized electron system of the aromatic nucleus lends the molecule the role of proton exchanger. Due to this characteristic, when carvacrol comes into contact with the microbial cell membrane, it generates an alteration in permeability resulting in the leakage of protons, phosphates and potassium, and eventually cell death (Ben Arfa et al. 2006). This antimicrobial effect has been proven on both Gram (-) and Gram (+) bacteria (Ben Arfa et al. 2006; Ultee et al. 1998), as well as on various fungi (Tunc et al. 2007). Some studies

have also reported on its free radical scavenging and DNA protective activity (Horvathova et al. 2014), proving carvacrol to be a very promising antioxidant too. Given its proven benefits and natural origin, it has been officially accepted as a food additive (Joint FAO/WHO, 2001) and as a flavouring substance (EFSA, 2012).

In recent years, various methods have been described, for the incorporation of active compounds into polymer materials, including encapsulation. The selection of the carrier matrix (compatible with the active compound and the foodstuff type) and the encapsulation method play a crucial role in maintaining the agent's activity, while also allowing for its optimal diffusion from the polymer to the foodstuffs. Table 2 shows several recent studies of active materials for the preservation of different food systems, focusing on the usage of plant-derived active compounds. Whereas these are some of the successful applications of these kinds of active materials, there are also authors that report either the absence of any effect (Sapper et al. 2019), or the appearance of off-flavours due to the absorption of the agent into the food matrix (Higuera et al. 2014). Thus, the efficiency of the active packaging needs to be tested for the specific food matrix for which it is intended.

Table 2. Some studies into active materials developed with biopolymers and compounds of plant origin. Application type (coating/dipping or stand-alone dry film) and material structure (mono- or multi-layer) are specified.

Biopolymer type		Active compound	Application method	Material structure	Tested food system	Effect	Reference
carbohydrates	Starch	Eugenol	Cast film	Mono	Sunflower oil	Antioxidant	Talón et al. 2019
	Hydroxypropylmethyl-cellulose	Bergamot EO	Dipping	Mono (one application)	Table grapes (<i>Vitis vinifera</i> cv. <i>Muscatel</i>)	Antimicrobial	Sánchez-González et al. 2011
	Chitosan						
	Chitosan	Rosemary EO Oregano EO	Dipping	Multi (2-3 applications)	Goat's milk cheese	Antimicrobial	Cano et al. 2017
	Chitosan	Lemon EO	Dipping	Mono (one application)	Strawberries	Antifungal	Perdones et al. 2012
	Chitosan	Basil EO Thyme EO	Cast film	Mono (one layer)	Minced pork meat patties	Antimicrobial Antioxidant	Bonilla et al. 2014
	Chitosan	Bitter apricot kernel EO	Cast film	Mono (one layer)	Bread	Antifungal	Priyadarshi et al. 2018

Table 2. continued

Biopolymer type		Active compound	Application method	Material structure	Tested food system	Effect	Reference
proteins	Gliadin	Cinnamaldehyde	Cast film	Mono (one layer)	Bread and cheese spreads	Antimicrobial	Balaguer et al. 2013
	Milk protein	Oregano EO Pimento EO	Cast film	Mono (one layer)	Whole beef muscle	Antimicrobial Antioxidant	Oussalah et al. 2004
	Soy protein	Oregano EO Thyme EO	Cast film	Mono (one layer)	Freshly ground beef patties	Antimicrobial	Emiroğlu et al. 2010
	Zein	Cinnamon EO Mustard EO	Spray coating	Mono (one application)	Cherry tomatoes	Antimicrobial	Yun et al. 2015
biodegradable polyesters	PHBV	Oregano EO Clove EO Carvacrol Eugenol	Thermo-processed film	Multi	Fresh cheese, chicken breast fillets, fresh-cut melon and pumpkin	Antimicrobial	Requena et al. 2019

Although the results of studies presented in Table 2 point to successful applications, there are several shortcomings that need to be considered in the process of forming the active material. The casting or dipping method requires that the active-loaded polymeric solution be spread over a surface (another film or food product) and the evaporation of large amounts of solvent. As concerns the spreading process, the wettability of the solution on the applied surface (food or other polymeric films) is critical to ensure a good, effective coating. The wettability depends on the surface energy of the coated surface and the surface tension and contact angle of the extended liquid, all of which depend on the chemical nature of the compounds involved (Sapper et al. 2019). The lack of chemical affinity between the solid surface and the coating-forming systems would lead to heterogeneous coatings with poor adhesion force. Then, the composition of the coating or of the coated surface should be modified to favour an effective extension (Sapper & Chiralt, 2018).

For casting processes, when the polymer is water soluble and the active compound is hydrophobic, the active is required to be previously emulsified in the polymer solution. In this sense, it is important to obtain a highly stable emulsion that resists the solvent evaporation process during the film formation. In this step, droplet flocculation and creaming can occur in line with the progressive increase in the concentration of the dispersed phase. Factors such as the viscosity of the continuous phase and stabilising interfacial agents are decisive for the purposes of limiting both the emulsion destabilization process and the creaming of the active compound to the film surface where water evaporates (Perdones et al. 2012). Water evaporation enhances the losses of active compounds by means of the steam-drag effect and promotes the losses of volatile compounds, stripping the polymer matrix of the active compound it is intended to carry. Different studies reported that the hydrophilic films retained a greater proportion of volatile active compounds, such as essential oils, via their previous encapsulation in lecithin liposomes (Valencia-Sullca, et al. 2016; Jimenez et al. 2014; Sapper et al. 2019). The active incorporated within polar biopolymer matrices can be homogeneously incorporated into the matrix or a separated dispersed phase (droplets) depending on the polymer-compound affinity. When the biopolymer is soluble in non-polar solvents, such as polyesters, greater compatibility between active and polymer is usually achieved, although it depends on the chemical nature of both compounds. In this sense, Muller et al. (2017a) obtained active PLA films with cinnamaldehyde by casting PLA-cinnamaldehyde solutions in ethyl acetate, with no phase separation of the active in the polymeric matrix. However, the cinnamaldehyde migration from PLA films into food

simulants was greatly inhibited due to the strong interactions between polymer and active, which limited the active function of the compounds in the food substrate.

When biopolymers are thermo-processed, the active can be incorporated before or after melt blending. However, the high temperatures used during thermo-processing could inactivate or lead to great losses of this compound. To offset this drawback, Requena et al. (2016) applied carvacrol and eugenol by spraying them directly onto the surface of the thermoformed film, and then thermo-sealed it with another film. Nevertheless, the authors reported a loss of 20% for carvacrol and 40 % for eugenol, respectively (determined through spectrophotometric quantification), caused by the thermo-sealing. Other authors encapsulate the active compound in other supports, such as different nanoparticles, which in turn can act as reinforcing agents, (Mikulcová et al. 2016; Lee et al. 2018; Adel et al. 2019; Sogut, 2020) or spray-dried capsules (Talon et al. 2019), prior to the thermal process. Encapsulation prevents the losses at the same time as the compound is vehiculated by another material that modifies and controls its release rate. Another strategy used to avoid thermal effects on active compounds is the use of the electrospinning of the polymer-active solutions to obtain active mats that can be deposited on another polymeric support, forming multilayer assemblies and providing it with active properties. Different aspects of this technique used in the present study are discussed below.

3. Use of electrospinning to develop active films

3.1. Description of the technique

In order to prevent some of the above-mentioned challenges, new techniques are being considered for the incorporation of active substances into bioplastics. Such is the case of **Electrospinning**, an old (Formhals, A., US patent, 1975504, 1934) (Bardwaj and Kundu, 2010; Sakai et al. 2008) but fascinating technology currently enjoying great market applicability. One of its initial purposes was that of textile fabrication, being patented by Formhals to spin cellulose acetate fibres from a solvent solution. With a few exceptions of patents being filed for synthetic vascular grafts (US Patent 4552707, 1985) and fibrillary lining for prosthetic devices (US Patent 4044404, 1977) (Zhang et al. 2005), electrospinning was only applied very little outside the textile field until the early 1990s when several research groups demonstrated this technique's versatility by spinning thin fibres from a wide range of organic polymers (Li and Xia, 2004). Due precisely to this technique's versatility

and simplicity, it has been opened up through these studies to new applications, delivering an impactful result. Through this method, ultrafine continuous fibres can be obtained, down to a nanometric size. Due to recent increased interest in nanotechnology, electrospinning is being studied for potential applications in many fields, such as drug delivery systems (Hamori et al. 2014; Sill and Recum, 2008), tissue engineering (Sill and Recum, 2008), biosensors (Mishra et al. 2017; Ramon-Marquez et al. 2018; Wu & Yin 2013), nanofibrous scaffolds for biomedical architecture (Wade and Burdick, 2014) and active food packaging (Fabra et al. 2016b; Wen et al. 2016).

The working principle of this technique is based on the electrostatic interactions induced in a fluid (polymeric solution or melt) when an electric field is applied. The “draw” of fibres becomes possible due to an inequality (imbalance) between the surface tension and the electric field strength.

The basic setup of the ES system consists of three elements: a spinneret that feeds the solution or melt, a grounded collector and a high voltage power supply. The polymeric fluid is pumped through the spinneret tip into the electric field that is being applied. At this initial moment, the fluid droplet is held in place by its surface tension. But as the electric field force increases, electric charges are induced on the surface of the fluid, exerting a repelling effect and the droplet slowly changes its shape into a conical structure, named the Taylor cone after Geoffrey Taylor, the scientist who studied this effect in 1964 (McClellan and Landis, 2016). With the increase in the electric field strength, the electric charges accumulating on the fluid surface reach a critical value where they overcome the surface tension. At this moment, a jet of fluid is ejected into the space between the spinneret tip and the collector. The excess charges on the surface of the ejected jet continue to repel each other, stretching and splitting the jet into many secondary strands, thus increasing its contact surface with the atmosphere. This allows for the solvent to evaporate (if applying from a solution) or the polymer to solidify (if applying from a melt), reaching the collector as solid fibres ((Bardwaj and Kundu, 2010; McClellan and Landis, 2016)

This simple, yet innovative, fibre-obtaining method allows structures to be obtained with ultra-fine fibres and high porosity, enjoying very large surface to volume ratios. Nakane et al. (2007) reported that the specific surface of electrospun PVA nanofibres was about 250 times larger than that of the PVA cast film. Thus, these authors point out that the diameters of ES fibres are one or two orders of magnitude smaller than the fibres obtained through the conventional methods.

3.2. Encapsulation of active compounds by electrospinning and development of multilayer active films

The high porosity of the electrospun materials, combined with the sub-micron fibre dimensions, make these structures attractive as carriers of active molecules and has paved the way for exploring the encapsulation of compounds of interest in carrier polymers through electrospinning. Additionally, electrospinning presents the possibility of running the process at room temperature, which in the case of temperature-sensitive, volatile actives is a big advantage, when compared with other encapsulation methods. Furthermore, due to the sub-micron scale that can be achieved through this technique, the active materials are more receptive to changes in the environment (such as temperature, relative humidity), and can enable a faster response, by triggering the release of the actives. Thus, Vega-Lugo and Lim (2009) reported that the release kinetics of natural antimicrobial allyl isothiocyanate from electrospun fibres of soy protein isolate / poly(ethylene oxide) blend and poly(lactic acid) changed with the relative humidity of the test environment, registering higher values when this parameter increased. Table 3 presents an overview of various naturally-occurring compounds encapsulated in different polymers by this process. The tested compounds vary from plant essential oils and their main constituents, to anti-inflammatory extracts, enzymes and vitamins. To this end, Wen et al. (2016) used poly(vinyl alcohol) to encapsulate cinnamon essential oil previously entrapped in β -cyclodextrin. The authors point out that the bioactive compound maintained its functionality when encapsulated in electrospun fibres, which retained more essential oil than the cast film. The electrospun films had very good antibacterial results against G(-) and G(+) bacteria and when applied over fresh strawberries it effectively prolonged their shelf-life.

Zhang et al. (2017) obtained electrospun PLA fibres encapsulating tea tree and manuka EO. The resulting fibres showed a 60 % lower glass transition temperature and increased tensile strength and elongation at break, due to EO's strong plasticizing effect. When testing the efficacy of the fibres against *Staphylococcus epidermidis*, only the ones containing Manuka tree EO were successful. The authors concluded that some components of the tea tree EO are lost during the ES encapsulation process, whereas the Manuka oil does not suffer losses. Sakai et al. (2008) used lipase entrapped in PVA by ES and reported that its transesterification rate was remarkably faster, by a factor of 5.2 when compared to the non-treated lipase. Liu et al. (2011) developed a biosensor for determining phenolic compounds by using laccase enzyme encapsulated by ES. The obtained biosensor had good sensing

performance, due to the high specific surface area (10.42 m²/g), biocompatibility and the excellent mechanical properties of the electrospun fibres used in its construction.

Given the advantages of this process, several studies have attempted to use the electrospun encapsulated molecules to develop active food packaging. Table 4 summarizes recent studies using this technique to deposit the electrospun encapsulated bioactive on biodegradable support material, thus generating multilayer structures with enhanced functionalities. Quiles-Carillo et al. (2019) reported on developing PLA-based multilayers by applying gallic acid (GA)-loaded PLA electrospun fibres onto PLA cast films. The authors found that the PLA matrix is protected by the presence of GA, experiencing a delay in its thermal degradation, while providing a sustained release of the active for over 1000 h. Castro-Mayorga et al. (2017) developed antibacterial multilayer material based on depositing electrospun polyhydroxyalkanoate (PHA) with silver nanoparticles onto PHA support. This material was effective at reducing *Salmonella enterica* below detection limits, even at very low silver loading. Other authors (Figueroa-Lopez et al. 2018) electrospun polycaprolactone carrying black pepper oleoresin over gelatin cast films. The electrospun coating reduced the cast film's permeability to water vapour, while increasing its thermal resistance and conferring antimicrobial activity against *Staphylococcus aureus*. Fabra et al. (2016a, 2016b, 2016c) did extensive work in encapsulating by means of ES different compounds. They used cinnamaldehyde, α -tocopherol and bacterial cellulose nanowhiskers (BCNW) respectively, to develop multilayers with potential applications as active food packaging. The cinnamaldehyde electrospun with zein on a polyhydroxybutyrate base exhibited promising inhibitory activity towards calicivirus, by exerting a complete inhibitory effect. The α -tocopherol was electrospayed with different protein carriers over thermoplastic wheat gluten films. The applied coating improved the water vapour barrier of the starch film. Moreover, the authors reported that the antioxidant's stability was preserved during a typical sterilization process, especially when entrapped in zein. Similarly, hybrid poly(3-hydroxybutyrate) with BCNW was applied by ES as a coating over thermoplastic corn starch that had been previously melt-mixed with BCNW. The presence of BCNW in only one of the layers led to a decrease of oxygen permeability values but it showed no significant differences between the multilayers containing BCNW, independent of the layer which contained the nanowhiskers. Nevertheless, the biggest reduction in water vapour permeability was noticed in the multilayers carrying BCNW in both layers (the inner layer of starch and the outer coating of polyhydroxybutyrate). Saeed et al. 2017 used the electrohydrodynamic process to construct a trilayer active would dressing by ES. The authors used

polycaprolactone and PVA as carriers for curcumin, a substance with antibacterial and anti-inflammatory activity for active wound bandaging. The dressing with 16 % active exhibited a good antibacterial effect while maintaining an acceptable cell viability level during *in vitro* biocompatibility tests.

Despite these successful reports, one look at the process conditions reveals that many solvents (not food grade) are being employed for the carrier polymer solutions (e.g. dichloromethane, N,N-dimethylformamide, chloroform) and, thus, do not comply with the legislation for food contact materials, limiting their use. Additionally, given the different chemical affinity between the active and the carrier matrix, it is necessary to assess the possible interactions that would prevent the active from being released effectively. Therefore, further studies are required to develop active materials for food packaging applications.

Table 3. Recent studies on the encapsulation of active compounds of natural origin by electrospinning. Active compound, solvent used, process conditions (D: distance between spinneret and collector, FR: flow rate, and voltage: V) and obtained microstructure are summarized.

Compound	Encapsulating polymer	Solvents	Processing conditions	Microstructure	Reference
Cinnamon EO	PVA (with β -cyclodextrin inclusions)	Ultrapure (Milli Q) water	26 °C , 56% RH; D= 12 -16 cm; FR= 3.3-10 μ L/min; V= 25 kV.	Smooth uniform fibres (average diameter 240 ± 40 nm) in optimal conditions: D= 14 cm; FR= 6.6 μ L/min; V= 15 kV.	Wen et al. 2016
Thyme EO	gelatine with TEO/ β -cyclodextrin/ ϵ -polylysine nanoparticles	Aqueous solution	25 °C , 35% RH; D= 15 cm; FR= 6.6 μ L/min; V= 20 kV.	Good continuous fibres, without beads. Diameter increases as content of nanoparticles rises	Lin et al. 2018
Tea tree EO	PLA	Acetone	20 °C ; D= 15 cm; FR= 33.3 μ L/min; V= 18.5 kV.	EO-free fibres with a cylindrical, well-defined shape, overlapping but not merged.	Zhang et al. 2017
Manuka tree EO				EO-loaded fibres without a cylindrical shape and more points of fusion where they overlap	

Compound	Encapsulating polymer	Solvents	Processing conditions	Microstructure	Reference
Cinnamaldehyde	Chitosan : poly(ethylene oxide) (1:1 wt.%)	Analytical reagent grade acetic acid	22 ± 1 °C , 24–28 % RH; D= 12, 14, and 16 cm; FR= 60 µL/min; V= 25 kV.	Continuous, fine, cylindrical fibres	Rieger and Schiffman, (2014)
Eugenol	PVA	Aqueous non-ionic micellar surfactant solution with Surfynol _{VR} 465	25 °C; D= 10 cm; FR= 20 µL/min; V= 20 kV	Fibres (mean diameter 57-126 nm). Thickness increases and fewer bead defects when surfactant and active concentrations increase.	Kriegel et al. 2010
Thymol	Zein (with γ-cyclodextrin inclusions)	-Aqueous solution for thymol-γ-cyclodextrin complex -Dimethylformamide (DMF) for zein	25 °C , 18 % RH; D= 17 cm; FR= 8.3 µL/min; V= 17 kV.	Bead-free, uniform nanofibres (average diameter between 155 ± 30 nm and 415 ± 100 nm)	Aytac et al. 2017
Carvacrol	Zein	Ethanol (80 % v/v)	24 °C; 21 %RH; D= 20 cm; FR= 16.6 µL/min;	Fibres with ribbon-like morphology and smooth surfaces, free of pores and pits	Altan et al. 2018

Compound	Encapsulating polymer	Solvents	Processing conditions	Microstructure	Reference
	PLA	Chloroform : DMF (9:1, v/v)	V= 15kV	Unevenly sized fibres, with textured surface topography as CA content increases	
Quercetin	Amaranth protein isolate (API): pullulan (50:50 wt.% and 80:20 wt.%)	Formic acid (95%)	24 °C; 60 % RH; D= 10 cm; FR= 0.4 mL/h; V= 22kV.	-Only the 50:50 API:pullulan solutions (w/w) with the active were suitable for stable electrospinning; -Relatively homogenous fibres, with smaller diameter than the active-free mats	Aceituno-Medina et al. 2015
Gallic acid	PLA (with cyclodextrin inclusions)	Dichloromethane (DCM) : N,N-dimethylformamide (DMF) (7:3)	24–25 °C, 17–18 % RH D= 10 cm; FR= 16.6 µL/min; V= 15 kV.	Bead-free nanofibres	Aytac et al. 2016
	Zein	Ethanol : water (4:1 w/w)	24–25 °C, 17–18 % RH D= 13 cm; FR= 13.3 µL/min; V= 16 kV.	Fibres (morphology details not specified)	Neo et al. 2013

Compound	Encapsulating polymer	Solvents	Processing conditions	Microstructure	Reference
Curcumin	Zein	Trifluoroethanol (100%)	Room temperature D= 10 cm; FR= 16.6 μ L/min; V= 20 kV.	Bead-free nanofibrous mat (average fibre diameter 200–350nm)	Brahatheeswaran et al. 2012
	PCL/ gum tragacanth	Acetic acid (90 % v/v)	D= 15 cm; FR= 16.6 μ L/min; V= 15 kV.	Bead-free, but irregular, surface nanofibres (average diameter between 667 \pm 33 and 836 \pm 23nm)	Ranjbar-Mohammadi and Bahrami, 2016
Lipase	PVA (M_w 146,000–186,000 and 98–99 % hydrolysed)	Aqueous solution	D= 12 cm; FR= 11.6 μ l/min; V= 15 kV.	Fibres (approximately 1 μ m in diameter)	Sakai et al. 2008
	PVA (polymerization degree 1,500)	Aqueous solution	D= 10 cm; FR= 0.015 mL/h; V= 25 kV.	Non-woven mat of nanofibres	Nakane et al. 2007

Compound	Encapsulating polymer	Solvents	Processing conditions	Microstructure	Reference
Laccase	PVA (polymerization degree: 2400, degree of alcoholysis: 98-99 %) with PEO–PPO–PEO triblock copolymer as enzyme stabilizer and gold nanoparticles as biosensor conductivity enhancer)	Aqueous solution	Room temperature, 25±2 % RH D= 9 cm; FR= 3.3 µl/min; V= 13.2 kV.	Irregular fibres interspersed with spindle-like beads	Liu et al. 2011
β-carotene	Zein prolamine	Ethanol : water (80:20 vol. %)	Room temperature, 60 % RH D= 10 cm; FR= 4.6 µl/min; V= 12 kV.	Ribbon-like structures mixed with cylindrical morphologies	Fernandez et al. 2009

Table 4. Recent studies on the development of multilayer active materials using electrospinning deposition on a polymeric support. Active compound, encapsulating polymer, solvent and processing conditions (D=distance between spinneret and collector; FR=flowrate; V= voltage) are presented.

Support	Electrospun material components		Solvent	Processing conditions	Reference
	active compound	encapsulating polymer			
Poly lactide (PLA)	Gallic acid	PLA	Dichloromethane (DCM) / N,N-dimethylformamide (DMF) 7:3 (v/v)	25 °C, 40 % RH; D= 18 cm; FR= 2.2 mL/h; V= 18 kV.	Quiles-Carrillo et al. 2019
Polyhydroxyalkanoate (PHA)	Silver nanoparticles	PHA	2,2,2-Trifluoroethanol	23 ± 2 °C; D= 20 cm; FR= 80 mL/h; V= 24kV and -18 kV.	Castro-Mayorga et al. 2017
Gelatine sheets	Black pepper oleoresin	PCL	Chloroform/butanol 75:25 (v/v)	D= 18 cm; FR= 1.5 mL/h; V= 20 kV.	Figueroa-Lopez et al. 2018
Polyhydroxybutyrate (PHB)	cinnamaldehyde	Zein	Ethanol/water (80:20 vol. %)	FR= 0.75 mL/h V= 14 kV	Fabra et al. 2016a
Thermoplastic wheat gluten	α-tocopherol	Whey protein isolate Zein Soy protein isolate	Aqueous solution Ethanol/water Aqueous solution	20 °C, 40 % RH; D=10 cm; FR=0.15-0.3 mL/h; V=10-15 kV.	Fabra et al. 2016b

Support	Electrospun material components		Solvent	Processing conditions	Reference
	active compound	encapsulating polymer			
Thermoplastic corn starch	Cellulose nanowhiskers	Polyhydroxyalkanoate (PHA)	2,2,2-Trifluoroethanol	23 °C, 40 % RH; D=10 cm; FR= 0.6 mL/h; V=14 kV.	Fabra et al. 2016c
Electrospun PCL or PCL+curcumin	Curcumin	PVA; PCL	For PCL: dimethylformamide :dichloromethane=2:1 (v/v) For PVA: aqueous solution	D=16 cm; FR= 1, 2 and 3 mL/h; V=12, 18 and 24 kV.	Saeed et al. 2017

4. References

<http://www.actinpak.eu/> (Accessed August 2019)

<https://www.european-bioplastics.org/bioplastics/> (Accessed September 2019)

<https://www.foodpackagingforum.org/food-packaging-health/bioplastics> (Accessed September 2019)

Aceituno-Medina, M., Mendoza, S., Rodríguez, B.A., Lagaron, J.M., López-Rubio, A., 2015. Improved antioxidant capacity of quercetin and ferulic acid during in-vitro digestion through encapsulation within food-grade electrospun fibers. *J. Funct. Foods* 12, 332–341. <https://doi.org/10.1016/j.jff.2014.11.028>

Adel, A.M., Ibrahim, A.A., El-Shafei, A.M., Al-Shemy, M.T., 2019. Inclusion complex of clove oil with chitosan/ β -cyclodextrin citrate/oxidized nanocellulose biocomposite for active food packaging. *Food Packag. Shelf Life* 20, 100307. <https://doi.org/10.1016/j.fpsl.2019.100307>

Altan, A., Aytac, Z., Uyar, T., 2018. Carvacrol loaded electrospun fibrous films from zein and poly(lactic acid) for active food packaging. *Food Hydrocoll.* 81, 48–59. <https://doi.org/10.1016/j.foodhyd.2018.02.028>

Auras, R., Harte, B., Selke, S., 2004. Effect of water on the oxygen barrier properties of poly(ethylene terephthalate) and polylactide films. *J. Appl. Polym. Sci.* 92, 1790–1803. <https://doi.org/10.1002/app.20148>

Aytac, Z., Kusku, S.I., Durgun, E., Uyar, T., 2016. Encapsulation of gallic acid/cyclodextrin inclusion complex in electrospun polylactic acid nanofibers: Release behaviour and antioxidant activity of gallic acid. *Mater. Sci. Eng. C* 63, 231–239. <https://doi.org/10.1016/j.msec.2016.02.063>

Aytac, Z., Ipek, S., Durgun, E., Tekinay, T., Uyar, T., 2017. Antibacterial electrospun zein nanofibrous web encapsulating thymol/cyclodextrin-inclusion complex for food packaging. *Food Chem.* 233, 117–124. <https://doi.org/10.1016/j.foodchem.2017.04.095>

Balaguer, M.P., Lopez-Carballo, G., Catala, R., Gavara, R., Hernandez-Munoz, P., 2013. Antifungal properties of gliadin films incorporating cinnamaldehyde and application in active food packaging of bread and cheese spread foodstuffs. *Int. J. Food Microbiol.* 166, 369–377. <https://doi.org/10.1016/j.ijfoodmicro.2013.08.012>

- Bassolé, I.H.N., Juliani, H.R., 2012. Essential oils in combination and their antimicrobial properties. *Molecules* 17, 3989–4006. <https://doi.org/10.3390/molecules17043989>
- Bhardwaj, N., Kundu, S.C., 2010. Electrospinning: A fascinating fiber fabrication technique. *Biotechnol. Adv.* 28, 325–347. <https://doi.org/10.1016/j.biotechadv.2010.01.004>
- Ben Arfa, A., Combes, S., Preziosi-Belloy, L., Gontard, N., Chalier, P., 2006. Antimicrobial activity of carvacrol related to its chemical structure. *Lett. Appl. Microbiol.* 43, 149–154. <https://doi.org/10.1111/j.1472-765X.2006.01938.x>
- Bonilla Lagos, M.J., Vargas, M., Atarés Huerta, L., Chiralt, A. (2014). Effect of Chitosan Essential Oil Films on the Storage-Keeping Quality of Pork Meat Products. *Food and Bioproc*, 2014. 2443–2450. <https://doi.org/10.1007/s11947-014-1329-3>.
- Brahatheeswaran, D., Mathew, A., Aswathy, R.G., Nagaoka, Y., Venugopal, K., Yoshida, Y., Maekawa, T., Sakthikumar, D., 2012. Hybrid fluorescent curcumin loaded zein electrospun nanofibrous scaffold for biomedical applications. *Biomed. Mater.* 7, 045001. <https://doi.org/10.1088/1748-6041/7/4/045001>
- Burt, S (2004). Essential oils: their antibacterial properties and potential applications in foods – a review. *International Journal of Food Microbiology* 94 (3) 223 – 253. <http://dx.doi.org/10.1016/j.ijfoodmicro.2004.03.022>
- Cano, A., Fortunati, E., Cháfer, M., Kenny, J.M., Chiralt, A., González-Martínez, C., 2015. Properties and ageing behaviour of pea starch films as affected by blend with poly(vinyl alcohol). *Food Hydrocoll.* 48, 84–93. <https://doi.org/10.1016/j.foodhyd.2015.01.008>
- Cano Embuena, A.I., Cháfer Nácher, M., Chiralt Boix, A., Molina Pons, M.P., Borrás Llopis, M., Beltran Martínez, M.C., González Martínez, C., 2017. Quality of goat's milk cheese as affected by coating with edible chitosan-essential oil films. *Int. J. Dairy Technol.* 70, 68–76. <https://doi.org/10.1111/1471-0307.12306>
- Castro-Mayorga, J.L., Fabra, M.J., Cabedo, L., Lagaron, J.M., 2017. On the use of the electrospinning coating technique to produce antimicrobial polyhydroxyalkanoate materials containing in situ-stabilized silver nanoparticles. *Nanomaterials* 7. <https://doi.org/10.3390/nano7010004>
- Chen, N., Li, L., Wang, Q., 2007. New technology for thermal processing of poly(vinyl alcohol). *Plast. Rubber Compos.* 36, 283–290. <https://doi.org/10.1179/174328907X237575>
- Collazo-Bigliardi, S., Ortega-Toro, R., Chiralt, A., 2018. Properties of Micro- and Nano-Reinforced Biopolymers for Food Applications, in: Gutiérrez, T.J. (Ed.), *Polymers for*

- Food Applications. Springer International Publishing, Cham, pp. 61–99. https://doi.org/10.1007/978-3-319-94625-2_4
- Conn, R.E., Kolstad, J.J., Borzelleca, J.F., Dixler, D.S., Filer, L.J., Ladu, B.N., Pariza, M.W., 1995. Safety assessment of polylactide (PLA) for use as a food-contact polymer. *Food Chem. Toxicol.* 33, 273–283. [https://doi.org/10.1016/0278-6915\(94\)00145-E](https://doi.org/10.1016/0278-6915(94)00145-E)
- DeMerlis, C.C., Schoneker, D.R., 2003. Review of the oral toxicity of polyvinyl alcohol (PVA). *Food Chem. Toxicol.* 41, 319–326. [https://doi.org/10.1016/S0278-6915\(02\)00258-2](https://doi.org/10.1016/S0278-6915(02)00258-2)
- De Vincenzi, M., Stamatii, A., De Vincenzi, A., & Silano, M. (2004). Constituents of aromatic plants: Carvacrol. *Fitoterapia*, 75(7–8), 801–804. <https://doi.org/10.1016/j.fitote.2004.05.002>
- Dhifi, W., Bellili, S., Jazi, S., Bahloul, N., Mnif, W., 2016. Essential Oils' Chemical Characterization and Investigation of Some Biological Activities: A Critical Review. *Medicines* 3, 25. <https://doi.org/10.3390/medicines3040025>
- Efsa, 2012. Scientific Opinion on the Safety and efficacy of phenol derivates containing ring-alkyl, ring-alkoxy and side- chains with an oxygenated functional group (chemical group 25) when used as flavourings for all species. *Efsa J.* 10, 2573. <https://doi.org/10.2903/j.efsa.2012.2573>.
- Emadian, S.M., Onay, T.T., Demirel, B., 2017. Biodegradation of bioplastics in natural environments. *Waste Manag.* 59, 526–536. <https://doi.org/10.1016/j.wasman.2016.10.006>
- Emiroğlu, Z.K., Yemiş, G.P., Coşkun, B.K., Candoğan, K., 2010. Antimicrobial activity of soy edible films incorporated with thyme and oregano essential oils on fresh ground beef patties. *Meat Sci.* 86, 283–288. <https://doi.org/10.1016/j.meatsci.2010.04.016>
- Fabra, M.J., Randazzo, W., Lagaro, J.M., Aznar, R., Sa, G., Lo, A., 2016 (a). Efficacy of Cinnamaldehyde Against Enteric Viruses and Its Activity After Incorporation Into Biodegradable Multilayer Systems of Interest in Food Packaging 125–132. <https://doi.org/10.1007/s12560-016-9235-7>
- Fabra, M.J., López-Rubio, A., Lagaron, J.M., 2016 (b). Use of the electrohydrodynamic process to develop active/bioactive bilayer films for food packaging applications. *Food Hydrocoll.* 55, 11–18. <https://doi.org/10.1016/j.foodhyd.2015.10.026>
- Fabra, M.J., López-Rubio, A., Ambrosio-Martín, J., Lagaron, J.M., 2016 (c). Food Hydrocolloids Improving the barrier properties of thermoplastic corn starch-based films containing bacterial cellulose nanowhiskers by means of PHA electrospun coatings of

- interest in food packaging. *Food Hydrocoll.* 61, 261–268. <https://doi.org/10.1016/j.foodhyd.2016.05.025>
- Fang, J.M., Fowler, P.A., Escrig, C., Gonzalez, R., Costa, J.A., Chamudis, L., 2005. Development of biodegradable laminate films derived from naturally occurring carbohydrate polymers. *Carbohydr. Polym.* 60, 39–42. <https://doi.org/10.1016/j.carbpol.2004.11.018>
- Fernandez, A., Torres-Giner, S., Lagaron, J.M., 2009. Novel route to stabilization of bioactive antioxidants by encapsulation in electrospun fibers of zein prolamine. *Food Hydrocoll.* 23, 1427–1432. <https://doi.org/10.1016/j.foodhyd.2008.10.011>
- Figueroa-Lopez, K., Castro-Mayorga, J., Andrade-Mahecha, M., Cabedo, L., Lagaron, J., 2018. Antibacterial and Barrier Properties of Gelatin Coated by Electrospun Polycaprolactone Ultrathin Fibres Containing Black Pepper Oleoresin of Interest in Active Food Biopackaging Applications. *Nanomaterials* 8, 199. <https://doi.org/10.3390/nano8040199>
- Hamori, M., Yoshimatsu, S., Hukuchi, Y., Shimizu, Y., Fukushima, K., Sugioka, N., Nishimura, A., Shibata, N., 2014. Preparation and pharmaceutical evaluation of nano-fiber matrix supported drug delivery system using the solvent-based electrospinning method. *Int. J. Pharm.* 464, 243–251. <https://doi.org/10.1016/j.ijpharm.2013.12.036>
- Higuera, L., López-Carballo, G., Hernández-Muñoz, P., Catalá, R., Gavara, R., 2014. Antimicrobial packaging of chicken fillets based on the release of carvacrol from chitosan/cyclodextrin films. *Int. J. Food Microbiol.* 188, 53–59. <https://doi.org/10.1016/j.ijfoodmicro.2014.07.018>
- Horvathova, E., Navarova, J., Galova, E., Sevcovicova, A., Chodakova, L., Snahnicanova, Z., Slamenova, D. (2014). Assessment of antioxidative, chelating, and DNA-Protective effects of selected essential oil components (Eugenol, Carvacrol, Thymol, Borneol, Eucalyptol) of plants and intact *rosmarinus officinalis* oil. *Journal of Agricultural and Food Chemistry*, 62(28), 6632–6639. <https://doi.org/10.1021/jf501006y>
- Jamshidian, M., Tehrany, E.A., Imran, M., Jacquot, M., Desobry, S., 2010. Poly-Lactic Acid: Production, applications, nanocomposites, and release studies. *Compr. Rev. Food Sci. Food Saf.* 9, 552–571. <https://doi.org/10.1111/j.1541-4337.2010.00126.x>
- Jiménez, A., Sánchez-González, L., Desobry, S., Chiralt, A., & Tehrany, E. A. (2014). Influence of nanoliposomes incorporation on properties of film forming dispersions and films based on corn starch and sodium caseinate. *Food Hydrocolloids*, 35, 159–169. <https://doi.org/10.1016/j.foodhyd.2013.05.006>

- Joint FAO/WHO, June 2001. Expert Committee on Food Additives Fifty-fifth report. http://apps.who.int/iris/bitstream/10665/42388/1/WHO_TRS_901.pdf (accessed in August, 2017).
- Kriegel, C., Kit, K.M., McClements, D.J., Weiss, J., 2010. Nanofibers as carrier systems for antimicrobial microemulsions. II. Release characteristics and antimicrobial activity. *J. Appl. Polym. Sci.* 118, 2859–2868. <https://doi.org/10.1002/app.32563>
- Lee, M.H., Kim, S.Y., Park, H.J., 2018. Effect of halloysite nanoclay on the physical, mechanical, and antioxidant properties of chitosan films incorporated with clove essential oil. *Food Hydrocoll.* 84, 58–67. <https://doi.org/10.1016/j.foodhyd.2018.05.048>
- Li, D., Xia, Y., 2004. Electrospinning of nanofibers: Reinventing the wheel? *Adv. Mater.* 16, 1151–1170. <https://doi.org/10.1002/adma.200400719>
- Lin, L., Zhu, Y., Cui, H., 2018. Electrospun thyme essential oil/gelatin nanofibers for active packaging against *Campylobacter jejuni* in chicken. *Lwt* 97, 711–718. <https://doi.org/10.1016/j.lwt.2018.08.015>
- Liu, J., Niu, J., Yin, L., Jiang, F., 2011. *In situ* encapsulation of laccase in nanofibers by electrospinning for development of enzyme biosensors for chlorophenol monitoring. *Analyst* 136, 4802–4808. <https://doi.org/10.1039/c1an15649g>
- López-Mata, M., Ruiz-Cruz, S., Silva-Beltrán, N., Ornelas-Paz, J., Zamudio-Flores, P., Burruel-Ibarra, S., 2013. Physicochemical, Antimicrobial and Antioxidant Properties of Chitosan Films Incorporated with Carvacrol. *Molecules* 18, 13735–13753. <https://doi.org/10.3390/molecules181113735>
- McClellan, P., Landis, W.J., 2016. Recent Applications of Coaxial and Emulsion Electrospinning Methods in the Field of Tissue Engineering. *Biores. Open Access* 5, 212–227. <https://doi.org/10.1089/biores.2016.0022>
- Mikulcová, V., Bordes, R., Kašpárková, V., 2016. On the preparation and antibacterial activity of emulsions stabilized with nanocellulose particles. *Food Hydrocoll.* 61, 780–792. <https://doi.org/10.1016/j.foodhyd.2016.06.031>
- Mishra, R.K., Nawaz, M.H., Hayat, A., Nawaz, M.A.H., Sharma, V., Marty, J.L., 2017. Electrospinning of graphene-oxide onto screen printed electrodes for heavy metal biosensor. *Sensors Actuators, B Chem.* 247, 366–373. <https://doi.org/10.1016/j.snb.2017.03.059>
- Muller, J., González-Martínez, C., Chiralt, A., 2017a. Combination Of Poly(lactic) acid and starch for biodegradable food packaging. *Materials (Basel)*. 10. <https://doi.org/10.3390/ma10080952>

- Muller, J., Casado Quesada, A., González-Martínez, C., Chiralt, A., 2017b. Antimicrobial properties and release of cinnamaldehyde in bilayer films based on polylactic acid (PLA) and starch. *Eur. Polym. J.* 96, 316–325. <https://doi.org/10.1016/j.eurpolymj.2017.09.009>
- Nakane, K., Hotta, T., Ogihara, T., Ogata, N., Yamaguchi, S., 2007. Synthesis of (Z)-3-hexen-1-yl acetate by lipase immobilized in polyvinyl alcohol nanofibers. *J. Appl. Polym. Sci.*, 106, 863–867. <https://doi.org/10.1002/app.26710>
- Neo, Y.P., Swift, S., Ray, S., Gizdavic-Nikolaidis, M., Jin, J., Perera, C.O., 2013. Evaluation of gallic acid loaded zein sub-micron electrospun fibre mats as novel active packaging materials. *Food Chem.* 141, 3192–3200. <https://doi.org/10.1016/j.foodchem.2013.06.018>
- Ortega-Toro, R., Bonilla, J., Talens, P., Chiralt, A., 2017. Future of Starch-Based Materials in Food Packaging, in: *Starch-Based Materials in Food Packaging*. Elsevier, pp. 257–312. <https://doi.org/10.1016/B978-0-12-809439-6.00009-1>
- Oussalah, M., Caillet, S., Salmiéri, S., Saucier, L., Lacroix, M., 2004. Antimicrobial and antioxidant effects of milk protein-based film containing essential oils for the preservation of whole beef muscle. *J. Agric. Food Chem.* 52, 5598–5605. <https://doi.org/10.1021/jf049389q>
- Peixoto, L.S., Silva, F.M., Niemeyer, M.A.L., Espinosa, G., Melo, P.A., Nele, M., Pinto, J.C., 2006. Synthesis of poly(vinyl alcohol) and/or poly(vinyl acetate) particles with spherical morphology and core-shell structure and its use in vascular embolization. *Macromol. Symp.* 243, 190–199. <https://doi.org/10.1002/masy.200651118>
- Perdones, A., Sánchez-González, L., Chiralt, A., Vargas, M., 2012. Effect of chitosan-lemon essential oil coatings on storage-keeping quality of strawberry. *Postharvest Biol. Technol.* 70, 32–41. <https://doi.org/10.1016/j.postharvbio.2012.04.002>
- Priyadarshi, R., Sauraj, Kumar, B., Deeba, F., Kulshreshtha, A., Negi, Y.S., 2018. Chitosan films incorporated with Apricot (*Prunus armeniaca*) kernel essential oil as active food packaging material. *Food Hydrocoll.* 85, 158–166. <https://doi.org/10.1016/j.foodhyd.2018.07.003>
- Quiles-Carrillo, L., Montanes, N., Lagaron, J., Balart, R., Torres-Giner, S., 2019. Bioactive Multilayer Polylactide Films with Controlled Release Capacity of Gallic Acid Accomplished by Incorporating Electrospun Nanostructured Coatings and Interlayers. *Appl. Sci.* 9, 533. <https://doi.org/10.3390/app9030533>

- Ramon-Marquez, T., Medina-Castillo, A.L., Nagiah, N., Fernandez-Gutierrez, A., Fernandez-Sanchez, J.F., 2018. A multifunctional material based on co-electrospinning for developing biosensors with optical oxygen transduction. *Anal. Chim. Acta* 1015, 66–73. <https://doi.org/10.1016/j.aca.2018.02.010>
- Ranjbar-Mohammadi, M., Bahrami, S.H., 2016. Electrospun curcumin loaded poly(ϵ -caprolactone)/gum tragacanth nanofibers for biomedical application. *Int. J. Biol. Macromol.* 84, 448–456. <https://doi.org/10.1016/j.ijbiomac.2015.12.024>
- Requena, R., Jiménez, A., Vargas, M., Chiralt, A., 2016. Poly[(3-hydroxybutyrate)-co-(3-hydroxyvalerate)] active bilayer films obtained by compression moulding and applying essential oils at the interface. *Polym. Int.* 65, 883–891. <https://doi.org/10.1002/pi.5091>
- Requena, R., Vargas, M., Chiralt, A., 2019. Eugenol and carvacrol migration from PHBV films and antibacterial action in different food matrices. *Food Chem.* 277, 38–45. <https://doi.org/10.1016/j.foodchem.2018.10.093>
- Ribeiro-Santos, R., Andrade, M., Melo, N.R. de, Sanches-Silva, A., 2017. Use of essential oils in active food packaging: Recent advances and future trends. *Trends Food Sci. Technol.* 61, 132–140. <https://doi.org/10.1016/j.tifs.2016.11.021>
- Rieger, K.A., Schiffman, J.D., 2014. Electrospinning an essential oil: Cinnamaldehyde enhances the antimicrobial efficacy of chitosan/poly(ethylene oxide) nanofibers. *Carbohydr. Polym.* 113, 561–568. <https://doi.org/10.1016/j.carbpol.2014.06.075>
- Rooney, M.L., 1995. Overview of active food packaging, in: Rooney, M.L. (Ed.), *Active Food Packaging*. Springer US, Boston, MA, pp. 1–37. https://doi.org/10.1007/978-1-4615-2175-4_1
- Saeed, S.M., Mirzadeh, H., Zandi, M., Barzin, J., 2017. Designing and fabrication of curcumin loaded PCL/PVA multi-layer nanofibrous electrospun structures as active wound dressing. *Prog. Biomater.* 6, 39–48. <https://doi.org/10.1007/s40204-017-0062-1>
- Sanchez-Gonzalez, L., Pastor, C., Vargas, M., Chiralt, A., Gonzalez-Martinez, C., Chafer, M., 2011. Effect of hydroxypropylmethylcellulose and chitosan coatings with and without bergamot essential oil on quality and safety of cold-stored grapes. *Postharvest Biol. Technol.* 60, 57–63. <https://doi.org/10.1016/j.postharvbio.2010.11.004>
- Sakai, S., Antoku, K., Yamaguchi, T., Kawakami, K., 2008. Transesterification by lipase entrapped in electrospun poly(vinyl alcohol) fibers and its application to a flow-through reactor. *J. Biosci. Bioeng.* 105, 687–689. <https://doi.org/10.1263/jbb.105.687>
- Sapper, M., Chiralt, A., 2018. Starch-Based Coatings for Preservation of Fruits and Vegetables. <https://doi.org/10.3390/coatings8050152>

- Sapper, M., Bonet, M., & Chiralt, A. (2019). Wettability of starch-gellan coatings on fruits, as affected by the incorporation of essential oil and/or surfactants. *LWT*, 116 (March), 108574. <https://doi.org/10.1016/j.lwt.2019.108574>
- Sill, T.J., von Recum, H.A., 2008. Electrospinning: Applications in drug delivery and tissue engineering. *Biomaterials* 29, 1989–2006. <https://doi.org/10.1016/j.biomaterials.2008.01.011>
- Sogut, E., 2020. Active whey protein isolate films including bergamot oil emulsion stabilized by nanocellulose. *Food Packag. Shelf Life* 23, 100430. <https://doi.org/10.1016/j.fpsl.2019.100430>
- Talón, E., Vargas, M., Chiralt, A., González-Martínez, C., 2019. Antioxidant starch-based films with encapsulated eugenol. Application to sunflower oil preservation. *Lwt* 113, 2019 v.113. <https://doi.org/10.1016/j.lwt.2019.108290> 105, 687–689. <https://doi.org/10.1263/jbb.105.687>
- Thakur, R., Pristijono, P., Scarlett, C.J., Bowyer, M., Singh, S.P., Vuong, Q. V., 2019. Starch-based films: Major factors affecting their properties. *Int. J. Biol. Macromol.* 132, 1079–1089. <https://doi.org/10.1016/j.ijbiomac.2019.03.190>
- Tian, H., Yan, J., Rajulu, A.V., Xiang, A., Luo, X., 2017. Fabrication and properties of polyvinyl alcohol/starch blend films: Effect of composition and humidity. *Int. J. Biol. Macromol.* 96, 518–523. <https://doi.org/10.1016/j.ijbiomac.2016.12.067>
- Ultee, A., Gorris, L. G. M., & Smid, E. J. (1998). Bactericidal activity of carvacrol towards the food-borne pathogen *Bacillus cereus*. *Journal of Applied Microbiology*, 85(2), 211–218. <https://doi.org/10.1046/j.1365-2672.1998.00467.x>
- Ultee, A., Bennik, M.H.J. and Moezelaar, R. (2002) The phenolic hydroxyl group of carvacrol is essential for action against the food borne pathogen *Bacillus cereus*. *Appl Environ Microbiol* 68, 1561–1568.
- Valencia-Sullca, C., Jiménez, M., Jiménez, A., Atarés, L., Vargas, M., & Chiralt, A. (2016). Influence of liposome encapsulated essential oils on properties of chitosan films. *Polymer International*, 65(8), 979–987. <https://doi.org/10.1002/pi.5143>
- Vega-Lugo, A.C., Lim, L.T., 2009. Controlled release of allyl isothiocyanate using soy protein and poly(lactic acid) electrospun fibers. *Food Res. Int.* 42, 933–940. <https://doi.org/10.1016/j.foodres.2009.05.005>
- Yun, J., Fan, X., Li, X., Jin, T.Z., Jia, X., Mattheis, J.P., 2015. Natural surface coating to inactivate *Salmonella enterica serovar Typhimurium* and maintain quality of cherry

tomatoes. *Int. J. Food Microbiol.* 193, 59–67.
<https://doi.org/10.1016/j.ijfoodmicro.2014.10.013>

Wade, R.J., Burdick, J. a., 2014. Advances in nanofibrous scaffolds for biomedical applications: From electrospinning to self-assembly. *Nano Today* 9, 722–742.
<https://doi.org/10.1016/j.nantod.2014.10.002>

Wen, P., Zhu, D.-H., Wu, H., Zong, M.-H., Jing, Y.-R., Han, S.-Y., 2016. Encapsulation of cinnamon essential oil in electrospun nanofibrous film for active food packaging. *Food Control* 59, 366–376. <https://doi.org/10.1016/j.foodcont.2015.06.005>

Wen, P., Zong, M.H., Linhardt, R.J., Feng, K., Wu, H., 2017. Electrospinning: A novel nano-encapsulation approach for bioactive compounds. *Trends Food Sci. Technol.* 70, 56–68. <https://doi.org/10.1016/j.tifs.2017.10.009>

Wu, J., Yin, F., 2013. Sensitive enzymatic glucose biosensor fabricated by electrospinning composite nanofibers and electrodepositing Prussian blue film. *J. Electroanal. Chem.* 694, 1–5. <https://doi.org/10.1016/j.jelechem.2013.02.003>

Zhang, Y., Chwee, T. L., Ramakrishna, S., & Huang, Z. M. (2005). Recent development of polymer nanofibers for biomedical and biotechnological applications. *Journal of Materials Science: Materials in Medicine*, 16(10), 933–946.
<https://doi.org/10.1007/s10856-005-4428-x>

Zhang, W., Huang, C., Kusmartseva, O., Thomas, N.L., Mele, E., 2017. Electrospinning of polylactic acid fibres containing tea tree and manuka oil 117, 106–111.
<https://doi.org/10.1016/j.reactfunctpolym.2017.06.013>

OBJECTIVES

The **general objective of this thesis** was to encapsulate carvacrol in different polymer matrices by using electrospinning or casting to develop biodegradable multilayer films with antioxidant and antimicrobial properties and a high barrier capacity against water vapour and gases for food packaging applications. To this end, polar and non-polar polymers (starch and PCL or PVA and PLA) have been combined in order to take advantage of their complementary barrier properties. Different combination strategies have been considered, taking into account the food contact layer and the polymer carrying the carvacrol.

Specific objectives

1. To study the electrospinning behaviour of polar (starch) and non-polar (PCL) polymers carrying carvacrol to obtain active multilayer films.
2. To obtain starch-electrospun PCL multilayer films and study both the release kinetics and antimicrobial properties of the carvacrol encapsulated in PCL nanofibres.
3. To study the biodegradation behaviour of the starch-PCL multilayer films containing, or not, carvacrol.
4. To study the electrospinning behaviour of polar PVA to encapsulate carvacrol, compared to cast films, in order to obtain active multilayer films.
5. To study the electrospinning behaviour of non-polar PLA to encapsulate carvacrol, compared to cast films, in order to obtain active multilayer films.
6. To obtain PVA-PLA multilayer films by the reactive functionalization of the PLA surface, by casting PVA coatings encapsulating carvacrol.

CHAPTERS

CHAPTER I

Multilayer films combining starch and poly-(ϵ -caprolactone)

1. Carvacrol encapsulation in starch or PCL based matrices by electrospinning
2. Release kinetics and antimicrobial properties of carvacrol encapsulated in electrospun poly-(ϵ -caprolactone) nanofibres. Application in starch multilayer films
3. Biodegradation of thermoplastic starch films containing electrospun poly-(ϵ -caprolactone) encapsulating carvacrol

CHAPTER II

Multilayer films combining PVA and PLA

1. Poly(vinyl alcohol)-based materials encapsulating carvacrol obtained by solvent casting and electrospinning
2. Poly(lactic acid) based materials encapsulating carvacrol obtained by solvent casting and electrospinning
3. Enhancement of PLA-PVA surface adhesion in bilayer assemblies by PLA aminolization

Carvacrol encapsulation in starch or PCL based matrices by electrospinning

Alina Tampau^a, Chelo González-Martínez^b, Amparo Chiralt^c

^{a,b,c} Instituto Universitario de Ingeniería de Alimentos para el Desarrollo, Ciudad Politécnica de la Innovación, Universitat Politècnica de Valencia, Camino de Vera, s/n, 46022 Valencia, Spain

Journal of Food Engineering (2017) 214, 245-256

altam@upvnet.upv.es

Abstract

Carvacrol (CA) was encapsulated in polar (corn starch-Sodium caseinate, CS:NaCas) or non-polar (poly- ϵ -caprolactone, PCL) matrices by electrospinning (ES). Electrospun formulations were prepared with CS:NaCas (9:1 w/w ratio), at 2, 4 and 6 wt. % in water, or PCL at 5, 10 and 15 wt.% in glacial acetic acid using different CA ratios (0, 5, 10 and 15 wt.% with respect to the polymer). The liquid formulations were characterized for electrical conductivity, rheological behaviour and surface tension, and ES process conditions were established. The electrospun structures were analysed as to their nanostructure and CA retention. Geometry of the nanostructures obtained from the PCL systems was nanofibrillar with some beads, whereas it is particles that are mainly deposited for starch systems. PCL systems yielded better CA encapsulation efficiency (EE) than the polar ones, where greater variability was observed. The best EE (around 80%) was obtained for 15% PCL regardless of the CA ratio.

Keywords

Electrospinning; nanostructure; active compound; encapsulation efficiency.

Chemical compounds

Corn starch (PubChem CID: 24836924); Sodium Caseinate (PubChem CID: 73995022); Poly- ϵ -caprolactone (PubChem CID: 10401); Carvacrol (PubChem CID: 10364); Glacial acetic acid (PubChem CID: 73995022); Absolute ethanol (PubChem CID: 702).

1. Introduction

Microbial contamination and loss of nutrients due to oxidation are two of the major concerns of the food industry. An average per capita food losses of 280-300 kg/year in Europe and North-America was reported in a study carried out by The Swedish Institute for Food and Biotechnology (SIK) on behalf of the Food and Agriculture Organization of the United Nations (FAO, 2011). Significant percentage (>50%) of these losses occurs early in the food supply chain, even before it reaches the final consumer. In an effort to reduce pre-consumer food wastes, several alternatives are being under study. Among them, the use of active packaging material to enhance food preservation represents a promising technology. According to the Regulation (EC) No. 450/2009 (EU, 2009), active packaging materials are designed to purposely incorporate components that would interact with the packaged food or the environment surrounding it, extending its shelf life, while maintaining its quality. One possibility to incorporate these active agents into the packaging material is the use of multi-layered films, where one of these layers incorporates the active component. With a growing demand for a reduced use of synthetic antioxidants and preservatives coming in contact with the food, interest is focusing on natural based compounds, namely plant essential oils (EO) (Bakkali et al., 2008). Special attention is being paid to their active compounds (AC), terpenoid or phenolic in nature (Burt, 2004), which can provide foodstuffs with antioxidant and antimicrobial protection (Rivera Calo et al., 2015; Ündeğer et al., 2009). Because of their volatility and degradability when exposed to light, oxygen and/or heat, these active compounds need to be encapsulated in matrices that retain them efficiently, protect them from degradation and allow their sustained release. Various methods of EO encapsulation have been investigated in the last few years, using different matrices and techniques. Some of the techniques that have been used consist of nanoprecipitation, coacervation, and encapsulation in liposomes, spray-drying and the rapid expansion of supercritical solutions (Asbahani et al., 2015).

Of the encapsulation methods, specific interest is currently being centred on electrospinning (ES) technology due to its ease of use, wide applicability (Bhardwaj and Kundu, 2010) and the possibility of obtaining structures that possess high surface-to-volume ratio (nanostructures) (Zhang et al., 2005). The versatility of this technology is proven by the growing number of applications and the variety of electrospunable materials (dissolutions or melts) being tested successfully (Bhardwaj and Kundu, 2010; Kim and Lee, 2000).

ES is a technique that uses electrostatic forces to create polymer fibres. The ES equipment consists of an electrically conductive needle tip or spinneret, a grounded collector and a power supply, responsible for generating the high voltage (around 5 to 50kV). During the process, a polymer solution is loaded into the spinneret and held by its surface tension at the end of the capillary tip. As the intensity of the electric field increases, the hemispherical surface of the polymer solution at the tip of the capillary tube elongates to form a cone-shaped structure known as the Taylor cone. When the applied electric field reaches a critical value, the repulsive electrical forces exceed the surface tension forces, and the charged jet of the polymer solution is ejected from the tip of the Taylor cone, which becomes very long and thin. Meanwhile, the solvent evaporates leaving behind a charged polymer fibre which accelerates towards the collector of opposite polarity (Ghorani and Tucker, 2015).

Although initially the ES technique was employed to obtain fibres and filaments (Garg and Bowlin, 2011) and for medical purposes (drug delivery systems, tissue engineering (Hamori et al., 2014; Sill and von Recum, 2008; Wade and Burdick, 2014) and grafts (Ahn et al., 2015)), it is gaining ground in the field of food packaging, where the application of electrospun layers of different polymers on the film packaging surface, with or without active compounds, can provide the films with active or tailored functional properties (Fabra et al., 2016; Fabra et al., 2014; Wen et al., 2016). The absence of high temperatures during this process makes it very useful for encapsulating volatile or organic active agents that would otherwise lose their desirable properties (Ghorani and Tucker, 2015). The process allows for the creation of film-like structures (when fibres are electrospun) or the obtaining of a coating effect (electrospraying). Attempts to use natural, biodegradable polymers to obtain electrospun structures that can encapsulate active compounds (*Bifidobacterium spp.*, cinnamaldehyde and cinnamon EO) have already been reported (López-Rubio et al., 2009; Rieger and Schiffman, 2014; Wen et al., 2016). Nevertheless, little information is available, and more research is needed in order to optimize the process for specific matrices and the AC they carry.

Of the natural antimicrobials, carvacrol (CA) is a monoterpenoid phenol found in the essential oil of oregano (*Origanum vulgare*), thyme (*Thymus vulgaris L.*), marjoram (*Origanum majorana*) and similar aromatic plants (De Vincenzi et al., 2004). Its antimicrobial effects have been proven with remarkable results on strains of bacteria, such as *Escherichia coli*, *Staphylococcus aureus*, *Bacillus subtilis*, *Pseudomonas fluorescens* (Ben Arfa, et al., 2006), *Baccillus cereus* (Ultee et al., 1998) and moulds, such as *Penicillium notatum* (Tunc

et al., 2007). Studies into the antioxidant properties of CA reported that this compound is highly effective at protecting the cells, especially their DNA, from the damaging action of free radicals (Horvathova et al., 2014).

The incorporation of active compounds from EOs to hydrophilic biopolymer films requires the use of emulsifying techniques to obtain the film forming aqueous dispersions due to the hydrophobic nature of active compounds and their lack of water solubility. Afterwards, films are obtained by casting and subsequent drying under controlled conditions. During the drying step, a part of the water-immiscible active compounds evaporates by steam drag effect, depending on the system viscosity, lipid droplet size and emulsion stability (Perdones et al., 2016). The EO incorporation in biopolymer films during thermoplastic processing (melt blending, extrusion, etc.) also presents problems due to the high volatility and temperature sensitivity of these compounds (Chew and Nyam, 2016). Likewise, the fast release of active compounds embedded in polar biopolymers, in contact with aqueous systems as is the case in most of the foods, also represents a problem for the control of their sustained action (antimicrobial or antioxidant) and their sensory impact, associated with their usually strong flavour. In this sense, encapsulation of these kinds of compounds by ES and their application as an active layer in packaging films could represent a good alternative to control both the fast release and the sensory impact, since the delivered dose could be better optimized over time. Likewise, the functional properties of the films could be modulated, by combining hydrophobic (with high water barrier capacity) and hydrophilic (with high gas barrier capacity) materials in multilayer films (Fabra et al., 2016).

In this study, the capacity of polar and less polar polymers to encapsulate CA by ES has been analysed in order to use these kinds of electrospun layers as active coatings for packaging films. Of the available biopolymers, starch has the advantage of being widely available, low-cost and highly compatible in food applications, as well as being water soluble, with the subsequent advantages of using water as solvent. Nevertheless, its aqueous solutions exhibit high surface tension, which can negatively affect their electrospinning behaviour (Bhardwaj and Kundu, 2010). In this sense, blends of starch and proteins, such as sodium caseinate (NaCas), could offer more appropriate properties. On the other hand, the more hydrophobic poly- ϵ -caprolactone (PCL) exhibits very good electrospinning behaviour in glacial acetic acid (GAA) (Ferreira et al., 2014; Gholipour-Kanani and Bahrami, 2011) and could be highly effective as an encapsulating agent by using electrospinning (Martínez-Abad et al., 2013).

The aim of this work is to analyse the CA encapsulation efficiency in two different polymer systems: polar (starch-sodium caseinate blends) and non-polar (PCL) dissolved in water and glacial acetic acid, respectively, as a function of the polymer concentration and the CA:polymer ratio. In this sense, the physical properties of the initial solutions/dispersions of components (polymer and active compound) relevant to the ES process were determined. Likewise, the microstructure of the electrospun material and the encapsulating efficacy of CA was analysed in each case and modelled as a function of the compositional variables of the initial dispersions or solutions.

2. Materials and methods

2.1. Raw materials and reagents

Corn starch (CS) (with 21 % amylose content) was purchased from Roquette (Roquette Laisa España, Benifaió (Valencia), Spain). NaCas, PCL and CA were supplied by Sigma (Sigma-Aldrich Chemie, Steinheim, Germany). Glacial acetic acid (GAA) and UV-grade absolute ethanol were obtained from Panreac (Panreac Química S.L.U., Castellar del Vallès (Barcelona), Spain). Purified water (with a resistivity of 18.2 M Ω cm) was obtained with a MilliQ Advantage A10 equipment from Millipore S.A.S., Molsheim, France.

2.2. Preparation of formulations

2.2.1. Polar systems

Starch dispersions (2, 4 and 6 % w/w) were prepared by mixing 2, 4 and 6 g respectively of CS with milli-Q water up to 100 g total weight. The dispersions were kept at 95 °C for 30 minutes, with stirring, to allow the gelatinization of the polysaccharide. NaCas (2, 4 and 6 %, w/w) was dissolved in milli-Q water using a magnetic stirrer (Model RCT Basic, IKA, Germany). Emulsions were then prepared by blending the respective starch and NaCas solution of the same concentration (in a ratio of 9:1) with CA, using different ratios of this compound: 0, 5, 10 and 15 % w/w with respect to the total polymer content. Mixtures were thoroughly emulsified for 4 minutes using an Ultra Turrax rotor–stator homogenizer (Model T25D, IKA Germany) at 12,000 rpm. Thus, 12 different aqueous formulations were obtained.

2.2.2. Non-polar systems

PCL pellets were dissolved, under constant stirring for 24 hours, in GAA at 5, 10 and 15 % w/w and CA was added at 0, 5, 10 and 15 % w/w with respect to the polymer, thus obtaining 12 different non-polar formulations.

All formulations were prepared immediately prior to their analysis. Samples were coded as **P_iC_j** or **N_iC_j**, where: **P** and **N** indicate a polar or non-polar system (polymer-solvent mixture), **subscript i** reflects the % of polymer in the solvent (2, 4 or 6 for CS-NaCas blend and 5, 10 or 15 for PCL) and **subscript j** stands for the % of CA with respect to the polymer content (0, 5, 10 or 15). The concentration range of each polymer was established taking into account its solubility in the respective solvent and the limiting viscosity for the liquid flow in the equipment.

2.3. Characterization of the initial solution/dispersion properties

Rheological behaviour was analyzed in duplicate at 25°C, using a rotational rheometer (HAAKE Rheostress 1, Thermo Electric Corporation, Karlsruhe, Germany) with a sensor system of coaxial cylinders, type Z34DIN Ti. Measurements were taken between 0-200 s⁻¹. The obtained data was fitted to the Ostwald de Waale power law model (eq. 1) in order to determine the consistency (K) and the flow behaviour indices (n).

$$\sigma = K \cdot \left(\frac{\partial u}{\partial y}\right)^n \quad (\text{eq.1})$$

where σ is the shear stress (Pa), **K** is the flow consistency index (Pa · sⁿ), $\frac{\partial u}{\partial y}$ represents the shear rate (s⁻¹), **n** is the flow behaviour index (dimensionless) (n=1 Newtonian fluid, n<1 shear-thinning fluid, n>1 shear thickening fluid).

Particle size distribution of the starch-based emulsions was carried out in triplicate using a laser diffractometer (MasterSizer, 2000; Malvern Instruments, Worcestershire, UK). The emulsions were dispersed in distilled water, at 2,000 rpm until an obscuration rate was obtained in the range 5-8%. The volume-length mean diameter (d_{4,3}) was determined. **ζ-potential** was also measured for the CA-water emulsions in triplicate using ZetaSizer nano series equipment (Malvern Instruments, Worcestershire, UK) with a DTS1070 cuvette. The Smoluchowski model (eq. 2) was selected to analyse the recorded data.

$$v_E = 4 \cdot \pi \cdot \varepsilon_0 \cdot \varepsilon_r \cdot \frac{\zeta}{6 \cdot \pi \cdot \mu} (1 + \kappa \cdot r) \quad (\text{eq.2})$$

where ε_0 is the relative dielectric constant of a vacuum, ε_r is the electrical permittivity of a vacuum, ζ is the ζ -potential, μ is the solution viscosity, r represents the particle radius and

κ is the Debye-Hückel parameter calculated as $\kappa = \sqrt{\frac{2 \cdot n_0 \cdot z^2 \cdot e^2}{\varepsilon_r \cdot \varepsilon_0 \cdot k_B \cdot T}}$ (in which n_0 -the bulk

ionic concentration, z -the valence of the ion, e -the charge of an electron, k_B -the Boltzmann constant and T -the absolute temperature) (Sze et al., 2003).

Electrical conductivity was measured for aqueous and GAA systems using a Mettler Toledo device, model SevenEasy Conductivity (Mettler Toledo, Schwerzenbach, Switzerland). **Surface tension** of liquid systems was analysed by means of the pendant drop method, using the OCA 20 instrument (Dataphysics, Germany), with SCA 20 Software package. Ten measurements were taken per formula.

2.4. Electrospinning process

The electrospinning of the liquid systems was carried out under ambient conditions (25°C and 45 % RH) by using a Fluidnatek apparatus, acquired from Biolnacia S.L. (Valencia, Spain). The equipment presents a simple setup (Figure 1) that consists of a sample feeder (a 5 mL plastic Luer Lok syringe by BD Plastik), connected through a PTFE tube to a stainless-steel spinneret needle with an internal diameter of 0.6 mm, a stainless-steel collector and a high voltage power supply (0-30KV). The flow rate of the liquid through the needle and the applied voltage were empirically fitted for each liquid to obtain a stable Taylor cone, on the basis of previously reported data (Gholipour-Kanani and Bahrami, 2011; Kong and Ziegler, 2012). Thus, the digitally controlled syringe fed the emulsions at a steady flow-rate that varied from 0.15 to 0,2 mL/h for polar systems and from 0.4 to 1.2 for non-polar, while the needle was positioned horizontally 15 cm away from the collector. A voltage value between 12 and 22 kV was applied for polar systems, whereas it ranged between 9.5 and 14.5 in non-polar systems.

2.5. Characterization of electrospun products

2.5.1. Nanostructure of electrospun material

Micrographs of the electrospun samples were obtained by means of Field Emission Scanning Electron Microscopy (FESEM Ultra 55, Zeiss, Oxford Instruments, UK). In order to microscopically analyse the obtained electrospun structures, the product was deposited over a support surface and stored in desiccators with phosphorus pentoxide (P_2O_5) at 25°C prior to observation. Samples were mounted on support stubs and, after platinum coating, were observed using an accelerating voltage of 2 kV. Image analysis, by using the ImageJ software (National Institutes of Health, USA), was carried out to measure the size of particles and fibres in the obtained electrospun structures.

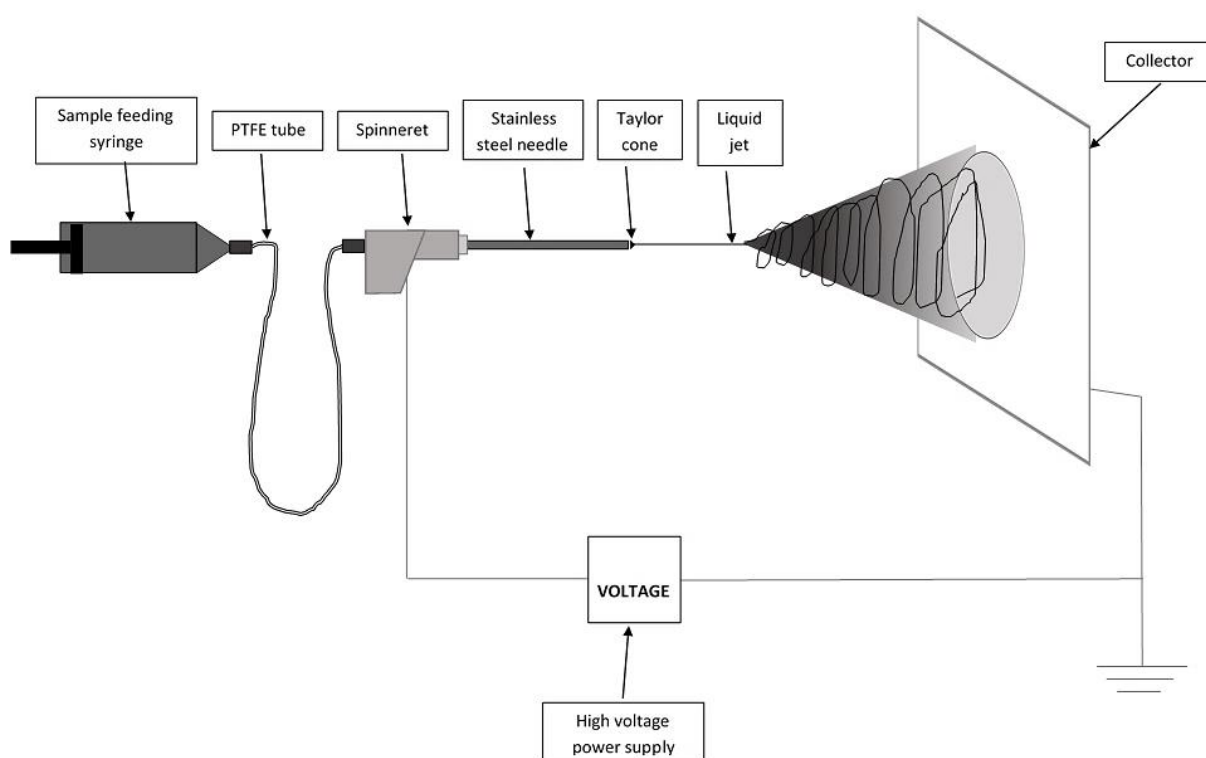


Figure 1. Schematic diagram of the electrospinning setup used during the experiment.

2.5.2. Encapsulating efficiency of CA

Degreased aluminium foils were used as support of the electrospun material from each formulation. Each foil was weighed before and after electrospinning the material for a determined time. Then, the coated foils were introduced into amber vials containing 15 mL of absolute ethanol, hermetically sealed and submitted to magnetic stirring for 24 h at room temperature to promote CA extraction. The extract was analysed as to its CA content by

using a UV/Vis spectrophotometer (Evolution 201 UV-Vis, Thermo Fisher Scientific Inc.) at 275 nm. As blank, an extract of the respective polymer matrix without the CA (samples P_iC₀ and N_iC₀, respectively) was used in each case. The results were expressed in µg carvacrol/mL using the corresponding calibration curve for CA concentrations between 5-80 µg/mL (concentration= 68.277 · Absorbance, r²=0.999). The encapsulating efficiency (in percentage) was determined through the quotient between the total extracted CA in the electrospun material and the theoretical CA content of the electrospun mass of each solution/dispersion liquid.

2.6. Statistical analysis

Statgraphics centurion XVI.I (StatPoint Technologies Inc., Warrenton, VA, USA) was used for data statistical analysis of variance (ANOVA) and the stepwise regression analysis for the EE and process variables.

3. Results and discussion

3.1. Properties of the carvacrol liquid formulations

The physical properties of the liquid systems provide useful information for the purposes of understanding their electrospinning behaviour. The morphology of the electrospun material is greatly affected by the viscosity of the solution (related to the concentration and the molecular weight of the polymer), surface tension, electrical conductivity and surface charge density of the solution, as well as by the processing parameters, such as voltage, flow rate and collectors (Li and Wang, 2013). A suitable viscosity is required for electrospinning and it can be tuned by adjusting the polymer concentration of the solution. Both the polymer concentration and the subsequent viscosity of the liquid influence the stability of the Taylor cone and an optimal value of these parameters allows for the greater stability of the cone and jet during the process (Shastri et al., 2009). For solutions of low viscosity, the surface tension is the controlling factor, which determines whether beads or beaded fibres are formed. By reducing the surface tension, for a determined concentration of the solution, beaded fibres can be converted into smooth fibres. Likewise, an increase in the solution conductivity favours the formation of thinner fibres. However, for natural polymers, which are generally polyelectrolytes, the ions increase the charge carrying ability of the polymer jet under the electric field, leading to poor fibre formation. Good ES results can be obtained

when the liquid phase has low surface tension, which permits the use of a low voltage, thus obtaining thinner fibres (Garg and Bowlin, 2011) and increasing the surface-to-volume ratio of the formed structures.

The physical properties of the studied systems used to encapsulate CA by ES are very different, as shown in Tables 1, 2 and 3. Aqueous systems are CA emulsions, whereas non-polar blends are true dissolutions of PCL and CA in GAA. This aspect confers important differences in terms of their ability for electrospinning behaviour.

For CA aqueous emulsions, the droplet size distributions are plotted in Figure 2 for the different formulations and their volume-length mean diameters $d_{4,3}$ are shown in Table 2. All of the emulsions presented a quasi-monomodal particle distribution, showing small shoulders in some cases. In the case of samples without CA, it is remarkable that particles were also detected in the same size range (20 - 50 μm) as that of CA emulsions and only small changes occurred when CA was incorporated at the different ratios. This indicates that starch and NaCas were not isolated, unfolded chains in water, but formed clusters measurable in size, while CA droplets seem to exhibit sizes in the same range. Samples with 2 and 6 % polymer without CA exhibit a small fraction of bigger particles (aggregates) that disappeared when CA was incorporated, which implied a reduction in the mean diameter value ($d_{4,3}$), regardless of the CA content. However, this effect was not observed for 4 % polymer where the size distribution curves were broader but slightly shifted to smaller sizes. All aqueous systems contained negatively charged particles, as revealed by the ζ -potential values. This is attributable to the surface action of negatively charged caseinate at the pH of the systems (average value 6.96), above its isoelectric point (ranging between 4.1 and 5.8, (Sigma Aldrich CAS 9005-46-3 information sheet)).

The ζ -potential values tend to increase when the CA ratio rises, which suggests that CA droplets competitively adsorb protein, reaching a greater surface charge, which will help to stabilize the emulsions through the promotion of the electrostatic repulsion and the steric effect. Such behaviour could be relevant to an enhancement of the encapsulating efficiency during electrospinning, since emulsion destabilization in the ES-formed jet could lead to CA evaporation by means of the steam drag effect.

CA emulsions were also stabilized by the viscous effect, as revealed by the rheological parameters (Table 1). All of the polar formulations exhibited shear thinning ($n < 1$) behaviour, while all of the samples containing 6 % polymer, or 4 % polymer and 5 or 10 % CA, exhibited

time-dependent shear thinning (hysteresis loop within the up and down curves). This indicates that weak gel structures are formed when the polymer reaches 6 %, or total CA content exceeds 0.30 % in the emulsion. This weak gel breaks down through the disaggregation of chains and droplets occurring under shear rate conditions. This flocculation could negatively affect the behaviour of the ES, since the capacity of macromolecules to unfold during the jet formation, favouring adequate solvent evaporation, would be limited. As expected, K values increased when the polymer concentration rose, whereas the incorporation of CA has a different effect, depending on the polymer concentration. 5 % CA hardly affected the rheological behaviour of 2 % polymer dispersions, whereas it promoted consistency when the polymer was at 4 or 6 %. Nevertheless, in general, the addition of CA enhanced the shear thinning behaviour and consistency index of the liquid systems in line with its ratio increase, this being especially remarkable for emulsions with 4 % polymer. This suggests that CA-Polymer interactions were promoted to a different extent, depending on the total content of both components in the blend.

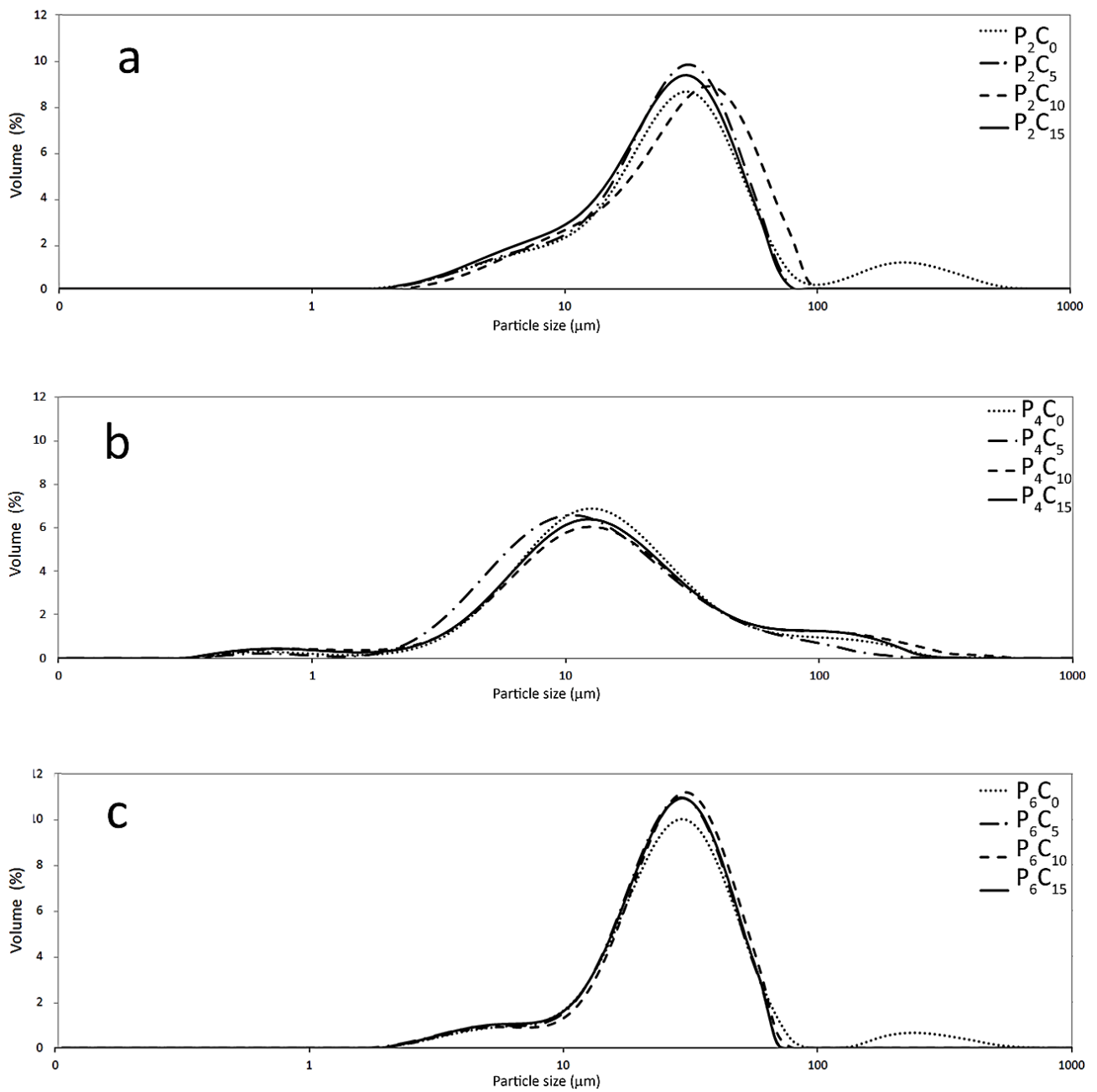


Figure 2. Particle size distribution in terms of volume for the polar systems with different polymer concentrations (a: 2 %, b: 4 %, c: 6 %) and carvacrol ratios.

Table 1: Rheological parameters for both polar and non-polar series: flow behaviour index (n), consistency index (K [Pa·sⁿ]) and viscosity (μ [Pa·s]). Average values and standard deviations.

		Polymer concentration (%)							
		Polar system				Non-polar system			
			2	4	6		5	10	15
CA concentration (g/100g polymer)	0	n	0.93±0.05 ^e	0.85±0.07 ^{de}	0.48±0.03 ^b	μ [Pa·s]	0.0389±0.0007 ^a	0.499±0.002 ^c	1.464±0.002 ^e
		K	0.0064±0.0009 ^a	0.034±0.013 ^a	1.3±0.2 ^{bc}		0.0393±0.0013 ^a	0.480±0.014 ^b	1.483±0.002 ^f
	5	n	0.86±0.08 ^{de}	0.65±0.02 ^c	0.40±0.02 ^{ab}		0.0424±0.0006 ^a	0.5003±0.0008 ^c	1.4983±0.0007 ^g
		K	0.008±0.003 ^a	0.15±0.02 ^a	2.3±0.9 ^d		0.0398±0.0006 ^a	0.499±0.003 ^c	1.434±0.003 ^d
	10	n	0.85±0.04 ^{de}	0.466±0.014 ^b	0.409±0.011 ^{ab}				
		k	0.008±0.002 ^a	0.58±0.14 ^{ab}	1.9±0.2 ^{cd}				
	15	n	0.81±0.05 ^d	0.429±0.003 ^{ab}	0.37±0.02 ^a				
		K	0.013±0.003 ^a	0.72±0.04 ^{ab}	3.4±0.8 ^e				

Different superscripts (a, b, c...) in each series indicate significant differences according to ANOVA test (p<0.05) for the respective parameter.

Table 2: Emulsion properties for polar series: particle volume-length mean diameter ($d_{4,3}$), $d_{4,3}-d_{3,2}$ difference and ζ -potential of the particles. Average values and standard deviations.

		Polymer concentration (%)							
		2		4		6			
Carvacrol concentration (g/100g polymer)	0	$d_{4,3}$	50±14 ^d	27±4 ^{ab}	43.5±1.4 ^d	ζ -potential (mV)	-8.5±0.4 ^f	-14±2 ^{cd}	-18±1 ^a
		$d_{4,3}-d_{3,2}$	30±13 ^e	19±4 ^{bc}	22±1 ^{cd}		-11±1 ^{ef}	-13±1 ^{de}	-14±2 ^{de}
	5	$d_{4,3}$	29.46±0.08 ^{bc}	20±1 ^a	32±4 ^{bc}		-12.6±0.4 ^{de}	-16±1 ^{abcd}	-14±3 ^{de}
		$d_{4,3}-d_{3,2}$	11.01±0.11 ^a	12±2 ^{ab}	12±3 ^{ab}		-15±1 ^{bcd}	-18±4 ^{ab}	-17±1 ^{abc}
10	$d_{4,3}$	26±2 ^{ab}	35±4 ^c	30.9±0.2 ^{bc}					
	$d_{4,3}-d_{3,2}$	10.18±0.46 ^a	27±4 ^{de}	9.95±0.03 ^a					
15	$d_{4,3}$	28.26±0.02 ^{bc}	28±2 ^{bc}	29.7±0.2 ^{bc}					
	$d_{4,3}-d_{3,2}$	10.75±0.03 ^{bc}	21±3 ^{cd}	9.89±0.13 ^a					

Different superscripts (a, b, c...) indicate, for the respective parameter, significant differences according to ANOVA test ($p < 0.05$).

Table 3: Physical properties for both polar and non-polar series: surface tension (γ) and conductivity (κ). Average values and standard deviations.

		Polymer concentration (%)						
		Polar system			Non-polar system			
		2	4	6	5	10	15	
Carvacrol concentration (g /100g polymer)	γ (mN/m)	0	54±1 ^d	51±1 ^c	48±1 ^d	25.5±0.4 ^a	26.1±0.4 ^{bc}	26.5±0.2 ^{de}
		5	39±1 ^a	39.7±0.4 ^a	40±1 ^c	25.3±0.3 ^a	26.2±0.4 ^{bcd}	26.3±0.2 ^{cd}
		10	42.2±0.3 ^c	41±1 ^b	31±1 ^b	25.4±0.4 ^a	26.4±0.4 ^{cd}	26.7±0.2 ^e
		15	40.5±0.1 ^b	40.2±0.2 ^b	30±1 ^a	26.0±0.2 ^b	26.3±0.2 ^{cd}	26.9±0.2 ^f
	κ [μ S/cm]	0	133±2 ^c	387±7 ⁱ	321.1±0.3 ^f	0.143±0.006 ^{bc}	0.243±0.006 ^f	0.123±0.006 ^a
		5	124±1 ^b	393±2 ⁱ	291±3 ^e	0.157±0.006 ^{cd}	0.32±0.03 ^g	0.117±0.006 ^a
		10	117±2 ^a	371±2 ^h	288±3 ^e	0.143±0.006 ^{bc}	0.16±0.02 ^d	0.12±0 ^a
		15	112.3±0.4 ^a	345±9 ^g	277±2 ^d	0.203±0.006 ^e	0.123±0.006 ^a	0.127±0.006 ^{ab}

Different superscripts (a, b, c...) within each series indicate, for the respective parameter, significant differences according to ANOVA test ($p < 0.05$).

For the non-polar systems, polymer-CA solutions exhibited Newtonian behaviour in every case and the obtained viscosity values are shown in Table 1. The viscosity of these solutions was basically determined by the PCL concentration and no relevant changes were induced by adding CA in the studied concentration range. These viscosity values ranged between 0.39-1.49 Pa·s. Taking into account the very low shear rate acting in the needle (range: 0.6-1.8 s⁻¹), estimated through the flow rates and the needle internal diameter, the apparent viscosity at 1 s⁻¹ (equal to the K value) could be used to compare the flow resistance of both kinds of fluids. These values ranged between 0.006 and 3.35, which cover a wider range of consistency than that obtained in non-polar systems. The consistency index of polar dispersions with 6 % polymer and CA exceeded the upper viscosity limit of the non-polar solutions.

Every polar formulation showed surface tension values (Table 3) which were significantly lower than those of the solvent (72 mN/m). Likewise, an increase in polymer concentration provoked a decrease in the surface tension in line with the surfactant effect of protein at the interface. The incorporation of the smallest amount of CA led to a significant surfactant effect, which could be explained by its interaction with protein, affecting its surface adsorption capacity; however, the increase in the CA content did not produce any additional effects, except for the higher protein content where a greater reduction in surface tension was observed when the CA ratio rose. Thus, this parameter ranged from 54 to 30 mN·m⁻¹ in the different polar systems. On the contrary, the surface tension values were very homogenous (25-27 mN/m) in the non-polar systems, these being in the range of the values of pure GAA (27.10 mN/m at 25 °C, Haynes, 2013-2014). So, no relevant surfactant action of PCL or CA can be deduced from the obtained surface tension values, according to their good solubility in the GGA.

The conductivity values of the different systems are shown in Table 3 where, as expected, the much higher values of the aqueous systems can be observed. In polar dispersions, the conductivity values increased when the polymer content rose which must be attributable to the greater ionic strength associated with the caseinate content; at the highest concentration, however, a reduction was observed associated with the fact that ion mobility was more limited as a consequence of the effects of aggregation and the higher viscosity. The addition of CA implied a slight decrease in the conductivity values for a determined polymer concentration, which could be attributed to different effects, such as a viscosity increase, changes in the mobility of the charged species or the attenuation of the electric

field in the presence of a greater fraction of non-polar dispersed phase. Most of the lipid components are not conductive and interfere with the salts, thereby reducing their conducting power (Mucchetti et al., 1994). The conductivity values of non-polar solutions were affected by the polymer concentration and, to a much lesser extent, by the CA content. The conductivity increased (twice) when PCL reached 10 % in GAA, but decreased at 15 %, nearly to the value obtained for 5 %, probably due to the viscous effects. The addition of CA enhanced solution conductivity for the smallest ratio (5 %), but reduced it for the highest. All of the values were about ten times higher than that of pure GAA (0.0112 $\mu\text{S}/\text{cm}$ at 25 °C) (Dean and Lange, 1999). Trace amounts of water from the polymer could be responsible for these differences, since small amounts of water greatly modify the electrical conductivity of GAA (Analytical, 2010).

3.2. Characterization of the electrospun product

The morphology of the material electrospun from polar and non-polar systems is shown in Figures 3 and 4, respectively. Great microstructural differences can be observed for starch and PCL based matrices. PCL matrices showed a bead-and-tail morphology, depending on the polymer concentration, whereas a more undefined bead structure was obtained for a large proportion of the starch formulations, as previously reported by Li et al., (2016) for electrospun native starch material. Excepting the dispersions with 4 % polymer and 10 or 15 % CA, quite unstructured material was obtained for the rest of the aqueous systems, exhibiting the typical appearance of a wet deposition due to the non-efficient water evaporation in the jet formed. These products adhered weakly to the collector and detached from its surface as a non-sticky powder. The poor electrospinning behaviour of emulsions with 2 or 6 % polymer might mainly be due to the very low viscosity of the first and to the flocculation that occurs to a great extent in the second. This implied the formation of an unstable Taylor cone and a non-homogeneous jet. An intermediate concentration of polymer (4 %) better fits the viscosity requirements for electrospinning and also exhibits higher conductivity values. The greatest ratios of CA (10 and 15 %) also promote flow viscosity and seem to favour the beaded fibre formation. With the increase in polymer content, more fibrous structures were expected. However, for the series with 6 % polymer, the rheological behaviour indicated weak gel formation, which makes jet stabilization and stretching difficult, leading to the formation of irregular round-shaped particles on the collector. Likewise, even in samples with good electrospinning behaviour and 4 % polymer, the macromolecules did

not wrap and form fibres but beads. Kong and Ziegler (2014) attributed the appearance of discrete structures in electrospun starch to the inability of the amylose helices to unfold fully during the process. Only when a complete helix-to-coil transition occurs, do the required entanglements occur and the polymer can be electrospun into continuous fibres. On the other hand, the branched amylopectin does not exhibit properties suitable for unfolding and entangling, as reported by the same authors for amylopectin-rich native starches. Blends with NaCas and CA did not notably improve the electrospinning behaviour of starch in the conditions that could be applied. The flow rate was between 0.1 and 0.2 mL/h and the voltage ranged from 12 to 22 kV, depending on the polymer and CA concentrations. The highest flow rate was required to process dispersions with 4% polymer, whereas the greatest voltage was applied for those containing 2 % polymer. In contrast, a higher flow rate could be applied in non-polar systems (0.4 to 1.2 mL/h) with a lower voltage (9.5 to 14.5 kV); the higher the PCL and CA concentrations, the greater the flow rate and the lower the voltage. No evidence of CA droplets was observed in starch-based electrospun material, which indicates that the compound was intimately absorbed in the polymer structure. Carvacrol could be entrapped in the central cavity of the single-helical V-amylose molecules, similarly to the structure formed by cyclodextrins when used to encapsulate lipophilic substances (Itthisoponkul et al., 2007).

Figure 4 shows the morphology of the material electrospun from the GAA-PCL systems, when a much more defined microstructure could be observed. In general, microstructure shows a mesh of fibres with entrapped bead formations, although fewer fibres were obtained at the lowest PCL concentration, in line with the lowest viscosity. The increase in the CA ratio for a determined polymer concentration also reduced the fibre formation, promoting the beads, which could be related with the interactions of CA with the polymer chains that make the chain unfolding more difficult. At very high magnification, it was noted that the beads are an entanglement of nanofibres. With the increase in polymer content, the beads exhibited more elongated shapes, probably due to the stretching of the more viscous jet by the electric forces, and more fibres were formed. A higher polymer concentration also gave rise to thicker fibres, as reported by Kanani and Bahrami (2011) for PCL dissolved in GAA at similar concentration levels, which was attributed to the promotion of the polymer chain entanglements when the concentration rose in the solution. On the basis of the obtained microstructure, the ability of PCL solutions with CA to be electrospun was much better than that of starch-based aqueous systems, despite the low electrical conductivity values.

Nevertheless, the viscosity and surface tension values were adequate for this purpose and the linearity of the chain greatly favours the development of electrospinning. In fact, the element size analysis of the electrospun material revealed a more nanostructured arrangement for PCL samples. In the polar systems, for cases with fibre formation, diameters of the obtained structures ranged between 40 nm (for the fibres) and 3.4 μm (for spherical morphologies), while in the non-polar systems, fibres exhibited diameters ranging between 15.0 nm and 1.4 μm and beads with diameters spanning from 0.25 μm up to 25 μm (maximum diameter in the case of the elongated structures).

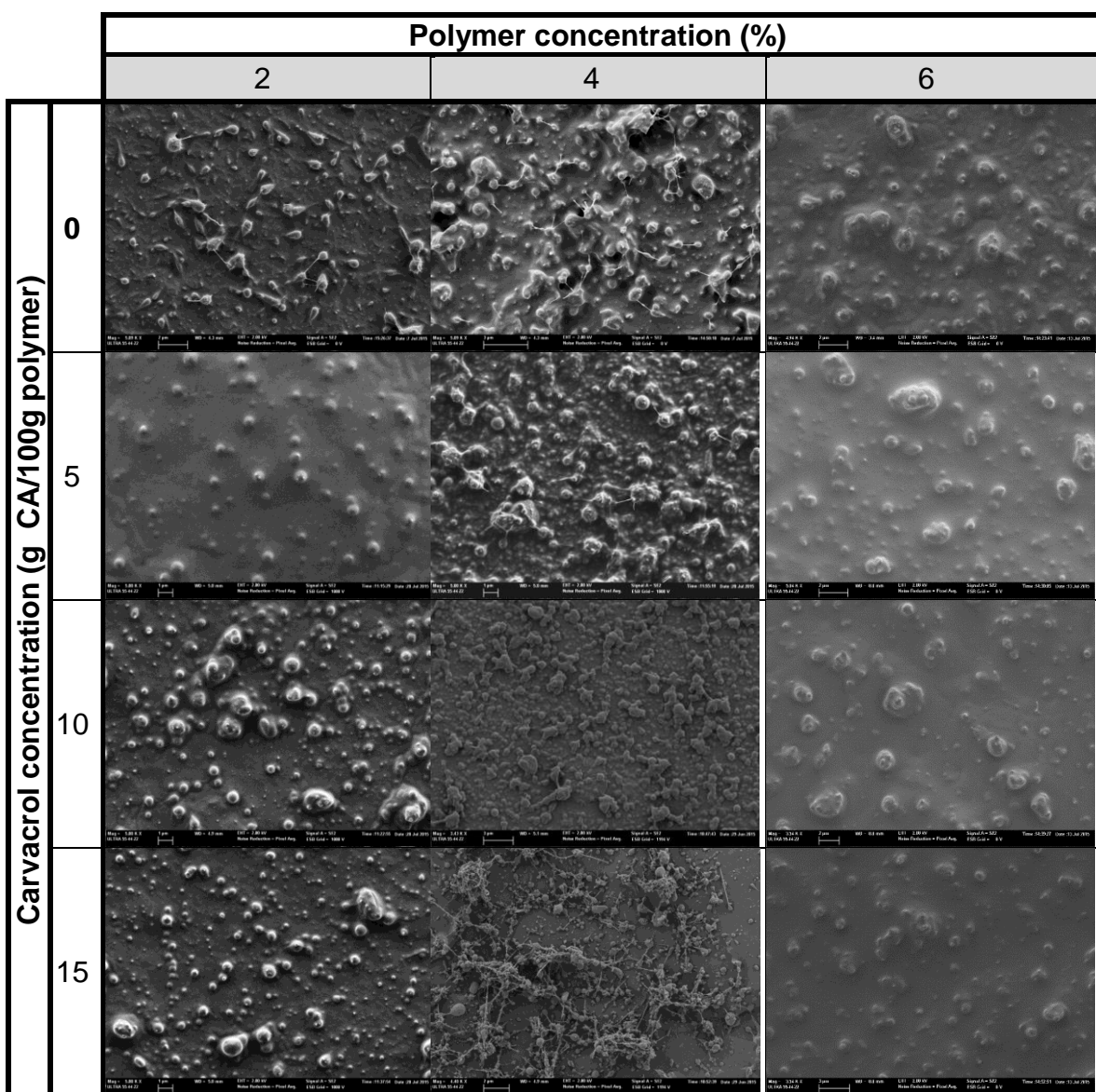


Figure 3. FESEM micrographs of nanostructure obtained for the electrospun material from polar matrices. Magnification factor between 2500x and 5100x.

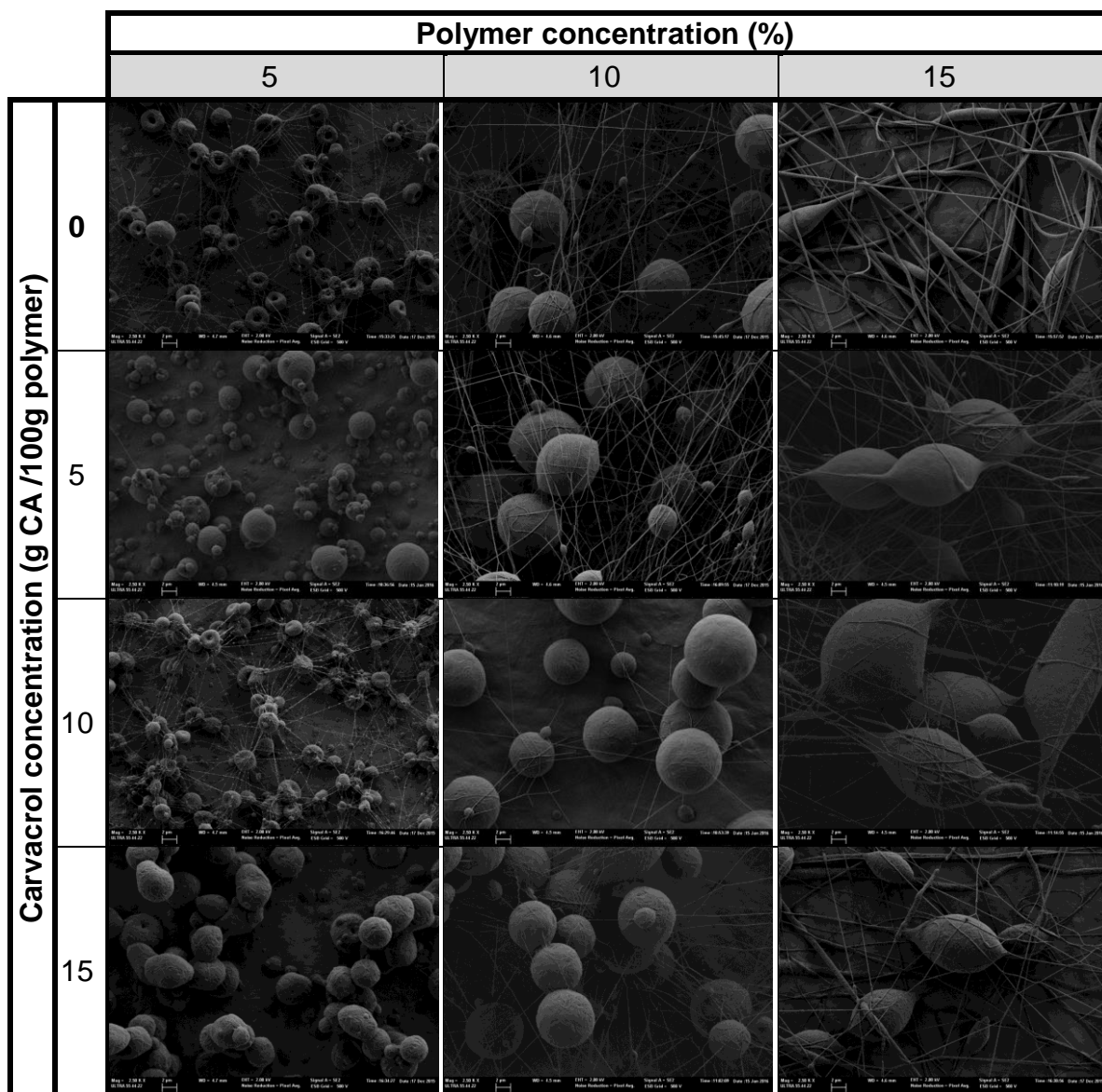


Figure 4. FESEM micrographs of nanostructure obtained for the electrospun material from non-polar matrices. Magnification factor of 2500x.

3.3. CA encapsulation efficiency

The potential of both polar and non-polar polymer matrices to encapsulate CA when electrospun is shown in Figure 5. The percentage of CA retained in the matrix, in relation to that originally present in the electrospun dispersion, was plotted as a function of the polymer concentration in the dispersion/solution for the different ratios of CA. It was noted that for the starch-based system, the percentage of retention is relatively low and is heavily dependent on the polymer concentration, while exhibiting a high degree of variation, as compared to the values in the PCL-GAA system, where higher polymer concentrations could be used on the basis of the greater PCL solubility in GAA.

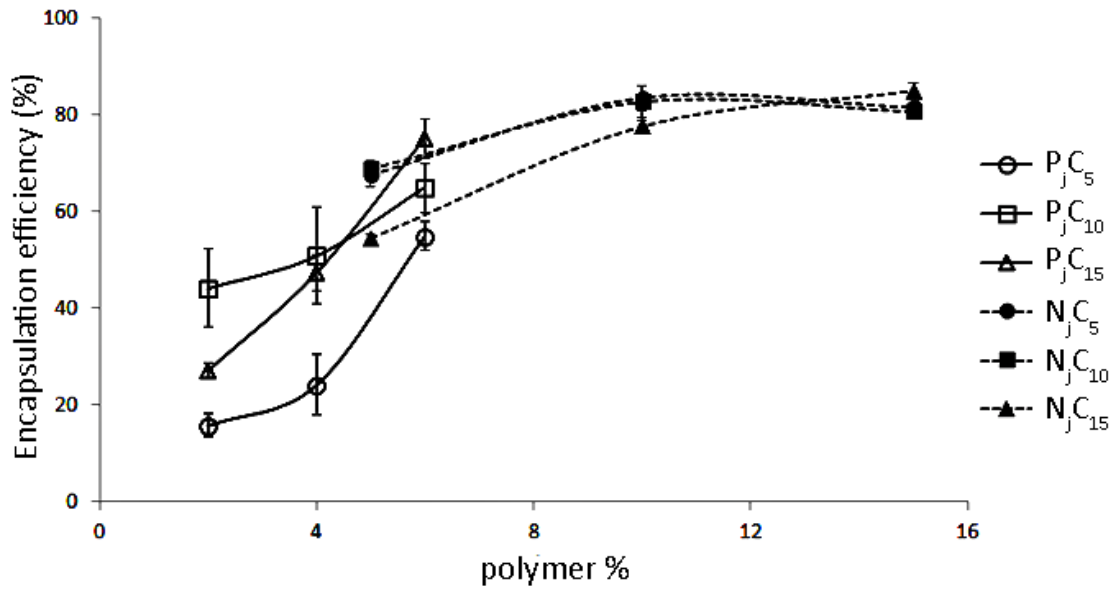


Figure 5. Encapsulation efficiency of carvacrol as a function of the polymer concentration in the liquid system, for polar and non-polar polymers with different carvacrol ratios. Mean values and standard deviations.

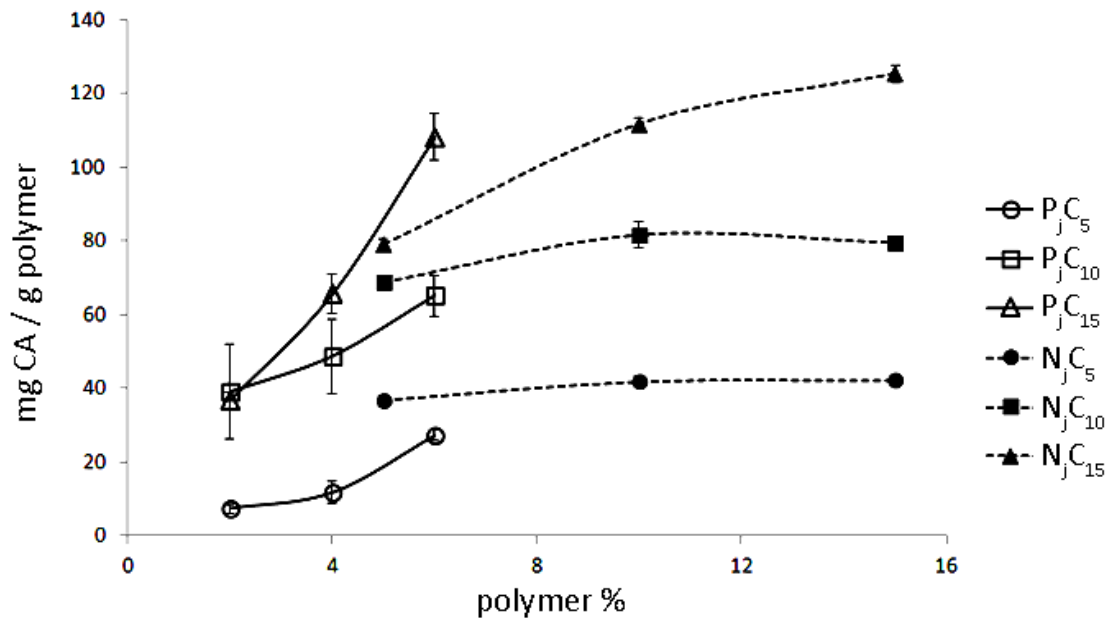


Figure 6. Carvacrol load of the polymer, expressed as mg CA/ g of polymer, as a function of the polymer concentration, for polar and non-polar polymers with different carvacrol ratios. Mean values and standard deviations.

The variation in the values could be explained by the steam drag effect of CA with water evaporation due to the immiscibility of CA in water, which provokes the evaporation of CA-

water mixtures at a temperature lower than that of pure water (steam distillation). Polymer adsorption on the surface of CA droplets could limit this effect during the jet stretching, but destabilization phenomena of the emulsion during the process will enhance the CA steam drag. Likewise, the limited compatibility of CA with the more polar matrix (starch-NaCas) could contribute to the less effective CA retention. Using this aqueous system, the retention capacity varied from 15-75%, depending on the polymer content and CA ratio. The increase in the polymer concentration improved the encapsulation capacity of the matrix, which could be explained by the promotion of viscosity, which enhances the viscous stabilization of the emulsified CA, thus limiting the steam drag effect. The greatest CA retention occurred with the highest polymer concentration and CA ratio. It should be mentioned that the CA retained in the matrix could be both included inside the electrospun droplets and fibres and on the surface of these structures. Nevertheless, it was assumed that the carvacrol extracted from the fibres was effectively encapsulated since, given the volatile nature of the compound, the amount retained at surface level would evaporate quickly and it would be not present when the ethanol extraction was carried out to quantify the encapsulated ratio in the fibres.

A stepwise regression analyses was carried out in order to evaluate the influence of independent variables, both physical properties and compositional variables (polymer concentration and carvacrol polymer ratio in the initial solution) on the encapsulation efficiency of carvacrol (dependent variable). Given the different range of the independent variables for polar and non-polar systems, the analyses were carried separately for each kind of system. A second grade polynomial model was considered in each case, thus taking lineal and square terms, to identify potential interactions between independent variables. The stepwise regression procedure allows for eliminating the polynomial terms without statistical significance in the model, thus giving a more simple equation with the minimum prediction error, where only variables with statistical significance appeared in the equation.

For polar system, eq. 3 was obtained for the EE as a function of the physical properties of liquid dispersions (surface tension, consistency index and conductivity). This regression revealed that the three considered properties affected the EE, but the properties that had the greatest statistical significance (p value) in the model were consistency index and conductivity.

$$\% EE = -1.7K\gamma + 0.5K\kappa + 1.5\kappa - 9\gamma - 14K^2 - 0.004\kappa^2 + 0.16\gamma^2 \quad (R^2= 98.31) \quad (\text{eq.3})$$

When using the non-polar system, a greater EE was obtained, up to 50-86%, which increased when the polymer concentration rose, as observed in the case of the polar systems. The best CA retention (>80%) was reached when 15% PCL and 15 % CA were used, with very small differences when the other CA ratio was employed. When non-polar systems contained 5 and 10 % CA with respect to the polymer, no differences in the CA retention behaviour were observed, showing a limited effect of the polymer concentration on the EE. However, with 15 % CA, the percentage of retention was more sensitive to the polymer concentration, probably due to the fact that the capacity of the polymer matrix to entrap the greatest amount of the compound was limited.

In contrast to the polar system, the stepwise regression analysis revealed that the surface tension (γ) and the products of viscosity (μ) and conductivity (κ) or surface tension are the properties with the greatest statistical significance in the obtained model for the non-polar systems (eq. 4).

$$\%EE = 565\mu\kappa - 2.5\mu\gamma - 44\kappa\gamma + 885\kappa + 0.161\gamma^2 (R^2=99.86) \quad (\text{eq.4})$$

Predictive equations of EE as a function of the polymer concentration and CA ratio in the liquid system for polar and non-polar systems were also obtained (eqs. 5 and 6, respectively). These equations fit the experimental points shown in Figure 5 for polar and non-polar systems, with a standard error of the estimate of 7 and 5 %, respectively, allowing for obtaining good predicted values of the EE. From the predicted EE value, the load of CA in the electrospun polymer (g CA/g polymer) can be estimated by multiplying it by the nominal ratio in the initial solution.

$$\% EE = 3(\%polymer)^2 - 0.4(\%CA)^2 - 15(\%polymer) + 10(\%CA) (R^2 = 98.07) \quad (\text{eq. 5})$$

$$\%EE= 11(\%polymer) + 4(\%CA) - 0.47(\%polymer)^2 - 0.24(\%CA)^2 (R^2 = 99.65) \quad (\text{eq. 6})$$

The capacity of the polymer matrix to entrap CA could be better observed in Figure 6, where the amount of CA retained per mass unit of polymer can be observed for the different conditions tested. An upward trend in the CA load in the polymer when the polymer concentration rose in the liquid system can be observed for all CA: polymer ratios. Nevertheless, this was more marked when the CA ratio increased in the liquid system with respect to the polymer. This points to both the greater viscosity requirements for CA encapsulation when its ratio rises with respect to the polymer and to the key role that viscosity plays in the outcome of the electrospinning process when employed to encapsulate these kinds of compounds.

The obtained results allow for selecting the adequate concentrations and ratios of polymer and active to reach the maximum EE. In this sense, using non-polar system, it is recommended that the highest concentrations of PCL and CA be used in the liquid system in order to obtain a good CA load in the matrix, while the process time needed to obtain a determined amount of coating material is shorter, since the process yield increases when a lower amount of solvent is evaporated. Likewise, for a given flow rate and electrospinning time of the optimum solution/dispersion on a defined surface, it is possible to determine the surface density (g/cm^2) of the electrospun material and the surface density of active compound (g/cm^2) by applying the obtained equations for EE. In this way, the available active compound per surface unit of a electrospun film can be predicted in order to evaluate if it exceeds or not the necessary concentration for inhibiting microbial growth. However, other factors must be taken into account. Namely, the required dose of the active compound applied to a determined food system from an electrospun active packaging film will depend on several factors: 1) the amount of carvacrol per mass unit of electrospun fibre, which in turn, is affected by the encapsulation efficiency of the polymer; 2) the flow rate and time of electrospinning process which determine the thickness of the electrospun layer and the mass of fibre per surface unit in the film, 3) the minimally inhibitory concentration (MIC) of the active for a target microorganism, 4) the active release capacity from the fibre into a determined food system, according to the respective affinity or partition coefficient and 5) the interactions of the active within the food matrix which can affect its antimicrobial activity. The obtained results are relevant to predict the active concentration per surface unit of active film for a determined flow rate and time of the electrospinning process. Nevertheless, release studies and *in vitro* and *in vivo* antimicrobial tests are required for a complete assessment of the active film development. Likewise, sensory evaluation of the potential impact of the active on the food system organoleptic properties is required to guarantee food quality.

4. Conclusions

Greater CA encapsulating efficiency (>80 %), with lower variability, was obtained for the PCL-based systems than for the starch-based ones. This may be explained by different factors: the greater solubility of PCL in GAA, allowing for the use of higher polymer concentrations with adequate viscosity, the greater compatibility of CA and PCL and the linearity of the polymer chain, which permits the chain to unfold in the electric field and its

subsequent entanglement to form fibres. This nanostructure presented better cohesiveness and adhesiveness in the electrospun material, which also contribute to the coating performance. The lower variability in the CA retention, associated with the lack of water in the liquid systems, which helps to avoid steam drag effects, also represents an advantage with respect to the aqueous systems. Therefore, in order to obtain tightly adhered electrospun layers with the highest CA load in the matrix, it is recommended that the highest PCL concentration (15 %) and CA ratio (15 %) be used.

5. Acknowledgments

The authors would like to thank the Ministerio de Economía y Competitividad of Spain, for funding this study as part of projects AGL2013-42989-R and AGL2016-76699-R and predoctoral research grant # BES-2014-068100.

6. References

- Ahn, H., Ju, Y. M., Takahashi, H., Williams, D. F., Yoo, J. J., Lee, S. J., Atala, A. (2015). Engineered small diameter vascular grafts by combining cell sheet engineering and electrospinning technology. *Acta Biomaterialia*, 16(1), 14–22. <https://doi.org/10.1016/j.actbio.2015.01.030>
- Analytical, R. (2010). Conductance Data For Commonly Used Chemicals. *Emerson Process Management*, (December), 44-6039/rev. B, 6. <http://www.emerson.com/resource/blob/68896/20a2feae1092b9763fee29d39c49a5a7/manual--conductance-data-for-commonly-used-chemicals-data.pdf>
- Asbahani, A. El, Miladi, K., Badri, W., Sala, M., Addi, E. H. A., Casabianca, H., Elaissari, A. (2015). Essential oils: From extraction to encapsulation. *International Journal of Pharmaceutics*, 483(1–2), 220–243. <https://doi.org/10.1016/j.ijpharm.2014.12.069>
- Bahrami, S. H., & Gholipour Kanani, A. (2011). Effect of changing solvents on poly(ϵ -Caprolactone) nanofibrous webs morphology. *Journal of Nanomaterials*, 2011. <https://doi.org/10.1155/2011/724153>

- Bakkali, F., Averbeck, S., Averbeck, D., & Idaomar, M. (2008). Biological effects of essential oils- A review. *Food and Chemical Toxicology*.
<https://doi.org/10.1016/j.fct.2007.09.106>
- Ben Arfa, A., Combes, S., Preziosi-Belloy, L., Gontard, N., & Chalier, P. (2006). Antimicrobial activity of carvacrol related to its chemical structure. *Letters in Applied Microbiology*, 43(2), 149–154. <https://doi.org/10.1111/j.1472-765X.2006.01938.x>
- Bhardwaj, N., & Kundu, S. C. (2010). Electrospinning: A fascinating fiber fabrication technique. *Biotechnology Advances*, 28(3), 325–347.
<https://doi.org/10.1016/j.biotechadv.2010.01.004>
- Burt, S (2004). Essential oils: their antibacterial properties and potential applications in foods—a review. *International Journal of Food Microbiology* 94 (3) 223– 253
<http://dx.doi.org/10.1016/j.ijfoodmicro.2004.03.022>
- Calo, J. R., Crandall, P. G., O'Bryan, C. A., & Ricke, S. C. (2015). Essential oils as antimicrobials in food systems - A review. *Food Control*, 54, 111–119.
<https://doi.org/10.1016/j.foodcont.2014.12.040>
- Chew, S. C., & Nyam, K. L. (2016). Microencapsulation of kenaf seed oil by co-extrusion technology. *Journal of Food Engineering*, 175, 43–50.
<https://doi.org/10.1016/j.jfoodeng.2015.12.002>
- Dean, J. A., & Lange, N. A. (1999). Lange's Handbook of Chemistry. McGraw-Hill. table 8.34, 8.161-8.162
- De Vincenzi, M., Stammati, A., De Vincenzi, A., & Silano, M. (2004). Constituents of aromatic plants: Carvacrol. *Fitoterapia*, 75(7–8), 801–804.
<https://doi.org/10.1016/j.fitote.2004.05.002>
- EU, (2009). Guidance to the commission regulation (EC) No 450/2009 of 29 May 2009 on active and intelligent materials and articles intended to come into contact with food. Version 10. European Commission Health and Consumers Directorate-General Directorate E-Safety of the Food chain. E6 - Innovation and sustainability.
<http://eur-lex.europa.eu/legal-content/EN/ALL/?uri=CELEX%3A32009R0450>

- Fabra, M. J., López-Rubio, A., & Lagaron, J. M. (2016). Use of the electrohydrodynamic process to develop active/bioactive bilayer films for food packaging applications. *Food Hydrocolloids*, 55, 11–18. <https://doi.org/10.1016/j.foodhyd.2015.10.026>
- Fabra, M. J., López-Rubio, A., & Lagaron, J. M. (2014). On the use of different hydrocolloids as electrospun adhesive interlayers to enhance the barrier properties of polyhydroxyalkanoates of interest in fully renewable food packaging concepts. *Food Hydrocolloids*, 39, 77–84. <https://doi.org/10.1016/j.foodhyd.2013.12.023>
- FAO. (2011). *Global food losses and food waste – Extent, causes and prevention*. Rome
- Ferreira, J. L., Gomes, S., Henriques, C., Borges, J. P., & Silva, J. C. (2014). Electrospinning polycaprolactone dissolved in glacial acetic acid: Fiber production, nonwoven characterization, and *In Vitro* evaluation. *Journal of Applied Polymer Science*, (September 2016). <https://doi.org/10.1002/app.41068>
- Garg, K., & Bowlin, G. L. (2011). Electrospinning jets and nanofibrous structures. *Biomicrofluidics*, 5(1), 1–19. <https://doi.org/10.1063/1.3567097>
- Ghorani, B., & Tucker, N. (2015). Fundamentals of electrospinning as a novel delivery vehicle for bioactive compounds in food nanotechnology. *Food Hydrocolloids*, 51, 227–240. <https://doi.org/10.1016/j.foodhyd.2015.05.024>
- Hamori, M., Yoshimatsu, S., Hukuchi, Y., Shimizu, Y., Fukushima, K., Sugioka, N., Shibata, N. (2014). Preparation and pharmaceutical evaluation of nano-fiber matrix supported drug delivery system using the solvent-based electrospinning method. *International Journal of Pharmaceutics*, 464(1–2), 243–251. <https://doi.org/10.1016/j.ijpharm.2013.12.036>
- Haynes, W.M. (ed.) (2013-2014). *CRC Handbook of Chemistry and Physics*. 94th Edition. CRC Press LLC, Boca Raton: FL, 6-182. <https://toxnet.nlm.nih.gov/cgi-bin/sis/search2/r?dbs+hsdb:@term+@rn+@rel+64-19-7>
- Horvathova, E., Navarova, J., Galova, E., Sevcovicova, A., Chodakova, L., Snahnicanova, Z., Slamenova, D. (2014). Assessment of antioxidative, chelating, and DNA-Protective effects of selected essential oil components (Eugenol, Carvacrol, Thymol, Borneol,

Eucalyptol) of plants and intact rosmarinus officinalis oil. *Journal of Agricultural and Food Chemistry*, 62(28), 6632–6639. <https://doi.org/10.1021/jf501006y>

Itthisoponkul, T., Mitchell, J. R., Taylor, A. J., & Farhat, I. A. (2007). Inclusion complexes of tapioca starch with flavour compounds. *Carbohydrate Polymers*, 69(1), 106–115. <https://doi.org/10.1016/j.carbpol.2006.09.012>

Kim, J. S., & Lee, D. (2000). Thermal properties of electrospun polyesters. *Polymer Journal*. <https://doi.org/10.1295/polymj.32.616>

Kong, L., & Ziegler, G. R. (2014). Fabrication of pure starch fibers by electrospinning. *Food Hydrocolloids*, 36, 20–25. <https://doi.org/10.1016/j.foodhyd.2013.08.021>

Kong, L., & Ziegler, G. R. (2012). Role of molecular entanglements in starch fiber formation by electrospinning. *Biomacromolecules*, 13(8), 2247–2253. <https://doi.org/10.1021/bm300396j>

Li, X., Chen, H., & Yang, B. (2016). Centrifugally spun starch-based fibers from amylopectin rich starches. *Carbohydrate Polymers*, 137, 459–465. <https://doi.org/10.1016/j.carbpol.2015.10.079>

Li, Z., & Wang, C. (2013). One-Dimensional nanostructures, 15–29. <https://doi.org/10.1007/978-3-642-36427-3>

López-Rubio, A., Sanchez, E., Sanz, Y., & Lagaron, J. M. (2009). Encapsulation of living bifidobacteria in ultrathin PVOH electrospun fibers. *Biomacromolecules*, 10(10), 2823–2829. <https://doi.org/10.1021/bm900660b>

Martínez-Abad, A., Sánchez, G., Fuster, V., Lagaron, J. M., & Ocio, M. J. (2013). Antibacterial performance of solvent cast polycaprolactone (PCL) films containing essential oils. *Food Control*, 34(1), 214–220. <https://doi.org/10.1016/j.foodcont.2013.04.025>

Mucchetti, G., Gatti, M., & Neviani, E. (1994). Electrical Conductivity Changes in Milk Caused by Acidification: Determining Factors. *Journal of Dairy Science*, 77(4), 940–944. [https://doi.org/http://dx.doi.org/10.3168/jds.S0022-0302\(94\)77029-6](https://doi.org/http://dx.doi.org/10.3168/jds.S0022-0302(94)77029-6)

- Perdones, Á., Chiralt, A., & Vargas, M. (2016). Properties of film-forming dispersions and films based on chitosan containing basil or thyme essential oil. *Food Hydrocolloids*, 57, 271–279. <https://doi.org/10.1016/j.foodhyd.2016.02.006>
- Rieger, K. A., & Schiffman, J. D. (2014). Electrospinning an essential oil: Cinnamaldehyde enhances the antimicrobial efficacy of chitosan/poly (ethylene oxide) nanofibers. *Carbohydrate Polymers*, 113, 561–568. <https://doi.org/10.1016/j.carbpol.2014.06.075>
- Shastri, V. P., Sy, J. C., & Klemm, A. S. (2009). Emulsion as a means of controlling electrospinning of polymers. *Advanced Materials*, 21(18), 1814–1819. <https://doi.org/10.1002/adma.200701630>
- Sigma Aldrich CAS 9005-46-3 information sheet
http://www.sigmaaldrich.com/content/dam/sigma-aldrich/docs/Sigma/Product_Information_Sheet/c8654pis.pdf
- Sill, T. J., & von Recum, H. A. (2008). Electrospinning: Applications in drug delivery and tissue engineering. *Biomaterials*, 29(13), 1989–2006. <https://doi.org/10.1016/j.biomaterials.2008.01.011>
- Sze, A., Erickson, D., Ren, L., & Li, D. (2003). Zeta-potential measurement using the Smoluchowski equation and the slope of the current – time relationship in electroosmotic flow. *Journal of Colloid and Interface Science*, 261, 402–410. [https://doi.org/10.1016/S0021-9797\(03\)00142-5](https://doi.org/10.1016/S0021-9797(03)00142-5)
- Tunc, S., Chollet, E., Chalier, P., Preziosi-Belloy, L., & Gontard, N. (2007). Combined effect of volatile antimicrobial agents on the growth of *Penicillium notatum*. *International Journal of Food Microbiology*, 113(3), 263–270. <https://doi.org/10.1016/j.ijfoodmicro.2006.07.004>
- Ultee, A., Gorris, L. G. M., & Smid, E. J. (1998). Bactericidal activity of carvacrol towards the food-borne pathogen *Bacillus cereus*. *Journal of Applied Microbiology*, 85(2), 211–218. <https://doi.org/10.1046/j.1365-2672.1998.00467.x>
- Ündeğer, Ü., Başaran, A., Degen, G. H., & Başaran, N. (2009). Antioxidant activities of major thyme ingredients and lack of (oxidative) DNA damage in V79 Chinese hamster lung

fibroblast cells at low levels of carvacrol and thymol. *Food and Chemical Toxicology*, 47(8), 2037–2043. <https://doi.org/10.1016/j.fct.2009.05.020>

Wade, R. J., & Burdick, J. a. (2014). Advances in nanofibrous scaffolds for biomedical applications: From electrospinning to self-assembly. *Nano Today*, 9(6), 722–742. <https://doi.org/10.1016/j.nantod.2014.10.002>

Wen, P., Zhu, D.-H., Wu, H., Zong, M.-H., Jing, Y.-R., & Han, S.-Y. (2016). Encapsulation of cinnamon essential oil in electrospun nanofibrous film for active food packaging. *Food Control*, 59, 366–376. <https://doi.org/10.1016/j.foodcont.2015.06.005>

Zhang, Y., Chwee, T. L., Ramakrishna, S., & Huang, Z. M. (2005). Recent development of polymer nanofibers for biomedical and biotechnological applications. *Journal of Materials Science: Materials in Medicine*, 16(10), 933–946. <https://doi.org/10.1007/s10856-005-4428-x>

Release kinetics and antimicrobial properties
of carvacrol encapsulated in electrospun
poly-(ϵ -caprolactone) nanofibres.
Application in starch multilayer films.

Alina Tampau ^a, Chelo González-Martínez ^b, Amparo Chiralt ^c

^{a, b, c} Instituto Universitario de Ingeniería de Alimentos para el Desarrollo, Ciudad
Politécnica de la Innovación, Universitat Politècnica de Valencia, Camino de Vera, s/n,
46022 Valencia, Spain.

Food Hydrocolloids (2018)79, 158-169

altam@upvnet.upv.es

Abstract

Electrospun poly-(ϵ -caprolactone) (PCL) fibre mats encapsulating Carvacrol (CA) were obtained with good encapsulation efficiency (85 %) and CA load (11 % in the fibre). These mats were effective at controlling the growth of *Escherichia coli*, when the surface density of CA loaded fibres was 1.2 or 1.8 mg/cm², in line with the CA released into the culture medium that exceeded the MIC of the bacteria. However, they were not effective at controlling the growth of *Listeria innocua*, since a greater release of CA was necessary to achieve the MIC of this bacterium. It was not only the CA load in the fibres, but also its release capacity in the media that determined the antimicrobial effect. The fibre showed higher release rate and ratio in less polar simulants, D1 (50 % ethanol) and D2 (isooctane) (representing fatty foodstuff), where practically the total amount of CA was released; whereas in more polar systems (simulants A (10 % ethanol) and B (3 % acetic acid)) a more limited CA delivery (60-75 %) occurred, at a slower rate. The antimicrobial action of the active PCL mats was reproduced in multilayer starch films containing the CA-loaded electrospun PCL fibres between two starch sheets, with a slightly delayed response. In the multilayer films, a great reduction in the water vapour permeability was also observed with respect to that of starch films, without relevant changes in other functional properties of the films for packaging purposes.

Keywords

PCL, carvacrol, release kinetics, antimicrobial action, starch multilayer films.

1. Introduction

The electrohydrodynamic process known as electrospinning is an efficient and straightforward method with a simple working principle (Bhardwaj & Kundu, 2010) that allows micro- and nanoscale polymer structures to be obtained. It can generate continuous (fibres) or discrete (particles) polymer delivery systems able to encapsulate compounds of specific interest for applications in many fields, such as that of medicine (Hamori et al., 2014; Sill & von Recum, 2008), optoelectronics (Hernández-Martínez, Nicho, Hu, León-Silva & Arenas-Arrocena, 2017; Xue et al, 2017), sensor technology (Mercante, Scagion, Migliorini, Mattoso & Correa, 2017; Macagnano & De Cesare, 2017) or food packaging (Fabra, López-Rubio & Lagaron, 2016). Incorporating active natural compounds into biodegradable food packaging materials is an innovative trend that focuses on the enhancement of the quality and shelf-life lengthening of the packaged foods (Majid, Nayik, Dar & Nanda, 2016; Padgett & Han, 1998), while these biodegradable materials reduce the environmental impact of the packaging waste. The electrospinning technique could be a feasible way to encapsulate the active compound, while providing a controlled delivery system (electrospun layer) when applied to such packaging materials. Electrospun layers provide structures with a large specific surface area for the compound diffusion, while the losses of active compounds during the process are minimized due to the use of room temperatures.

Of the active agents that are currently used in the development of active food packaging, plant essential oils (and their constituents) are a prominent group of interest. Plant-derived phenolic terpenoids have been successfully incorporated in different polymers with food packaging potential, as reported by Requena, Vargas & Chiralt, (2017) for eugenol encapsulated in poly(hydroxybutyrate-co-hydroxyvalerate), Fernandez-Pan, Maté, Gardrat & Coma, (2015) for carvacrol in chitosan, Rieger & Schiffman, (2014) for cinnamaldehyde in chitosan/poly(ethylene-oxide) or Ramos, Beltrán, Peltzer, Valente & Garrigós, (2014) for carvacrol and thymol in polypropylene. Carvacrol is one of the most widely used active compounds (Higueras, López- Carballo, Hernández-Muñoz, Catalá & Gavara, 2014) recognized as a food additive (Joint FAO/WHO, 2001) and as a flavouring substance (EFSA, 2012). It is a phenolic terpenoid present at great concentration in several essential oils, such as oregano or thyme oil (Burt, 2004), which exhibits high antimicrobial activity against both Gram positive and Gram negative bacteria (Ben Arfa, Combes, Preziosi-Belloy, Gontard & Chalier, 2006; Ultee, Gorris & Smid, 1998), as well as different fungi (Tunc, Chollet, Chalier,

Preziosi-Belloy & Gontard, 2007). Its incorporation in food-grade polymers would offer alternative active packaging materials, replacing some of the synthetic antimicrobials currently in use such as weak organic acids or salts (Fu, Sarkar, Bhunia & Yao, 2016). Its controlled delivery, until the minimal inhibitory concentration of the microorganisms is reached at the target point, is required to ensure its antimicrobial activity. This controlled release should also prevent any overdose in the food system in order to limit the dilution effects by diffusion and the food sensory impact.

A previous study (Tampau, González-Martínez & Chiralt, 2017) reported a good encapsulation efficiency (EE) of carvacrol in electrospun poly- ϵ -caprolactone (PCL) mats, using 15 % glacial acetic acid solution of PCL containing 0.15 g carvacrol/g polymer. These mats exhibited a fibrous structure, which could adequately coat biodegradable packaging films to obtain active materials for food applications. 85 % of the carvacrol content of the solution could be encapsulated in the PCL fibres, which is highly efficient when taking into account the volatile nature of the active and the high losses incurred by other techniques. Despite the high EE, the antimicrobial effect of the encapsulated compound will be affected by its initial load in the active material and its active release capacity into the applied medium. All of this defines the active effective concentration on the target point, which must exceed the minimal inhibitory concentration of the contaminating bacteria.

Likewise, electrospun PCL fibres carrying carvacrol could be applied to obtain multilayer starch films including carvacrol loaded fibres between the starch sheets, thus contributing to the improvement of the functional properties of the packaging material. The multilayer assembly of biopolymers with complementary properties allows packaging material to be obtained that better meets the specific requirements of different kinds of foods. In fact, more and more of the food available in the stores comes in high-tech plastic packaging multilayer films, ensuring the food is preserved for longer than when using a monolayer structure. Starch is a good candidate since it is widely available and cheap, while its films are extensible with very good oxygen barrier properties (López, Zaritzky, Grossmann, & García, 2013). However, starch films exhibit poor water vapour barrier capacity, being water sensitive (Pushpadass et al., 2009). In this sense, PCL exhibits good barrier capacity to water vapour (Ortega-Toro, Morey, Talens & Chiralt, 2015) and its inclusion in the starch multilayer assembly has been demonstrated to enhance the film functionality (Ortega-Toro et al., 2015). Likewise, the incorporation of carvacrol into the PCL electrospun layer can confer antimicrobial properties on the starch/PCL/starch multilayers.

The aim of the study was to develop active electrospun layers of poly- ϵ -caprolactone with encapsulated carvacrol with a high enough load of the active to be applied on food packaging films, by analysing the release kinetics of carvacrol in different food simulants (solvents with different polarity) and verifying their antibacterial activity. Likewise, the improvement in the functional properties of the starch multilayer films, containing electrospun PCL fibres between the starch sheets, has been analysed in terms of the barrier and tensile properties and antimicrobial activity.

2. Materials and methods

2.1. Materials and reagents

Poly-(ϵ -caprolactone) (PCL) pellets (average Mn 80,000) and carvacrol (CA) were acquired from Sigma-Aldrich (Sigma–Aldrich Chemie, Steinheim, Germany). All UV-grade solvents used (ethanol, glacial acetic acid and isooctane) were from Panreac AppliChem (Panreac Química S.L.U, Barcelona, Spain).

2.2. Obtaining and characterizing the electrospun fibre of CA-loaded PCL

On the basis of previous studies (Tampau et al., 2017), nanofibres were obtained from PCL in glacial acetic acid (GAA) with and without CA. Briefly, PCL (15 wt. %) and CA (15 wt. % with respect to the polymer) were dissolved in GAA under stirring for 24 h at room temperature. The solutions were electrospun using Fluidnatek equipment (BioInicia S.L., Valencia, Spain), at a flow rate of 1.2 mL/h through the syringe needle (internal diameter=0.6 mm), by applying an electric field of 12.0 kV. The electrospun fibre material was collected on aluminium foil disks placed on the collector at 20 cm from the tip of the needle. In these conditions, an encapsulation efficiency (EE) of CA in the fibres of about 85 % was expected, which would suppose 12 g CA/100 g fibres in the obtained mat.

Nanofibres were obtained for different electrospinning (ES) times on aluminium foil to determine the process yield (g fibre/cm²) as a function of the process time. Carvacrol content in the fibre (mg/g fibre) was analysed at the longest process time (90 min) and the expected EE from the previous study (Tampau et al. 2017) was verified. The CA surface density (mg CA/cm²) vs the ES time was estimated from this analysis, in order to determine the time required to reach enough CA load in the mat. This is for the purposes of ensuring that the minimum inhibitory concentration (MIC) of CA for different bacteria can be reached

when the active mat is applied on a target product surface. Likewise, CA content was also determined in different zones of the circular electrospun surface, considering radial distance and angle with respect to the centre (6 zones), to analyse the CA distribution homogeneity on the mat surface electrospun for 90 min.

CA quantification was carried out by extraction of fibre (with a determined surface and weight) with UV grade absolute ethanol and spectrophotometric determination at 275 nm using a UV/Vis spectrophotometer (Evolution 201 UV-Vis, Thermo Fisher Scientific Inc.), as previously described by Tampau et al. (2017). The obtained results were expressed as $\mu\text{g CA}/\text{cm}^2$ or $\mu\text{g CA}/\text{g fibre}$.

Structural characterization of the fibres was performed using Field Emission Scanning Electron Microscopy (FESEM Ultra 55, Zeiss, Germany). Samples were mounted on support stubs and, after platinum coating, were observed using an accelerating voltage of 2 kV. ImageJ software (National Institutes of Health, U.S.A.) was employed for the image analysis, in order to assess the morphological differences between the two types of matrices with or without the active.

2.3. Release kinetics of CA in different food simulants

The kinetic study of CA release from the electrospun PCL fibres was carried out in four types of solvents, acting as food simulants of different polarities or pH (Regulation 10/2011/EC). As described by Requena et al. (2017), ethanol 10 % (v/v) (simulant A) and acetic acid 3 % (w/v) (simulant B) were chosen to emulate aqueous foodstuffs neutral and acidic (pH<4.5) in character, respectively. Ethanol 50 % (v/v) (simulant D1) was used to imitate foods with alcohol content higher than 20 % or oil-in-water emulsions, whereas isooctane (simulant D2) was used for foods with a highly lipophilic surface. For this purpose, fibre samples of 50 mg were placed in glass bottles containing 100 mL of the corresponding simulant, and kept under stirring at 22 ± 2 °C. Aliquots of the samples were extracted at different times of contact (ranging from 1 min upward, until equilibrium is reached) and absorbance was determined spectrophotometrically at 275 nm. CA quantification in the liquid phase was established using the previously obtained calibration curves in each simulant. All analyses were carried out in triplicate, using the respective simulant, in contact with CA-free fibres for the equivalent time, as blank.

2.3.1 CA release mathematical modelling

Three models were considered to describe the behaviour of the CA loaded PCL fibres in the four food simulants. Considering that the electrospun fibres fuse together at different points throughout their length to form a mat-like matrix, the CA release from the mat can be analysed as a one-dimensional mass transfer process from an infinite plane sheet (Crank, 1975) of half-thickness e , with a characteristic diffusion coefficient D (m^2/s). The diffusion coefficients for each simulant were determined by modelling the obtained data to Fick's second law for long-time diffusion (eq.1), considering that i) the distribution of the active is homogenous within the matrix, ii) the initial concentration of CA in each simulant is zero, and iii) there is no degradation of CA during the migration process.

$$\frac{M_t}{M_\infty} = \frac{8}{\pi^2} \sum_{n=0}^{\infty} \left[\frac{1}{(2n+1)^2} \exp \left\{ \frac{-D(2n+1)^2 \pi^2 t}{4e^2} \right\} \right] \quad (\text{eq. 1})$$

where:

t = release process time (s),

M_t = mass of CA released at time t ,

M_∞ = mass of CA released at equilibrium,

e : half thickness of the fibre layer (m).

The boundary conditions taken into account for eq.1 are as follows:

$$\begin{array}{lll} t = 0 & -e < x < e & c = c_0 \\ t > 0 & x = \pm e & c = 0 \end{array}$$

The mathematical solutions from Fick's equation with eleven terms ($n= 0\div 10$) were optimized using the Solver tool (Microsoft Excel 2016®) by minimizing the Sum of Squared Errors (SSE).

Peleg's model (eq. 2) (Peleg, 1988) was also applied to the data, in order to obtain the equilibrium value for the carvacrol release and the release rate for each simulant.

$$\frac{t}{M_t} = k_1 + k_2 t \quad (\text{eq. 2})$$

where:

t = release process time,

M_t = mass of CA released at time t ,

$1/k_1$ = release rate,

$1/k_2$ = mass of CA released at equilibrium (M_∞).

Lastly, the Korsmeyer-Peppas model (Siepmann & Peppas, 2011) (eq. 3) was considered in order to analyse the mechanisms controlling the CA release, with the caveat that it can only be applied for $(\frac{M_t}{M_\infty} \leq 0.6)$, which means a progress of the mass transfer process of 60% (Hines & Kaplan, 2011).

$$\frac{M_t}{M_\infty} = kt^n \quad (\text{eq. 3})$$

where:

M_t / M_∞ = mass of CA released at time t with respect to the mass released at equilibrium;

t = release process time (h);

k = rate constant (h^{-n});

n = diffusional exponent which takes values in the 0÷1 interval (dimensionless).

2.3.2. Prediction of CA antimicrobial effect based on the release study

Peleg's parameters determined in the modelling step were employed to predict the amount of CA released throughout time in the target product, which must reach the minimum inhibitory concentration (MIC) of the target microorganism to exert the antimicrobial effect. To this end, a contact surface equivalent to a Petri dish of 5.5 cm in diameter with a volume of 10 mL of agar medium (pH=5.6±0.2) was considered. For this simulation, two ES deposition times of 60 and 90 minutes (with the subsequent total amount of CA in the mat) and the release profile of CA from PCL mats in A simulant were considered. Simulant A was the most similar in water content to the culture medium.

2.4. Incorporation of PCL fibres in multilayer starch films

PCL fibres were electrodeposited on thermoplastic starch films (S) in order to obtain multilayer films (S-PCL-S). To this end, corn starch films were obtained by melt blending of

starch-glycerol-water (mass ratios: 100:30:50) at 160 °C and 8 rpm for 30 min in a two-roll mill (Model LRM-M-100, Labtech Engineering, Thailand). The obtained pellets were conditioned at 53 % relative humidity for 1 week and compression moulded in a press (Model LP20, Labtech Engineering, Thailand), initially at 50 bars/160 °C for 2 min, then at 130 bars/160 °C for 6 min, and cooled down to 50 °C for 3 min (Ortega-Toro et al., 2015). Multilayer films were prepared by electrodeposition of the 15 % PCL solution in GAA with or without CA (15 g/100 g PCL). Electrodeposition times were 60 and 90 min to obtain the same CA surface concentration as in previously described fibre mats. Multilayer films with the ES PCL in the middle were obtained by thermo-compression of two S layers (one of these containing the ES PCL fibres of 60 or 90 min) at 130 bars and 80 °C for 4 min, and cooled down to 50 °C for 2 min.

Multilayer films conditioned for 1 week at 53 % RH were characterized as to their thickness (measured at 5 different points by a Palmer digital micrometre from Comecta, Barcelona, Spain), water content (assessed gravimetrically), water vapour permeability (determined at 25 °C using a modified (Gennadios, Weller & Gooding, 1994) ASTM E96-95 gravimetric method (ASTM, 1995), as described by Perdonés, Chiralt & Vargas, (2016)), oxygen permeability (Standard Method D3985-95 (ASTM, 2002)) and tensile properties (ASTM standard method D882 (ASTM, 2001)), as previously described by Ortega-Toro et al. (2015).

Antimicrobial *in vitro* tests were also carried out for multilayer films using the below described method (section 2.6) for fibre mats.

2.5. Thermal analysis

Thermal analyses were carried out in PCL fibres and multilayer assemblies in order to analyse the carvacrol effect on phase transitions and thermal stability of PCL or starch. Differential scanning calorimetry analyses were performed, using a DSC (1 StareSystem, Mettler-Toledo, Inc., Switzerland). Samples (5-15 mg), previously conditioned in P₂O₅, were placed into aluminium pans (Seiko Instruments, P/N SSC000C008) and sealed. Samples were heated from 25 °C to 120 °C at 10 K/min. Then, they were kept at 120 °C for 5 min, cooled to -60 °C at -10 K/min, kept at -60 °C for 5 min and heated again to 200 °C at 10 K/min. An empty aluminium pan was used as reference. Each sample was analysed in triplicate.

A thermogravimetric analyser (TGA/SDTA 851e, Mettler Toledo, Schwarzenbach, Switzerland) was used to characterize the sample thermal degradation. The analysis was

performed from room temperature to 500 °C at 20 °C/min under a nitrogen flow (50 mL/min). DTA and DGTA curves were analysed and the temperature at which the maximum degradation rate occurs was determined (T_{max}). Each sample was analysed in duplicate.

2.6. Antimicrobial properties

Gram (-) *Escherichia coli* (CECT 101) and Gram (+) *Listeria innocua* (CECT 910) obtained from Spanish Type Culture Collection (CECT, Burjassot, Spain) were used to test the antimicrobial efficiency of the electrospun PCL fibre mats. The model bacterial strains, stored in protective conditions (glycerol 30%) at -25 °C, were regenerated as described by Valencia-Sullca et al. (2016), by incubating them at 37 °C for 24 h in tryptic soy broth (TSB) (Scharlab, S.L., Barcelona, Spain) and harvested in their exponential growth phase. The revived cultures were properly diluted in TSB to obtain a target inoculum of 10^6 colony forming units (CFU)/ml for *E. coli* and 10^5 CFU/ml for *L. innocua*.

Circular samples (55 mm in diameter), consisting of starch multilayers or PCL fibre mats (with and without CA) electrospun over thermoplastic starch film acting as support, were placed (with the electrospun side face down) on inoculated plates (1 ml inoculum on the plate surface) containing 10 mL of tryptic soy agar (TSA) (Scharlab, S.L., Barcelona, Spain). CA-free PCL samples and uncoated inoculated TSA plates were used as controls. Immediately after the inoculation and after 2, 6, 9 and 14 days of storage at 10 °C, microbial counts were performed. To this end, the Petri dish content was placed aseptically in a sterile stomacher strainer bag (Seward Limited, West Sussex, UK) along with 90 mL of buffered peptone water (BPW) (Scharlab, S.L., Barcelona, Spain) and homogenized for 2 min by means of a Masticator Paddle Blender (IUL S.A., Barcelona, Spain). Serial dilutions of this liquid were plated and covered with violet red bile agar (VRBA) (Scharlab, S.L., Barcelona, Spain) for *E. coli* and palcam agar base (PAB) (Scharlab, S.L., Barcelona, Spain) enriched with palcam selective supplement for *Listeria* (Scharlab, S.L., Barcelona, Spain). After incubation at 37 °C for 48 h, the colonies were counted. All determinations were performed in duplicate.

2.7. Statistical analysis

The experimental data was processed using one-way analysis of variance (ANOVA) with the statistics program Statgraphics centurion XVI.I (StatPoint Technologies Inc. Warrenton, VA, USA).

3. Results and discussion

3.1. Electrospun fibre layers of CA loaded PCL

The structure of the obtained electrospun matrices can be observed in Figure 1. The mat has a fibrous appearance, with occasional beads of spindle-like geometry which appear more frequently in the case of the CA-loaded fibres. The average diameter of active-loaded fibres was 200 ± 40 nm, whereas in the case of the CA-free matrix this reached higher values of 500 ± 350 nm. CA affected the morphology of the electrospun fibres, giving rise to thinner fibrous forms, but with more beads, such as previously observed (Tampau et al., 2017). These changes must be attributed to the differences in the liquid phase properties induced by CA addition and the CA interactions with the polymer chains that affected the chain entanglements, responsible for fibre formation (Bahrami & Gholipour Kanani, 2011).

The mass fibre accumulation on the collector surface as a function of the ES time (Figure 2a) reveals the expected linear trend where the slope is coherent with the liquid flow applied in the equipment, the concentration of the compounds (PCL and CA) and the EE of CA. The quantified amount of CA in the fibre obtained for 90 min was 11.1 ± 0.1 g CA/100g fibre. This concentration represents an encapsulation efficiency of CA in the fibres of 83 ± 1 % (expressed as the ratio between the final amount in the fibre and the initial content in the solution), which agrees with the values previously reported by Tampau et al. (2017). From the mean CA content in the fibre, the CA surface density in the ES layer as a function of time was predicted (Figure 2b). Figure 2b also shows the values of the minimal inhibitory concentration (MIC) reported by some authors for *Escherichia coli* and *Listeria monocytogenes*, expressed as $\mu\text{g}/\text{cm}^2$. To obtain these values, the reported MIC values of CA against *E. coli* ($2.2\cdot 10^{-4}$ g/ml) and *L. monocytogenes* ($3.7\cdot 10^{-4}$ g/ml) (Burt, 2004), and the *in vitro* test conditions for the antimicrobial activity of the fibres used in the present study (section 2.4), were considered. Then, the MIC ($\mu\text{g}/\text{ml}$) was assumed to be reached in 10 ml of medium with a contact surface of 23.76 cm^2 (in a plate of 5.5 cm diameter) with the fibre mat. Figure 2b is a useful tool with which to estimate the ES time required to obtain active electrospun layers of PLC-CA fibres with enough CA to exceed the MIC of different microorganisms.

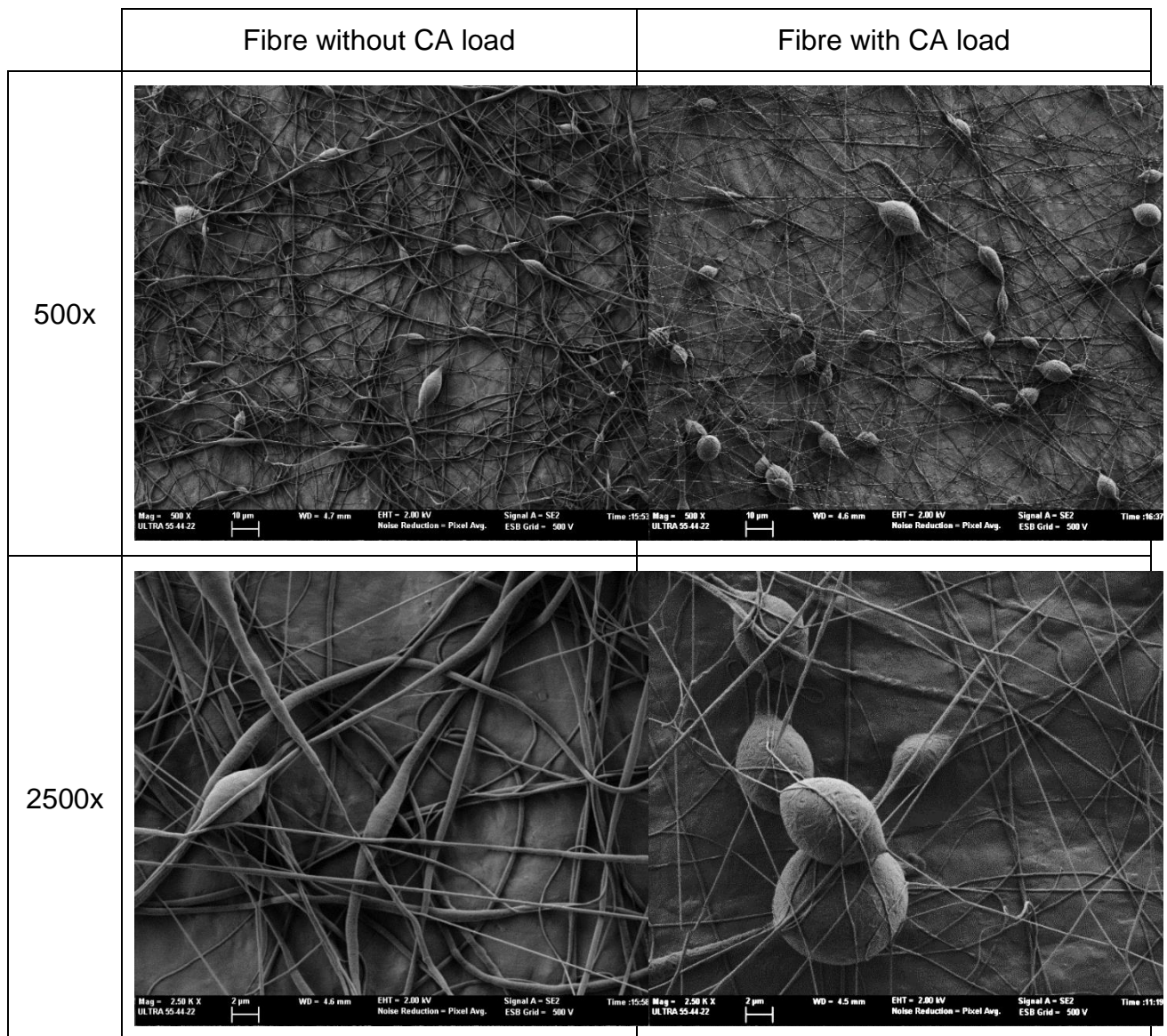


Figure 1. FESEM micrographs of the electrospun fibres for 10 minutes.

An ES time of 37 min and 62 min, respectively, would be required to obtain a CA mass in the fibres equivalent to the respective MICs of each bacterium. In order to ensure this quantity of active is reached, 60 and 90 min of ES time were applied to obtain potentially active layers, assuming that the complete release of the active in the culture media could not occur. By analysing the active's surface distribution, additional data was obtained to support this decision; this revealed that the ES process with the used equipment provided an uneven coating, creating a concentric concentration gradient (Figure 2c), where the external area of the obtained electrospun disc contained a smaller amount of fibres and so of CA. In this sense, four tangent sample disks obtained from each of the four quadrants of the main circle were considered for each analysis.

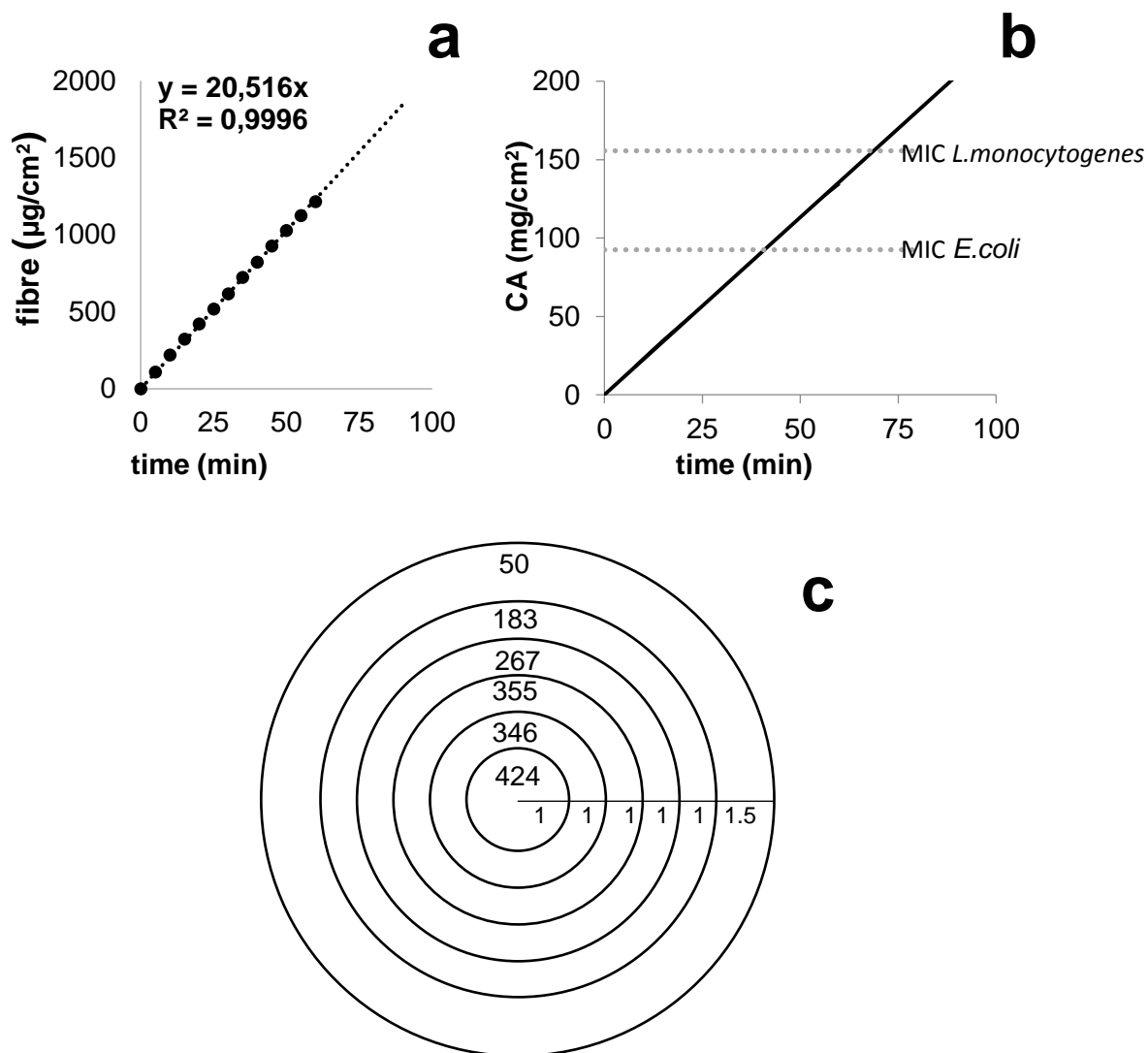


Figure 2. a) Mass of ES fibre layer as a function of time; b) Mean surface density of CA ($\mu\text{g}/\text{cm}^2$) as a function of ES time and c) surface CA distribution ($\mu\text{g}/\text{cm}^2$) in different zones of ES layer) for 90 min of ES (radius increments shown in cm). MICs in $\mu\text{g}/\text{cm}^2$ are indicated as a dashed line, assuming a CA diffusion in 10 ml medium through 23.76 cm^2 of sample surface in contact with the fibres (equivalent to 0.42 cm of characteristic dimension for diffusion).

3.2. Release kinetics of CA from PCL fibres in different food simulants

The release kinetics of CA from the fibre mat obtained for 90 min was analysed in order to find out how the active compound can be delivered in different food systems. To this end, four liquid simulants of different polarity have been considered, as commented in section 2.3. The release mass of CA was determined at different contact times with simulants and Figures 3 and 4 show the mean values, for each food simulant.

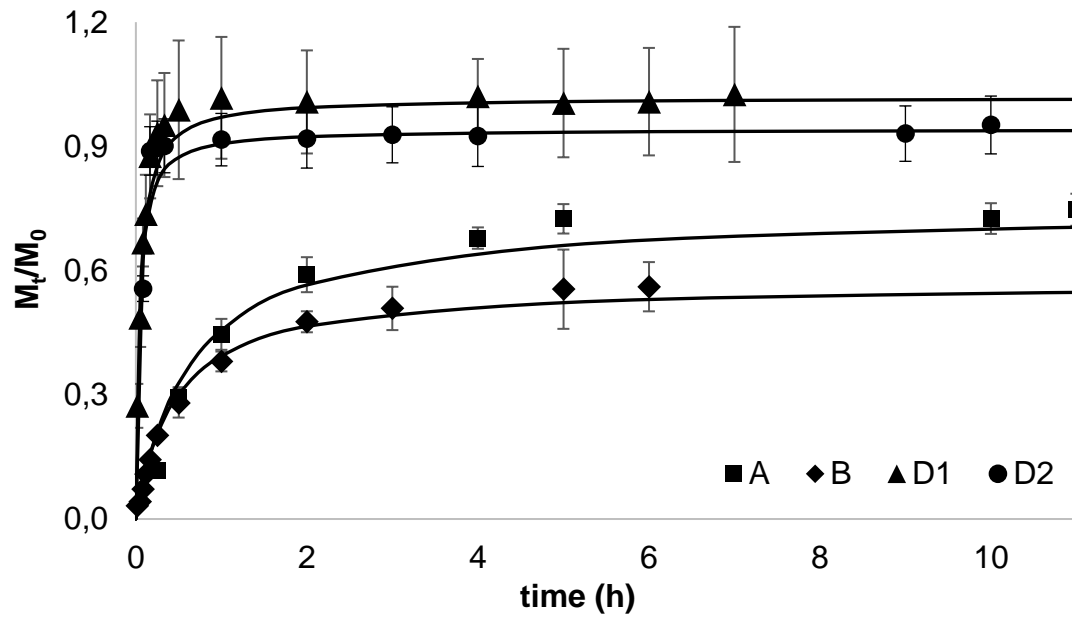


Figure 3. M_t/M_0 ratio (fraction of the active released from the fibres at each time, referred to the initial content in the fibres) as a function of time for the different solvents: experimental data (points) and Peleg's fitted model (continuous lines).

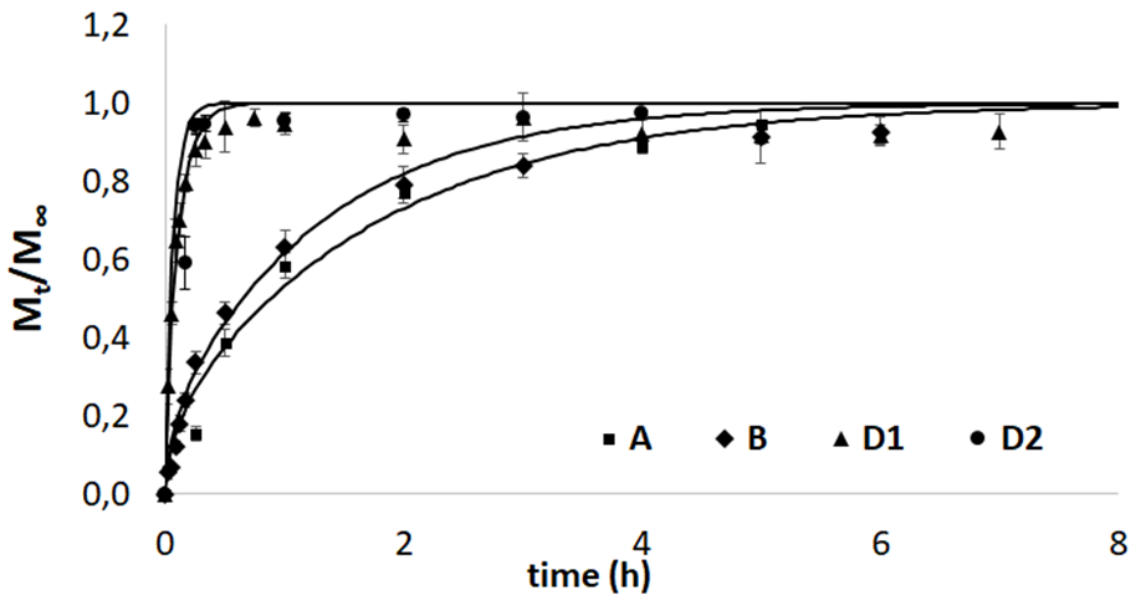


Figure 4. M_t/M_∞ ratio (fraction of the active released from the fibres at each time, referred to the maximum value released at equilibrium) as a function of time for the different simulants: experimental data (points) and Fick's fitted model (continuous lines).

Table 1 shows the maximum values released (M_∞), referred to 100 g of the initial ES layer, and estimated by applying Peleg's model to the experimental data. Table 1 also includes the values of $1/k_1$ Peleg's parameter, related to the release rate. A good fit of the model was

achieved in every case ($R^2 > 0.998$), as can be seen in Figure 3. Both the release rate and asymptotic value were greatly affected by the polarity of the food simulants. The fastest release of CA was observed in 50% ethanol (D1 simulant) and isooctane (D2 simulant), whereas the slowest delivery occurred in the more polar solvents (A: 10% ethanol and B: 3% acetic acid). Those less polar solvents also allow for the maximum delivery of CA from the PCL mats (near 100% of their content), whereas only 75 and 57 % of the content was released at equilibrium in polar solvents (simulants A and B, respectively). This behaviour agrees with the differences in polarity of the solvent and the corresponding chemical affinity between the polymer matrix, the active compound and the solvent, as previously reported by Tehrani (2007).

In fact, three steps can be described for the active release from the polymeric matrix: 1) solvent diffusion into the polymer network, 2) network relaxation due to solvent plasticization effects, and 3) the diffusion of the compound through the relaxed polymer network, until the thermodynamic equilibrium between the polymer and food system phases is reached (Requena et al., 2017). These steps can be coupled, especially 2 and 3, depending on the characteristic relaxation time of polymers and the diffusion times of the diffusing compound, giving rise to anomalous transport behaviour (Siepmann & Peppas, 2011). At equilibrium, the relative compound affinity with the solvated polymer and its solubility in the liquid food system determine its partition coefficient, defined as the ratio between the mass of active released at equilibrium in the simulant (M^∞) and its corresponding residual mass in the film ($M_0 - M^\infty$). The solubility of CA increases in less polar solvents with respect to the more aqueous solvents (CA water solubility is 1250 mg/L, Yalkowsky, He & Jain, 2010), while the PCL matrix could be more relaxed in contact with non-polar solvents than with the more aqueous systems, considering the non-polar nature of the polymer. Both the increase in the active solubility and polymer relaxation in less polar food simulants led to a faster CA release and a higher amount of CA delivered at equilibrium.

Table 1. Parameters of the Peleg (M_∞ - CA mass released at equilibrium; $1/k_1$ - CA release rate) and Korsmeyer-Peppas (n - diffusional exponent; k - rate constant) models, and Fick's diffusion coefficient in the different food simulants. The M_∞/M_0 ratio represents the CA mass released in the simulant liquid at equilibrium, with respect to the total amount in the fibres determined by ethanol extraction. Different superscript letters in the same column indicate significant differences ($p < 0.05$) between simulants.

Simulant	Adjusted model								
	Peleg				Fick		Korsmeyer-Peppas		
	$1/k_1$ ($\mu\text{g CA/g film}$)	$M_\infty=1/k_2$ (g CA/100 g film)*	M_∞/M_0 (%)	R^2	$D \times 10^{13}$ (m^2/s)	SSE	n	K (h^{-n})	R^2
A	34.1±0.4 ^a	7.8±0.3 ^b	75±3 ^b	0.9993	3.9±0.3 ^a	0.03	0.9±0.2 ^c	0.63±0.05 ^a	0.9468
B	38±2 ^a	6.1±0.6 ^a	57±5 ^a	0.9998	5.3±1 ^a	0.12	0.68±0.04 ^b	0.67±0.01 ^a	0.9502
D1	700±150 ^b	11±1 ^c	100±10 ^c	0.9981	46±7 ^b	0.04	0.53±0.07 ^{ab}	2.3±0.3 ^c	0.9979
D2	800±100 ^b	11.5±0.8 ^c	96±7 ^c	0.9998	109±14 ^c	0.05	0.46±0.11 ^a	1.8±0.4 ^b	0.8747

*corresponding to 100 mL volume of simulant

Table 1 also shows the parameters of the Korsmeyer and Peppas model. The values for the “n” exponent reveal that a Fickian diffusion ($n \approx 0.5$) takes place when the matrix is in contact with the less polar simulants, whereas an anomalous transport ($0.5 < n < 1.0$) can be assumed in the aqueous media (Siepmann & Peppas, 2011), which reveals the coupling of the polymer relaxation in contact with the solvent and the diffusion of CA in the matrix. This agrees with the low solvent-polymer affinity, which will imply a poor capacity of the solvent to penetrate the polymer network. Nevertheless, an apparent diffusion value (D) was estimated in every case (Table 1) considering the electrospun layer thickness (0.16 ± 0.08 mm) and assuming a homogenous medium, despite the nano-porous structure generated in the ES process (Figure 1), where the solvent could also penetrate by means of capillarity.

Figure 4 shows the curves fitted considering the Fickian equation (eq. 1), where the good fit of the model can be appreciated, ($SSE < 0.12$). The obtained D values also reflect the effect of the solvent polarity, showing the highest values for simulant D (isooctane) and the lowest value for 10% ethanol in water (simulant A). Other authors also report similar behaviour for the CA release from non-polar polymer matrices, such as polypropylene (Ramos et al., 2014) and poly (butylene succinate) (Petchwattana & Naknaen, 2015). Kuorwel, Cran, Sonneveld, Miltz & Bigger (2013) obtained lower diffusion values (about 15 times lower) for the CA diffusion from starch films in isooctane, which can be explained by the lower chemical affinity of starch matrix and isooctane, which affects the polymer relaxation and plasticization level, and so, the compound diffusion. From the obtained kinetic behaviour, no total CA release would be expected from PCL mats in the more polar food systems regardless of their pH, whereas it would be fully delivered in more fatty foods, due to the greater CA solubility and polymer relaxation during the food contact. Likewise, less time will be required for the maximum release in fatty foods (emulated by D1 and D2 simulants), than in more aqueous products (emulated by A and B simulants), where longer times would be needed.

3.3. Antibacterial properties of the CA loaded fibres

Based on the release profile, the amount of CA released in the incubation plates (55 mm in diameter, with 10 mL of agar medium), used in the *in vitro* antimicrobial test, was predicted, considering the behaviour of the medium to be similar to that of the simulant A (10 % ethanol in water). Figure 5 shows the predicted concentration of active reached over time for two CA-loaded PCL mats of different thicknesses (60 and 90 min of electrodeposition), and so, with different total amounts of CA in the mat. Likewise, the previously reported range for the

MIC values of the tested foodborne bacteria, namely *E. coli* ($0.225\text{-}5\text{ mg}\cdot\text{mL}^{-1}$) and *L. monocytogenes* ($0.375\text{-}5\text{ mg}\cdot\text{mL}^{-1}$) (Burt, 2004) were reflected in the plot (shadow areas). The predicted equilibrium values for CA release for 60 and 90 min processed PCL mats greatly differed. In the case of the 60-min process, the MIC value for *E. coli* was barely reached, while the MIC value for *L. innocua* was higher than the amount of CA released. For the 90-min process, both MIC values were reached, but for *L. innocua*, the amount released at equilibrium was in the range limit after about 5 h of contact. This can imply a lack of antilisterial activity, since a high degree of bacterial growth will occur during this period.

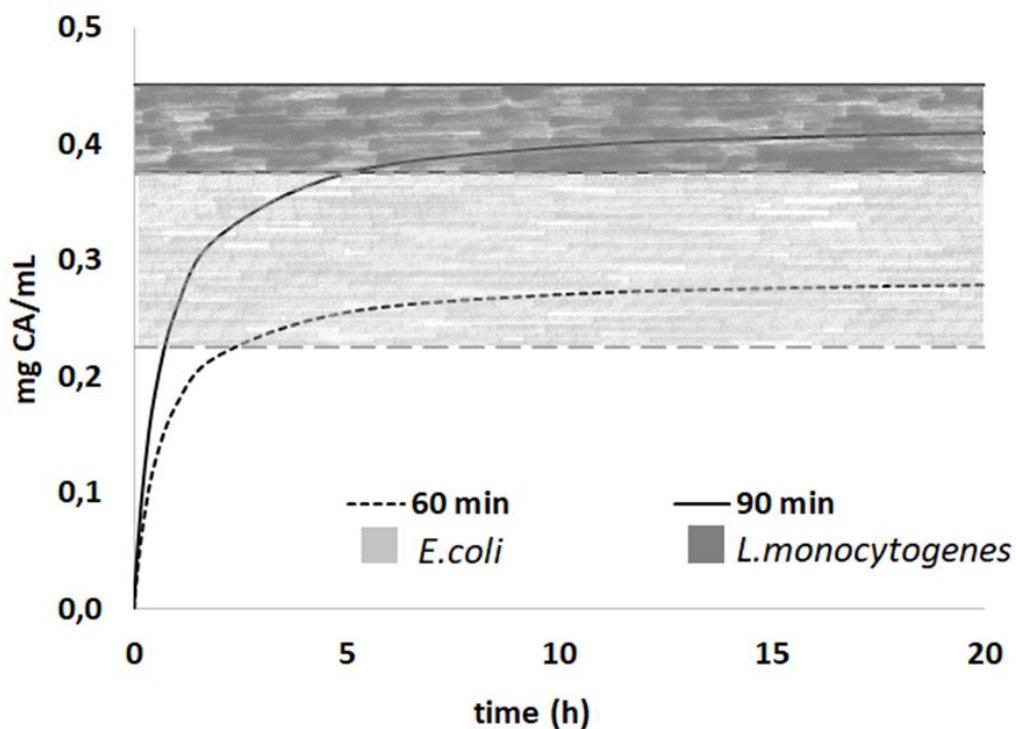


Figure 5. CA release prediction as a function of time in the microbial plate, assuming the behaviour of A simulant (10% ethanol). MIC range for *E. coli* is from $2.25\cdot 10^{-4}$ g/mL (Cosentino et al., 1999) to $3.75\cdot 10^{-4}$ g/mL (Du et al., 2015); MIC range for *L. monocytogenes* is from $3.75\cdot 10^{-4}$ g/mL (Pol & Smid, 1999) to $4.5\cdot 10^{-4}$ g/mL (Cosentino et al., 1999).

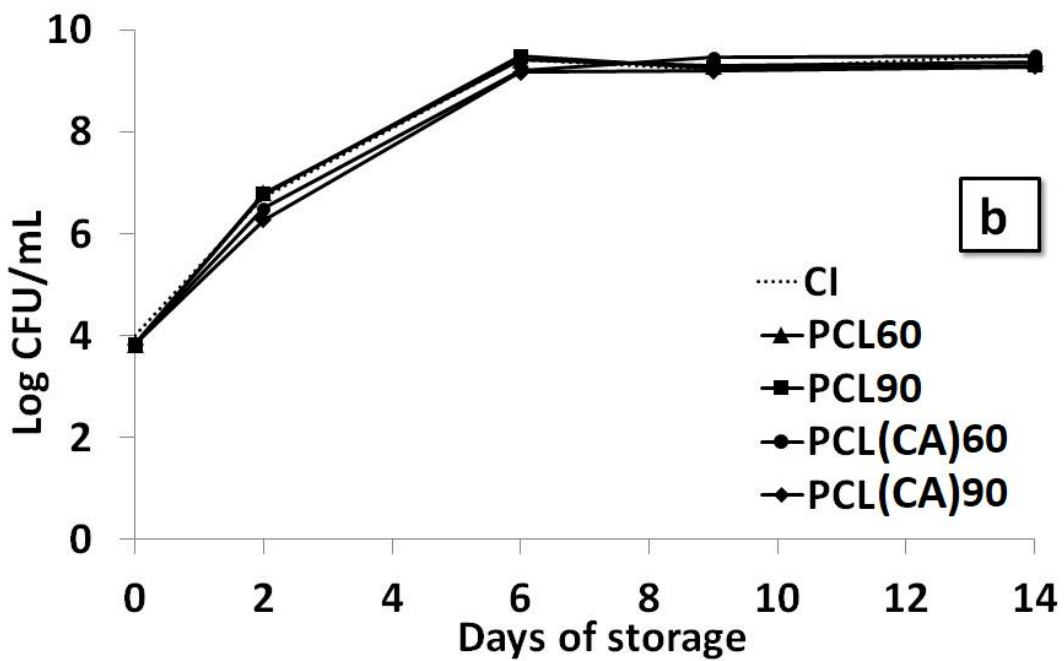
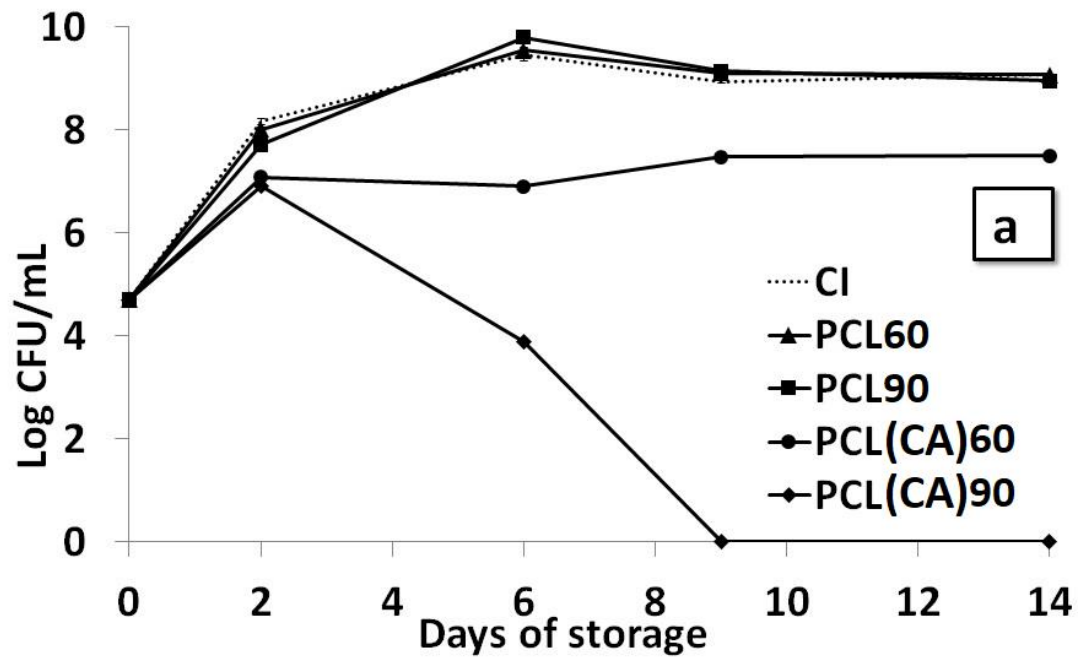


Figure 6. Growth of *E. coli* (a) and *L. innocua* (b) in the culture media at 10 °C in the uncoated inoculum control plate (CI) and plates coated with electrospun PCL without CA (PCL60; PCL90) and with electrospun PCL with CA (PCL(CA)60; PCL(CA)90). The numbers 60 and 90 indicate the electrodeposition time of fibres.

Figure 6 shows the growth curves of both *E. coli* and *L. innocua* for 14 days, obtained in the *in vitro* test, for the control samples (uncoated and CA-free PCL coated) and for the samples coated with CA-loaded PCL mats electrodeposited for 60 and 90 min. No antilisterial effect was observed for either CA loaded PCL mat, according to the predicted CA release which did not reach or barely attained the MIC levels at longer contact times when the bacteria have grown to a great extent. Limitations in the CA release from PCL mat to aqueous systems compromise the antilisterial activity of the CA loaded mats, despite the enough CA load revealed by Figure 2b. For *E. coli*, a bacteriostatic effect was observed from 2 incubation days onwards, revealing that enough CA was released from the mat electrodeposited for 60 min at this contact time. For the 90-min electrodeposited mat, bacterial death progressively occurred from 2 days of contact onwards, when more CA release occurred in the culture medium. The obtained antimicrobial action of the CA-loaded PCL mats was coherent with the total load of CA, its release kinetics in the culture medium (assuming its behaviour as simulant A) and the MIC values of the respective bacteria.

From this analysis, thicker CA-loaded PCL mats, with a greater surface density of CA, would be required to obtain antilisterial activity, whereas 90-min electrodeposited mats were able to exert an antibacterial effect against *E. coli*, taking into account the total CA load and its release kinetics in the culture medium.

3.4 Multilayer starch films with electrospun PLC fibres with and without CA

The efficiency with which PCL electrospun fibres improve the functional properties of starch films, either as packaging material or antimicrobial activity, was analysed through the measurement of the tensile, barrier and optical properties of the films as well as the *in vitro* antibacterial capacity for *E. coli* and *L. innocua*. Table 2 shows the different film properties, where the effect of the electrospun PCL layer between the two starch sheets can be observed.

Table 2. Barrier (water vapour permeability: WVP and Oxygen permeability: OP), tensile (Elastic modulus: EM, tensile strength: TS and deformation at break: % ϵ and optical properties (Internal transmittance: T_i , Gloss (60°), lightness: L^* , chrome: C_{ab} and hue: h_{ab}) of starch multilayer films containing electrospun PCL fibres. Different superscript letters in the same row indicate significant differences ($p < 0.05$) between multilayers.

	Multilayer				
	S-S	S-PCL60-S	S-PCL(CA)60-S	S-PCL90-S	S-PCL(CA)90-S
Thickness [mm]	0.38 ± 0.07 ^a	0.45 ± 0.01 ^b	0.45 ± 0.01 ^b	0.44 ± 0.03 ^b	0.5 ± 0.02 ^b
WVP x 10¹⁰ [g/(Pa·s·m)]	57 ± 4 ^c	18 ± 6 ^b	19 ± 4 ^b	12 ± 2 ^a	9 ± 1 ^a
OP x 10¹⁴ [cm³/ Pa·s·m]	5 ± 3 ^a	3.6 ± 0.4 ^a	5 ± 1 ^a	4 ± 2 ^a	2.9 ± 0.6 ^a
EM [MPa]	206 ± 21 ^b	149 ± 23 ^a	126 ± 34 ^a	192 ± 32 ^b	126 ± 23 ^a
TS [MPa]	9.7 ± 0.7 ^d	7 ± 2 ^{bc}	6.2 ± 0.9 ^{ab}	8 ± 1 ^c	5.8 ± 0.8 ^a
% ϵ	39 ± 4 ^b	34 ± 15 ^{ab}	34 ± 10 ^{ab}	36 ± 5 ^{ab}	29 ± 6 ^a
T_i [460 nm]	0.73 ± 0.01 ^c	0.72 ± 0.01 ^{bc}	0.69 ± 0.01 ^{ab}	0.69 ± 0.04 ^{ab}	0.69 ± 0.02 ^a
Gloss [60°]	15 ± 2 ^b	17 ± 4 ^b	9 ± 2 ^a	18 ± 5 ^b	10 ± 3 ^a
L^*	65.7 ± 0.6 ^b	64.8 ± 0.9 ^{ab}	64.6 ± 0.8 ^{ab}	66 ± 2 ^b	64.2 ± 0.4 ^a
C_{ab}	21.3 ± 0.3 ^{ab}	21.2 ± 0.3 ^{ab}	21.0 ± 0.6 ^{ab}	21 ± 1 ^a	21.7 ± 0.3 ^b
h_{ab}	79.8 ± 0.4 ^c	79.4 ± 0.4 ^{bc}	78.9 ± 0.6 ^{ab}	79.5 ± 0.5 ^c	78.7 ± 0.2 ^a

The ES layer thickness in the multilayer film can be deduced from the respective difference values as regards the SS bilayer. The resulting thickness was affected not only by the ES layer thickness but also by the relative radial flow of the PCL in the mats during the thermo-compression step of multilayer. In general, no significant differences were observed in the measured thicknesses of the multilayer films, all of which were about 70-120 μm thicker than the SS bilayer. This indicates that, regardless of the initial thickness of the ES layer, its flow and compaction during thermo-compression led to non-significant differences in the multilayer film thicknesses. The equilibrium moisture content of the multilayers was not significantly affected by the presence of the PCL fibre, this being 7.3 ± 0.2 g/100 g dry film.

As concerns the barrier properties, the WVP was greatly reduced when PCL fibres were present between the starch layers: 65 and 80 % reductions for 60 and 90-min electrodeposited layers, respectively (Table 2). This indicates the effectiveness of the parallel assembly of the PCL sheet, with a different surface density in the multilayer film, at limiting the transport of water molecules, as previously observed in starch-PCL bilayer films by Ortega-Toro et al. (2015). Nevertheless, no changes in the oxygen permeability of the SS films were observed, due to the fact that starch layers are actually the limiting material for the gas transport. As concerns tensile behaviour, the inclusion of PCL mats in multilayer films implied a slight reduction of the film stiffness and tensile at break, which can be attributed to the discontinuity introduced at the interlayer zone in the multilayer. This reduced the film's cohesion forces at the interfacial area, where no great chemical affinity could be expected for the PCL chains in contact with the starch matrix. However, no significant changes in the film extensibility were observed, except when CA-loaded PCL fibre produced for 90 min was included. In this case, films become slightly less stretchable and resistant, which could be attributed to a certain degree of CA diffusion into the starch matrix of bilayer, giving rise to a weakening effect in the starch multilayer. This effect was also observed at lower intensity in multilayers containing 60 min electrospun PCL with CA. The optical properties of the multilayer films were hardly affected by the PCL mat inclusion. The internal transparency (T_i) was the most affected optical property due to the greater opacity of PCL than starch (Ortega-Toro et al., 2015).

DSC and TGA analyses of isolated PCL fibres and multilayers were carried out to identify changes in phase transitions or thermal stability of the polymers, either starch or PCL, associated with the presence of CA or with its internal diffusion in the multilayer.

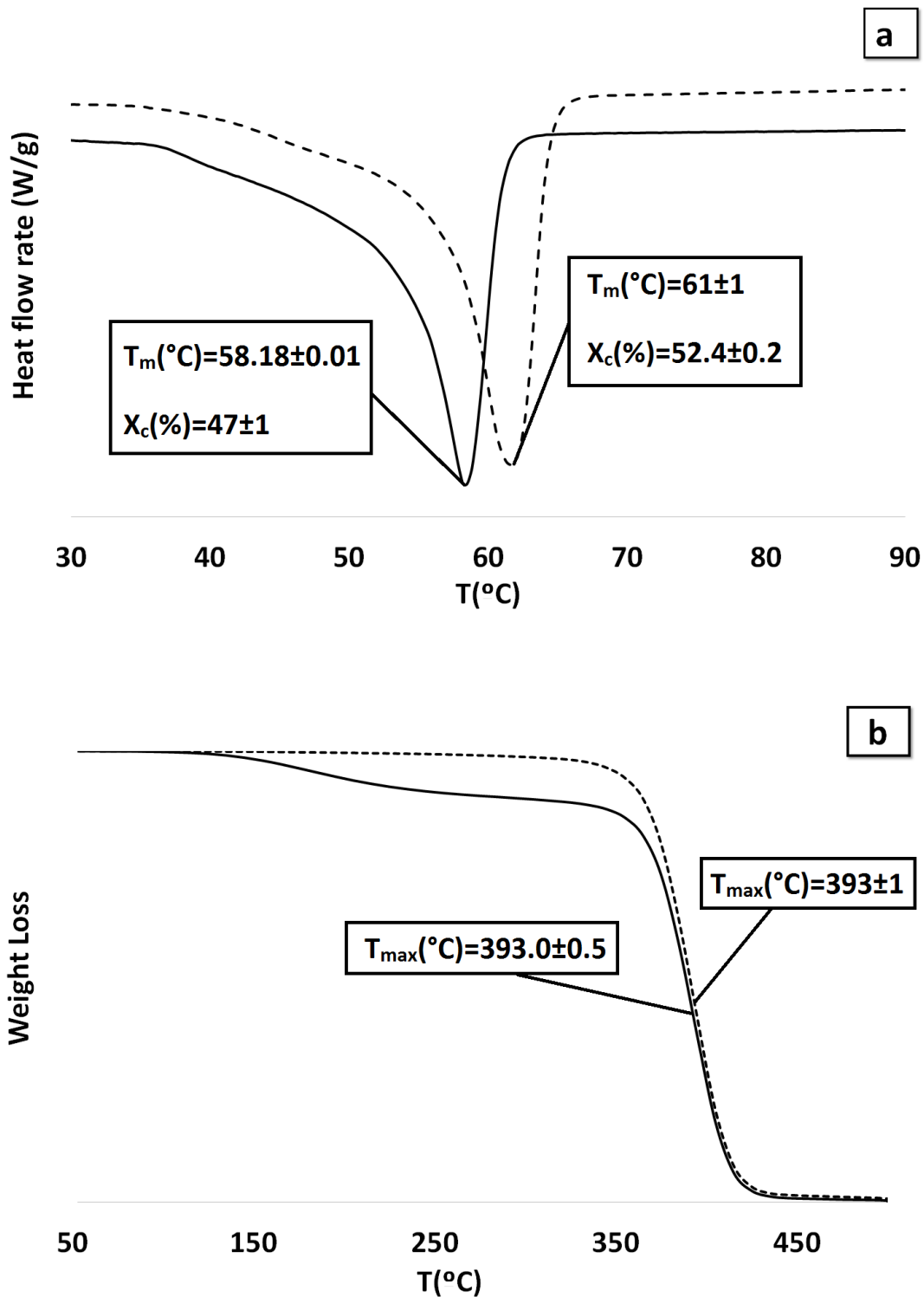


Figure 7. a) DSC thermograms and b) TGA curves of electrospun PCL fibres carrying (continuous line) or not (dashed line) CA. Melting temperature (T_m) and crystallization degree (X_c) as well as temperature for the maximum degradation rate (T_{\max}) of PCL are shown for each sample.

Figures 7a and b show the DSC thermograms (first heating step) for both fibres as well as the TGA curves. The melting endotherm of PCL can be observed for both mats, showing a shift of the melting peak to lower temperatures when fibres contained CA. From the melting enthalpy and the mass of PCL in each sample, the crystallization degree of PCL was estimated, by considering the enthalpy value of completely crystallized PCL (139.3 J/g, as reported by Koenig & Huang, 1995). A decrease in the PCL crystallization degree was also observed in CA-loaded fibres. These results point to the effective miscibility of CA and PCL in the fibres, which reduced the melting point and crystallinity of the polymer, as previously reported for CA containing PHBV (Requena, Jiménez, Vargas & Chiralt, 2016). TGA curves (Figure 7b) show the influence of the CA-load on the thermal behaviour of the mats. Weight losses at temperatures below the PCL thermo-degradation must be attributed to the CA evaporation from the mat, which did not affect the temperature of the maximum degradation rate (393.2 ± 0.6 °C) of the polymer, but overlapped the starting degradation step.

In contrast, DSC thermograms of multilayer films also revealed the crystalline structure of PCL in the electrospun layer, although no effect of CA was observed on its crystallization and melting temperatures (Table 3), which coincided with those observed for pure PCL mats, these being in the range previously reported for PCL films (Ortega-Toro et al., 2015). The values of crystallization and melting enthalpy from the different scans did not show significant differences for a determined sample, which indicates that the film process formation induced similar PCL crystallization to that obtained in the DSC scan conditions. Small differences in the enthalpy values among the different samples can be attributed to the fluctuations in the electrospun layer thickness in the different small bilayer samples used in the DSC analysis. This melting behaviour of PCL in multilayers, similar to that of pure PCL fibres, suggests that a high proportion of CA migrated to the starch sheets in the multilayer assembly, since the potential remaining amount in the PCL internal sheet was not enough to affect the PCL melting behaviour. On the other hand, the glass transition temperature of the starch (Table 3) was slightly reduced in multilayers containing CA-loaded fibres, particularly when this fibre mat was thicker, with the subsequent higher load of CA. This is coherent with the aforementioned small changes in the tensile behaviour of multilayers containing carvacrol.

Table 3. Phase transitions in the starch multilayer films containing electrospun PCL fibres (glass transition temperature of starch (T_g), and melting and crystallization temperatures and enthalpy of PCL). Different superscript letters in the same row indicate significant differences ($p < 0.05$) between multilayers.

		Multilayer				
		S-S	S-PCL60-S	S-PCL(CA)60-S	S-PCL90-S	S-PCL(CA)90-S
T_g (mid point)	1 st scan	107 ± 3 ^{ab}	108.0 ± 0.6 ^{ab}	108 ± 8 ^b	101 ± 2 ^{ab}	98 ± 4 ^a
1 st heating step	ΔH_m (J/g)	-	1.36 ± 0.12 ^a	3.45 ± 0.04 ^b	1.9 ± 0.2 ^a	3.8 ± 0.5 ^b
	T_m (peak)	-	62.7 ± 0.5 ^b	62.8 ± 0.6 ^b	60.9 ± 0.4 ^a	61.6 ± 0.4 ^a
2 nd heating step	ΔH_m (J/g)	-	0.90 ± 0.04 ^a	2.5 ± 0.2 ^{bc}	1.5 ± 0.2 ^{ab}	3 ± 1 ^c
	T_m (peak)	-	55.79 ± 0.09 ^a	55.6 ± 0.5 ^a	55.9 ± 0.2 ^a	56.6 ± 0.4 ^b
Cooling step	ΔH_c (J/g)	-	1.20 ± 0.04 ^a	3.1 ± 0.2 ^b	1.9 ± 0.7 ^a	3.6 ± 0.8 ^b
	T_c	-	29 ± 1 ^a	28.4 ± 0.9 ^a	28.5 ± 0.6 ^a	27.5 ± 0.4 ^a

Likewise, the thermal degradation (Figure 8a and b) of multilayer films exhibited the two typical steps associated with starch and PCL degradation, where the influence of CA can also be observed. Weight loss started earlier in 60-min electrospun CA-loaded fibres (from about 130 °C), associated with the CA evaporation, but had no significant effect on the temperature of maximum degradation rate of starch. Nevertheless, in 90-min electrospun fibres, with a greater CA load, a shifting of this temperature occurred which indicated the CA-starch interactions as a result of the CA diffusion into the starch layers. On the other hand, the thermo-degradation of PCL was also affected by CA interactions, exhibiting a lower temperature in the maximum degradation rate. A higher residual mass was also observed in CA-loaded multilayers. This behaviour suggests the participation of CA in both starch and PCL matrices with enough interaction forces to modify their thermal stability and modify the tensile behaviour of the films, as previously commented.

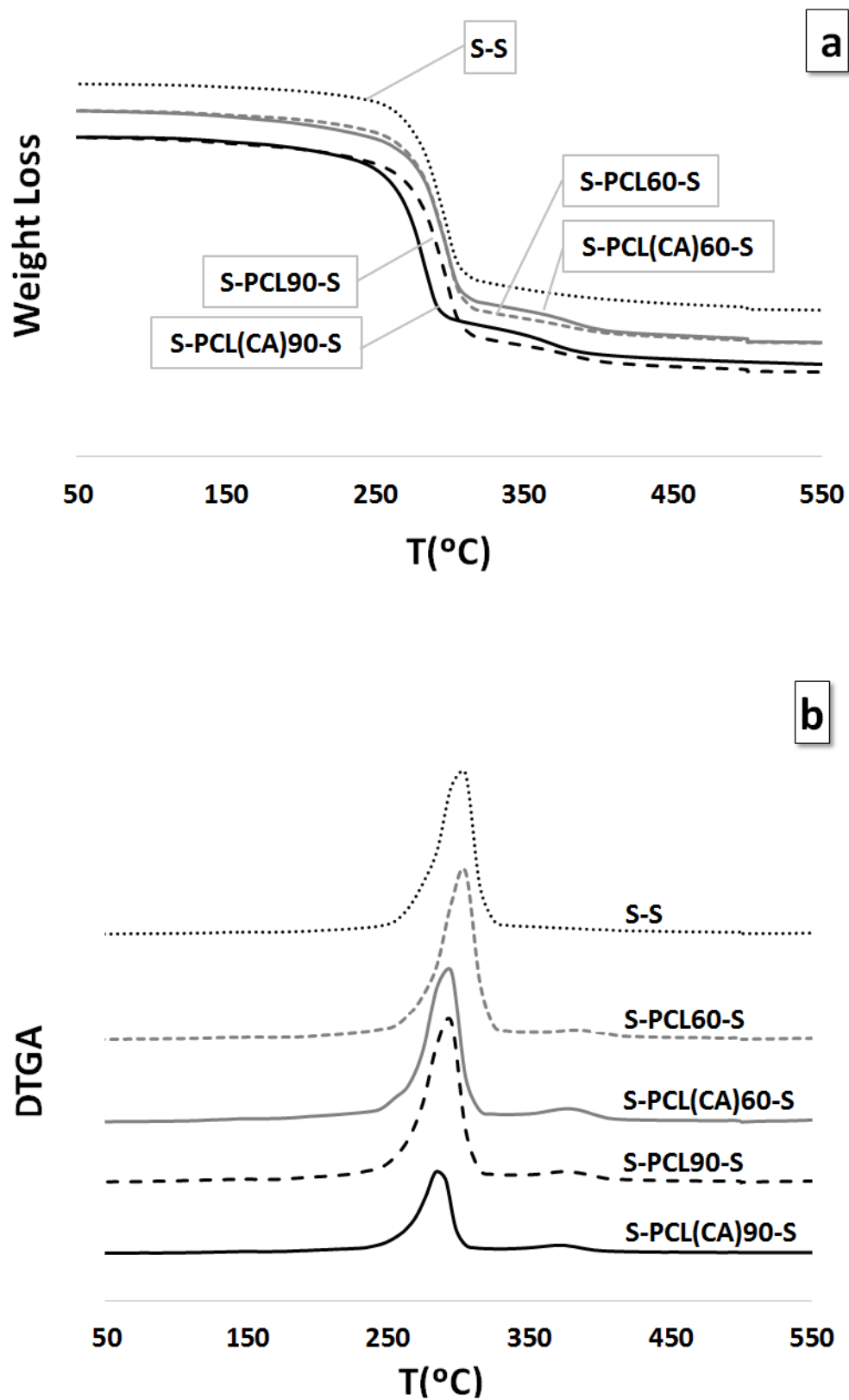


Figure 8. TGA (a) and DGTA(b) curves of starch multilayer films containing 60 (grey) or 90 (black) min electrospun PCL fibres, with (continuous line) and without (dashed line) CA.

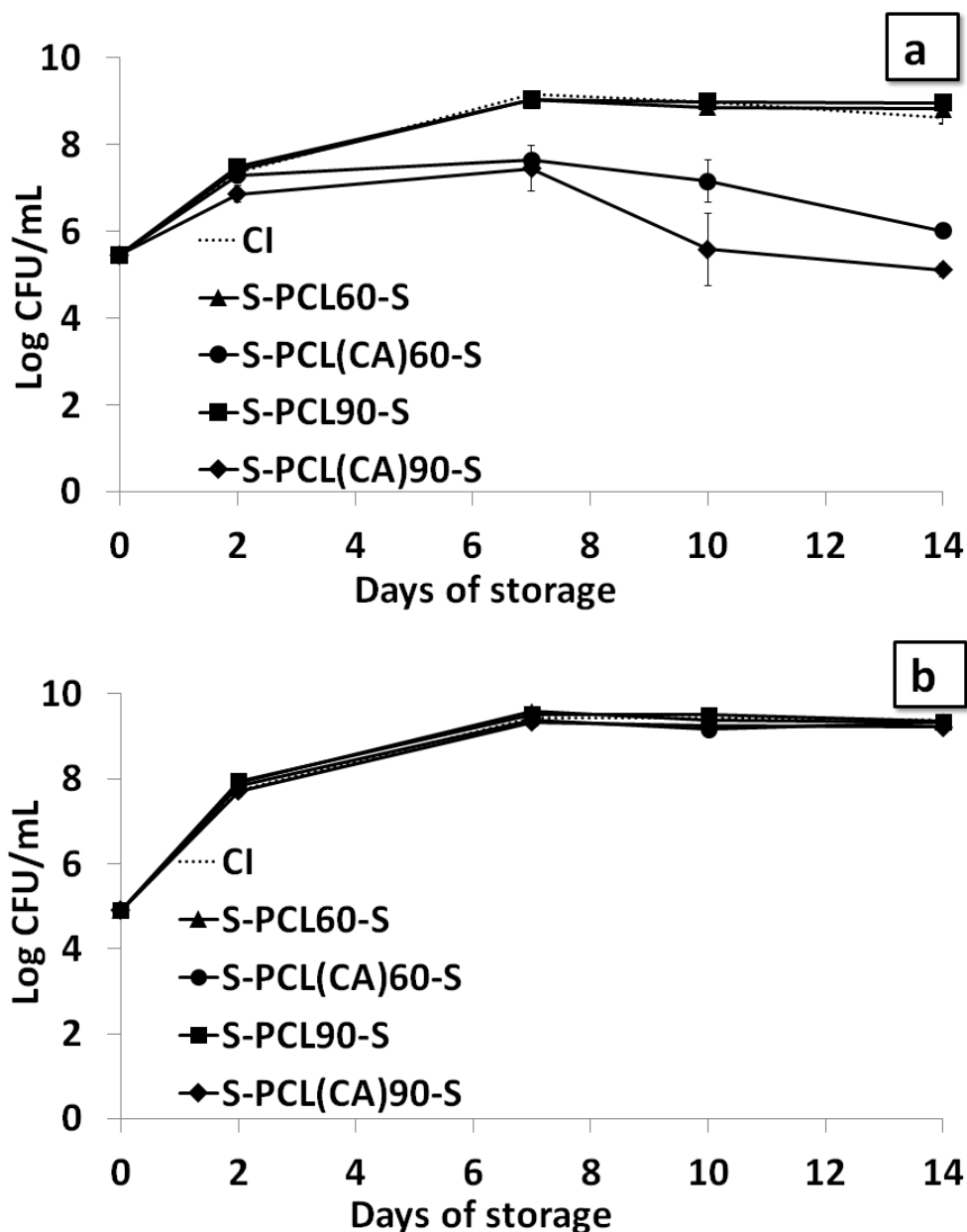


Figure 9. Growth of *E. coli* (a) and *L. innocua* (b) in the culture media at 10°C in the inoculum plates, coated with starch multilayers with 60 or 90 min electrospun CA loaded layers (S-PCL(CA)60-S and S-PCL(CA)90-S). Controls: uncoated inoculated plates (CI) and those coated with CA-free multilayers (S-PCL60-S and S-PCL90-S).

The CA diffusion into the starch layers could affect the antimicrobial activity of the multilayer films, with respect to that observed for CA-loaded mats, which was analysed. The antibacterial activity of the multilayer films revealed from the *in vitro* test (Figure 9), indicates a similar behaviour to that observed for the CA-loaded PCL mats. No antilisterial effect was observed, while a delayed action against *E. coli* was observed. This delay can be explained

by the thicker layer (starch layer) where CA must diffuse to reach the target point in the culture medium. From 2 to 7 contact days, a bacteriostatic effect could be appreciated; from 7 contact days onwards, however, a bactericidal action was observed both for 60 and 90-min CA-loaded electrospun PCL. This effect was more intense when CA-loaded fibres were thicker (90 min electrodeposited), in agreement with the higher CA load in the multilayer. Then, CA-loaded electrospun PCL fibres applied to multilayer starch films allows for effective antibacterial action against *E. coli* to a similar extent to that observed in the isolated fibres, but with a slightly retarded effect. Likewise, the electrospun PCL layers were greatly effective at reducing the WVP values of starch films, without relevant changes in their tensile or optical properties.

4. Conclusions

Electrospun PCL fibre mats encapsulating CA were effective at controlling the growth of *E. coli*, when the surface density of CA loaded fibres was 1.2 and 1.8 mg/cm², the latter being more effective. In both cases, the CA released into the culture medium exceeded the MIC of the bacteria. Nevertheless, these mats were not effective at controlling the growth of *L. innocua*, since a greater release of CA was necessary to achieve the MIC of this bacterium. Not only did the CA load in the fibres determine their antimicrobial effect, but also its release capacity into the aqueous media. In this sense, the fibre showed a faster release and higher release capacity of the active in fatty foodstuffs (simulants D1 and D2), where practically the total amount of CA could be released from the fibres. However, in more aqueous food systems (simulants A and B), such as the bacteria culture medium, a more limited CA delivery (60-75 %) occurred with a slower rate, which reduced the potential effectiveness of the encapsulated active. This meant that the Gram negative bacteria (*E. coli*) could be effectively inhibited, whereas no growth inhibition was observed for Gram positive (*L. innocua*), which would require a greater surface density of the electrospun CA-loaded PCL fibres. This behaviour was reproduced in multilayer starch films containing the CA-loaded electrospun PCL fibres between two starch sheets, although a delayed response was observed for the antimicrobial action. In these multilayer films, a great reduction in the water vapour permeability was also observed with respect to that of starch films, without any notable changes in the other packaging functions. Therefore, active electrospun PCL fibre in multilayer starch films represents an interesting alternative for the purposes of active food packaging.

5. Acknowledgements

The authors thank the Ministerio de Economía y Competitividad (MINECO) of Spain, for the financial support for this study as a part of projects AGL2013-42989-R and AGL2016-76699-R. The author A. Tampau thanks MINECO for the pre-doctoral research grant # BES-2014-068100.

6. References

- ASTM. (1995). Standard test methods for water vapor transmission of materials. standard designations: E96-95. In *ASTM, annual book of ASTM* (pp. 406-413). Philadelphia, PA: American Society for Testing and Materials.
- ASTM. (2001). Standard test method for tensile properties of thin plastic sheeting. Standard Designations: D882. In *Annual book of ASTM standards* (pp 162-170). Philadelphia, PA: American Society for Testing and Materials.
- ASTM. (2002). Standard test method for oxygen gas transmission rate through plastic film and sheeting using a coulometric sensor. Standard Designations: 3985-95. In *Annual book of ASTM standards* (pp 472-477). Philadelphia, PA: American Society for Testing and Materials.
- Bahrami, S. H., & Gholipour Kanani, A. (2011). Effect of changing solvents on poly(ϵ -Caprolactone) nanofibrous webs morphology. *Journal of Nanomaterials*, 2011. <https://doi.org/10.1155/2011/724153>
- Ben Arfa, A., Combes, S., Preziosi-Belloy, L., Gontard, N., & Chalier, P. (2006). Antimicrobial activity of carvacrol related to its chemical structure. *Letters in Applied Microbiology*, 43(2), 149–154. <https://doi.org/10.1111/j.1472-765X.2006.01938.x>
- Bhardwaj, N., & Kundu, S. C. (2010). Electrospinning: A fascinating fiber fabrication technique. *Biotechnology Advances*, 28(3), 325–347. <https://doi.org/10.1016/j.biotechadv.2010.01.004>

- Burt, S (2004). Essential oils: their antibacterial properties and potential applications in foods—a review. *International Journal of Food Microbiology* 94 (3) 223– 253
<http://dx.doi.org/10.1016/j.ijfoodmicro.2004.03.022>
- Commission, E. (2011). EU Guidance to the Commission Regulation (EC) No 450 / 2009 of 29 May 2009 on active and intelligent materials and articles intended to come into contact with food. (450), 1–26.
- Cosentino, S., Tuberoso, C. I. G., Pisano, B., Satta, M., Mascia, V., Arzedi, E., & Palmas, F. (1999). *In-vitro* antimicrobial activity and chemical composition of Sardinian Thymus essential oils. *Letters in Applied Microbiology*, 29(2), 130–135.
<https://doi.org/10.1046/j.1472-765X.1999.00605.x>
- Crank, J. (1979). *The Mathematics of Diffusion*, (2nd ed.) London: Oxford University Press, (Chapter 4).
- Du, E., Gan, L., Li, Z., Wang, W., Liu, D., & Guo, Y. (2015). *In vitro* antibacterial activity of thymol and carvacrol and their effects on broiler chickens challenged with *Clostridium perfringens*. *Journal of Animal Science and Biotechnology*, 6(1), 58.
<https://doi.org/10.1186/s40104-015-0055-7>
- Efsa. (2012). Scientific Opinion on the Safety and efficacy of phenol derivates containing ring-alkyl, ring-alkoxy and side- chains with an oxygenated functional group (chemical group 25) when used as flavourings for all species. *Efsa J.*, 10(2), 2573.
<https://doi.org/10.2903/j.efsa.2012.2573>.
- Fabra, M. J., López-Rubio, A., & Lagaron, J. M. (2016). Use of the electrohydrodynamic process to develop active/bioactive bilayer films for food packaging applications. *Food Hydrocolloids*, 55, 11–18. <https://doi.org/10.1016/j.foodhyd.2015.10.026>
- Fernández-Pan, I., Maté, J. I., Gardrat, C., & Coma, V. (2015). Effect of chitosan molecular weight on the antimicrobial activity and release rate of carvacrol-enriched films. *Food Hydrocolloids*, 51, 60–68. <https://doi.org/10.1016/j.foodhyd.2015.04.033>

- Fu, Y., Sarkar, P., Bhunia, A. K., & Yao, Y. (2016). Delivery systems of antimicrobial compounds to food. *Trends in Food Science and Technology*, 57, 165–177. <https://doi.org/10.1016/j.tifs.2016.09.013>
- Gennadios A., Weller C. L., & Gooding C. H. (1994). Measurement errors in water vapor permeability of highly permeable, hydrophilic edible films. *Journal of Food Engineering*, Volume 21, Issue 4, pp 395-409, ISSN 0260-8774. [https://doi.org/10.1016/0260-8774\(94\)90062-0](https://doi.org/10.1016/0260-8774(94)90062-0)
- Hamori, M., Yoshimatsu, S., Hukuchi, Y., Shimizu, Y., Fukushima, K., Sugioka, N., Nishimura, A., & Shibata, N. (2014). Preparation and pharmaceutical evaluation of nano-fiber matrix supported drug delivery system using the solvent-based electrospinning method. *International Journal of Pharmaceutics*, 464(1–2), 243–251. <https://doi.org/10.1016/j.ijpharm.2013.12.036>
- Hernández-Martínez, D., Nicho, M. E., Hu, H., León-Silva, U., Arenas-Arrocena, M. C., & García-Escobar, C. H. (2017). Electrospinning of P3HT-PEO-CdS fibers by solution method and their properties. *Materials Science in Semiconductor Processing*, 61 (November 2016), 50–56. <https://doi.org/10.1016/j.mssp.2016.12.039>
- Higuera, L., López-Carballo, G., Hernández-Muñoz, P., Catalá, R., & Gavara, R. (2014). Antimicrobial packaging of chicken fillets based on the release of carvacrol from chitosan/cyclodextrin films. *International Journal of Food Microbiology*, 188, 53–59. <https://doi.org/10.1016/j.ijfoodmicro.2014.07.018>
- Hines, D. J., & Kaplan, D. L. (2012). Mechanisms of controlled release from silk fibroin films. *Changes*, 29(6), 997–1003. <https://doi.org/10.1016/j.biotechadv.2011.08.021>. Secreted
- Joint FAO/WHO, June 2001. Expert Committee on Food Additives Fifty-fifth report. http://apps.who.int/iris/bitstream/10665/42388/1/WHO_TRS_901.pdf (accessed on August 04, 2017).
- Koenig, M. F., & Huang, S. J. (1995). Biodegradable blends and composites of polycaprolactone and starch derivatives. *Polymer*, 36(9), 1877–1882.

- Kuorwel, K. K., Cran, M. J., Sonneveld, K., Miltz, J., & Bigger, S. W. (2013). Migration of antimicrobial agents from starch-based films into a food simulant. *LWT - Food Science and Technology*, *50*(2), 432–438. <https://doi.org/10.1016/j.lwt.2012.08.023>
- López, O. V., Zaritzky, N. E., Grossmann, M. V. E., & García, M. A. (2013). Acetylated and native corn starch blend films produced by blown extrusion. *Journal of Food Engineering*, *116*(2), 286–297. <https://doi.org/10.1016/j.jfoodeng.2012.12.032>
- Macagnano, A., & De Cesare, F. (2017). 17 - Electrospinning: A versatile technology to design biosensors and sensors for diagnostics. In E. B. T.-E. M. for T. E. and B. A. Kny (Ed.) (pp. 385–417). Woodhead Publishing. <https://doi.org/10.1016/B978-0-08-101022-8.00016-8>
- Majid, I., Ahmad Nayik, G., Mohammad Dar, S., & Nanda, V. (2016). Novel food packaging technologies: Innovations and future prospective. *Journal of the Saudi Society of Agricultural Sciences*. <https://doi.org/10.1016/j.jssas.2016.11.003>
- Mercante, L. A., Scagion, V. P., Migliorini, F. L., Mattoso, L. H. C., & Correa, D. S. (2017). Electrospinning-based (bio)sensors for food and agricultural applications: A review. *TrAC - Trends in Analytical Chemistry*, *91*, 91–103. <https://doi.org/10.1016/j.trac.2017.04.004>
- Ortega-Toro, R., Morey, I., Talens, P., & Chiralt, A. (2015). Active bilayer films of thermoplastic starch and polycaprolactone obtained by compression molding. *Carbohydrate Polymers*, *127*, 282–290. <https://doi.org/10.1016/j.carbpol.2015.03.080>
- Padgett, T., Han, I. Y., & Dawson, P. L. (1998). Incorporation of food-grade antimicrobial compounds into biodegradable packaging films. *Journal of Food Protection*, *61*(10), 1330–1335.
- Peleg, M. (1988). An Empirical Model for the Description Moisture Sorption Curves. *Journal of Food Science*, *53*(4), 1216–1217. <https://doi.org/10.1111/j.1365-2621.1988.tb13565.x>
- Perdones, Á., Chiralt, A., & Vargas, M. (2016). Properties of film-forming dispersions and films based on chitosan containing basil or thyme essential oil. *Food Hydrocolloids*, *57*, 271–279. <https://doi.org/10.1016/j.foodhyd.2016.02.006>

- Petchwattana, N., & Naknaen, P. (2015). Utilization of thymol as an antimicrobial agent for biodegradable poly (butylene succinate). *Materials Chemistry and Physics*, 163, 369–375. <https://doi.org/10.1016/j.matchemphys.2015.07.052>
- Pol, I. E., & Smid, E. J. (1999). Combined action of nisin and carvacrol on *Bacillus cereus* and *Listeria monocytogenes*. *Letters in Applied Microbiology*, 29(3), 166–170. <https://doi.org/10.1046/j.1365-2672.1999.00606.x>
- Pushpadassa, H. A., Kumara, A., Jackson, D. S., Wehling, R. L., Dumaise, J. J., & Hannaa, M. A. (2009). Macromolecular changes in extruded starch-films plasticized with glycerol, water and stearic acid. *Starch/Staerke*, 61(5), 256–266. <https://doi.org/10.1002/star.200800046>
- Ramos, M., Beltrán, A., Peltzer, M., Valente, A. J. M., & Garrigós, M. del C. (2014). Release and antioxidant activity of carvacrol and thymol from polypropylene active packaging films. *LWT - Food Science and Technology*, 58(2), 470–477. <https://doi.org/10.1016/j.lwt.2014.04.019>
- Requena, R., Jiménez, A., Vargas, M., & Chiralt, A. (2016). Poly[(3-hydroxybutyrate)-co-(3-hydroxyvalerate)] active bilayer films obtained by compression moulding and applying essential oils at the interface. *Polymer International*, 65(8), 883–891. <https://doi.org/10.1002/pi.5091>
- Requena, R., Vargas, M., & Chiralt, A. (2017). Release kinetics of carvacrol and eugenol from poly(hydroxybutyrate-co-hydroxyvalerate) (PHBV) films for food packaging applications. *European Polymer Journal*, 92(May), 185–193. <https://doi.org/10.1016/j.eurpolymj.2017.05.008>
- Rieger, K. A., & Schiffman, J. D. (2014). Electrospinning an essential oil: Cinnamaldehyde enhances the antimicrobial efficacy of chitosan/poly (ethylene oxide) nanofibers. *Carbohydrate Polymers*, 113, 561–568. <https://doi.org/10.1016/j.carbpol.2014.06.075>
- Siepmann, J., & Peppas, N. A. (2011). Higuchi equation: Derivation, applications, use and misuse. *International Journal of Pharmaceutics*, 418(1), 6–12. <https://doi.org/10.1016/j.ijpharm.2011.03.051>

- Sill, T. J., & von Recum, H. A. (2008). Electrospinning: Applications in drug delivery and tissue engineering. *Biomaterials*, 29(13), 1989–2006. <https://doi.org/10.1016/j.biomaterials.2008.01.011>
- Tampau, A., González-Martinez, C., & Chiralt, A. (2017). Carvacrol encapsulation in starch or PCL based matrices by electrospinning. *Journal of Food Engineering*, 214, 245–256. <https://doi.org/10.1016/j.jfoodeng.2017.07.005>
- Tehrany, E. A., & Desobry, S. (2007). Partition coefficient of migrants in food simulants/polymers systems. *Food Chemistry*, 101(4), 1714–1718. <https://doi.org/10.1016/j.foodchem.2006.03.058>
- Tunc, S., Chollet, E., Chalier, P., Preziosi-Belloy, L., & Gontard, N. (2007). Combined effect of volatile antimicrobial agents on the growth of *Penicillium notatum*. *International Journal of Food Microbiology*, 113(3), 263–270. <https://doi.org/10.1016/j.ijfoodmicro.2006.07.004>
- Ultee, A., Gorris, L. G. M., & Smid, E. J. (1998). Bactericidal activity of carvacrol towards the food-borne pathogen *Bacillus cereus*. *Journal of Applied Microbiology*, 85(2), 211–218. <https://doi.org/10.1046/j.1365-2672.1998.00467.x>
- Valencia-Sullca, C., Jiménez, M., Jiménez, A., Atarés, L., Vargas, M., & Chiralt, A. (2016). Influence of liposome encapsulated essential oils on properties of chitosan films. *Polymer International*, 65(8), 979–987. <https://doi.org/10.1002/pi.5143>
- Yalkowsky, S.H., He, Y., & Jain, P. (2010). Handbook of Aqueous Solubility Data (second ed.) (pp 710). Florida, CRC Press.
- Xue, J., Song, J., Dong, Y., Xu, L., Li, J., & Zeng, H. (2017). Nanowire-based transparent conductors for flexible electronics and optoelectronics. *Science Bulletin*, 62(2), 143–156. <https://doi.org/10.1016/j.scib.2016.11.009>

Biodegradation of thermoplastic starch films containing electrospun poly-(ϵ -caprolactone) encapsulating carvacrol

Alina Tampau ^a, Chelo González-Martínez ^b, Amparo Chiralt ^c

^{a, b, c} Instituto Universitario de Ingeniería de Alimentos para el Desarrollo, Ciudad Politécnica de la Innovación, Universitat Politècnica de Valencia, Camino de Vera, s/n, 46022 Valencia, Spain.

Polymer Degradation and Stability- BIOPOL 2019 special issue

<https://doi.org/10.1016/j.polymdegradstab.2020.109100>

altam@upvnet.upv.es

Abstract

The biodegradation and disintegration of thermoplastic starch multilayers containing carvacrol(CA)-loaded poly-(ϵ -caprolactone) electrospun mats were evaluated under thermophilic composting conditions for 45 and 84 days, respectively, and compared with non-loaded carvacrol films and pure starch films. Sample mass loss, thermogravimetric and visual analyses were performed throughout the disintegration test. The disintegration behaviour of all multilayers was similar, reaching values of 75-80 % after 84 days. Biodegradation, assessed by carbon dioxide measurements, revealed that all the carvacrol-free films completely biodegraded after 25 composting days. However, the presence of CA notably affected the compost inoculum activity, thus limiting the biodegradability of the CA-loaded multilayers to a maximum value of around 85 % after 45 days. Nevertheless, this value was close to that established by the standard ISO method to qualify as biodegradable material.

Keywords

thermoplastic starch; poly-(ϵ -caprolactone); carvacrol; TGA; disintegration; biodegradation.

Abbreviations

EFSA, European Food Safety Authority; S, starch; PCL, poly-(ϵ -caprolactone); CA, carvacrol; GAA, glacial acetic acid; MCC, microcrystalline cellulose; TGA, thermogravimetric analysis; DTGA, derivative thermogravimetric analysis; SSR, synthetic solid residue; DS, dry solids; VS, volatile solids; MC, moisture content.

1. Introduction

The quantity of plastics produced in the first 10 years of the current century is likely to approach the quantity produced in the entire preceding century [1] and only a modest percentage of these packaging materials ends up being recycled (plastic recycling rates of 9.1% in the US in 2015 [2] and 40.9% in the EU in 2016 [3]). The usage and disposal of plastics is controversial and there are growing concerns about waste accumulation, problems for wildlife resulting from ingestion and the potential for plastics to transfer harmful chemicals to wildlife and humans. There are numerous studies alerting to the alarming levels of microplastics found in oysters [4], mussels [5],[6],[7] crabs [8] and fish [9], [10] which move up through the food chain, ending up in the human body. Risk assessments developed by the European Food Safety Authority (EFSA) [11] have taken these considerations into account. However, perhaps the most important overriding concern is that our current usage is not sustainable [1].

Due to the environmental impact these plastics generate owing to their long degradation times, more effort is being made to develop packaging from biodegradable materials. This trend is aligned with consumer demand for more natural products for food contact materials. As a result, new materials have been developed, using biodegradable polymers from renewable sources, such as polysaccharides and proteins, and natural active agents of plant or marine origin.

Starch (S) is one of the most commonly studied, readily available carbohydrates, obtainable from renewable sources at relatively low cost. Starch films present very good oxygen barrier capacity, but due to their hydrophilic nature, films exhibit water sensitivity and poor water vapour barrier properties. Combining starch layers with sheets of hydrophobic polymers — creating multilayer assemblies — could provide adequate materials for food packaging. Following this strategy, poly-(ϵ -caprolactone) (PCL) (a completely biodegradable aliphatic polyester) [12] has been used in combination with thermoplastic corn starch, forming bilayers with improved properties when compared to net starch films [13], [14]. These multilayer films became active films with antimicrobial properties by incorporating carvacrol encapsulated into electrospun PCL layers [14]. Carvacrol (CA) is a phenolic monoterpene, one of the major constituents of oregano and thyme essential oil [15]. It exhibits significant *in vitro* antimicrobial [16], [17], [18] and antioxidant activity [19], [20], and has been approved as a food additive by Joint FAO/WHO [21] and as flavouring substance by EFSA [22]. It is currently being used

as a bioactive in packaging materials [23], [24], [25]. Thus, the addition of active compounds to biopolymer layers confers antimicrobial and/or antioxidant properties, making these materials more attractive as food packaging candidates. Given the inhibiting effect of such antimicrobial compounds on microflora, it is likely that the biodegradation of these matrices could be altered by the presence of active compounds [26], [27].

Composting is a form of organic recycling, based on the activity of the microbiota population, which breaks down the biodegradable parts of the waste, generating stabilized organic residue [28]. The resulting compost could be used as soil conditioner to increase soil productivity by replenishing some of its nutrients, and reduce the excessive use of synthetic fertilizers [26]. As pointed out by Balaguer et al. [26], not all biodegradable polymers are compostable. Moreover, Adamcová et al. [29] have reported that even though a polymer is labelled by its maker as 100% degradable, those samples did not show any visual signs of degradation in the laboratory or in real life composting tests. Therefore, the biodegradability as well as the compostability of the developed active packaging material made with biodegradable materials cannot be assumed as such. It must be analysed to ensure that the newly created materials comply with the requirements specified by law [28].

The aim of this study is to assess the disintegration and biodegradation behaviour under laboratory composting conditions of starch-PCL multilayer films, incorporating or not carvacrol.

2. Materials and experimental design

2.1. Materials

Starch for film preparation was provided by Roquette Laisa España S.A. (Benifaió, Valencia, Spain), while PCL pellets (average Mn 80,000), CA and glacial acetic acid (GAA) were obtained from Sigma-Aldrich (Sigma–Aldrich Chemie, Steinheim, Germany).

For the biodegradation and disintegration studies, ripe compost (no older than 4 months) was offered by a local solid residue treatment plant (Valencia, Spain). Other components used for the disintegration test consisted of urea (Urea 46 % Prill, Tarazona, Spain), sawdust (Productos de Limpieza Adrian, Almacera, Valencia, Spain), corn starch (Roquette Laisa España S.A. (Benifaió, Valencia, Spain), rabbit-feed (Super Feed S.L., Madrid, Spain), saccharose (White sugar, Azucarera Ebro, Madrid, Spain) and corn seed oil (Hacendado

brand, Mercadona supermarkets, Spain). For the biodegradation test, vermiculite from a local market was used. Microcrystalline cellulose (MCC) was purchased from Sigma Aldrich Química S.L., Madrid, Spain.

Magnesium nitrate ($\text{Mg}(\text{NO}_3)_2$) and Phosphorous pentoxide (P_2O_5) used for creating controlled relative humidity environments for sample storage were purchased from Panreac Química S.A. (Castellar de Valles, Barcelona, Spain).

2.2. Films preparation

The starch films were prepared by compression moulding, following the protocol described previously by Tampau et al. [14]. Briefly, a mixture of starch : glycerol : water=1 : 0.3 : 0.5 (wt. / wt.) was processed in a two-roll mill (Model LRM-M-100, Labtech Engineering, Thailand) at 160 °C and 8 rpm for 30 minutes. The resulting pellets were conditioned for one week at 25 °C in a desiccator with saturated $\text{Mg}(\text{NO}_3)_2$ aqueous solution, to ensure a 53 % relative humidity. Each individual starch film was obtained from 4 grams of conditioned pellet, moulded by thermo-compression in a press (Model LP20, Labtech Engineering, Thailand), at 50 bars / 160 °C for 2 min, then at 130 bars / 160 °C for 6 min and cooled down to 50 °C for 3 min. Multilayer films were prepared by coating one side of a starch film with an electrospun layer (application time of 90 minutes) of a PCL solution (15 % wt. / wt.) in GAA with or without CA (15 g carvacrol / 100 g PCL), following the methodology described by Tampau et al. [14]. Later on, the PCL-coated starch films were thermo-compressed with another net starch film at 130 bars / 80 °C for 4 min followed by a cooling at 50 °C for 2 min. Thus, three multilayer films were obtained: starch-starch (SS), starch-PCL (SPS) and starch-PCL containing carvacrol (SPCAS).

2.3. Samples characterization

2.3.1. Moisture content and visual appearance

Prior to the tests, the multilayer films were analysed as to their moisture content (as described by Cano et al. [27]) and thickness, measured in 5 different points using a Palmer digital micrometre (Comecta, Barcelona, Spain). In order to determine the C, N and H composition of the samples, an elemental analysis was performed by means of a Euro EA3000 analyser (EUROVECTOR, Milan, Italy). Analyses were carried out in triplicate.

The visual changes that samples presented throughout the disintegration experiments were analysed. For this purpose, the samples extracted from the reactors were previously dried in

a vacuum oven at 40 °C for a week. Pictures were taken by means of a digital camera (EOS 5D Mark II, Canon, Japan).

2.3.2. Thermogravimetric analysis

The samples were submitted to a thermogravimetric analysis (TGA) at different times of the composting process (day 0, 14, 21, 42 and 84). Prior to this analysis, the composted samples were conditioned by drying in a vacuum oven at 40 °C for one week and later transferred to a desiccator with P₂O₅ until constant weight. A TGA/SDTA 851e analyser (Mettler Toledo, Schwarzenbach, Switzerland) working under nitrogen flow (20 mL / min) was used to obtain the weight loss curves vs. temperature (TGA) and the first derivatives (DTGA). Between 5 and 10 mg of conditioned sample was placed in a 70 µL alumina crucible and heated from 25 to 600 °C at 10 K / min. With the software provided by the Mettler Toledo analyser, the onset, peak and end temperatures of the degradation steps were obtained. All measurements were done in triplicate.

2.4. Compost and synthetic solid residue (SSR)

The ripe compost (acting as the inoculum) was prepared by removing any inert pieces like shards of glass and stones, and then sieved. Its pH was assessed by mixing 1 part compost to 5 parts deionized water and measured immediately, to ensure a value between 7 and 9.

Following the ISO 20200 International Standard (2004) [30], a synthetic solid residue (SSR) was prepared for the disintegration test, by manually mixing the required components. For the purpose of the biodegradation test, the inoculum was mixed only with vermiculite to prevent compacting and thus ensuring good oxygenation. For both tests, the water content was adjusted to 55 % (wt. / wt.) by adding de-ionized water and gently stirring. This ensured the compost was moist, but without visible free water.

The SSR was characterized as to its dry solids (DS) and volatile solids (VS) content, as specified by ISO 20200 [30], both at the beginning, as well as at the end of the composting process (84 days). The DS was determined by drying the analysed sample in an oven at 105 °C until constant mass was reached and expressed as a percentage of the total mass of the analysed sample. The VS was obtained from the previously dried sample by calcination at 550 °C in a muffle (Selecta, Barcelona, Spain) until constant weight, and expressed as a percentage with respect to the DS. The ripe compost used for the biodegradation study was also characterized in terms of DS and VS at initial time.

2.5. Disintegration test

A composting study was carried out in the laboratory, following the International Standard guidelines [30]. Roughly 5 grams of film samples (cut into 25 x 25 mm squares) were placed with 1 kg of wet SSR in each composting unit (reactor) consisting of a polypropylene box with lid. On each one of the narrow sides of the reactor, one hole (5 mm in diameter) was made at approximately 6.5 cm from the bottom, to allow gas exchange between the inside and outside atmospheres. The filled reactors were placed in an oven (Selecta, J.P. Selecta S.A., Barcelona, Spain) at 58 ± 2 °C to ensure controlled thermophilic conditions. Their initial weight was recorded and was closely monitored throughout the duration of the essay (84 days), restoring it totally or partially with de-ionised water, as specified by the aforementioned ISO standard [30]. Three reactors per formulation were prepared, each reactor containing a mesh bag with around 5 g of sample together with individual sample squares to be used in the TGA and visual analysis. Prior to these analysis, the samples were gently cleaned with a soft brush. The disintegration percentage after 84 days ($D_{84}(\%)$) was calculated by means of the eq. 1:

$$D_{84}(\%) = \frac{m_0 - m_{84}}{m_0} \cdot 100 \quad (\text{eq. 1})$$

where m_0 is sample dry mass at the start of test and m_{84} is dry mass of the final disintegrated samples after 84 composting days.

2.6. Biodegradation test

The starch films containing electrospun PCL material were also submitted to an aerobic biodegradation assessment under controlled composting conditions following the guidelines of the ISO 14855-1 standard method [31]. The principle of this method assumes that the CO_2 that forms during the biodegradation of a sample is directly proportional to the carbon percentage that is biodegraded from that respective sample.

This test was performed inside airtight glass jars of 2000 mL in volume, whose lids were modified with a covered septum. Inside the jars, 2 polypropylene cups were placed: one containing 3 g of dry compost mixed with 1 g of vermiculite and a sample quantity equivalent to 50 mg of carbon, while the second one, contained water to ensure 100% relative humidity inside the jar. The samples were maintained up to 45 days at 58 ± 2 °C. A control sample was also prepared using MCC as reference material [26]. A blank sample contained just compost with vermiculite. The percentage of CO_2 generated inside the reactors was measured in

triplicate using a CO₂ analyser (CheckMate 9900 PBI Dansensor, Ringsted, Denmark) throughout the biodegradation process.

The theoretical amount of CO₂ that could be generated from the sample ($CO_2^{Th}_S$) was estimated from its carbon content applying eq. 2. The biodegradation percentage (B%) at each time was calculated as the ratio between the cumulative amounts of CO₂ produced by the sample throughout the 45 days with respect to the theoretical amount ($CO_2^{Th}_S$), applying eq. 3 [31].

$$CO_2^{Th}_S = DW_S \cdot C_S \cdot \frac{Mw_{CO_2}}{Mw_C} \quad (\text{eq. 2})$$

$$B\% = \frac{\sum CO_{2S} - \sum CO_{2B}}{CO_2^{Th}_S} \quad (\text{eq. 3})$$

where:

- DW_S is the dry weight of sample (g);
- C_S is the percentage of carbon in the dry sample, as determined by elemental analysis (%);
- Mw_{CO_2} and Mw_C are the molecular weights of CO₂ and of C respectively;
- $\sum CO_{2S}$ is the cumulative amount of carbon dioxide in the sample reactors at each time throughout test period (g);
- $\sum CO_{2B}$ is the cumulative amount of carbon dioxide detected in the blank reactor at each time (g).

The experimental data obtained from the biodegradation test was modelled using Hill's equation (eq.4) in order to describe the kinetics of the process.

$$B\% = B\%_{max} \cdot \frac{t^n}{k^n + t^n} \quad (\text{eq. 4})$$

where:

- B%_{max} is the percentage of biodegradation at infinite time (%);
- t is the time (days);
- k is the time at which 0.5B%_{max} has occurred;
- n is the curve radius of the sigmoid function.

2.7. Statistical analysis

All statistical analysis were performed through analysis of variance (ANOVA) using the application STATGRAPHICS Centurion XVI (Statgraphics Technologies, Inc., The Plains,

Virginia 20198, USA). Fisher's least significant difference (LSD) procedure was used at the 95% confidence level.

3. Results

3.1. Properties of multilayer films

Table 1 presents the properties of the starch film samples prior to the tests. As can be observed, while the films presented similar moisture content values among formulations, the presence of the electrospun layer of PCL significantly increased the film thickness and the carbon content of these multilayers, according to the presence of PCL with higher C ratio in the molecule. The thickness of multilayer films notably increased with respect to the usual thickness of monolayer films. [32].

Table 1. Samples' moisture content (MC), thickness and elemental carbon (C %) analysis prior to the composting test. Mean values and standard deviation.

Sample / reactor	MC (%)	Thickness (µm)	C %
SS	6.73±0.16 ^{ab}	430±30 ^a	40.4±0.2 ^a
SPS	6.59±0.16 ^a	500±30 ^b	41.2±0.6 ^{ab}
SPCAS	6.956±0.010 ^b	490±20 ^b	42.3±1.3 ^b

Different superscript letters (a, b, c...) in the same column indicate significant differences (p<0.05) among samples.

3.2. Compost characteristics

The active compost used as inoculum for both tests presented a pH of 8.25 (measured according to the ISO method), total dry solids (DS) content of 70±1 % and organic matter content of 56±1 % (expressed as volatile solids (VS) with respect to the dry solids). Characteristics of the pre-composting SSR prepared for the disintegration test are shown in Table 2. The volatile solids content decreased slightly at the end of the composting process with respect to the initial value, as an indicator of the organic matter being converted into CO₂ by the compost microflora. Then, the test was validated taking into account the standard method, which established a reduction of the volatile content in the sample after the composting period (R values, Table 2) of over 30 % as well as the standard deviation the

disintegration values of the samples (D_{84} (%), in Table 2) lower than 10 units. Likewise, throughout the duration of the test, the colour changes described by the ISO 20200 standard [30] were observed in the compost (from lighter yellow (due to sawdust presence) to a darker brown). The odour of the compost was strongly ammoniacal within the first week, and it disappeared gradually, according to that described in ISO 20200 standard [30].

Table 2. Volatile solids VS (g volatiles / 100 g compost DS) before and after the composting period of the disintegration test, the difference between these values (R: expressed as % with respect to the initial value) and disintegration percentage for the samples. Mean values and standard deviations.

Reactor	VS (g / 100 g DS)		R (%)	Disintegration D_{84} (%)
	Pre composting	Post composting	Decrease in VS	
SSR (blank)	95.0±0.3	91.3±0.6 ^c	43±1 ^a	-
SS		80.5±0.7 ^a	55±1 ^b	75±6 ^a
SPS		85.9±1.1 ^b	52± 2 ^b	81.1±0.5 ^a
SPCAS		84.5±0.5 ^b	51± 2 ^b	75±4 ^a

Different superscript letters (a,b,c...) in the same column indicate significant differences ($p < 0.05$) among samples.

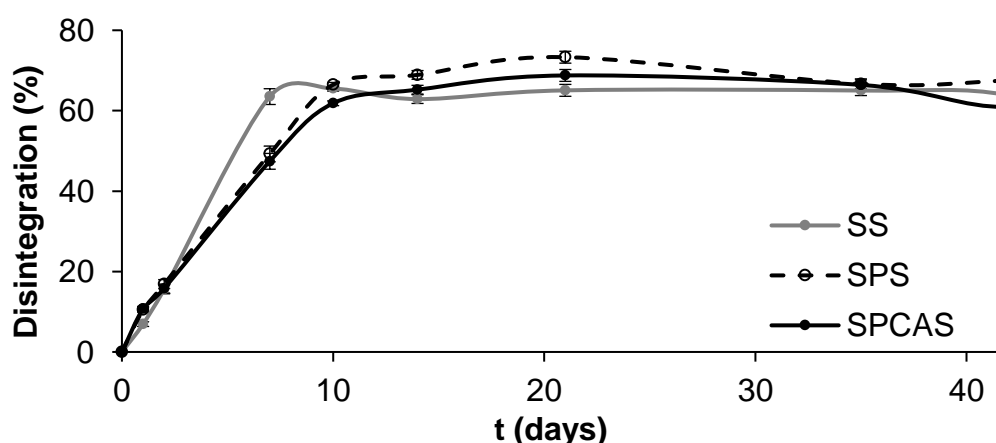


Figure 1. Development of sample disintegration as a function of time for the different multilayer films. (Mean values and LSD intervals ($p < 0.05$)).

3.3. Disintegration test

The degree of disintegration (D) of films when exposed to laboratory-scale composting environmental conditions (58 ± 2 °C for 84 days) provided information about the physical breakdown of films into smaller fractions. Figure 1 shows the disintegration values as a function of time for the different samples. As shown, all films presented similar disintegration patterns, but a faster disintegration rate within the first 7 days can be observed for pure starch bilayer films (SS). Similar asymptotic values were attained for the different samples (75-80%) at the end of the test period (Table 2).

The visual appearance of the samples at different composting times is also presented in Figure 2. Non-significant differences ($p < 0.05$) in the D_{84} (%) values were found among samples at the end of the composting period, being the mean D_{84} (%) value 77 ± 5 %. These values are in agreement with those mentioned by Castro-Aguirre et al. [33] for trays with similar composition.

As reported by Balaguer et al. [26], the erosion kinetics are affected by two major factors: 1) the water diffusion through the polymer layer and 2) the rate of degradation of the polymeric chains. Other authors [27] observed higher disintegration rates for starch films obtained by casting which could be attributed to differences in the films thickness and polymer arrangements in the film structure obtained by different processing methods. Nevertheless, this disintegration process in the obtained bilayer films was very similar according to their similar specific surface. This permits the water diffusion and uptake, favouring the microbial action and bulk erosion, thus breaking the matrix in small fragments.

The degradation degree of polymer throughout the disintegration period has been analysed via thermogravimetric analysis at different times. Figure 3 shows TGA and DTGA curves obtained for the films at different times and Table 3 gives the onset and peak temperatures for the degradation steps of the samples at initial and final time of the disintegration test. As can be observed in Figure 3, samples presented a first degradation step at around 61-63 °C (T_p), corresponding to the evaporation of bound water. This step was not detected in the samples at initial time ($t=0$), which suggests that the partially degraded samples exhibit greater water binding capacity due to the changes in the mean molecular weight or composition of the substrate. The main peak corresponding to the starch degradation showed the maximum degradation rate at T_p around 280-290 °C, in agreement with the value reported

by Collazo-Bigliardi et al. [34] for starch films. However, it is remarkable that the peak became wider and split throughout the composting period.
















day	Sample		
	SS	SPS	SPCAS
0			
1			
7			
14			
42			

Figure 2. Visual appearance of the samples throughout the disintegration period.

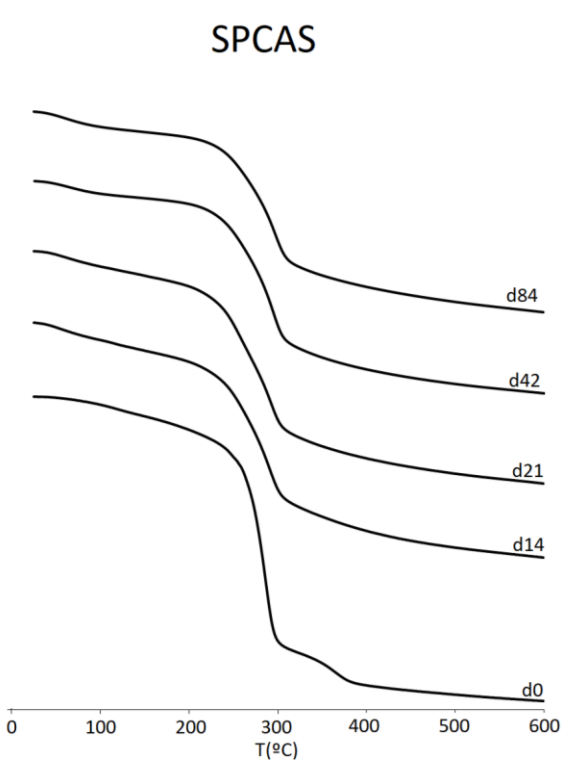
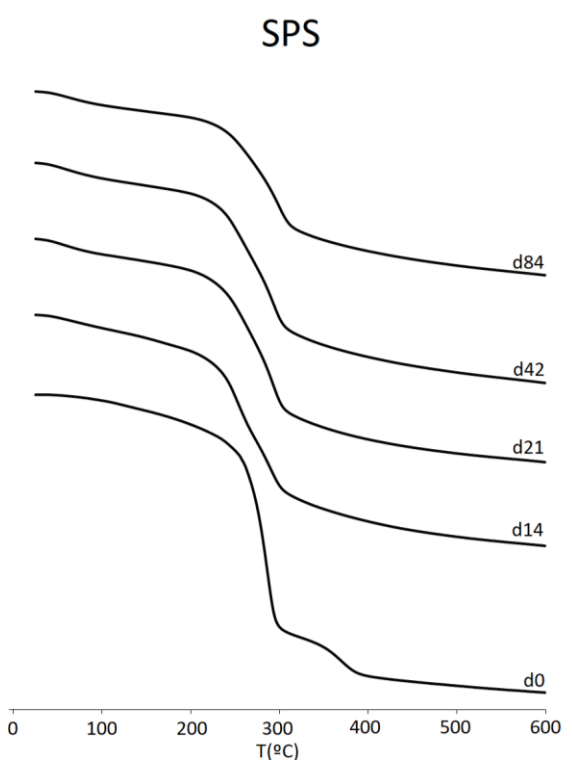
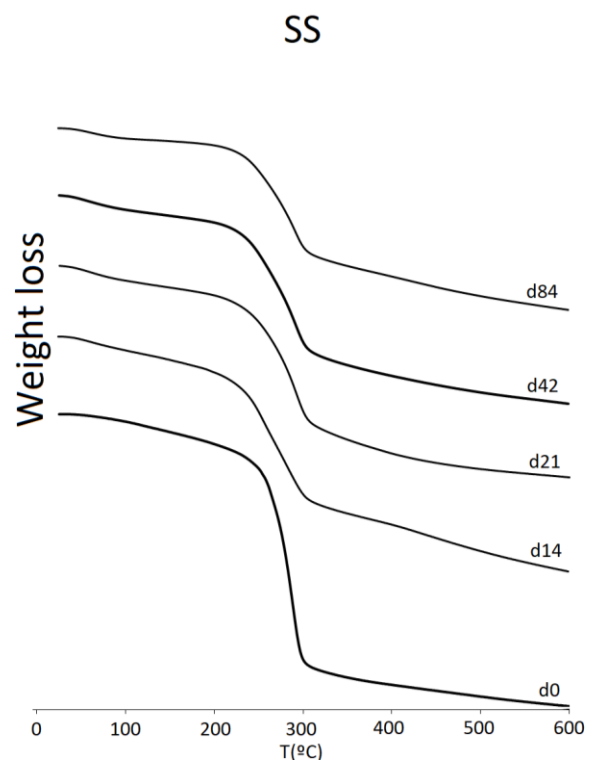
This reflects the formation of starch subunits of lower molecular weight that degrade at lower temperature, as has been observed by other authors [35], [36]. The mass loss profiles (DTGA curves) slightly vary for the different multilayers. This suggests differences in the degradation

mechanisms in each case, depending on the presence of PCL and carvacrol. The degradation step of electrospun PCL at about 360 °C (as described by Tampau et al. [14]) only appeared in the initial samples, and it was no longer observed in samples at 14 days of the process. This suggests most of the PCL polymer chains were quickly broken down by the composting bacteria due to the low thickness (less than 60 µm) of the electrospun layer and the possible detachment of the multilayer assembly, promoted by the starch swelling in the wet compost environment, which increases the specific surface area of the PCL sheet and the disintegration's effectiveness. No quantitative thermo-release of carvacrol was observed at any time of the disintegration process, probably due to its low mass fraction in the bilayer, as reported in a previous study [14].

The percentage of residual mass at 600 °C is also presented in Table 3. All initial samples showed low values for this parameter, which significantly ($p < 0.05$) increased after the composting period. This was in agreement with the mineralization process, as reported by others authors [27].

Table 3. TGA parameters obtained for the pre- and post- composting samples: onset (T_o), peak (T_p), endset (T_e) temperatures, and pyrolysis residual mass at 600 °C. Different superscript letters in the same column indicate significant differences ($p < 0.05$) among samples.

Sample	Day	1 st step			2 nd step		3 rd step		Residual mass (%)
		T_o	T_p	T_e	T_o	T_p	T_o	T_p	
SS	0	-	-	-	257±1 ^b	286±2 ^b	-	-	3±3 ^a
	84	37±4 ^a	63±1 ^a	109±3 ^a	223±11 ^a	290±1 ^c	-	-	34±5 ^b
SPS	0	-	-	-	244±2 ^b	281±1 ^a	331±15 ^a	366±5 ^a	6±1 ^a
	84	39±4 ^a	62±3 ^a	104±4 ^a	227±15 ^a	293±2 ^d	-	-	37±4 ^b
SPCAS	0	-	-	-	244±1 ^b	282±1 ^a	321±28 ^a	362±8 ^a	5±2 ^a
	84	37±4 ^a	61±4 ^a	105±3 ^a	243±6 ^b	293±1 ^d	-	-	34±2 ^b



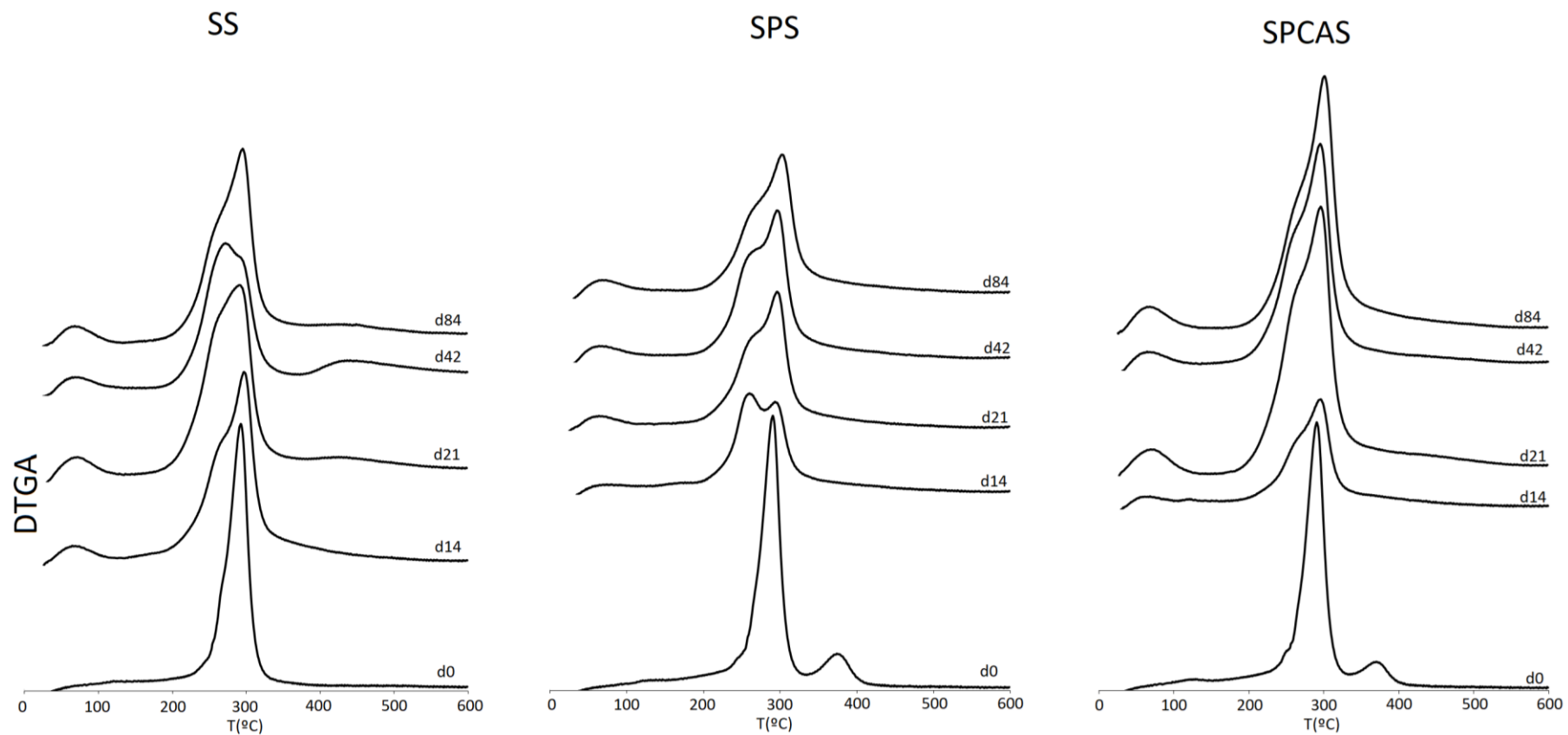


Figure 3. TGA (previous page) and DGTA curves of starch multilayer films submitted to the disintegration process at different composting times (0, 14, 21, 42 and 84 days).

3.4. Biodegradation test

The samples' biodegradability potential was assessed in a laboratory setup by direct measurement of the CO₂ generated during aerobic composting at 58±2 °C for 45 days. The compostable material is used by microorganisms as an energy source for their metabolic activities and cellular growth, which under aerobic conditions means the transformation of the samples' carbon into CO₂. The maximum amount of CO₂ that could be generated from the samples was theoretically calculated based on the carbon content (Table 1) previously determined through elemental analysis.

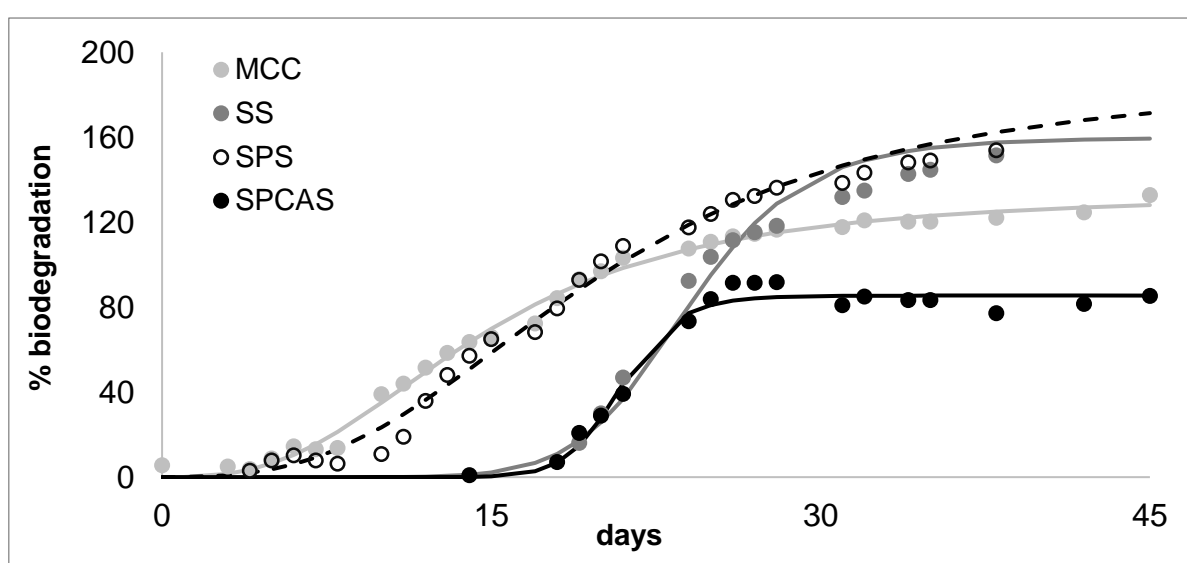


Figure 4. Biodegradation kinetics of MCC and the different films with and without carvacrol throughout the composting time. Experimental data (symbols) and Hill's fitted model (lines).

Figure 4 presents the biodegradation kinetics of the starch based multilayers and the microcrystalline cellulose used as reference material. All samples exhibited the typical sigmoid profile of the respirometric test in agreement with other studies [26], [27], with an initial lag period lasting among 4-18 days depending on the sample, a biodegradation phase and a plateau after around 30 days. The initial lag period for MCC sample was similar to those found by others authors [27]. For the multilayers, this period was longer than those found in the literature for cast starch based films [27], which could be due to the different film thickness and polymer structure or crystalline content, affected by the film's processing method. Furthermore, SPS displayed a shorter initial lag period than SS films, probably because of the lack of adherence among hydrophilic (SS) and hydrophobic (PCL) layers

[37] and the multilayer detachment throughout the process that enhances the specific film surface area and biodegradation rate. The effect of specific surface area on the biodegradation behaviour of films has also been previously reported by other authors [38].

For starch and cellulose, amylases and cellulases are responsible for the cleavage of glycosidic bonds [39]. The degradation of PCL mainly takes place by enzymatic hydrolytic ester cleavage, which is attributed to microorganisms that secrete extracellular PCL depolymerases such as esterase, cutinase and lipase [40], [41], [42]. The PCL also undergoes hydrolytic degradation due to the presence of hydrolytically labile aliphatic ester linkages, but this degradation is rather slow because of the hydrophobic nature of PCL [43]. After 25 days, biodegradation of the reference sample (MCC) was greater than 70%, thus meeting the requirements established by the ISO 14855 standard [31], and the CA-free film samples reached values of around 100 % of biodegradation (B25% values, Table 4).

The biodegradation experimental values were fitted by the Hill's model, and the obtained parameters are shown in Table 4. As can be observed, MCC, SS and SPS films reached maximum biodegradation values greater than 100%, which can be due to the priming effect. This effect occurs when the compost inoculum in the samples' reactors produces more CO₂ than the one in the blank reactors [44], as microflora is overstimulated by small molecules being released into the medium as consequence of the polymer degradation. On the other hand, SPCAS was not fully degraded during the composting period, which must be attributed to the presence of carvacrol, reaching a B_{max} (%) value of around 85 %. The CA loaded electrospun PCL fibres in multilayer films have been reported to exert an effective antimicrobial action due to the CA diffusion into the starch layers [14]. These authors reported that glass transition temperature of starch and melting properties of PCL were modified when carvacrol was present in the multilayer, due to the expected migration of the compound occurred into the global film thickness. This migration of the antimicrobial carvacrol to the starch layers in the multilayer assembly will affect biodegradation under composting conditions of both PCL and S sheets, thus reaching lower final biodegradation values. Other studies carried out with starch and gluten films incorporating active essential oils showed that the presence of these antimicrobials did not significantly inhibit the biodegradation process of the films [26], [27]. In these cases, the use of hydrophilic films, which absorb water easily, contributed to the plasticization of the polymer matrix and thus, to the fast antimicrobial compound release and volatilization, and so, it doesn't affect the microbial assimilation of the films under composting exposure. In contrast, the presence of

carvacrol in the multilayer assembly with greater thickness seems to increase the persistence of the antimicrobial in the films, thus partially inhibiting the microbial action and the enzyme access to the polymer, further limiting the biodegradation processes.

Table 4. Hill's parameters: n , k (the time needed for 50 % of B_{max} to occur), B_{max} (percentage of biodegradation at infinite time), maximum biodegradation rate (τ_{max}), time at this maximum ($t_{\tau max}$) for the different films and microcrystalline cellulose (MCC, reference) and R^2 (correlation coefficient for the fitted model).

Sample	n	k (days)	B_{max} (%)	B_{25} (%)	τ_{max} (%B/day)	$t_{\tau max}$ (days)	R^2
MCC	2.8	14.5	134	110	7.3	11	0.90
SS	9.1	24.0	160	95	15.2	24	0.85
SPS	2.8	19.8	188	124	7.6	15	0.96
SPCAS	16.2	20.9	85	81	16.5	21	0.80

Figure 5 shows the biodegradation rates obtained from the first derivative of Hill's equation as a function of time for each sample. In Table 4, the maximum biodegradation rate (τ_{max}) and the time needed to reach this maximum ($t_{\tau max}$) value are shown. SS bilayer exhibited greater degradation rates than SPS (around 15.2 and 7.6 %B/day, respectively) but delayed in time. This can be attributed to the greatest adhesion force between the two starch layers in the SS assembly that limit the water diffusion between layers, making the greater sample thickness more effective than in the SPS assembly. In the latter, the starch swelling in the wet ambient should enhance the detachment of the layers, reducing the effective thickness of the multilayer. This should favour a more extended biodegradation process with lower maximum biodegradation rate, in line with the progressive increase in the specific surface area of the multilayer assembly.

Additionally, the polyester enzymatic degradation (leading to small organic acid fractions) could also affect the biochemical route of starch degradation. SPS films with and without carvacrol exhibited different maximum biodegradation rates (16.5 and 7.6 %B/day, respectively) and these values were reached at different incubation times (21 and 15 days for SPCAS and SPS, respectively). So, those films incorporating CA needed a longer composting exposure time to reach the maximum biodegradation rate than those films

without the antimicrobial agent. This could be attributed to the time necessary for carvacrol volatilization and the reduction of its inhibitory effect.

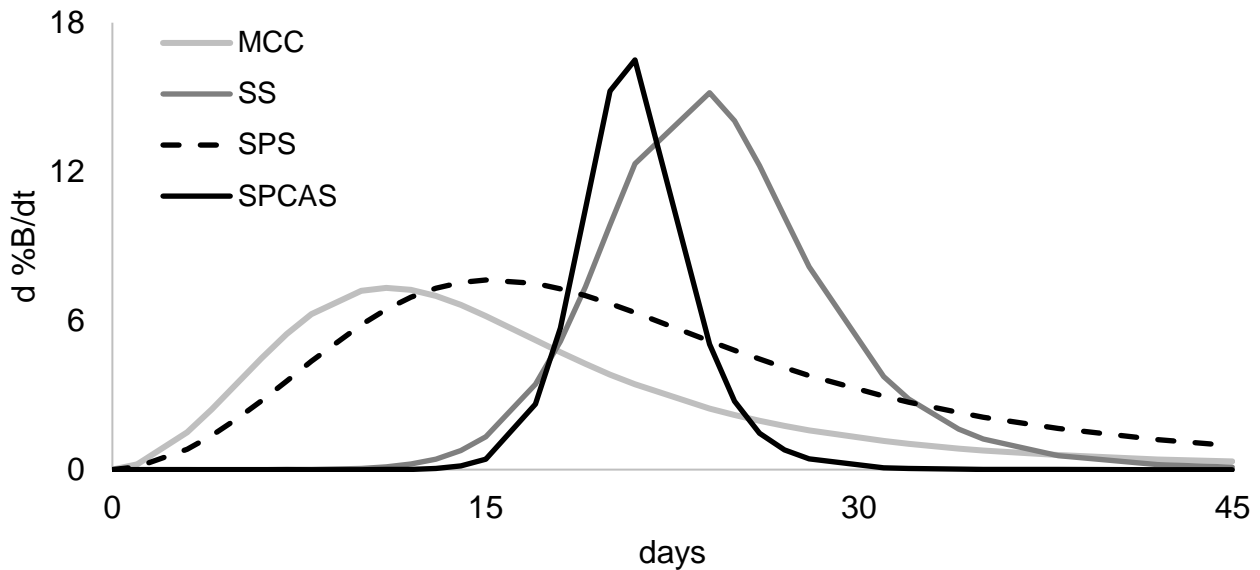


Figure 5. Biodegradation rates of CMC and the different films with and without carvacrol throughout the composting time.

4. Conclusions

All multilayer films (containing or not CA) exhibited the same trend of disintegration throughout the composting exposure time. The biodegradation process of pure bilayer starch films was retarded, in comparison with starch-PCL multilayer, by the greater effective thickness of the bilayer, due to the highest adhesion forces between the starch sheets. In contrast, starch-PCL multilayers, exhibited an earlier, more extended degradation behaviour with lower peak rate. The biodegradation test revealed that the presence of CA notably affected the compost inoculum activity, thus limiting the biodegradability of the CA-loaded multilayers to a maximum value of around 85 %. Nevertheless, the biodegradation values reached by the CA loaded films were very close to that established by the standard ISO method to be considered as biodegradable material (90 %). Further biodegradation studies under longer composting times are recommended to evaluate the total biodegradation of carvacrol-loaded SPS films.

5. Acknowledgements

The authors thank the Ministerio de Economía y Competitividad (MINECO, Spain) for funding this study through the pre-doctoral grant BES-2014-068100 and through the investigation project AGL2016-76699-R.

6. References

- [1]. R. C. Thompson, C. J. Moore, F. S. vom Saal, S. H. Swan. Plastics, the environment and human health: current consensus and future trends 364. *Phil. Trans. R. Soc. B* 364 (2009) 1526. <http://doi.org/10.1098/rstb.2009.0053>
- [2]. www.epa.gov (page accessed in May 2019)
- [3]. <http://www.euro-plasticsrecycling.org> (page accessed in May 2019).
- [4]. S. Jahan, V. Strezov, H. Weldekidan, R. Kumar, T. Kan, S.A. Sarkodie, J. He, B. Dastjerdi, S.P. Wilson, Interrelationship of microplastic pollution in sediments and oysters in a seaport environment of the eastern coast of Australia, *Sci. Total Environ.* 695 (2019) 133924. doi:10.1016/j.scitotenv.2019.133924.
- [5]. J. Li, X. Qu, L. Su, W. Zhang, D. Yang, P. Kolandhasamy, D. Li, H. Shi, Microplastics in mussels along the coastal waters of China, *Environ. Pollut.* 214 (2016) 177–184. doi:10.1016/j.envpol.2016.04.012.
- [6]. M. Renzi, C. Guerranti, A. Blašković, Microplastic contents from maricultured and natural mussels, *Mar. Pollut. Bull.* 131 (2018) 248–251. doi:10.1016/j.marpolbul.2018.04.035.
- [7]. M.F.M. Santana, L.G. Ascer, M.R. Custódio, F.T. Moreira, A. Turra, Microplastic contamination in natural mussel beds from a Brazilian urbanized coastal region: Rapid evaluation through bioassessment, *Mar. Pollut. Bull.* 106 (2016) 183–189. doi:10.1016/j.marpolbul.2016.02.074.
- [8]. A.J.R. Watts, M.A. Urbina, S. Corr, C. Lewis, T.S. Galloway, Ingestion of Plastic Microfibers by the Crab *Carcinus maenas* and Its Effect on Food Consumption and

Energy Balance, Environ. Sci. Technol. 49 (2015) 14597–14604. doi:10.1021/acs.est.5b04026.

- [9]. Jinhui, X. Sudong, N. Yan, P. Xia, Q. Jiahao, X. Yongjian, Effects of microplastics and attached heavy metals on growth, immunity, and heavy metal accumulation in the yellow seahorse, *Hippocampus kuda* Bleeker, Mar. Pollut. Bull. 149 (2019) 110510. doi:10.1016/j.marpolbul.2019.110510.
- [10]. R. Qiao, Y. Deng, S. Zhang, M.B. Wolosker, Q. Zhu, H. Ren, Y. Zhang, Accumulation of different shapes of microplastics initiates intestinal injury and gut microbiota dysbiosis in the gut of zebrafish, Chemosphere. 236 (2019) 124334. doi:10.1016/j.chemosphere.2019.07.065.
- [11]. EFSA CONTAM Panel (EFSA Panel on Contaminants in the Food Chain) Statement on the presence of microplastics and nanoplastics in food, with particular focus on seafood EFSA J., 14 (6) (2016), pp. 4501-4531
- [12]. A. Heimowska, M. Morawska, A. Bocho-Janiszewska, Biodegradation of poly(ϵ -caprolactone) in natural water environments, Polish J. Chem. Technol. 19 (2017) 120–126. doi:10.1515/pjct-2017-0017.
- [13]. R. Ortega-Toro, J. Contreras, P. Talens, A. Chiralt., Physical and structural properties and thermal behaviour of starch-poly(ϵ -caprolactone) blend films for food packaging, Food Packag. Shelf Life. 5 (2015) 10–20. doi:10.1016/j.fpsl.2015.04.001.
- [14]. A. Tampau, C. González-Martínez, A. Chiralt, Release kinetics and antimicrobial properties of carvacrol encapsulated in electrospun poly-(ϵ -caprolactone) nanofibres. Application in starch multilayer films, Food Hydrocoll. 79 (2018) 158–169. doi:10.1016/j.foodhyd.2017.12.021.
- [15]. M. Ramos, A. Jiménez, M. Peltzer, M.C. Garrigós, Characterization and antimicrobial activity studies of polypropylene films with carvacrol and thymol for active packaging, J. Food Eng. 109 (2012) 513–519. doi:10.1016/j.jfoodeng.2011.10.031.

- [16]. A. Ben Arfa, L. Preziosi-Belloy, P. Chalier, N. Gontard, Antimicrobial paper based on a soy protein isolate or modified starch coating including carvacrol and cinnamaldehyde, *J. Agric. Food Chem.* 55 (2007) 2155–2162. doi:10.1021/jf0626009.
- [17]. A. Ultee, M.H.J. Bennik, R. Moezelaar, The phenolic hydroxyl group of carvacrol is essential for action against the food-borne pathogen *Bacillus cereus*, *Appl. Environ. Microbiol.* 68 (2002) 1561–1568. doi:10.1128/AEM.68.4.1561-1568.2002.
- [18]. S. Tunc, E. Chollet, P. Chalier, L. Preziosi-Belloy, N. Gontard, Combined effect of volatile antimicrobial agents on the growth of *Penicillium notatum*, *Int. J. Food Microbiol.* 113 (2007) 263–270. doi:10.1016/j.ijfoodmicro.2006.07.004.
- [19]. B. Tepe, M. Sokmen, H.A. Akpulat, D. Daferera, M. Polissiou, A. Sokmen, Antioxidative activity of the essential oils of *Thymus sipyleus* subsp. *sipyleus* var. *sipyleus* and *Thymus sipyleus* subsp. *sipyleus* var. *rosulans*, *J. Food Eng.* 66 (2005) 447–454. doi:10.1016/j.jfoodeng.2004.04.015.
- [20]. S. Gursul, I. Karabulut, G. Durmaz, Antioxidant efficacy of thymol and carvacrol in microencapsulated walnut oil triacylglycerols, *Food Chem.* 278 (2019) 805–810. doi:10.1016/j.foodchem.2018.11.134.
- [21]. Joint FAO/WHO Expert Committee on Food Additives Fifty-seventh meeting Rome, 5-14 June 2001, (2001).
- [22]. EFSA, Scientific Opinion on the Safety and efficacy of phenol derivatives containing ring-alkyl, ring-alkoxy and side-chains with an oxygenated functional group (chemical group 25) when used as flavourings for all species, *EFSA J.* 10 (2012) 2573. doi:10.2903/j.efsa.2012.2573.
- [23]. G. Kavosi, S.M.M. Dadfar, A. Mohammadi Purfard, R. Mehrabi, Antioxidant and antibacterial properties of gelatin films incorporated with carvacrol, *J. Food Saf.* 33 (2013) 423–432. doi:10.1111/jfs.12071.
- [24]. M.A. López-Mata, S. Ruiz-Cruz, N.P. Silva-Beltrán, J.D.J. Ornelas-Paz, P.B. Zamudio-Flores, S.E. Burruel-Ibarra, Physicochemical, antimicrobial and antioxidant properties

of chitosan films incorporated with carvacrol, *Molecules*. 18 (2013) 13735–13753. doi:10.3390/molecules181113735.

- [25]. L. Higuera, G. López-Carballo, P. Hernández-Muñoz, R. Catalá, R. Gavara, Antimicrobial packaging of chicken fillets based on the release of carvacrol from chitosan/cyclodextrin films, *Int. J. Food Microbiol.* 188 (2014) 53–59. doi:10.1016/j.ijfoodmicro.2014.07.018.
- [26]. M.P. Balaguer, J. Villanova, G. Cesar, R. Gavara, P. Hernandez-Munoz, Compostable properties of antimicrobial bioplastics based on cinnamaldehyde cross-linked gliadins, *Chem. Eng. J.* 262 (2013) 447–455. doi:10.1016/j.cej.2014.09.099.
- [27]. A.I. Cano, M. Cháfer, A. Chiralt, C. González-Martínez, Biodegradation behaviour of starch-PVA films as affected by the incorporation of different antimicrobials, *Polym. Degrad. Stab.* 132 (2016) 11–20. doi:10.1016/j.polymdegradstab.2016.04.014.
- [28]. European Union, European Parliament and Council Directive 94/62/EC on Packaging and Packaging Waste, *Off. J. Eur. Communities No L 365/10*. 1993 (1994) 10–23. doi:10.1038/sj.bdj.4811054.
- [29]. D. Adamcová, J. Zloch, M. Brtnický, M.D. Vaverková, Biodegradation / Disintegration of Selected Range of Polymers: Impact on the Compost Quality, *J. Polym. Environ.* 27 (2019) 892–899. doi:10.1007/s10924-019-01393-3.
- [30]. ISO 20200, *Plastics - Determination of the Degree of Disintegration of Plastic Materials under Simulated Composting in a Laboratory-scale Test*, 2004.
- [31]. UNE-EN ISO 14855-1, *Determinación de la biodegradabilidad aeróbica final de materiales plásticos en condiciones de compostaje controladas, in: Método según el análisis de dióxido de carbono generado*, 2012. Parte 1: Método general.
- [32]. E. Talón, M. Vargas, A. Chiralt, C. González-Martínez, Eugenol incorporation into thermoprocessed starch films using different encapsulating materials, *Food Packag. Shelf Life.* 21 (2019) 100326. doi:10.1016/j.fpsl.2019.100326.

- [33]. E. Castro-Aguirre, R. Auras, S. Selke, M. Rubino, T. Marsh, Insights on the aerobic biodegradation of polymers by analysis of evolved carbon dioxide in simulated composting conditions, *Polym. Degrad. Stab.* 137 (2017) 251–271. doi:10.1016/j.polymdegradstab.2017.01.017.
- [34]. S. Collazo-Bigliardi, R. Ortega-Toro, A. Chiralt, Reinforcement of thermoplastic starch films with cellulose fibres obtained from rice and coffee husks, *J. Renew. Mater.* 6 (2018) 599–610. doi:10.32604/JRM.2018.00127.
- [35]. P.A. Sreekumar, M.A. Al-Harhi, S.K. De, Studies on compatibility of biodegradable starch/polyvinyl alcohol blends, *Polym. Eng. Sci.* 52 (2012) 2167–2172. doi:10.1002/pen.23178.
- [36]. E. Rudnik, Biodegradability testing of compostable polymer materials, in: *Compost. Polym. Mater*, Elsevier, 2008: pp. 112–166. doi:10.1016/B978-008045371-2.50008-1.
- [37]. R.P. Singh, J.K. Pandey, D. Rutot, P. Degée, P. Dubois, Biodegradation of poly(ϵ -caprolactone)/starch blends and composites in composting and culture environments: The effect of compatibilization on the inherent biodegradability of the host polymer, *Carbohydr. Res.* 338 (2003) 1759–1769. doi:10.1016/S0008-6215(03)00236-2.
- [38]. H.S. Yang, J.S. Yoon, M.N. Kim, Dependence of biodegradability of plastics in compost on the shape of specimens, *Polym. Degrad. Stab.* 87 (2005) 131–135. doi:10.1016/j.polymdegradstab.2004.07.016.
- [39]. B.P. Wasserman, *Principles of enzymology for the food sciences*, 2nd edition. John R. Whitaker, Marcel Dekker, Inc., 270 Madison Ave., New York, NY 10016. 1994. 648 pages. \$185.00, *J. Food Saf.* 15 (1995) 365a – 366. doi:10.1111/j.1745-4565.1995.tb00147.x.
- [40] C.A. Murphy, J.A. Cameron, S.J. Huang, R.T. Vinopal, Fusarium polycaprolactone depolymerase is cutinase, *Appl. Environ. Microbiol.* 62 (1996) 456–460.
- [41] C.A. Murphy, J.A. Cameron, S.J. Huang, R.T. Vinopal, A second polycaprolactone depolymerase from Fusarium, a lipase distinct from cutinase, *Appl. Microbiol. Biotechnol.* 50 (1998) 692–696. doi:10.1007/s002530051352.

- [42] Y. Tokiwa, B.P. Calabia, C.U. Ugwu, S. Aiba, Biodegradability of plastics, *Int. J. Mol. Sci.* 10 (2009) 3722–3742. doi:10.3390/ijms10093722.
- [43] A. Banerjee, K. Chatterjee, G. Madras, Enzymatic degradation of polycaprolactone-gelatin blend, *Mater. Res. Express.* 2 (2015). doi:10.1088/2053-1591/2/4/045303.
- [44] J. Shen, R. Bartha, Priming effect of glucose polymers in soil-based biodegradation tests, *Soil Biol. Biochem.* 29 (1997) 1195–1198. doi:10.1016/S0038-0717(97)00031-X.

Poly(vinyl alcohol)-based materials
encapsulating carvacrol
obtained by solvent casting and electrospinning

Alina Tampau ^a, Chelo González-Martínez ^b, Amparo Chiralt ^c

^{a, b, c} Instituto Universitario de Ingeniería de Alimentos para el Desarrollo, Ciudad
Politécnica de la Innovación, Universitat Politècnica de Valencia, Camino de Vera, s/n,
46022 Valencia, Spain.

submitted to Reactive and Functional Polymers

altam@upvnet.upv.es

Abstract

Carvacrol has been encapsulated in poly(vinyl alcohol) (PVA) matrices by electrospinning and casting. Aqueous solutions containing 15 % PVA and 15 % carvacrol with respect to polymer have been used, containing or not Tween 85 at 0.3 g/100 g carvacrol. Electrospun mats exhibited beads and thin fibres which became thinner and interrupted when carvacrol was present and retained up to 83 % of this compound. The encapsulation efficiency in the electrospun mats decreased in the presence of surfactant, reaching values similar to those of casting (75-77 %). The electrospun, surfactant free material was practically amorphous with 40 % of the total carvacrol non-thermally releasable. In contrast, when surfactant was present and in cast material, with 40 % crystallinity, the strongly bonded carvacrol ratio decreased. Specific PVA - phenolic hydroxyl interactions played an important role in the degree of carvacrol retention in the matrices, which depended on surfactant's presence and processing method.

Keywords

poly(vinyl alcohol); carvacrol; electrospinning; casting; encapsulation efficiency.

1. Introduction

Nowadays, we are increasingly witnessing a higher consumer demand for safer foods. A modern strategy that provides an increase in food quality and safety is the use of “smart” active packaging that interacts with the food and its environment [1], [2]. These active packaging materials could control the permeability for gases and/or moisture, scavenge oxygen (to prevent foodstuff oxidation) or limit microbial growth, safely extending product shelf life. Also, the packaging industry is actively changing direction towards environmentally-friendly biodegradable components, stimulating the creation of new kinds of coatings and multilayer packaging materials for the food industry [1]. Nevertheless, currently the great majority of food-preserving packaging is based on oil-derived synthetic plastics, which, despite having multiple advantages (such as low cost, versatility, good barrier qualities), are not biodegradable, thus generating a significant environmental impact [3]. Then, the new packaging concept should be based on biodegradable materials in order to address these concerns.

Poly(vinyl alcohol) (PVA) is a synthetic polymer that is widely used for different applications in various branches of the industry, medicine and food sectors, obtained easily through the polymerization of vinyl acetate followed by the hydrolysis of the acetate groups [4]. It is water soluble, completely biodegradable, colourless and odourless, with good mechanical properties and biocompatibility. PVA also has the potential to act as a carrier matrix for the incorporation of active compounds [5].

Regarding the active compounds, natural substances could be used, such as plant extracts and essential oils, for the purposes of replacing the synthetic food preservatives. The essential oils (EO) are a complex blend of volatile and semi volatile substances, mostly made up of terpenes, terpenoids and aromatic compounds of low molecular weight. Different EO have proven to exhibit antimicrobial properties against bacteria [6], [7], or fungi [8], and have been recognized as safe compounds (GRAS) to be used in the food industry by legal organisms, such as the Food and Drug Administration in the USA. Nevertheless, despite their advantages, the concentration levels of EO that would exert the desired effects could also introduce unwanted flavours and potential fitotoxicity into the foodstuffs they are required to protect. This is the case of carvacrol (CA), a monoterpenoid phenol that can be found in high concentrations in the EO of oregano or thyme [9], with proven antimicrobial and antioxidant effects. It is considered a good preservative for a wide range of foodstuffs

[10], but its direct application is limited because of its strong flavour, high volatility, low water solubility or its potential reactions with certain food components that might alter the food properties and limit its efficacy as a preservative [11], [12]. The encapsulation of the active compounds may favour their stability, their preservation efficiency while allowing for a controlled release towards the foodstuffs [13].

One encapsulation method that is gaining interest in the food packaging sector is the electrospinning (ES) technique [14], [15]. It has a simple working principle, using an electric field to stretch a polymeric solution, forming structures (mainly fibres) with high specific surface that can be used to coat support materials useful in the development of multilayer active packaging [16]. Some successful applications have been reported, such as antioxidant multilayers constituted by polylactide (PLA) cast films coated by ES with PLA mats encapsulating gallic acid [17], antimicrobial multilayer systems composed of a polyhydroxyalkanoate (PHA) support coated with an electrospun layer of PHA enriched with silver nanoparticles [18], and antibacterial multilayers with reduced water barrier properties developed from gelatine sheets coated by ES with poly- ϵ -caprolactone loaded with black pepper oleoresin [19].

In the development of active multilayer materials, the extension of a polymer solution containing the active compound on a polymeric support can also be used to obtain coated films with an active layer, where the active compound would be encapsulated into the polymer matrix of the cast layer. However, the effective extension of a determined active-polymer solution will be greatly affected by the solutions' wettability and spreadability on the supporting polymer layer, which in turn, depend on the contact angle of the polymer-solution system and surface tension of the solutions. All these factors play a crucial role in the coating thickness and effectiveness. Additionally, the concept of multilayer films involves the assembly of polar and non-polar polymers to take advantage of their respective complementary barrier properties to gases and water vapour. In this sense, the effective extension of polymer polar solutions on non-polar polymers or vice versa has the problems associated with the lack of chemical affinity. In contrast, the ES technique allows for the electrodeposition of the solvent-free polymer on the supporting film surface, thus avoiding the problems of the extension of the solution.

The electrodeposition of polyvinyl alcohol has been studied by several authors. [20] and [21] studied the influence of different parameters, such as molecular weight and concentration on the ES process. The electrospun fibre architecture depended on the PVA molecular

weight (M_w) and its concentration in the solution; beads and spindle-like formations being more present at lower concentrations or lower M_w than fibres. The diameter of fibres became larger as M_w or concentration increased, and a broader fibre distribution could be obtained. The presence of salts (such as NaCl) in the solution could disrupt the fibrous assembly for a low M_w polymer, however for the higher M_w the salt presence leads to thinner fibre diameters. The formation of PVA fibres was not affected by the pH variation, but an increase in voltage and salt concentration was not favourable to the ES process [21]. [14] reviewed the use of the electrospun PVA matrix as a carrier for different active substrates, such as silver particles, medicinal drugs, enzymes, bifidobacteria, or plant essential oils. [13] successfully obtained electrospun PVA nano-mats with uniform fibres containing cinnamon essential oil entrapped in β -cyclodextrin. The authors demonstrated that the ES process is favourable to maintaining the volatile active compound in the electrodeposited mat, which also presents thermal stability, due to the molecular interactions between the PVA, the essential oil and the β -cyclodextrin.

The purpose of this study was to analyse the ability of PVA to encapsulate carvacrol, incorporating or not surfactant, by means of the ES technique, in comparison with the casting method. The characterisation of the obtained materials in terms of the encapsulation efficiency, microstructure and thermal behaviour was carried out.

2. Materials and methods

2.1. Materials and reagents

Polyvinyl alcohol (PVA) (M_w 13,000-23,000; 87-89 % hydrolyzed), polyoxyethylene sorbitan trioleate Tween 85 (T85), carvacrol (CA) and phosphorous pentoxide (P_2O_5) were acquired from Sigma-Aldrich (Sigma–Aldrich Chemie, Steinheim, Germany). Purified water (resistivity of 18.2 $M\Omega$ cm) was prepared using a MilliQ Advantage A10 equipment from Millipore S.A.S., Molsheim, France. Absolute ethanol (UV grade) used for extraction was obtained from Panreac AppliChem (Panreac Química S.L.U, Barcelona, Spain).

2.2. Preparation of the liquid formulations

Aqueous solutions of PVA (15 wt. %) were prepared by dissolving the polymer in milli-Q water, under constant stirring at 80 °C, for one hour. This concentration was selected on the basis of preliminary trials using 12.5, 15 and 20 % of PVA, in which 15 % wt. of PVA imparted

the proper viscosity to the ES processing. CA was added in a ratio of 15 % (w/w) with respect to the PVA content. Formulations were prepared with and without surfactant (S), using a wt. ratio of 0.3:100 S:CA. This ratio was estimated on the basis of an expected CA droplet diameter of about 10 μm and considering an excess surface concentration for the surfactant of 5 mg/m^2 , in the range of the previously reported values [22]. The blend was mixed at 12,000 rpm for 3 minutes, using an Ultra Turrax rotor–stator homogenizer (Model T25D, IKA Germany). Control solutions with pure PVA were also prepared.

All the formulations were allowed to rest at room temperature for 24 h post-preparation, to assess their stability and promote the natural degassing process and, afterwards, these were degassed under vacuum. All the dispersions showed good stability without phase separation. Each liquid formulation was processed either by electrospinning (ES) or casting to obtain fibres or films, respectively, with entrapped carvacrol. The obtained materials were labelled as P for PVA, C for carvacrol and S for surfactant, preceded by C (casting) or ES (electrospinning), according to the processing method.

2.3. Obtaining the dry encapsulating material

To obtain the electrospun materials, the liquid formulations were loaded onto Fluidnatek **electrospinning** equipment (Bioinicia, Valencia, Spain) presenting the same setup as described by Tampau et al. (2017). The emulsions were fed through a BD luer-lock syringe (BD, Franklin Lakes, NJ, USA) at a flow rate varying between 0.25 and 0.5 mL/h, and a voltage in the range of 20-25 kV was applied. The collector plate was positioned 15 cm from the injector needle. All the applications were performed under room temperature conditions (25 °C and 45 % RH). The obtained material was placed in a desiccator with P_2O_5 to avoid moisture absorption till further analysis.

To obtain the **cast** films, an equivalent of 1.5 g of PVA/plate of the aqueous formulations was poured onto levelled Teflon plates of 15 cm in diameter and dried at 25 °C and 45 % RH for 48 h. The resulting dry films were peeled off and stored in a desiccator with P_2O_5 till further analysis.

2.4. Characterization of the liquid systems

2.4.1. Particle size distribution

The droplet size of the emulsions was evaluated using the laser diffractometer MasterSizer 2000 (Malvern Instruments, Worcestershire, UK) in order to assess their particle size distribution. Each formulation was dispersed in distilled water at 1000 rpm (to avoid formation of bubbles) until an obscuration range of 5 % was reached. The size distribution graphs were obtained.

2.4.2. Rheological behaviour

The rheological behaviour of the PVA-based formulations was assessed in triplicate by means of a rotational rheometer (HAAKE Rheostress 1, Thermo Electric Corporation, Karlsruhe, Germany) with a system of coaxial cylinders type Z34DIN Ti. The samples were stabilized for 15 minutes at 25 °C after being poured into the coaxial cylinder. The shear stress (σ) was measured as a function of shear rate ($\dot{\gamma}$) from 0 to 100 s⁻¹, allowing the equipment a 5 min ramp-up (to reach the maximum shear rate) and a 5 min ramp-down (to return to zero shear rate). The power law model (**eq. 1**) was used to determine the flow behaviour index (n) and the consistency index (K). The viscosity at near zero shear rate (η_0) was determined from the initial slope of the flow curves.

$$\sigma = K \cdot \dot{\gamma}^n \quad (\text{eq. 1})$$

2.4.3. Conductivity, surface tension and ζ potential

The **conductivity** of the emulsions was analysed by means of a conductimeter (model SevenEasy, Mettler Toledo, Schwerzenbach, Switzerland). Each formulation was measured in triplicate, after being diluted 1:100 (v/v) with milli-Q water.

The **surface tension** was determined using the pendant drop method, with OCA 20 equipment (Dataphysics, Germany) and the measurements were processed by SCA 20 software package. For each formulation, 20 measurements were performed.

Finally, the **ζ -potential** was assessed in triplicate in the diluted emulsions (1:100 (v/v)), using DTS1070 cuvettes and Zeta Sizer nano series equipment (Malvern Instruments,

Worcestershire, UK). The electrophoretic mobility registered by the equipment was converted into **ζ-potential** by applying the Smoluchowsky model [23].

2.5. Characterization of the solid material

2.5.1. Microstructure

The microstructure of the obtained materials was analysed by using Field Emission Scanning Electron Microscopy (FESEM Ultra 55, Zeiss, Oxford Instruments, UK). The cast films were cryo-fractured by immersion in liquid nitrogen (to allow for cross-section view), while the electrospun material was deposited over an aluminium foil support surface and observed directly. The samples were mounted on stubs with carbon tape, and after platinum sputtering in an EM MED020 (Leica Microsystems, Germany), were observed using an accelerating voltage of 1 kV.

2.5.2. Encapsulation efficiency

The CA retention in the films and in the electrospun material was quantified by using a UV/Vis spectrophotometer (Evolution 201 UV-Vis, Thermo Fisher Scientific Inc.), using quartz cuvettes, as described by Tampau et al. (2017). Briefly, samples of up to 30 mg of dry material were placed in amber vials along with 15 mL of absolute ethanol, and after being hermetically sealed, were maintained under stirring for 24 h at room temperature. The alcoholic extracts were analysed at 275 nm, using the extract of the CA-free matrix as blank. The absorbance data were converted into concentration units by using a calibration curve (concentration=66.643 x Abs, $R^2=0.999$), obtained previously from the absorbance measurements of standard carvacrol solutions (between 4-100 µg CA/mL). The encapsulating efficiency (EE) was expressed as a percentage, representing the quotient between the CA alcohol-extracted in the films and the theoretical CA content. This analysis was performed in triplicate for each formulation.

2.5.3. Thermogravimetric analysis (TGA) and differential scanning calorimetry (DSC)

The obtained films and ES material were submitted to thermal analyses, in order to characterize their thermal degradation (TGA) and assess the carvacrol effect on the thermal behaviour of the polymer by differential scanning calorimetry (DSC). For the TGA assay, the previously conditioned samples (10 mg) were placed in 70 µL alumina crucibles in a thermo-

gravimetric analyser (TGA/SDTA 851e, Mettler Toledo, Schwarzenbach, Switzerland) and heated from 25 to 700 °C at a rate of 10K/min, under a nitrogen flow (20 mL/min) to avoid oxidative processes. The DTA curves were obtained and the onset, peak and endset temperatures of the degradation peaks were determined, as well as the percentage of weight loss for each of them. The differential scanning calorimetry analysis was carried out in DSC (1 StarE System, Mettler-Toledo, Inc., Switzerland) equipment. Samples (5-10 mg) of the previously P₂O₅ conditioned films or fibres were placed into aluminium pans (Seiko Instruments, P/N SSC000C008) and tightly sealed. The samples were first kept at -25 °C for 5 minutes and then heated at a rate of 10 K/min from -25 to 225 °C, where they were maintained for 5 minutes. Then a cooling step was applied from 225 to -25 °C, at the same cooling rate. After being kept at -25 °C for 5 minutes, a second heating step followed, going from -25 to 250 °C, at 10 K/min. As reference, an empty aluminium pan was used. The weight fraction of crystalline regions (X_c: crystallinity index) was calculated from both heating steps, comparing the obtained enthalpy to the fusion enthalpy of 100 % crystalline PVA ($\Delta H=138.6$ J/g, [24]). Each sample was analysed in triplicate.

2.6. Statistical analysis

The analysis of the data was performed through variance analysis (ANOVA) using the Statgraphics Centurion XVII.64 software. To discern between formulations, the Fisher Least Significant Difference (LSD) ($p<0.05$) was used. DSC data were also analysed using a multifactor analysis of variance with 95 % significance level, considering as factors: type of formulation (P, PC, PCS) and processing method (C or ES).

3. Results and discussion

3.1. Properties of the liquid systems

Rheological behaviour, conductivity, surface tension and the emulsion droplet size (in the case of systems containing CA) of the liquid systems can affect their behaviour in ES processing as well as the microstructure of the electrospun material. So, these parameters were characterised in order to better understand differences between samples.

Figure 1 shows the droplet size distribution of the emulsions containing carvacrol with and without surfactant. The presence of the surfactant gave rise to a unimodal particle size

distribution, with smaller droplet diameters (under 1 μm), in agreement with the formation of small T85 micelle-entrapping CA. The particle size was lower than that expected from the surfactant-CA ratio used, which suggests that only a part of the incorporated carvacrol was inside the micelles. When no surfactant was added, the particle size distribution turned multimodal. This suggests the formation of aggregates of CA droplets through flocculation and coalescence processes, or even chain-droplet aggregations promoted by the CA interactions with the polymer. Specific CA-polymer interactions could be deduced from the sharp increase in the liquid phase viscosity when CA was incorporated into the PVA solution.

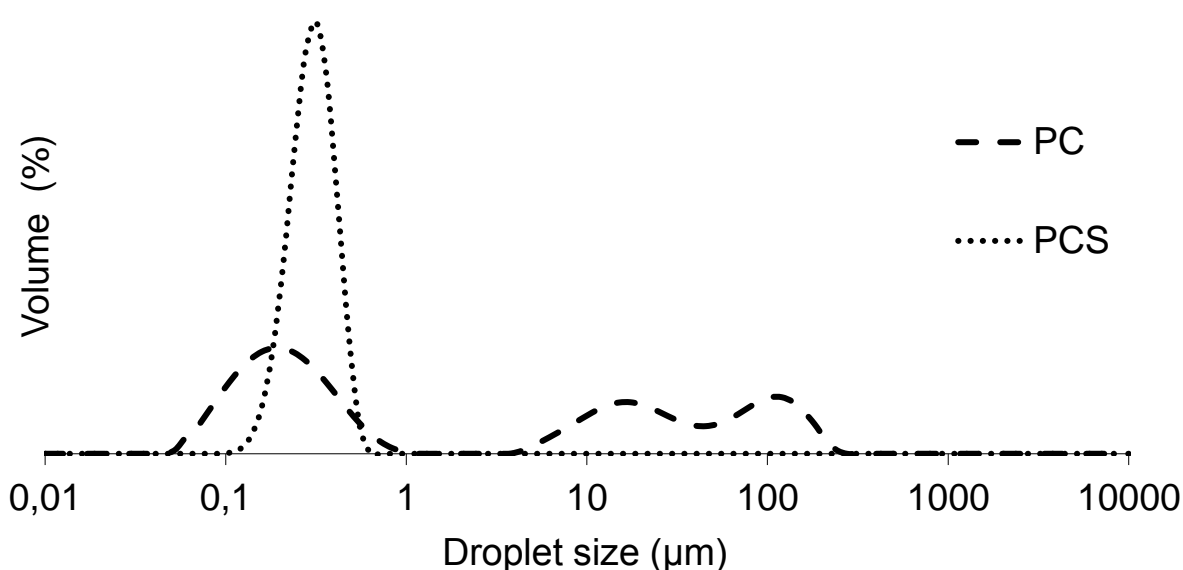


Figure 1. Typical particle size distribution of the different emulsions containing carvacrol.

Figure 2 shows the flow curves of the three aqueous formulations (P, PC and PCS) where the Newtonian flow of the PVA solution turned pseudoplastic when CA was incorporated for both surfactant-free liquid (PC) and that containing surfactant (PCS).

The volume fraction of the dispersed phase was about 2.3 % in both cases whereas the viscosity at near zero shear rate increased approximately 200 or 165 times (**Figure 2**), respectively for the surfactant-free emulsion and that containing surfactant. This marked rise in viscosity suggests specific interactions of CA with the polymer. In fact, acetylated groups of PVA chains can be ionized, exhibiting negative charge, according to the mechanism described by [25], which could promote the binding with the CA phenolic hydroxyl group, which can act as a Lewis electron acceptor, thus being bonded to the polymer chain, forming Lewis adducts. These interactions could lead to an increase in the liquid viscosity when CA is incorporated, additionally to the effect of the dispersed phase concentration, since the

hydrodynamic volume and intrinsic viscosity of PVA chains will increase by bonding the carvacrol molecules. When surfactant is present, the CA entrapment in the T85 micelles could limit the CA bonding to the PVA chains while the smaller droplet size in the emulsion may also contribute to the reduction in viscosity.

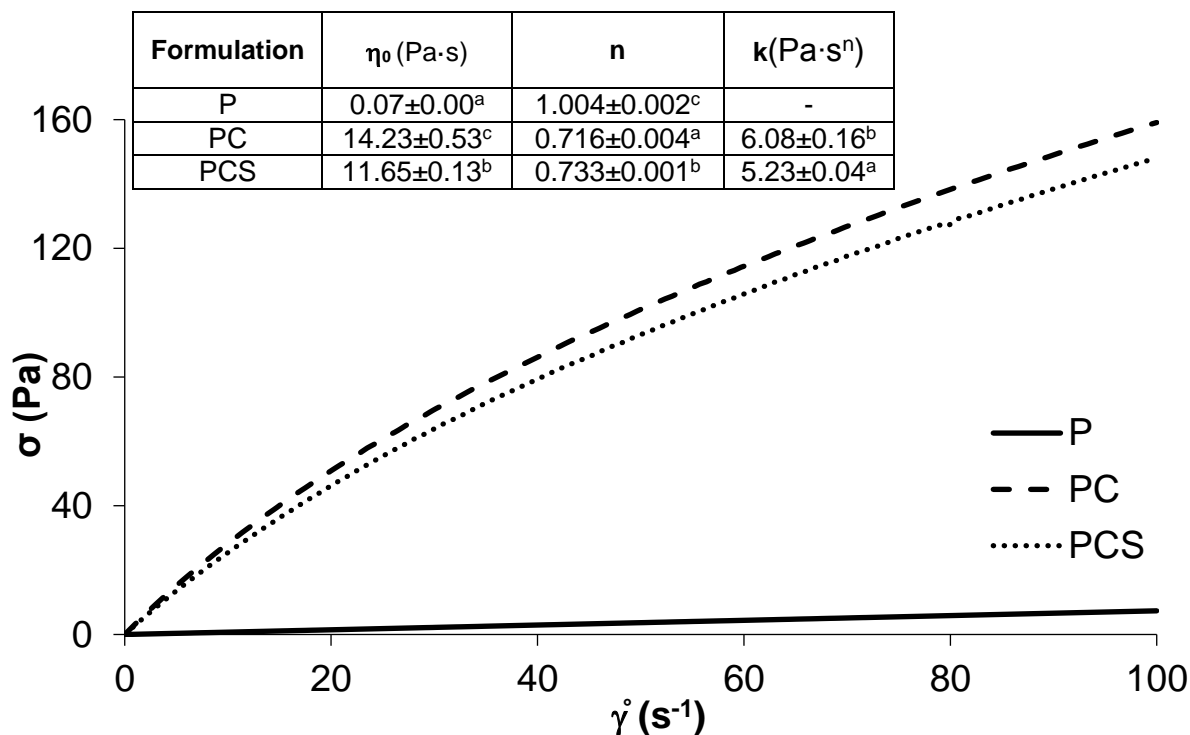


Figure 2. Rheological curves of the different PVA-based emulsions. Apparent viscosity η_0 (Pa·s) at a near zero shear rate $\dot{\gamma}$ (initial slope of the flow curves), flow behavior index (n) and consistency index (K) are also presented, with mean values and standard deviation.

Table 1. Conductivity (κ), surface tension (γ) and ζ -potential of the emulsions, diluted or not in milli-Q water. Average values and standard deviations. Different superscript letters in the same column indicate significant differences ($p < 0.05$) between samples.

Formulation	κ ($\mu\text{S/cm}$)	γ (mN/m)	ζ -potential (mV)
	dilution 1:100 (v/v)	without dilution	dilution 1:100 (v/v)
P	28.9±0.1 ^b	42.2 ± 0.7 ^b	-13±3 ^a
PC	21.5±0.4 ^a	31.5 ± 0.4 ^a	-7±2 ^b
PCS	44.5±0.1 ^c	31.3 ± 0.3 ^a	-11.6±0.6 ^a

The obtained values for conductivity, surface tension and ζ -potential of the liquid systems are shown in Table 1. Conductivity decreased in the liquid systems when CA was incorporated and increased when surfactant was present. Differences in the sample conductivity revealed a different surface charge density in the polymer chains or droplets. The PCS system exhibited the highest conductivity values, followed by the pure PVA formulation. The incorporation of CA decreased the conductivity values, probably due to the combination between the neutralizing effect upon acetate groups and the formation of aggregates with lower mobility, as revealed by the particle size distribution curve. The higher conductivity values registered for the PCS emulsion can be explained by the different interactions taking place in the presence of the surfactant, which lead to the formation of smaller particles, decreasing the viscosity and limiting CA-PVA interactions. Coherently with the changes in conductivity, the negative ζ -potential values of pure PVA associated with the ionization equilibrium decreased when the system contained CA, in agreement with the described mechanism shown in Figure 3. According to the acetylation degree of the chains, the molar ratio of the incorporated carvacrol and acetylated groups was estimated to be 1:3, which implies that there were not enough carvacrol molecules in the system to react with all the negative charges of the chains, in agreement with the negative ζ -potential value obtained for the PC system. In emulsions containing surfactant, the smaller reduction in ζ -potential is coherent with the fact that a part of the carvacrol molecules is entrapped in the core of the surfactant micelles. Then, a partition of carvacrol between the Lewis adducts in the polymer chains and T85 micelles seems to occur.

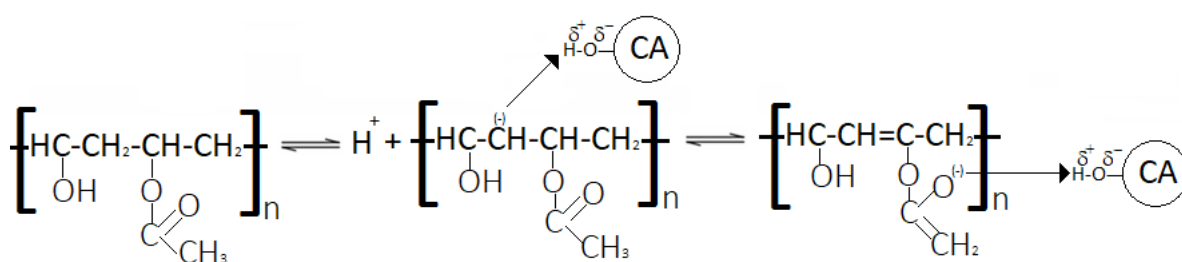


Figure 3. Ionization mechanism of the acetate group within the PVA polymer chain, according to [25] and proposed mechanism for PVA-carvacrol interactions.

As concerns the surface tension (ST) (Table 1), all PVA formulations presented ST values lower than the solvent ($72 \text{ mN}\cdot\text{m}^{-1}$) and in the range of that previously determined by other authors [26]. Because of the presence of -OH groups, PVA has the capability of H-bonding

with the solvent, exhibiting a tendency to migrate from bulk to the surface, thus decreasing its surface tension, like other surface-active agents [26]. The presence of carvacrol, with and without surfactant enhanced this surfactant effect, and lower values of surface tensions were obtained for these liquid systems. The changes in the chain hydrophobicity associated with the binding of carvacrol could explain this effect, due to the promotion of the polymer adsorption at the air-liquid interface. Likewise, the presence of droplets or micelles at the air-liquid interface will also reduce the liquid surface tension. The addition of the T85 did not significantly modify the ST value with respect to the PC system, probably due to its prevalent location at the water-carvacrol interface in the micelles. Relatively low values of surface tension favour the ES process, given that the electrostatic forces induced by the electric field must overcome the surface tension of the liquid.

It is remarkable that the obtained emulsions did not exhibit creaming or phase separation throughout more than 2 weeks and were considered stable and able to be processed by ES or casting.

3.2. Characterization of the solid material

The FESEM micrographs obtained for the cast and ES material are shown in Figure 4. It can be observed that the electrodeposition of the polymeric emulsions generated mostly thin fibres and spherical structures, with a few spindle-like shapes. Spherical formations could be mainly due to the low molecular weight of the polymer, reported by other authors [20], [27]. The presence of CA with and without T85 gave rise to thinner and less continuous fibres. This could be attributed to the previously commented on interactions of CA and PVA chains, which could modify the chain interactions under the electric field. Weak interactions could lead to thinner and more brittle fibres, which appear interrupted and that also break easily under the electron field during microscopy observations. Fibre formation was also limited in other emulsified systems [16]. In all cases, the specific surface generated through electrodeposition was large, providing a potentially wide surface for the active to be released.

The cross-sections of the cast films showed a fairly homogenous structure, without visible droplets of carvacrol when no surfactant was used, which suggested a complete integration of the active into the polymeric matrix through the aforementioned interactions between CA and PVA chains. Nevertheless, the PCS micrograph presented small spherical particles

distributed in the matrix, which can be assigned to the preserved T85-Carvacrol micelles. These can be more clearly observed at higher magnification.

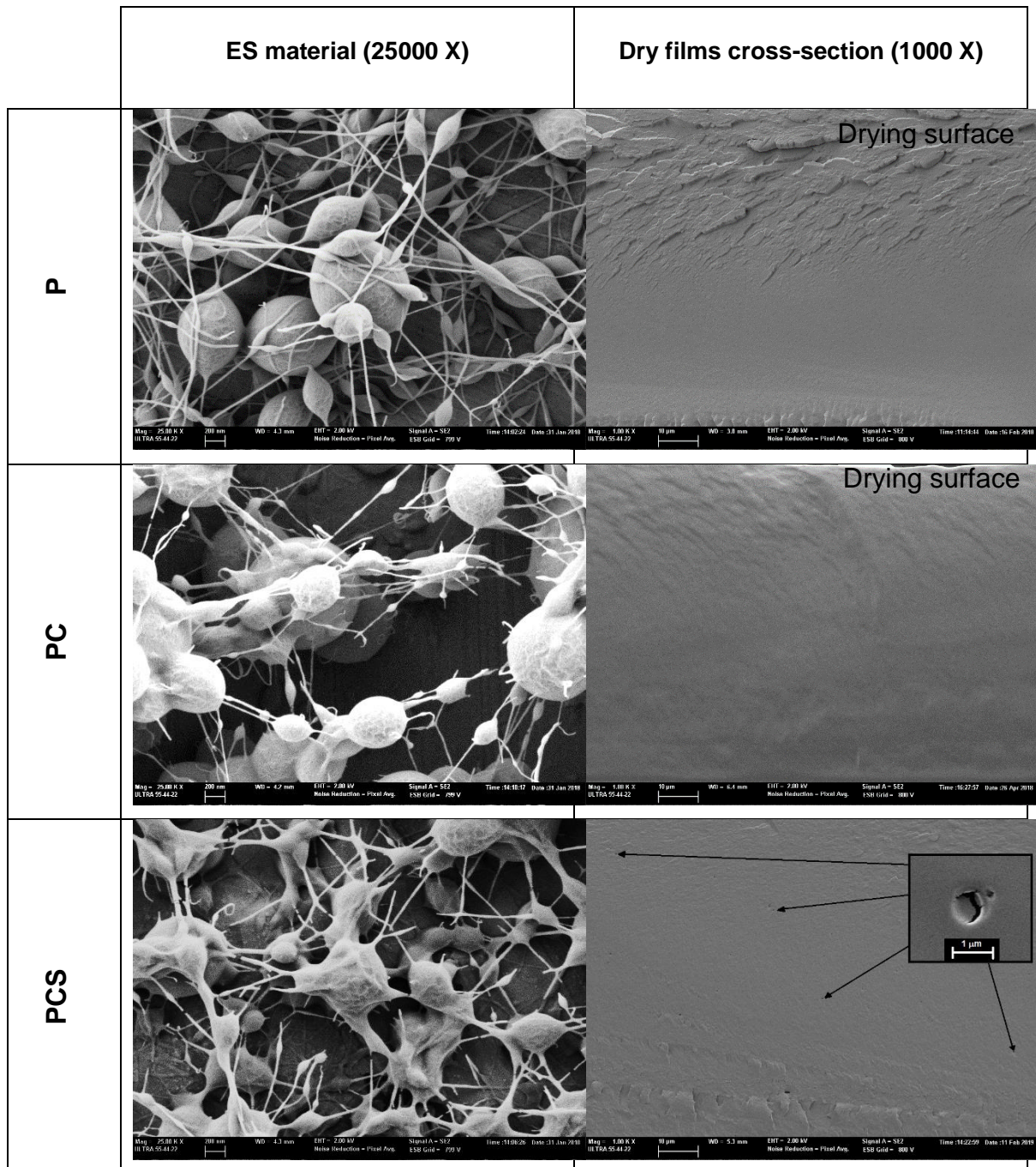


Figure 4. FESEM micrographs of the different ES materials and cross section of the PVA films. Higher magnification of small particles in the C-PCS sample was included.

The encapsulating efficiency (EE) determined by extraction with absolute ethanol for ES and cast materials is shown in Table 2. Given the aqueous nature of the solvent and the formation of immiscible blends with carvacrol, the losses of the active during water evaporation by steam drag effect can be expected in both processing methods, according

to previous studies [16], [28]. Nevertheless, CA-loaded samples exhibited high retention degree, with an encapsulation efficiency of about 80 % and 75 % for ES and cast materials, respectively. This could be attributed to the high viscosity of the liquid medium, which limited the emulsion destabilization during the solvent evaporation, as well as to the described specific CA-PVA interactions, which helped to efficiently retain CA molecules inside the fibres or film structure. No significant differences in the EE values were obtained when incorporating T85, which indicated that the surfactant did not contribute efficiently to improving the emulsion stability during the solvent evaporation period.

When carvacrol was encapsulated by using the ES process, the retention values were higher than when encapsulated by casting, although this difference was only significant ($p < 0.05$) for the T85-free formulation. This is coherent with the fact that the addition of T85 limited the CA binding to the PVA chains, as previously commented on. The bonded carvacrol would be less sensitive to evaporation by steam drag effect than the carvacrol in micelles, which are sensitive to destabilization mechanisms releasing carvacrol. Then, higher EE values would be obtained in the absence of surfactant, especially when a fast water evaporation occurred in the electrospinning process.

Table 2. Carvacrol encapsulating efficiency (EE) and content determined in the ES and cast samples. Average values and standard deviations.

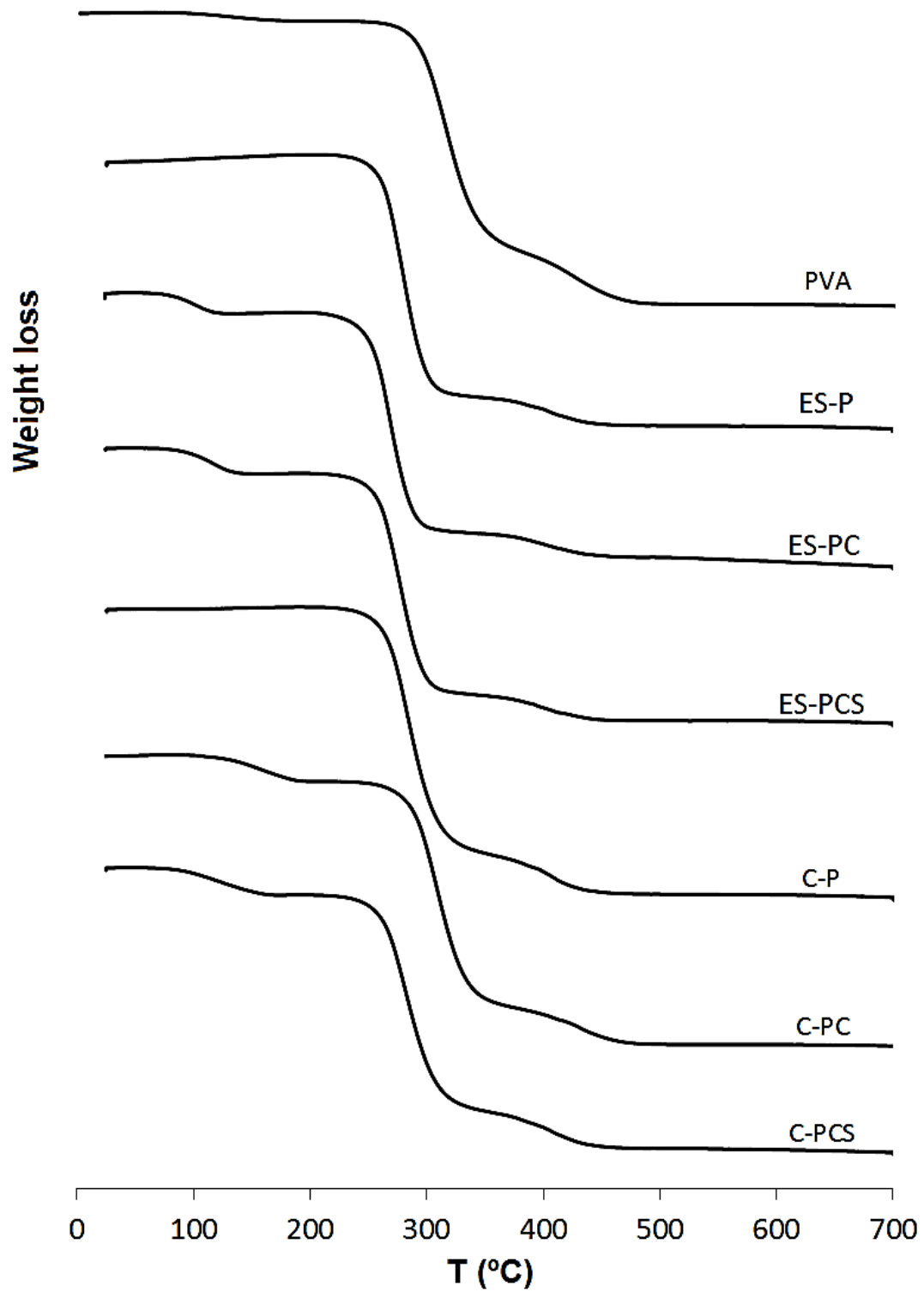
Formulation	EE (%)	g CA/ 100 g PVA	g CA/ 100 g fibre or film
ES-PC	83 ± 9 ^b	12±2 ^b	11±1 ^b
ES-PCS	77 ± 7 ^{ab}	11±1 ^{ab}	10±1 ^{ab}
C-PC	75 ± 2 ^a	10.9±0.3 ^a	9.8±0.2 ^a
C-PCS	76 ± 3 ^{ab}	11.0±0.4 ^{ab}	9.9±0.3 ^{ab}

^{a,b,c} Different superscript letters in the same column indicate significant differences ($p < 0.05$) between samples.

As concerns the thermal stability of the materials, Figure 5 shows the weight loss and derivative (DTGA) curves for the different material formulations, together with that obtained for the pure components. Likewise, the temperatures for the different degradation steps of the samples are summarized in Table 3.

For PVA films, two weight loss steps were observed: the first step between 200-300 °C, in which the dehydration, chain scission and decomposition of the polymer take place and the

second step, around 400 °C related with the degradation of the by-products generated by PVA during the thermal process [29].



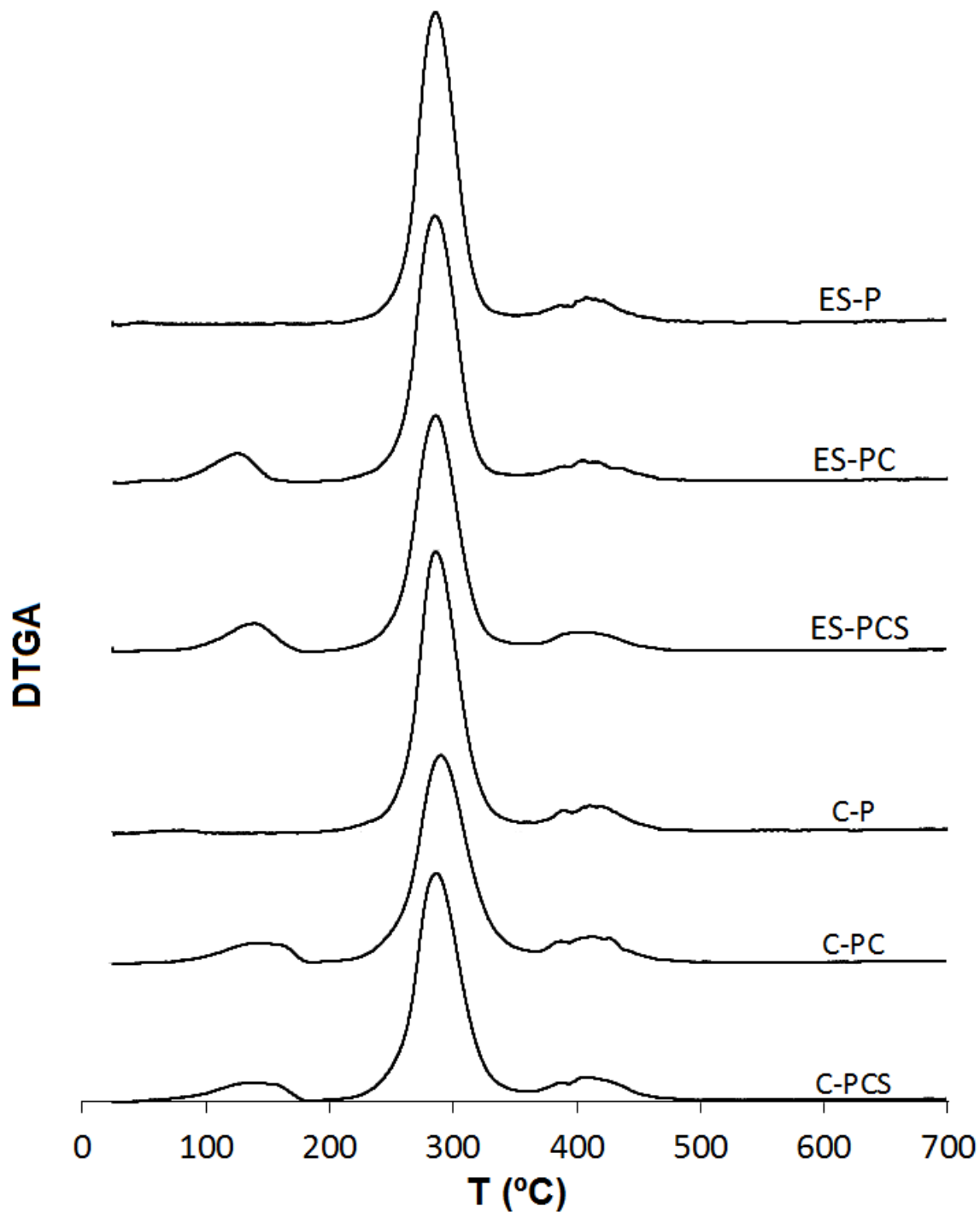


Figure 5. TGA (previous page) and DTGA thermograms of the electrospun (ES) and cast (C) samples.

Losses of adsorbed or bound water were not detected as the samples were previously conditioned with P_2O_5 . All CA-added formulations presented a first weight loss step, starting at around 50 °C, which could be attributed to the thermo-released fraction of the active (Figure 5), which showed the peak temperature between 109 and 135 °C, depending on the

sample. For cast films, the thermo-liberation of CA exhibited a similar pattern with a sustained release up to about 150 °C, whereas the ES samples showed a thermo-release of CA a lower temperature (peaks: 121 and 109 °C respectively for samples with and without surfactant). In contrast, by comparing the amounts of thermo-released CA (Table 3) with the determined content in the samples (Table 2), a strongly bonded fraction of this component to the polymer matrix could be deduced, since the total content was not thermo-released before the polymer degradation. This strongly bonded fraction represented 18 % of the total CA for cast films, regardless of the presence of surfactant, and 40 and 1 %, for ES samples without and with surfactant, respectively. These results indicate that CA was more strongly bonded to PVA in ES samples when no surfactant was added and the presence of surfactant did not affect the CA bonding degree in cast films. The thermo-release of CA at lower temperature in ES samples must be related with the greater specific surface area of the ES material, which facilitates the fast release of the compound. As previously commented on, the presence of surfactant limited the bonding of carvacrol to the polymer chains by the formation of the CA-surfactant micelles, which, as previously commented on, represent a weaker bonding of the compound within the polymer matrix. However, this effect was less remarkable in cast films where the longer drying times allow for the establishment of a structure nearer the equilibrium state (minimum free energy) where the components are arranged according to the more favourable interactions (affinity), with a higher CA ratio bonded to the PVA chains.

As regards the degradation temperature of PVA, the values were significantly affected ($p < 0.05$) by the film processing method. Thus, the thermogravimetric analysis revealed that the degradation temperature (T_p) was significantly lower ($p < 0.05$) in electrospun PVA films than in those obtained by casting. These differences could be attributed to the differing degree of polymer crystallization in each case, as crystallinity influences many polymer properties, including mechanical and thermal. In this sense, a lower crystallinity degree usually implies lower degradation temperatures [30]. Most electrospun fibres exhibit a lower crystalline structure due to fast water evaporation and polymer solidification during the electrospinning process [31], [32], as deduced from the DSC analysis commented on below, which could explain their lower thermal stability. Neither the presence of carvacrol nor T85 caused any significant differences in the degradation temperature of the polymer for samples obtained using the same processing method.

Table 3. Degradation temperatures (onset- T_o and peak- T_p) of **A**) individual components of the emulsions and **B**) the dry materials obtained by electrospinning and casting. Thermo-released CA fraction referred per 100 g polymer is also shown. Different superscript letters in the same column indicate significant differences ($p < 0.05$) between samples.

A	Component	T_o (°C)	T_p (°C)
	Carvacrol	77±6 ^a	159±7 ^a
	PVA	197±2 ^b	293±5 ^b
	Tween 85	335±2 ^c	380±2 ^c

B	Formulation	1st peak CA release		Thermo-released CA fraction	2nd peak PVA main degradation		3er peak by-product degradation	
		T_o (°C)	T_p (°C)	(g/100 g PVA)	T_o (°C)	T_p (°C)	T_o (°C)	T_p (°C)
	ES-P	-	-	-	190±3 ^{ab}	281±2 ^b	394±10 ^a	394±10 ^a
	ES-PC	48±1 ^a	109±7 ^a	7±1 ^a	187±4 ^a	275±6 ^a	402±8 ^a	406±6 ^b
	ES-PCS	46±3 ^a	121±8 ^b	10±1 ^b	189±1 ^{ab}	279±3 ^{ab}	395±3 ^a	395±3 ^a
	C-P	-	-	-	192±1 ^b	288±4 ^c	391±12 ^a	399±6 ^{ab}
	C-PC	44.8±0.4 ^a	135±3 ^c	9±1 ^b	191±1 ^b	289±2 ^c	397±4 ^a	397±4 ^{ab}
	C-PCS	47±3 ^a	129±4 ^{bc}	8.9±0.2 ^b	191±2 ^b	287±3 ^c	393±5 ^a	393±5 ^a

Table 4 shows the results obtained from the DSC analysis, in terms of the glass transition (T_g), melting temperatures (T_m), melting and crystallization enthalpies (ΔH) and percentage of crystallinity (X_c) of PVA-based films deduced from the 1st and 2nd heating scans.

In Figure 6, only the DSC curves from the 1st heating for the different samples are shown. After erasing the thermal history of the samples, the thermograms obtained in the 2nd heating (not shown) were very similar, exhibiting the glass transition and the melting endotherm, whose enthalpy and onset and peak temperature values are shown in Table 4.

Table 4. DSC parameters of the PVA phase transitions: enthalpies (ΔH), crystallinity index (X_c), melting (T_m), crystallization (T_c) and glass transition (T_g) temperatures obtained in the different heating and cooling scans. Different superscript letters in the same row indicate significant differences ($p < 0.05$) between samples.

		ES-P	ES-PC	ES-PCS	C-P	C-PC	C-PCS
1 st heating	ΔH_m (J/g PVA)	-	-	-	50±3 ^a	54±13 ^a	55±10 ^a
	X_c (%)	-	-	-	36±2 ^a	39±10 ^a	40±7 ^a
	T_m peak (°C)	196±4 ^{a*}	180±4 ^{a*}	174±31 ^{a*}	186±3 ^a	186±3 ^a	189±3 ^a
	T_g (°C)	37±3 ^{abc*}	31±2 ^{a*}	33±5 ^{a*}	55±2 ^d	41±8 ^{bc}	42±1 ^c
Cooling step	ΔH_c (J/g PVA)	24±4 ^a	30±3 ^a	25±6 ^a	29±2 ^a	26±5 ^a	22±6 ^a
	T_c onset (°C)	156±9 ^a	168±1 ^b	166±6 ^{ab}	164±1 ^{ab}	169±6 ^b	158±8 ^{ab}
	T_c peak (°C)	142±12 ^a	157.0±0.4 ^a	144±22 ^a	152±1 ^a	156±7 ^a	145±12 ^a
	T_g (°C)	62±1 ^c	43±3 ^a	56±3 ^b	60±2 ^c	49±6 ^a	56±5 ^b
2 nd heating	ΔH_m (J/g PVA)	26±7 ^a	39±2 ^c	28±4 ^{ab}	35±1 ^{bc}	29±5 ^{ab}	23±5 ^a
	X_c (%)	22±3 ^{abc}	29±2 ^d	24±3 ^{bc}	26±1 ^{cd}	21.7±0.4 ^{ab}	18±3 ^a
	T_m onset (°C)	150±11 ^a	157±4 ^a	155±13 ^a	160±2 ^a	145±9 ^a	146±10 ^a
	T_m peak (°C)	180±7 ^a	185.7±0.3 ^a	182±10 ^a	186±1 ^a	183±4 ^a	178±8 ^a
	T_g (°C)	66±1 ^e	45±3 ^a	59±4 ^{cd}	64±2 ^{de}	52±6 ^b	57±5 ^{bc}

*: onset T_g value and T_m values from the last endotherm

During the 1st heating, all the thermograms exhibited a glass transition at around 28-55 °C, typical of semi-crystalline polymers and coherent with that observed by other authors [33]. After the glass transition, multiple crystallization-melting behaviour of ES samples was observed to overlap. This multiple crystallization-melting behaviour reveals that the materials obtained by fast solvent evaporation were mainly in a non-equilibrium glassy state when maintained at temperatures below their T_g [34] and were prone to crystallization during DSC heating to achieve a more thermodynamically stable state [35]. A reduction in PVA crystallinity after the electrospinning process has also been reported by other authors [34], [36], related to the extremely short solvent evaporation time leading to the formation of highly metastable structures.

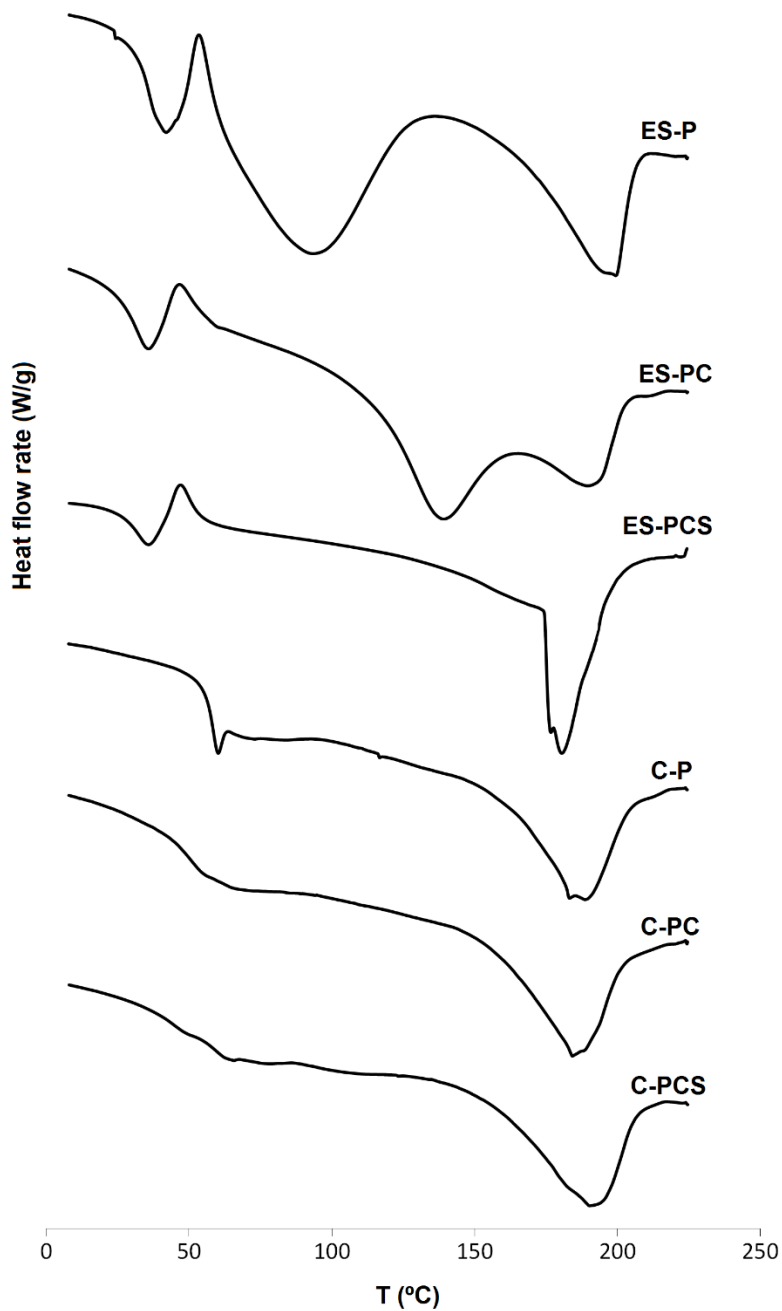


Figure 6. DSC thermograms showing the 1st heating scan of the different electrospun (ES) and cast (C) samples.

In some cases, polymer relaxation, characterized by an endothermic peak at the end of the glass transition, was observed. This relaxation is related with the aging of the glass fraction of the material. The presence of the relaxation endotherm and the overlapped crystallization-melting processes, which disrupt the construction of a realistic integration baseline, hamper the determination of the midpoint of the glass transition temperature in ES samples during the first heating step as well as the integration of the melting endotherm [37]. Due to this, for

ES samples, the onset T_g values and the peak temperature of the last endotherm in the 1st heating were only provided in Table 4. In the other cases, the midpoint T_g values were shown. The presence of carvacrol decreased the onset (ES samples) and midpoint (cast samples) T_g values of the polymer, to a greater extent than in the samples containing surfactant. This was coherent with the carvacrol plasticizing effect, which was more limited when surfactant entrapped a part of the compound within the micelles.

As concerns the cooling scan and second heating scan, where the sample thermal history was deleted, a multifactorial ANOVA revealed no significant differences in the T_g values from either scan and no significant effect of the processing method, but a significant effect of both the carvacrol and surfactant presence ($p < 0.05$). Samples without carvacrol exhibited a mean T_g value of 63 °C, which decreased to 56 °C with carvacrol and surfactant and to 48 °C with only carvacrol, corroborating the plasticizing effects observed from the onset T_g values of the first scan.

By comparing the crystallization (cooling scan) and melting (second heating) temperatures, a supercooling effect was inferred in every case since the T_c values ranged between 142-157 and the T_m between 178-186 °C. The crystallinity of PVA was obtained from the ΔH_m values (J/g PVA), taking into account the reported ΔH_m value (138.6 J/g PVA) of 100 % crystalline PVA [24]. In cast films, the crystallinity was estimated from the first and second (erased thermal history) heating scans. Neither the presence of carvacrol nor that of surfactant in the first heating was observed to cause any significant differences in these values (of about 40 %); however, under the thermal conditions of the DSC assay (second heating), significant differences in crystallinity were observed between the samples. The crystallinity increased in ES samples when these contained carvacrol (especially when there was no surfactant), whereas it decreased in cast samples with carvacrol with and without surfactant. This suggests that, after melting, different component interactions were established in the melt that affect the polymer crystallization differently. In the second heating step, the crystallinity of PVA ranged between 18-30 % concurring with the values obtained by other authors [24], and was lower than that reached during the casting process determined in the first heating scan.

Therefore, a practically amorphous structure can be assumed for the ES samples, which tend to crystallize at temperatures above the T_g value, whereas cast samples exhibited a structure that was highly crystalline in nature (nearly 40 %), as was also deduced from the thermal degradation behaviour of the different samples.

4. Conclusions

PVA aqueous solutions (15 % w/w) containing CA (15 g/100 g polymer) exhibited good electrospinning behaviour, leading to loaded mats with fibres and spherical beads, that retained up to 83 % of the active, giving rise to matrices with up to 12 g carvacrol/100 g polymer. The greatest encapsulation efficiency occurred in the blend without surfactant (83 %) and the formulations with surfactant exhibited similar encapsulation efficiency to that obtained in the casting process (75-77 %). Two fractions of carvacrol could be distinguished in the encapsulating materials; the more strongly bonded, non-thermo-releasable fraction was higher (40 % of the total) in ES samples without surfactant and lower in those containing surfactant, whereas in cast samples this fraction accounted for about 18 % of total carvacrol. Therefore, the addition of the Tween 85 surfactant limited the retention of CA by the PVA matrix, due to its less stable micelle-encapsulating effect that reduced the amount of carvacrol that was more strongly bonded to the polymer. PVA-CA interactions also promoted the plasticization of the polymer, which was practically amorphous in the ES samples and semi-crystalline (about 40 % crystallinity) in the cast samples. Thus, the use of electrospinning as a delivery system for the purposes of successfully applying carvacrol-loaded PVA fibres in active packaging materials represents an interesting strategy, while the PVA layer would provide oxygen barrier capacity coherent with its polar nature.

5. Acknowledgements

The authors thank the Ministerio de Economía y Competitividad (MINECO) of Spain, for the financial support provided for this study as part of the project AGL2016-76699-R. The author A. Tampau also thanks MINECO for the pre-doctoral research grant #BES-2014-068100.

6. References

- [1] L. Sánchez-González, M. Vargas, C. González-Martínez, A. Chiralt, M. Cháfer, Characterization of edible films based on hydroxypropylmethylcellulose and tea tree essential oil, *Food Hydrocoll.* 23 (2009) 2102–2109. doi:10.1016/j.foodhyd.2009.05.006.

- [2] R. Shemesh, M. Krepker, D. Goldman, Y. Danin-Poleg, Y. Kashi, N. Nitzan, A. Vaxman, E. Segal, Antibacterial and antifungal LDPE films for active packaging, *Polym. Adv. Technol.* 26 (2015) 110–116. doi:10.1002/pat.3434.
- [3] A. González, C.I. Alvarez Igarzabal, Soy protein – Poly (lactic acid) bilayer films as biodegradable material for active food packaging, *Food Hydrocoll.* 33 (2013) 289–296. doi:10.1016/j.foodhyd.2013.03.010.
- [4] C.C. Thong, D.C.L. Teo, C.K. Ng, Application of polyvinyl alcohol (PVA) in cement-based composite materials: A review of its engineering properties and microstructure behavior, *Constr. Build. Mater.* 107 (2016) 172–180. doi:10.1016/j.conbuildmat.2015.12.188.
- [5] Y. Di, J. Li, T. Ye, Y. Xiaoyun, The preparation and mechanical properties of novel PVA/SiO₂ film, *J. Exp. Nanosci.* 10 (2015) 1137–1142. doi:10.1080/17458080.2014.980447.
- [6] A. Ultee, L.G.M. Gorris, E.J. Smid, Bactericidal activity of carvacrol towards the food-borne pathogen *Bacillus cereus*, *J. Appl. Microbiol.* 85 (1998) 211–218. doi:10.1046/j.1365-2672.1998.00467.x.
- [7] A. Ben Arfa, S. Combes, L. Preziosi-Belloy, N. Gontard, P. Chalier, Antimicrobial activity of carvacrol related to its chemical structure, *Lett. Appl. Microbiol.* 43 (2006) 149–154. doi:10.1111/j.1472-765X.2006.01938.x.
- [8] S. Tunc, E. Chollet, P. Chalier, L. Preziosi-Belloy, N. Gontard, Combined effect of volatile antimicrobial agents on the growth of *Penicillium notatum*, *Int. J. Food Microbiol.* 113 (2007) 263–270. doi:10.1016/j.ijfoodmicro.2006.07.004.
- [9] S. Burt, Essential oils: Their antibacterial properties and potential applications in foods – A review, *Int. J. Food Microbiol.* 94 (2004) 223–253. doi:10.1016/j.ijfoodmicro.2004.03.022.
- [10] Z.E. Suntres, J. Coccimiglio, M. Alipour, The Bioactivity and Toxicological Actions of Carvacrol, *Crit. Rev. Food Sci. Nutr.* 55 (2015) 304–318. doi:10.1080/10408398.2011.653458.

- [11] M.A. López-Mata, S. Ruiz-Cruz, N.P. Silva-Beltrán, J.D.J. Ornelas-Paz, P.B. Zamudio-Flores, S.E. BurrueI-Ibarra, Physicochemical, antimicrobial and antioxidant properties of chitosan films incorporated with carvacrol, *Molecules*. 18 (2013) 13735–13753. doi:10.3390/molecules181113735.
- [12] L. Atarés, A. Chiralt, Essential oils as additives in biodegradable films and coatings for active food packaging, *Trends Food Sci. Technol.* 48 (2016) 51–62. doi:10.1016/j.tifs.2015.12.001.
- [13] P. Wen, D.-H.H. Zhu, H. Wu, M.-H.H. Zong, Y.-R.R. Jing, S.-Y.Y. Han, Encapsulation of cinnamon essential oil in electrospun nanofibrous film for active food packaging, *Food Control*. 59 (2016) 366–376. doi:10.1016/j.foodcont.2015.06.005.
- [14] S. Torres-Giner, Multifunctional and Nanoreinforced Polymers for Food Packaging, *Multifunct. Nanoreinforced Polym. Food Packag.* (2011) 108–125. doi:10.1533/9780857092786.1.108.
- [15] B. Ghorani, N. Tucker, Fundamentals of electrospinning as a novel delivery vehicle for bioactive compounds in food nanotechnology, *Food Hydrocoll.* 51 (2015) 227–240. doi:10.1016/j.foodhyd.2015.05.024.
- [16] A. Tampau, C. González-Martinez, A. Chiralt, Carvacrol encapsulation in starch or PCL based matrices by electrospinning, *J. Food Eng.* 214 (2017) 245–256. doi:10.1016/j.jfoodeng.2017.07.005.
- [17] L. Quiles-Carrillo, N. Montanes, J.M. Lagaron, R. Balart, S. Torres-Giner, Bioactive multilayer polylactide films with controlled release capacity of gallic acid accomplished by incorporating electrospun nanostructured coatings and interlayers, *Appl. Sci.* 9 (2019) 533. doi:10.3390/app9030533.
- [18] J.L. Castro-Mayorga, M.J. Fabra, L. Cabedo, J.M. Lagaron, On the use of the electrospinning coating technique to produce antimicrobial polyhydroxyalkanoate materials containing in situ-stabilized silver nanoparticles, *Nanomaterials*. 7 (2017). doi:10.3390/nano7010004.

- [19] K. Figueroa-Lopez, J. Castro-Mayorga, M. Andrade-Mahecha, L. Cabedo, J. Lagaron, Antibacterial and Barrier Properties of Gelatin Coated by Electrospun Polycaprolactone Ultrathin Fibers Containing Black Pepper Oleoresin of Interest in Active Food Biopackaging Applications, *Nanomaterials*. 8 (2018) 199. doi:10.3390/nano8040199.
- [20] J. Tao, Effects of Molecular Weight and Solution Concentration on Electrospinning of PVA, Master Thesis, Mater. Sci. Eng. Worcester Polytech. Inst. (2003) 1–107. <https://digitalcommons.wpi.edu/etd-theses/889>.
- [21] S.P. Rwei, C.C. Huang, Electrospinning PVA solution-rheology and morphology analyses, *Fibers Polym.* 13 (2012) 44–50. doi:10.1007/s12221-012-0044-9.
- [22] R.K. Owusu Apenten, Q.-H. Zhu, Interfacial parameters for selected Spans and Tweens at the hydrocarbon—water interface, *Food Hydrocoll.* 10 (1996) 27–30. doi:10.1016/S0268-005X(96)80050-6.
- [23] A. Sze, D. Erickson, L. Ren, D. Li, Zeta-potential measurement using the Smoluchowski equation and the slope of the current-time relationship in electroosmotic flow, *J. Colloid Interface Sci.* 261 (2003) 402–410. doi:10.1016/S0021-9797(03)00142-5.
- [24] M. Hdidar, S. Chouikhi, A. Fattoum, M. Arous, Effect of hydrolysis degree and mass molecular weight on the structure and properties of PVA films, *Ionics (Kiel)*. 23 (2017) 3125–3135. doi:10.1007/s11581-017-2103-0.
- [25] M. Wiśniewska, V. Bogatyrov, I. Ostolska, K. Szewczuk-Karpisz, K. Terpiłowski, A. Nosal-Wiercińska, Impact of poly(vinyl alcohol) adsorption on the surface characteristics of mixed oxide $Mn_xO_y-SiO_2$, *Adsorption*. 22 (2016) 417–423. doi:10.1007/s10450-015-9696-2.
- [26] A. Bhattacharya, P. Ray, Studies on surface tension of poly (vinyl alcohol): Effect of concentration, temperature, and addition of chaotropic agents, *J. Appl. Polym. Sci.* 93 (2004) 122–130. doi:10.1002/app.20436.
- [27] A. Koski, K. Yim, S. Shivkumar, Effect of molecular weight on fibrous PVA produced by electrospinning, *Mater. Lett.* 58 (2004) 493–497. doi:10.1016/S0167-577X(03)00532-9.

- [28] Á. Perdonés, A. Chiralt, M. Vargas, Properties of film-forming dispersions and films based on chitosan containing basil or thyme essential oil, *Food Hydrocoll.* 57 (2016) 271–279. doi:10.1016/j.foodhyd.2016.02.006.
- [29] A. Cano, E. Fortunati, M. Cháfer, J.M. Kenny, A. Chiralt, C. González-Martínez, Properties and ageing behaviour of pea starch films as affected by blend with poly(vinyl alcohol), *Food Hydrocoll.* 48 (2015) 84–93. doi:10.1016/j.foodhyd.2015.01.008.
- [30] S. Farah, D.G. Anderson, R. Langer, Physical and mechanical properties of PLA, and their functions in widespread applications — A comprehensive review, *Adv. Drug Deliv. Rev.* 107 (2016) 367–392. doi:10.1016/j.addr.2016.06.012.
- [31] R. Inai, M. Kotaki, S. Ramakrishna, Structure and properties of electrospun PLLA single nanofibres, *Nanotechnology.* 16 (2005) 208–213. doi:10.1088/0957-4484/16/2/005.
- [32] E.K. Kostakova, L. Meszaros, G. Maskova, L. Blazkova, T. Turcsan, D. Lukas, Crystallinity of Electrospun and Centrifugal Spun Polycaprolactone Fibers: A Comparative Study, *J. Nanomater.* 2017 (2017). doi:10.1155/2017/8952390.
- [33] I. Restrepo, C. Medina, V. Meruane, A. Akbari-Fakhrabadi, P. Flores, S. Rodríguez-Llamazares, The effect of molecular weight and hydrolysis degree of poly(vinyl alcohol)(PVA) on the thermal and mechanical properties of poly(lactic acid)/PVA blends, *Polimeros.* 28 (2018) 169–177. doi:10.1590/0104-1428.03117.
- [34] M.J. Parker, Test Methods for Physical Properties, in: A. Kelly, C.B.T.-C.C.M. Zweben (Eds.), *Compr. Compos. Mater.*, Elsevier, Oxford, 2000: pp. 183–226. doi:10.1016/B0-08-042993-9/00074-7.
- [35] B.B. Sauer, W.G. Kampert, E. Neal Blanchard, S.A. Threefoot, B.S. Hsiao, Temperature modulated DSC studies of melting and recrystallization in polymers exhibiting multiple endotherms, *Polymer (Guildf).* 41 (2000) 1099–1108. doi:10.1016/S0032-3861(99)00258-X.
- [36] M.S. Enayati, T. Behzad, P. Sajkiewicz, R. Bagheri, L. Ghasemi-Mobarakeh, W. Łojkowski, Z. Pahlevanneshan, M. Ahmadi, Crystallinity study of electrospun poly (vinyl

alcohol) nanofibers: effect of electrospinning, filler incorporation, and heat treatment, Iran. Polym. J. (English Ed. 25 (2016) 647–659. doi:10.1007/s13726-016-0455-3.

- [37] C.A. Avila-Orta, F.J. Medellín-Rodríguez, M. V. Dávila-Rodríguez, Y.A. Aguirre-Figueroa, K. Yoon, B.S. Hsiao, Morphological features and melting behavior of nanocomposites based on isotactic polypropylene and multiwalled carbon nanotubes, J. Appl. Polym. Sci. 106 (2007) 2640–2647. doi:10.1002/app.26823.

Poly(lactic acid) based materials encapsulating carvacrol obtained by solvent casting and electrospinning

Alina Tampau ^a, Chelo González-Martínez ^b, Amparo Chiralt ^c

^{a, b, c} Instituto Universitario de Ingeniería de Alimentos para el Desarrollo, Ciudad Politécnica de la Innovación, Universitat Politècnica de Valencia, Camino de Vera, s/n, 46022 Valencia, Spain.

Journal of Food Science (2020)-in press

altam@upvnet.upv.es

Abstract

Poly(lactic acid) (PLA) dissolved (15 wt. %) in ethyl acetate (EtAc) : dimethyl sulfoxide (DMSO) binary systems (0:1; 1:3 and 2:3 v/v) was used as carrier to obtain Carvacrol (CA) loaded (20 wt. % with respect to PLA) matrices by electrospinning, in comparison with solvent casting. Field Emission Scanning Electron Microscopy (FESEM) observations showed that CA-loaded electrospun fibers were thinner than the CA-free ones and their encapsulating efficiency (EE) increased when EtAc was present in the solvent. The cast films had higher EE (up to 89 %) than the electrospun mats (max. 68 %). Thermogravimetric analysis and differential scanning calorimetry revealed that CA-free matrices retain more solvent than the samples with CA, this effect being more noticeable in fibers rather than in cast films. The thermal analysis revealed stronger retention forces of CA in the fibers than in the cast material and the carvacrol plasticizing effect in the PLA matrices, in accordance with its retained amount.

Practical Application

The carvacrol-loaded polylactic acid materials obtained in this study are intended to serve as possible active layer in obtaining active (antimicrobial and/or antioxidant) multilayer materials for the packaging of foodstuffs, when applied onto a supporting polymer layer. Active properties of the material, as well as the potential carvacrol sensory impact, in packaged products should be assessed in further studies.

1. Introduction

Traditionally, the functions of food packaging were protection, communication, containment and transport safety. However, innovation in food packaging has been directed towards the development of new technologies that provide additional benefit, such as the so-called active and intelligent packaging (Martínez-Tenorio & López, 2011). The active packages (Regulation (EC) No. 450/2009 (EU, 2009)) can be obtained either by introducing the active element into the package together with the product or by introducing the active agent into the packaging material itself. This second option would be the most attractive from the consumer's point of view, as nothing strange would be found inside the packaging that would attract attention and cast doubt on the quality of the food (Catalá & Gavara, 2001).

In regards to food preservatives, due to growing consumer concern about synthetic ingredients, the use of natural active compounds extracted from plants represents an attractive alternative in active packaging materials for foods. Of these components, carvacrol (CA), a phenolic monoterpenoid abundant in oregano and thyme essential oils (De Vincenzi, Stammati, De Vincenzi, & Silano, 2004), is one of the most active in terms of antioxidant and antimicrobial activity and approved by the EFSA (2012) as a food flavoring agent. Despite its proven efficacy, carvacrol's use in active packaging materials is limited due to different drawbacks, such as its high volatility (Turek & Stintzing, 2013), low water solubility (1250 mg/L, Yalkowsky, He, & Jain, 2010) and high sensory impact (Hsieh, Mau, & Huang, 2001). Carvacrol encapsulation in a polymeric matrix could enhance the protection of the compound, mitigate its sensory impact and control its release from the material to develop its active functions (Majeed et al., 2015). Ramos, Jiménez, and Garrigós (2016) reviewed different studies and reported on the incorporation of carvacrol into synthetic polymers and biopolymers to obtain innovative materials for active food packaging.

One potential strategy to develop active packaging consists of obtaining multilayer materials in which polymers with complementary properties are assembled to meet the food packaging requirements--in terms of barrier capacity against water vapor or gases--while the active compound could be incorporated in one of the layers. To this end, one possibility is the extension of a polymeric layer containing the active compound over a supporting packaging material, and the subsequent evaporation of the solvent (casting method) (Rhim, Mohanty, & Singh, 2005). With this technique, Busolo, Fernandez, Ocio, and Lagaron (2010) obtained high water barrier PLA chloroform-cast films encapsulating a silver-based nanoclay

with strong antimicrobial activity. However, one of the shortcomings of casting is the effective extension of the active-polymer solution on the polymeric support layer. This process requires a high wettability of the polymeric support with the cast solution that is greatly affected by the chemical affinity of the solution and supporting layer, and their surface properties. Also, casting involves the evaporation of large amounts of solvent that constitute a limitation at the industrial level. Electrospinning (ES) is an alternative technique for depositing an active polymer layer on a polymeric sheet in order to obtain multilayer materials. The ES technique uses an electric field to produce the stretching of the polymeric solution. This allows the solvent in the sample stream to evaporate progressively due to the large contact area between the stream surface and air. Then the electro-drawn material reaches the collector in a dry state, producing nano or microfibers (Bhardwaj & Kundu, 2010). With this technique, polymer meshes with a high surface area / volume ratio, and very small pores are obtained (Liang, Hsiao, & Chu, 2007).

To reduce the environmental impact of synthetic plastics (García, 2004), the use of biodegradable polymers in the development of active food packaging is necessary. Of the available biodegradable materials, polylactic acid (PLA) is an interesting option since it is a biodegradable polyester obtained from the microbial fermentation of renewable sources with high carbohydrate content (Serna, Rodríguez, & Albán, 2003), and it is approved by the Food and Drug Administration (FDA, US) as food contact material. Previous studies reported the use of PLA in electrospun matrices, using solvents unfit for food contact. Alharbi, Luqman, Fouad, Khalil, and Alharthi (2018) obtained PLA-core/PVA-shell coaxially spun nanofibers, using chloroform: dimethylformamide (8:2) as solvent for the polylactide. The core/shell composites exhibited higher tensile strength and ductility than the pristine PLA fibers. Likewise, Li, Frey, and Baeumner (2006) successfully obtained PLA electrospun mats incorporating biotin -- intended as membranes for biosensors -- using chloroform: acetone (3:1) as solvent. A good distribution of the biotin along the length of the individual fibers was achieved, making it accessible for binding with the streptavidin used as detector of *E. coli*. Scafaro, Maio, and Lopresti (2019) obtained cast and electrospun materials with PLA, CA and graphene nanoplatelets (GNP), using chloroform-acetone mixtures. They reported that the incorporation of GNP strengthened and stiffened the cast films, whereas it had an opposite effect in the electrospun fibrous mats, decreasing their stiffness. Likewise, the CA amount and release kinetics could be modulated by the GNP, prolonging the active's release

time, making this kind of materials useful for applications in wound dressing or scaffolds for neuronal tissue engineering.

The aim of this study was to assess the capability of electrospun PLA matrices to encapsulate carvacrol in comparison with cast obtained films, by using different solvent systems approved for food contact. The obtained materials were characterized as to their encapsulation efficiency, microstructure and thermal behavior.

2. Materials and Methods

2.1. Materials

Amorphous poly(lactic acid) (PLA) 4060D, with a density of 1.24 g/cm³, was obtained from NatureWorks (Minnesota, USA) while carvacrol (CA) was supplied by Sigma-Aldrich (Steinheim, Germany). As for the solvents used, dimethyl sulfoxide (DMSO), glacial acetic acid (GAA) and absolute ethanol were purchased from Panreac Química S.L.U. (Castellar del Vallès, Barcelona, Spain); butyl acetate (ButAc) was purchased from Sigma-Aldrich (Steinheim, Germany) and ethyl acetate (EtAc) from Indukern (El Prat de Llobregat, Barcelona, Spain).

2.2. Obtaining the CA encapsulating matrices

15 wt. % PLA solutions (with or without 20 wt. % CA with respect to the polymer) were prepared by placing the PLA pellets in the selected solvent systems in hermetically sealed recipients and maintaining under magnetic stirring at room temperature for 24 h to ensure complete dissolution. Initially, EtAc was used in order to meet the requirements for food contact use. Nevertheless, to solve the problems associated with its fast evaporation at the tip of the spinneret, other solvents (DMSO, GAA and ButAc) with higher boiling points were considered as co-solvents on the basis of their miscibility with the EtAc and good solvent properties with respect to PLA (Scharlab, 2018). The properties of the chosen solvents, relevant for the electrospinning process, as well as the binary combinations tested, are given in Table 1.

The electrospinning of the polymer solutions was carried out under ambient conditions (25 °C, 45 % relative humidity (RH)) in Fluidnatek equipment (Bioinicia S.A., Valencia, Spain) with mono and coaxial mode. In the co-axial mode, only the solvent of the respective

polymeric solution passes through the exterior needle. The process parameters (flow rate, injector-collector distance and voltage) were empirically adjusted to ensure a stable "Taylor cone" formation at the tip of the spinneret. They were fitted on the basis of the previous screening with different solvent systems. For the selected solvents, the PLA solutions were electrodeposited for 1 hour at a flow rate of 1.0 mL/h. The material was deposited on sheets of aluminum foil (previously weighed) placed on the collector, 20 cm from the spinneret tip. The voltage (13.5-15 kV) was adjusted depending on the solution. The obtained material was preserved until its characterization in vacuum desiccators with silica gel to favor further drying and avoid moisture absorption.

The same selected solutions were used to obtain cast materials. These were poured onto Teflon plates of 15 cm in diameter to obtain a surface solid density of $5.6 \cdot 10^{-3}$ g polymer / cm² and placed in a fume hood for solvent evaporation and film formation. The films were peeled from the plate and stored in a vacuum desiccator, with silica gel, until their characterization.

2.3. Characterization of the obtained materials

2.3.1. Microstructure

The obtained ES and cast matrices were observed with a Field Emission Scanning Electron Microscopy equipment (FESEM Ultra 55, Zeiss, Oxford, UK). The samples were mounted with carbon tape on supports and, after being vacuum coated with platinum, were observed using an acceleration voltage of 1 kV. Image analysis, using the ImageJ software (National Institutes of Health, USA), was carried out to measure the size of fibers in the obtained electrospun structures. At least 25 measurements of the fibers were considered per formulation.

2.3.2. CA encapsulating efficiency

The CA retention of the matrices was assessed by means of the ethanol extraction of carvacrol and spectrophotometric determination at 275 nm, using a UV/Vis spectrophotometer (Evolution 201 UV-Vis, Thermo Fisher Scientific Inc.), as previously described by Tampau, González-Martínez and Chiralt (2017). Briefly, electrospun samples (deposited on aluminum foils) or cast film fragments (about 3-5 mg) were introduced into absolute ethanol (15 mL) in amber bottles that were hermetically sealed and kept under

stirring for 24 h at room temperature. The absorbance of the extracts was measured using the respective extract of the CA-free matrix as background. Carvacrol concentration was determined as $\mu\text{g CA/mL}$, using a calibration curve obtained for CA solutions with 10-85 $\mu\text{g/mL}$ (Concentration = $67.325 \cdot \text{Absorbance}$, $R^2=0.998$). The encapsulating efficiency (EE) was expressed as the percentage (%) of total ethanol-extracted CA with respect to the theoretical CA content. Each formulation was analyzed in triplicate.

2.3.3. Thermal analysis

Previously P_2O_5 -conditioned samples were submitted to thermal analyses in order to assess the effect of the carvacrol and processing method on phase transitions and thermal stability of the matrices.

Thermogravimetric analysis (TGA), evaluating the thermal degradation of the material, was performed using a thermogravimetric analyzer (TGA/SDTA 851e, Mettler Toledo, Schwarzenbach, Switzerland). Samples placed into an alumina crucible were heated at a rate of 10 K/min from 25 °C to 700 °C under inert nitrogen atmosphere (flow 20 mL/min). DTA and DGTA curves were analyzed, and the onset (T_o) and peak (T_p) temperatures for the different mass loss steps were determined, as well as the relative mass loss in the first step.

Differential scanning calorimetry (DSC) analyses were carried out using a DSC (1 StarE System, Mettler-Toledo, Inc., Switzerland). The samples (5-10 mg) were placed into aluminum pans (Seiko Instruments, P/N SSC000C008) and sealed. The samples, initially maintained at -25 °C for 5 min, were heated to 225 °C, then cooled to -25 °C, kept at -25 °C for 5 min and heated again to 275 °C. The thermal scanning was performed at 10 K/min. As reference, an empty aluminum pan was used. The thermograms were processed using the software of the equipment (Mettler-Toledo, Inc., Switzerland) to determine the glass transition (T_g) temperatures. The thermal analyses (TGA and DSC) of the samples were carried out in triplicate.

2.4. Statistical analysis

All the data were processed using the software Statgraphics Centurion XVI (Statpoint Technologies Inc., VA, USA) and applying analysis of simple variance (ANOVA). Fisher's least significant difference (LSD) (with a 95.0 % confidence level) was used in order to identify significantly different samples. DSC data were also analyzed using a multifactor

analysis of variance with 95 % significance level, considering the presence of CA in the matrix and the processing method (C or ES) as factors.

3. Results and Discussion

3.1. Solvent system screening

Electrospinning of the 15 wt. % PLA dissolved in pure EtAc revealed the obstruction of the spinneret after about 10 min processing due to the solidification of the polymer. This was attributed to the low boiling point (Table 1) of the solvent which promoted an overly fast evaporation rate. Combination of EtAc with other solvents with higher boiling points (Table 1) and the coaxial mode of the process were tested to mitigate this problem, fitting the process conditions to obtain a stable Taylor cone. Table 1 shows the fitted conditions, including or not co-axial flow, established for each binary solvent system, as well as the processing time during which no problems occurred with the jet flow.

It was observed that the use of DMSO in the solvent mixture allowed for a much longer duration of the process than with the rest of the solvents, without solidification at the tip of the injector (Table 1). However, the electrospun material was not completely free of solvent once the process was finished; the mats collected from the ES equipment produced a wet, translucent appearance. Blends of EtAc and GAA (1:1, v/v) were also tested on the basis of their higher boiling point, and good solvent properties of GAA (parameter of Flory-Huggins $\chi < 0.5$; Casasola, Thomas, & Georgiadou, 2016). However, this blend did not extend the useful process time enough, with or without coaxial flow (Table 1). The solutions using EtAc:GAA 2:1 and 4:1 and EtAc:ButAc 1:1 exhibited an opalescent appearance, which indicated a partial dissolution of the polymer, and were therefore discarded for their subsequent use.

The microstructural characteristics of the obtained fibers under the different operating conditions reflected in Table 1 are shown in Figure 1. In most cases, fibers with elongated droplets were obtained, depending on the solvent and process conditions. The samples obtained with co-axial solvent flow presented less fiber formation with a higher proportion of beads, in accordance with the drop in the polymer concentration at the spinneret needle, due to a local dilution induced by the outer flow of solvent. Yu, Li, Ge, Ye, & Wang (2013) also observed this effect for co-axial electrospinning of ethyl cellulose from an ethanol solution, using a sheath of solvent through the outer needle. When the solvent sheath

flowrate was above a certain ratio with respect to the solution flowrate, the electrospun fibers presented beads-on-string morphology.

Table 1. Process parameters and microscopic observations of the material obtained during ES of solutions with 15 % PLA in different binary solvent systems. Boiling point of each solvent (Smallwood, 1996) was indicated in brackets.

Solvents ratio (v/v)				Flowrate ($\mu\text{L/h}$)		Distance to collector (cm)	Micro-structure in Figure 1	Process time* (min)
EtAc (77 °C)	GAA (118 °C)	ButAc (126 °C)	DMSO (189 °C)	through interior needle	through exterior needle			
0	0	0	1	1000	0	20	A	>60
0	0	0	1	1000	15	20	B	>60
1	0	0	1	1000	0	20	C	>60
1	0	0	1	1000	25	20	D	>60
1	0	0	3	1000	0	20	E	>60
2	0	0	3	1000	0	20	F	>60
1	0	1	0	1100	0	15	G	~10
1	1	0	0	1200	0	15	H	~13
1	1	0	0	1100	100	15	I	~20

*without solidification at the injector tip

Therefore, based on the observed morphology of the material and the processing time without partial solidification at the injector tip, three EtAc:DMSO mixtures (0:1, 1:3 and 2:3) were chosen for further studies encapsulating carvacrol, by processing in monoaxial application mode. The distance between the injector and the collector was set at 20 cm and the voltage adjusted to achieve a stable application (between 14 and 18 kV, depending on the solvent).

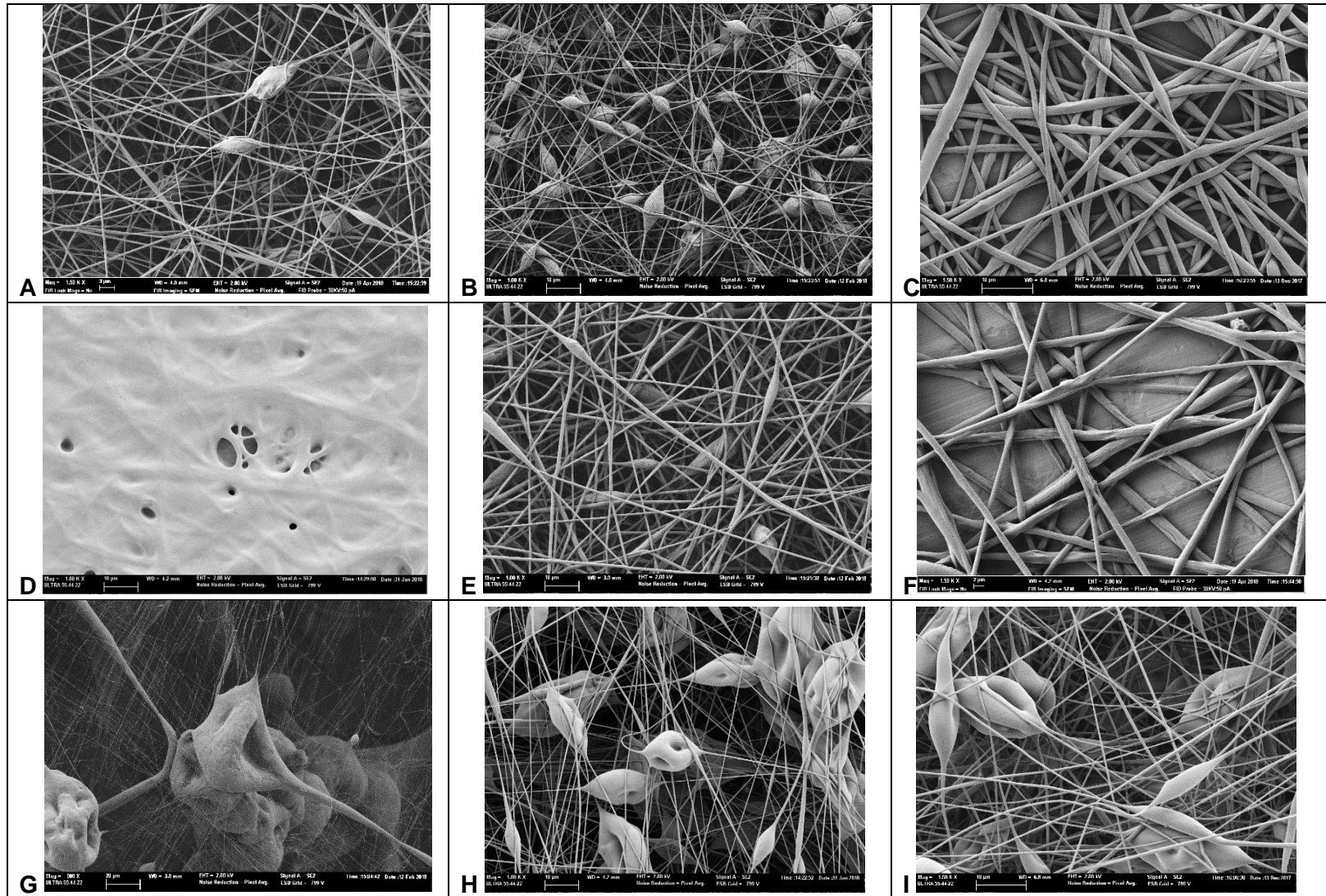


Figure 1. Microstructure of the electrospun PLA material using the different solvent systems and process conditions described in Table 1.

3.2. Microstructure of the ES matrices

With the selected binary solvent systems, matrices of PLA with and without encapsulated CA were obtained, in mono-axial mode, whose micrographs obtained by FESEM are shown in Figure 2. Fiber mats with few beads were obtained in all cases. The relatively flat structure of the obtained fibers revealed the lack of a complete solvent evaporation. The residual solvent plasticized the material and provoked its flattening on the collector surface.

The incorporation of carvacrol modified the structure of the electrospun material, mainly in the sample obtained with pure DMSO, where it presents a compact appearance likely attributable to fibers not being completely dry when deposited in the mesh on the collector. Except when solvent was pure DMSO, the presence of the CA promoted the formation of thinner fibers than those obtained for the respective CA-free controls (Figure 2). This could be related to the modification of the interactions between the chains of the polymer allowing a greater stretching of the fiber in the electric field. It can be observed in the micrographs that by increasing the proportion of EtAc in the solvent mixture, fibers with larger diameters were obtained, an effect verified by the image analysis results shown in Figure 2. This was consistent with the observations reported by other authors (Wannatong, Sirivat, & Supaphol, 2004; Casasola, Thomas, Trybala, & Georgiadou, 2014) who attributed this effect to the lower boiling point of the solvent. The higher the boiling point during electro-stretching, the longer the fiber remains wet, and the more it stretches in the electric field.

3.3. Carvacrol encapsulating efficiency

Table 2 shows the encapsulation efficiency (EE) for the different materials obtained by ES and casting. The EE values reflected a greater CA retention capacity in the matrix when the casting method was used. Likewise, the electrospun fibers obtained from the bisolvent mixtures presented higher encapsulating efficiency than those obtained with pure DMSO. This could be attributed to faster solvent evaporation in the mixtures with EtAc that enhanced the solidification of the polymer fiber, entrapping the active compound and preventing its evaporation. Therefore, the lower boiling point of the solvent caused the formation of thicker fibers, as previously discussed, with higher carvacrol content. In cast films, lower differences in the EE associated with the solvent boiling point were observed, probably due to the fact that the evaporation of the solvent occurs at the film surface, with much lower specific area.

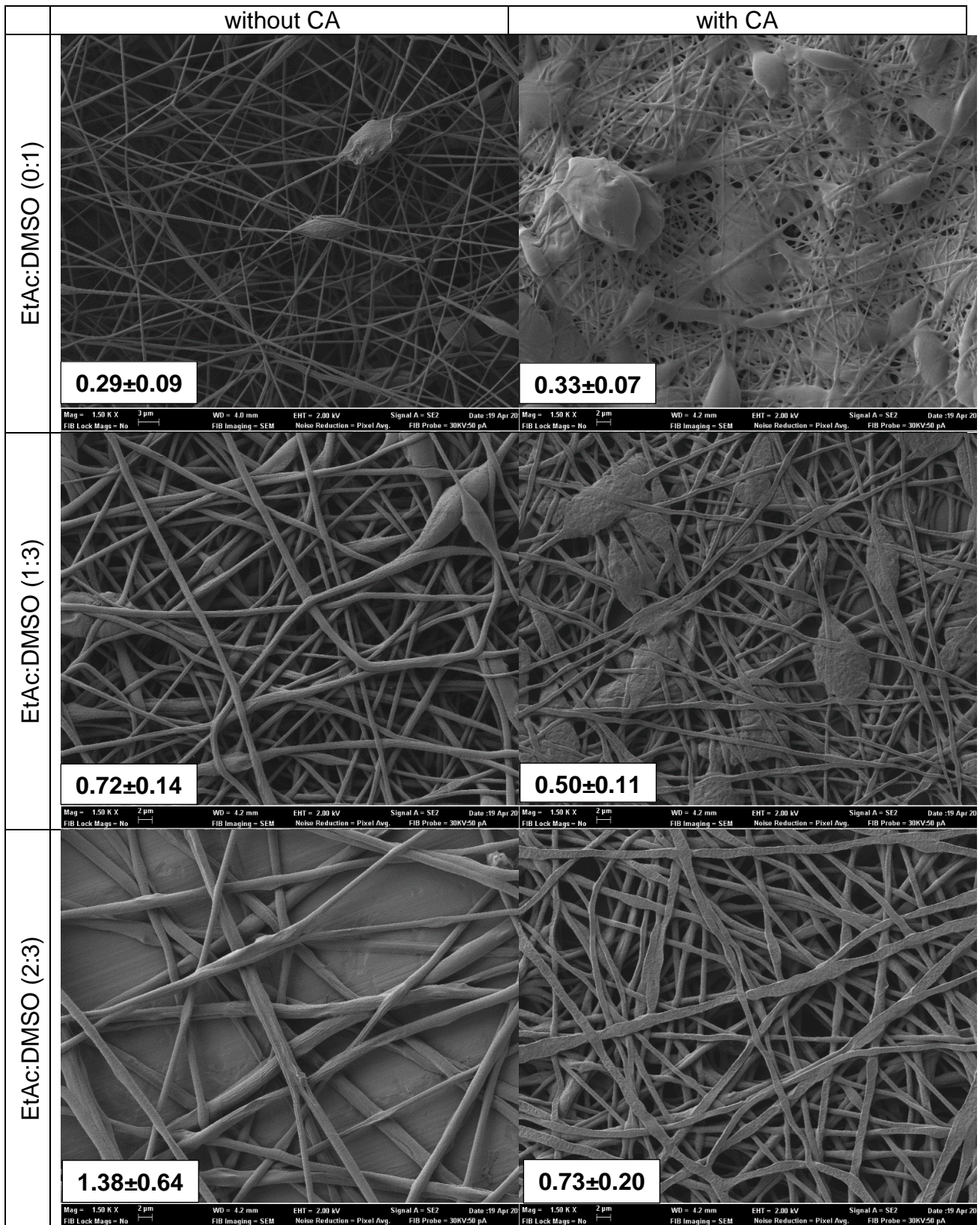


Figure 2. FESEM micrographs of the electrodeposited material, with and without carvacrol. Magnification of 1500x. Estimated mean values of fiber diameters (μm) were specified for each sample.

Table 2. Encapsulating efficacy (EE) values expressed as % of encapsulated CA referred to the initial amount and final carvacrol content (g / g polymer) in the electrospun and cast materials using different solvent systems. The different letters (superscripts) in each column indicate significant differences ($p < 0.05$) between the samples.

Solvent system	EE (%)		Carvacrol content (g /g PLA)	
	ES	Casting	ES	Casting
EtAc:DMSO (0:1)	52±4 ^a	78±4 ^a	0.103±0.008 ^a	0.156±0.008 ^a
EtAc:DMSO (1:3)	62±6 ^b	89±6 ^b	0.124±0.013 ^b	0.177±0.012 ^b
EtAc:DMSO (2:3)	68±2 ^b	76±3 ^a	0.136±0.005 ^b	0.151±0.005 ^a

3.4. Thermal analysis

Figure 3 and Table 3 present the results of the thermogravimetric analysis that showed two weight loss stages, as observed in the TGA curves. The first degradation step of less intensity, up to temperatures of about 150 °C (in CA-free samples) or 250 °C (in samples with CA), must be attributed to the thermo-release of solvent residues or both solvent and encapsulated CA, respectively. In fact, the peak temperature of this step was higher in samples containing carvacrol, coherently with the higher volatilization temperature of this compound. The second step, at higher temperatures, much more intense, corresponded to the thermo-degradation of the polymer. During the first stage, variable mass losses were detected depending on the sample. Losses of up to 40 % (Table 3) occurred in fibers without CA and indicate the retention of a large amount of solvent in the matrix that is released during heating. This retention increased with the content of EtAc in the solvent mixture. This suggests the appearance of specific interactions of the solvent with the polymer, which limit its evaporation during electrospinning. This solvent retention effect was also observed in casting films for the solvent EtAc:DMSO with ratio of 1:3 and was very slight for the 2:3 mixture and pure DMSO. In the samples carrying carvacrol, the first stage of weight loss extends to higher temperatures, given the higher boiling point of carvacrol compared to DMSO, and was more intense for casting films than for fibers. This could be related with the highest content of carvacrol retained in the film determined by spectrophotometry (Table 2).

Table 3. Thermal degradation temperatures (T_o – onset temperature at which degradation begins, T_p – peak temperature at maximum degradation rate), and mass fraction released in the first stage (M) before the polymer degradation step. The superscript letters indicate significant differences ($p < 0.05$) between the formulations with or without carvacrol in the respective columns.

Sample			First peak		Second peak		M (g/g sample)
			T_o (°C)	T_p (°C)	T_o (°C)	T_p (°C)	
Casting	with CA	EtAc:DMSO (0:1)	34±2 ^a	131±16 ^{ef}	234±5 ^a	283±4 ^{ab}	0.13
		EtAc:DMSO (1:3)	34±3 ^a	141±12 ^f	235±29 ^a	287±25 ^{ab}	0.17
		EtAc:DMSO (2:3)	35±4 ^a	141±6 ^f	272±1 ^{cd}	320±1 ^d	0.17
	without CA	EtAc:DMSO (0:1)	35±3 ^a	73±5 ^a	291 ±1 ^{de}	327±1 ^d	0.02
		EtAc:DMSO (1:3)	35±4 ^a	96±7 ^{abc}	264±7 ^{bc}	304±9 ^c	0.16
		EtAc:DMSO (2:3)	35±2 ^a	76±23 ^a	250±25 ^{ab}	297±17 ^{bc}	0.01
ES	with CA	EtAc:DMSO (0:1)	39 ±1 ^{ab}	178±2 ^g	242±3 ^a	291±3 ^{abc}	0.04
		EtAc:DMSO (1:3)	36±2 ^{ab}	131±17 ^{ef}	233±2 ^a	280±1 ^a	0.05
		EtAc:DMSO (2:3)	35±3 ^a	125±22 ^{def}	238±8 ^a	289±6 ^{abc}	0.03
	without CA	EtAc:DMSO (0:1)	43±5 ^{bc}	106±25 ^{bcd}	281±8 ^{cde}	323±4 ^d	0.14
		EtAc:DMSO (1:3)	48±9 ^c	88±15 ^{ab}	292±5 ^e	328±2 ^d	0.23
		EtAc:DMSO (2:3)	76±7 ^d	116±4 ^{cde}	290±5 ^{de}	326±2 ^d	0.46
Carvacrol			118±15	159±7	-	-	-
PLA pellet			-	-	272±4	311±4	-

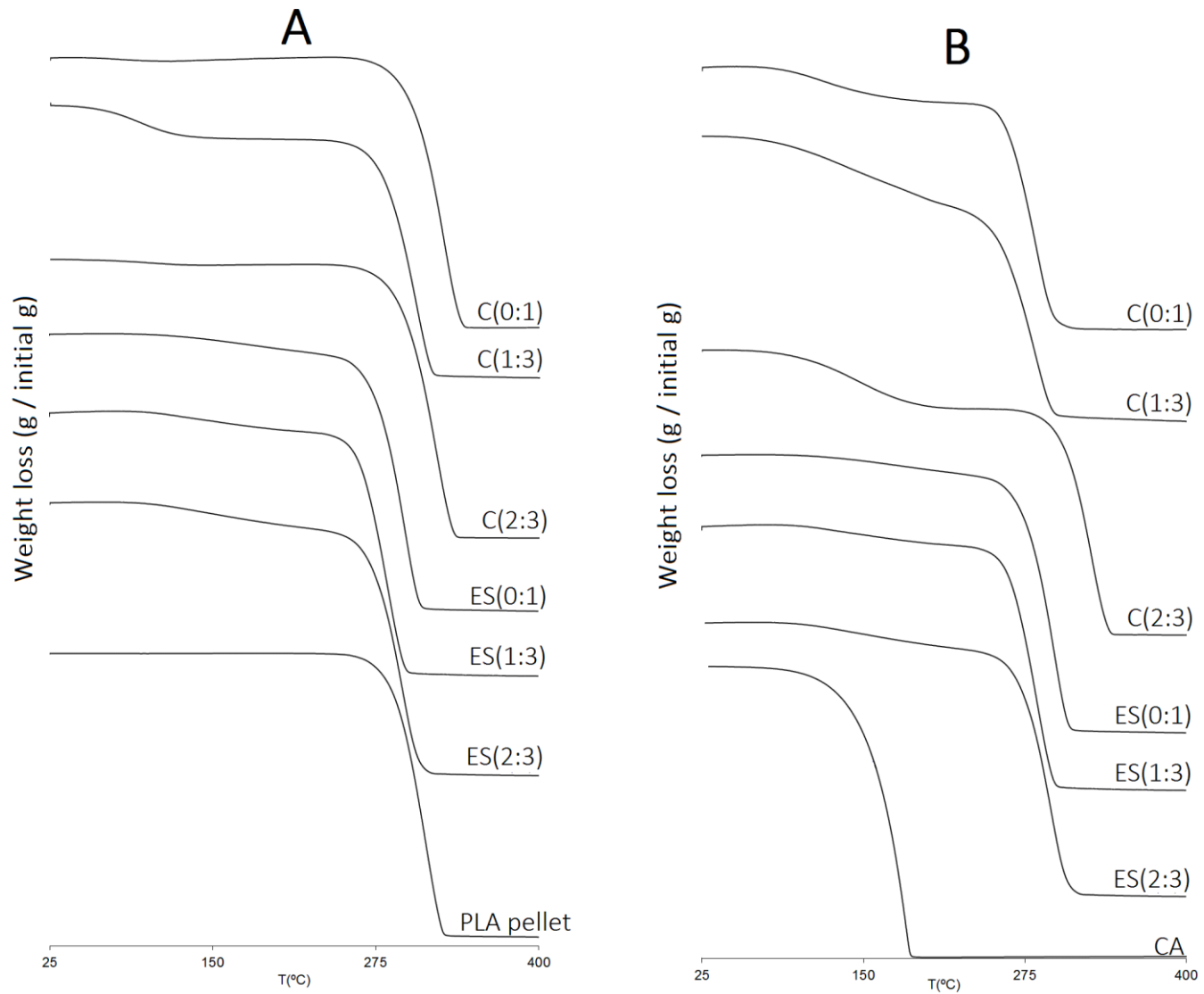


Figure 3. TGA curves of the cast (C) and electrospun (ES) PLA materials, using different EtAc:DMSO ratios (0:1, 1:3 and 2:3). A: samples without carvacrol, B: samples encapsulating carvacrol.

It is remarkable that the presence of CA seems to minimize the solvent retention since the mass loss occurs mainly in the temperature range corresponding to the release of carvacrol. In fact, assuming that the mass loss of the first temperature interval, corresponds to the thermo-release of carvacrol before the polymer degradation, it can be deduced that only a fraction of the encapsulated compound was delivered from the fibers, since the weight loss was lower than the corresponding total carvacrol content determined by spectrophotometry. This suggests that a part of the carvacrol (about 60 % of the total) was strongly bonded to the polymer and was not thermo-released before the polymer degradation. However, in cast samples, the mass loss that occurred during the first step was, in general, slightly higher than the carvacrol content in the samples, which indicates that a part of the thermo-released mass must also correspond to adsorbed solvent. This mainly occurred when solvent contained EtAc, which concurs with what was observed for carvacrol-free materials that retained significant amounts of solvent when there was more ratio of EtAc in the mixture.

The degradation step of the polymer occurred in a temperature range that was affected by the type of processing and the presence or absence of carvacrol. In CA-loaded cast material, the temperature of the degradation peak increased when the EtAc ratio in the solvent rose and reached values higher than those of the polymer pellets, whereas the opposite effect was observed with cast samples without carvacrol. In contrast, no significant effect of solvent was observed in the temperature peak of electrospun material with or without carvacrol. Nevertheless, carvacrol-loaded mats exhibited lower peak temperature than carvacrol free ones. These results suggested that in the obtained matrices the interactions of the residual solvent or carvacrol with the polymer chains affected the degree of packing of the chains in the matrix, giving rise to structures with different thermal resistance. The greater the polymer matrix's degree of compactness, the higher the expected degradation temperature of the matrix is.

On the other hand, the presence of carvacrol affected the interactions of the chains with the solvent, leading to lower solvent adsorption in the polymer matrix, especially in the electrospun material. These results indicate that the polymer chains in amorphous PLA interact specifically with the solvent (EtAc and DMSO) molecules and carvacrol, which affects the retention of these compounds in the matrix and its compactness. This, in turn, determines the thermal degradation temperature of the polymer. The effects of the solvent were more relevant in the absence of carvacrol, notably in fibers. This could be attributed to the blocking of the active points of the chains through preferential interactions with carvacrol,

thus limiting their ability to interact with the solvent molecules and limiting the solvent retention in the material.

The first heating scans in the DSC thermograms exhibited endotherms associated with the evaporation of the solvent retained in different proportions. Figure 4 shows an example of the obtained thermograms (first scan) for the samples prepared by ES and casting, with and without carvacrol, using EtAc:DMSO (2:3) where the solvent evaporation endotherms can be observed. The comparison of the vaporization enthalpy with the enthalpy of the DMSO allowed to determine variable amounts of solvent, depending on the analyzed sample. These enthalpies were greater in the samples without carvacrol, revealing that the presence of the active substance contributes to a better evaporation of the solvent from the fibers and the films, as previously deduced from the TGA analyses. It reveals that the active points of the polymer for the solvent adsorption (interacting groups) are shielded by the preferential interaction with carvacrol. In thermograms, the glass transition of the polymer could be observed with the typical relaxation endotherm whose enthalpy values ranged between 0.6 and 5.8 J/g, associated with aging of the matrix. As expected, this relaxation no longer appears in the cooling sweep or in the second heating scan.

Table 4 shows the T_g values of the different samples obtained in the heating (first and second) and cooling scans. In general, the values for a determined sample in the cooling and the second heating steps were higher than those of the first heating sweep. This reflects the plasticizing effect of the adsorbed solvent in the initial sample. This solvent is released, at least partially, during the first heating (as the endotherms shown in Figure 4 reveal). Then, the cooling or second heating step could be considered to obtain the T_g of the samples when these were free of solvent (after the first heating step). The variability observed in the values can be attributed to the different proportions of solvent remaining in the samples during the different thermal steps, or even to partial losses of carvacrol during the first heating. However, assuming the major release of the solvent in the first heating scan, the T_g of the second heating scan was taken to estimate the effect of CA on the T_g values. The average T_g values for all the ES samples containing carvacrol was 37 ± 5 °C while for the cast samples with carvacrol, this value was 26 ± 8 °C. In contrast, for all samples without CA the mean T_g was 44 ± 6 °C, which was in the range of the T_g obtained for the non-processed polymer pellets (52 ± 2 °C). These values indicate that carvacrol had a plasticizing effect on PLA, which will be affected by its load in the ES or cast matrices. The ES samples with carvacrol exhibited higher T_g values than the carvacrol loaded cast samples, which is

coherent with the lower amount of CA retained in the mats and so, the lower plasticizing effect of the retained compound.

Table 4. Glass transition temperature (T_g) obtained from different heating and cooling steps of the DSC thermograms for the different samples. The superscript letters indicate significant differences ($p < 0.05$) between the formulations in the same column.

		Sample	T_g (°C)		
			First heating	Cooling	Second heating
Casting	PLA + CA	EtAc:DMSO (0:1)	15±1 ^b	23±1 ^a	26±1 ^a
		EtAc:DMSO (1:3)	19±2 ^c	35±2 ^b	37±2 ^b
		EtAc:DMSO (2:3)	8±4 ^a	17±4 ^a	20±5 ^a
	PLA	EtAc:DMSO (0:1)	45±2 ⁱ	41±1 ^{bcd}	44±1 ^{cd}
		EtAc:DMSO (1:3)	40±1 ^{fg}	46 ^{cde}	49 ^{de}
		EtAc:DMSO (2:3)	44±3 ^{gh}	52±1 ^e	55±1 ^e
ES	PLA + CA	EtAc:DMSO (0:1)	35±1 ^e	37±3 ^{bc}	39±4 ^{bc}
		EtAc:DMSO (1:3)	30±1 ^d	34±1 ^b	36±2 ^c
		EtAc:DMSO (2:3)	30±2 ^d	39±7 ^{bc}	41±7 ^{bcd}
	PLA	EtAc:DMSO (0:1)	39±2 ^{ef}	46±8 ^{de}	49±7 ^{de}
		EtAc:DMSO (1:3)	40±5 ^f	39±3 ^{bcd}	41±3 ^{bcd}
		EtAc:DMSO (2:3)	37±1 ^{ef}	-	-
PLA pellet			56	52	55

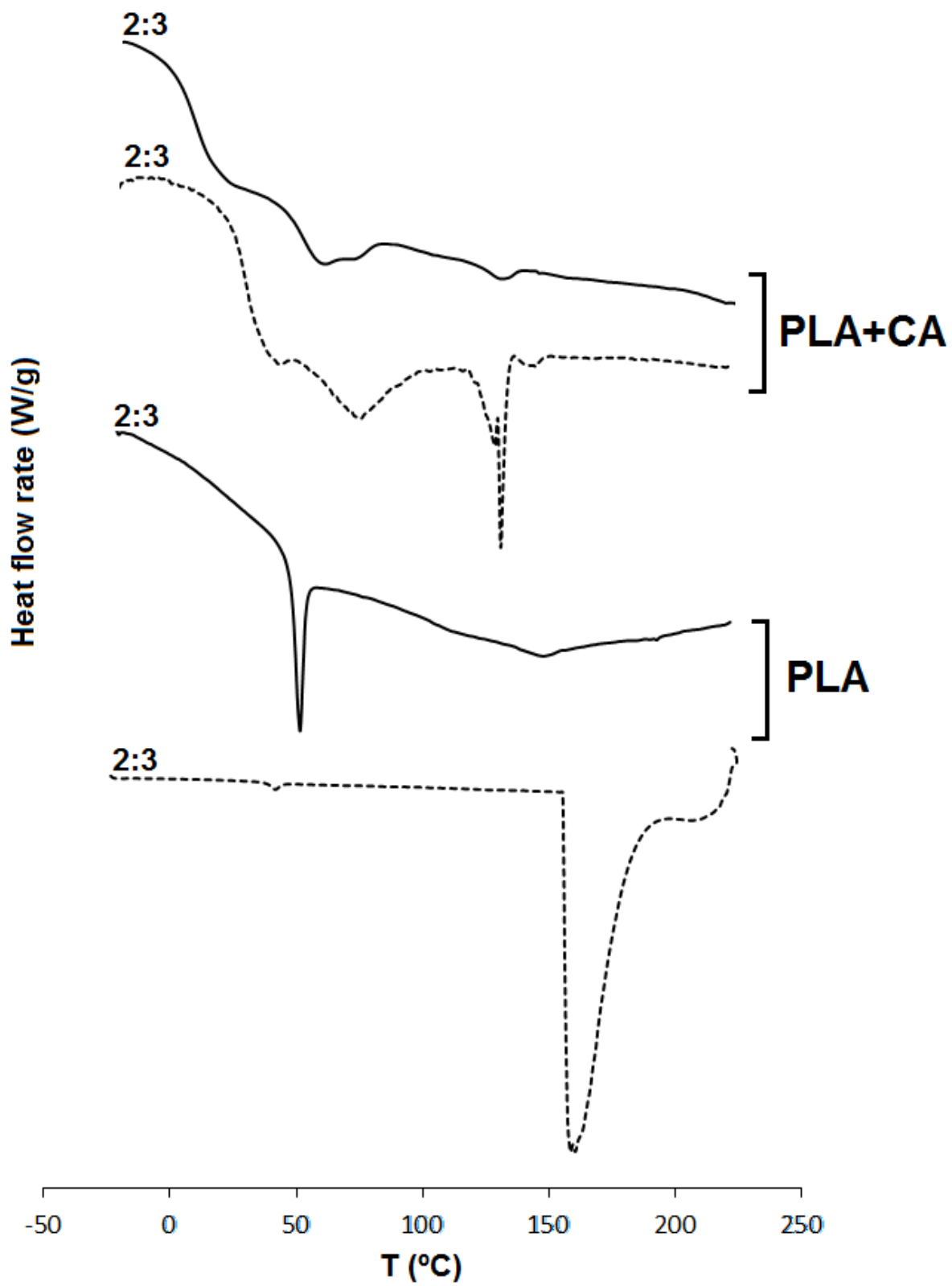


Figure 4. DSC thermograms of PLA materials obtained from the EtAc:DMSO (2:3) solution by casting (continuous line) or electrospinning (dashed line).

4. Conclusions

The carvacrol encapsulation efficiency in PLA matrices was higher for solvent casting (76-89 %) than for electrospinning (52-68 %) and was affected by the ratio EtAc:DMSO in the solvent mixture. Nevertheless, fibers reached a carvacrol-load of 10-13 g per 100 polymer (against 15-18 in cast samples), from which only about 40 % was thermo-released before the polymer degradation, which indicates its strong retention in the fibers. In contrast, carvacrol was practically thermo-released in total in cast samples, which indicates lower retention forces in the matrix. As far as the solvent, the incorporation of the EtAc to DMSO significantly increased the encapsulating efficiency in the fibers (from 50 to almost 70 %), although in the cast samples a higher efficiency was only observed for the smallest ratio of EtAc. The electrospun material of PLA with or without carvacrol, using EtAc:DMSO mixtures as solvents, exhibited a fiber structure with few beads. Fiber diameter decreased when it contained carvacrol and increased when the proportion of EtAc in the solvent mixture rose. Based on the current study, electrospinning of solutions of PLA and carvacrol (20 wt. % with respect to the polymer) in mixtures of EtAc:DMSO (both valid for food contact) could be used effectively in obtaining active multilayer materials for the packaging of foodstuffs when applied onto a supporting polymer layer.

5. Acknowledgments

The authors thank the Ministerio de Economía y Competitividad (MINECO) of Spain, for the financial support for this study as part of the project AGL2016-76699-R. The author A. Tampau also thanks MINECO for the pre-doctoral research grant #BES-2014-068100.

6. References

Alharbi, H. F., Luqman, M., Fouad, H., Khalil, K. A., & Alharthi, N. H. (2018). Viscoelastic behavior of core-shell structured nanofibers of PLA and PVA produced by coaxial electrospinning. *Polymer Testing*, 67, 136–143. <https://doi.org/10.1016/j.polymertesting.2018.02.026>

- Bhardwaj, N., & Kundu, S. C. (2010). Electrospinning: A fascinating fiber fabrication technique. *Biotechnology Advances*, 28(3), 325–347. <https://doi.org/10.1016/j.biotechadv.2010.01.004>
- Busolo, M. A., Fernandez, P., Ocio, M. J., & Lagaron, J. M. (2010). Novel silver-based nanoclay as an antimicrobial in polylactic acid food packaging coatings. *Food Additives & Contaminants: Part A*, 27(11), 1617–1626. <https://doi.org/10.1080/19440049.2010.506601>
- Casasola, R., Thomas, N. L., Trybala, A., & Georgiadou, S. (2014). Electrospun poly lactic acid (PLA) fibers: Effect of different solvent systems on fiber morphology and diameter. *Polymer*, 55(18), 4728–4737. <https://doi.org/10.1016/j.polymer.2014.06.032>
- Casasola, R., Thomas, N. L., & Georgiadou, S. (2016). Electrospinning of poly (lactic acid): Theoretical approach for the solvent selection to produce defect-free nanofibers. *Journal of Polymer Science, Part B: Polymer Physics*, 54(15), 1483–1498. <https://doi.org/10.1002/polb.24042>
- Catalá, R., & Gavara, R. (2001). Nuevos envases. De la protección pasiva a la defensa activa de los alimentos envasados. *Arbor*, 168(661), 109–127. <https://doi.org/10.3989/arbor.2001.i661.825>
- De Vincenzi, M., Stamatii, A., De Vincenzi, A., & Silano, M. (2004). Constituents of aromatic plants: Carvacrol. *Fitoterapia*, 75(7–8), 801–804. <https://doi.org/10.1016/j.fitote.2004.05.002>
- EC450. (2009). EC450, Regulation on active and intelligent materials and articles intended to come into contact with food. *Off J EU*, 450(29 May 2009), L 135/3-135/11.
- EFSA. (2012). Scientific Opinion on the Safety and efficacy of phenol derivates containing ring-alkyl, ring-alkoxy and side- chains with an oxygenated functional group (chemical group 25) when used as flavourings for all species. *EFSA J.*, 10(2), 2573. <https://doi.org/10.2903/j.efsa.2012.2573>.
- García, E. (2004). La civilización industrial y los límites del planeta. *Medio Ambiente y Sociedad.*, 59–99.

- Hsieh, P. C., Mau, J. L., & Huang, S. H. (2001). Antimicrobial effect of various combinations of plant extracts. *Food Microbiology*, 18(1), 35–43. <https://doi.org/10.1006/fmic.2000.0376>
- Li, D., Frey, M. W., & Baeumner, A. J. (2006). Electrospun polylactic acid nanofiber membranes as substrates for biosensor assemblies. *Journal of Membrane Science*, 279(1–2), 354–363. <https://doi.org/10.1016/j.memsci.2005.12.036>
- Liang, D., Hsiao, B. S., & Chu, B. (2007). Functional electrospun nanofibrous scaffolds for biomedical applications. *Advanced Drug Delivery Reviews*, 59(14), 1392–1412. <https://doi.org/10.1016/j.addr.2007.04.021>
- Majeed, H., Bian, Y., Ali, B., Jamil, A., Majeed, U., Khan, Q. F., Fang, Z. (2015). Essential oil encapsulations: uses, procedures, and trends. *RSC Advances*, 5(72), 58449–58463. <https://doi.org/10.1039/C5RA06556A>
- Martínez-Tenorio, Y., & López-Malo, A. (2011). Envases activos con agentes antimicrobianos y su aplicación en los alimentos. *Temas Selectos de Ingeniería De Alimentos*, Vol. 2, pp. 1–12. Retrieved from [https://www.udlap.mx/WP/tsia/files/No5-Vol-2/TSIA-5\(2\)-Martinez-Tenorio-et-al-2011.pdf](https://www.udlap.mx/WP/tsia/files/No5-Vol-2/TSIA-5(2)-Martinez-Tenorio-et-al-2011.pdf)
- Ramos, M., Jiménez, A., & Garrigós, M. C. (2016). Chapter 26 - Carvacrol-Based Films: Usage and Potential in Antimicrobial Packaging. In J. B. T.-A. F. P. Barros-Velázquez (Ed.), *Antimicrobial Food Packaging* (pp. 329–338). <https://doi.org/https://doi.org/10.1016/B978-0-12-800723-5.00026-7>
- Rhim, J. W., Mohanty, A. K., Singh, S. P., & Ng, P. K. W. (2006). Effect of the processing methods on the performance of polylactide films: Thermocompression versus solvent casting. *Journal of Applied Polymer Science*, 101(6), 3736–3742. <https://doi.org/10.1002/app.23403>
- Scaffaro, R., Maio, A., & Lopresti, F. (2019). Effect of graphene and fabrication technique on the release kinetics of carvacrol from polylactic acid. *Composites Science and Technology*, 169(October 2018), 60–69. <https://doi.org/10.1016/j.compscitech.2018.11.003>

- Scharlab (2018, September 17). Retrieved from <http://scharlab.com/tabla-reactivos-mezclabilidad.php>
- Serna, L., Rodríguez, A., & Albán, F. (2003). Ácido Poliláctico (PLA): Propiedades y Aplicaciones. *Ingeniería y Competitividad*, 5(1), 16–26.
- Smallwood, I. M. (1996). *Handbook of organic solvent properties*. London: Arnold Hodder Headline Group; New York: Halsted Press John Wiley & Sons.
- Tampau, A., González-Martínez, C., & Chiralt, A. (2017). Carvacrol encapsulation in starch or PCL based matrices by electrospinning. *Journal of Food Engineering*, 214, 245–256. <https://doi.org/10.1016/j.jfoodeng.2017.07.005>
- Turek, C., & Stintzing, F. C. (n.d.). *Stability of Essential Oils: A Review*. <https://doi.org/10.1111/1541-4337.12006>
- Wannatong, L., Sirivat, A., & Supaphol, P. (2004). Effects of solvents on electrospun polymeric fibers: preliminary study on polystyrene. *Polymer International*, 53(11), 1851–1859. <https://doi.org/10.1002/pi.1599>
- Yalkowsky, S. H., He, Y., & Jain, P. (2010). *Handbook of aqueous solubility data*. Second ed. CRC Press Taylor and Francis Group.
- Yu, D.-G., Li, X.-X., Ge, J.-W., Ye, P.-P., & Wang, X. (2013). The Influence of Sheath Solvent's Flow Rate on the Quality of Electrospun Ethyl Cellulose Nanofibers. *Modeling and Numerical Simulation of Material Science*, 03(04), 1–5. <https://doi.org/10.4236/mnsms.2013.34B001>

Enhancement of PLA-PVA surface adhesion in bilayer assemblies by PLA aminolization

Alina Tampau ^a, Chelo González-Martínez ^b, António A. Vicente ^c
Amparo Chiralt ^d

^{a, b, d} Instituto Universitario de Ingeniería de Alimentos para el Desarrollo, Ciudad Politécnica de la Innovación, Universitat Politècnica de Valencia, Camino de Vera, s/n, 46022 Valencia, Spain.

^c CEB – Centre of Biological Engineering, University of Minho, Campus de Gualtar, 4710-057 Braga, Portugal

submitted to Food and Bioprocess Technology

altam@upvnet.upv.es

Abstract

The surface energy of thermo-processed poly(lactic acid) (PLA) films was modified through chemical treatment with 1,6-hexanediamine in order to enhance the polar component and adhesion forces with polar poly(vinyl alcohol) (PVA) aqueous solutions. Treatment times longer than 10 min provoked a corrosive action in the films' internal structure, whereas 1 and 3 min treatments increased the polar component of surface energy. Extensibility analyses of PVA solutions containing or not carvacrol (15 wt. %) and different Tween 85 ratios on PLA activated surface led to select the 1 min aminolyzed surface for obtaining PLA-PVA bilayers, by casting PVA solutions on the PLA films. The bilayers were characterized as to their oxygen and water vapour barrier properties, microstructure, mechanical and thermal behaviour. Despite aminolization enhanced the PLA surface affinity with aqueous PVA solutions, casting provided a thin and heterogeneous thickness for PVA layer in the laminates that limited its oxygen barrier effectiveness.

Keywords

aminolization; surface activation; poly(lactic acid); poly(vinyl alcohol); carvacrol; bilayer assembly.

Abbreviations

PLA, poly(lactic acid); PVA, poly(vinyl alcohol); CA, carvacrol; M_w , molecular weight; T85, Tween 85 (polyoxyethylene sorbitan trioleate); P_2O_5 , phosphorous pentoxide; RH, relative humidity; S, surfactant; FFD, film-forming dispersion; SE, surface energy; FESEM, Field Emission Scanning Electron Microscopy; WVP, water vapour permeability; OP, oxygen permeability; TS, tensile strength at break; YM, Young modulus; $\epsilon\%$, elongation at break; TGA, thermogravimetric analysis; DTA, derivative TGA; T_o , onset degradation temperature; T_p , peak degradation temperature; DSC, differential scanning calorimetry; T_g , glass transition temperature; ΔH , enthalpy.

1. Introduction

Biodegradable polymers have generated an increased interest in the current packaging field, as the massive use of conventional petroleum-based plastics has led to a negative environmental impact world-wide. Some biobased aliphatic polyesters, such as the polylactides, constitute a very promising group of materials for applications in the packaging area [1]. Poly(lactic acid) (PLA) is biocompatible (Food and Drug Administration approved) [2], compostable [3], and made from renewable sources. Its lactic acid monomer is obtained by fermenting starch extracted from corn, cassava, sugar cane or beets and its environmentally-friendly manufacturing process requires less fossil energy and water consumption than conventional plastics [4]. Its degradation products are non-toxic, since lactic acid is a naturally occurring substance, widely found in nature and metabolized by organisms [5]. PLA presents potential as packaging material, as it can produce highly transparent, rigid films that exhibit good water vapour barrier (WVP) properties [6], [7]. Nevertheless, PLA also presents shortcomings, as it exhibits mechanical fragility/brittleness and limited oxygen barrier capacity [6].

A useful approach to offset/overcome drawbacks of individual films is by emulating/adopting the multilayer structure of commercial films. These are currently made of several sheets of polymers (3 to 12 layers according to [8]) imparting complementary properties to the final material (e.g. European Patent EP0175451A2 [9]). Some layers provide moisture resistance, while others act as gas barriers or provide mechanical support, creating materials more suitable for the intended applications. This strategy of pairing polymer sheets is already ongoing in the field of biopolymers.

Several authors have reported obtaining multilayers with improved physical properties, based on starch and polyester blends. Thus, Requena et al. (2018) [10] obtained bilayers by thermo-sealing cassava starch sheets and polylactic acid-polyhydroxybutyrate-co-hydroxyvalerate blend films. These materials presented effective WVP due to the layer of polyesters, whereas the good oxygen barrier was provided by the starch sheet. Similarly, Muller et al. (2017) [2] obtained bilayer assemblies from thermo-processed cassava starch and solvent-cast amorphous PLA that presented a greatly reduced WVP, high transparency and good oxygen barrier. Martucci and Ruseckaite (2010) [11] prepared a three layer laminate, by combining two external layers of PLA with a middle layer of heat-moulded

gelatine. This assembly maintained the transparency while increasing the moisture resistance of the protein. The multilayer material presented an increased tensile strength and a noticeable improvement in its water vapour and oxygen barrier properties with respect to its individual constituents. Rhim et al. (2006) [12] developed multilayer films based on a middle sheet of soy protein isolate (SPI) and exterior layers of polylactide obtained by casting. The tensile strength of the laminates showed a more than 5-fold increase when compared to the SPI sheet alone. The barrier properties also benefited from pairing the two polymers, the multilayer material presenting low water vapour and oxygen permeability.

Another interesting alternative to complement the polylactide's physical properties is represented by poly(vinyl alcohol) (PVA). This polymer is a fully degradable bioplastic, synthetically obtained via catalysed hydrolysis of polyvinyl acetate. PVA cast films exhibit very good oxygen barrier capacity, with good tensile strength and flexibility [13]. It already enjoys many applications in the market, given its non-toxic, water-soluble nature which allows for excellent hydrogel and film-forming properties. PVA has already been approved by the USDA to be used in the packaging of meat and poultry products [14]. However, PVA exhibits high WVP due to its hydrophilic nature. Thus, the laminated assembly with hydrophobic polymer sheets, such as PLA, could yield a multilayer material with enhanced mechanical and barrier features.

One of the possible strategies to obtain multilayer films is the casting of a polymeric solution on the surface of another polymeric layer support. This method requires a good extensibility/wettability of the solution on the polymeric film, which is greatly affected by the surface interactions of the polymer solution with the supporting polymer that, in turn, depends on the molecular interactions between the components in the solution and those on the contact surface [15]. However, when using polymers with complementary properties, such as PVA and PLA, these are hydrophilic and hydrophobic in nature, respectively. Therefore, chemical affinity between them or their solutions is low, which compromises the surface interactions to obtain adequate polymer adhesion. To address this shortcoming, a potential strategy is the functionalization of the PLA surface through the aminolization technique. This method uses a diamine solution to introduce radicals carrying free amino moieties onto the surface of the PLA film [16]. The ester (-COO-) groups in the polylactic acid chain would interact with one of the diamine's -NH₂ groups forming a covalent bond (O=C-NH-) (Figure 1). Thus, the diamine's structure carrying a free -NH₂ moiety would

become attached to the polymer surface. The surface modifications in the hydrophilic-lipophilic balance produced by the diamine can easily be monitored by observing the change in the surface energy components, through contact angle measurement. Then, the positively charged amino moieties (activated by immersion in a hydrochloric solution) could interact with a negatively charged polymer (such as partially acetylated PVA) in aqueous solution, generating a well-adhered coating on top of the PLA support material. This surface modification approach has found applications not only in constructing layer-by-layer assemblies [17], [18], [19], but also in live cell immobilization on the activated polyester surface [16], [20].

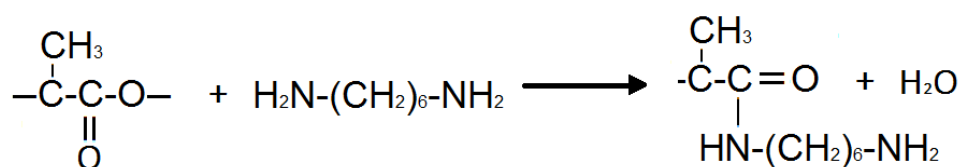


Figure 1. Mechanism of aminolization by 1,6-hexanediamine, occurring at the polylactide's surface.

The addition of antimicrobial or antioxidant molecules into the multilayer structure could provide additional benefits when used as packaging material, exerting an active protection on the packaged foodstuffs. In line with the trend for environmentally-friendly materials, natural extracts and plant essential oils, or their constituents, are good candidates to be added to the packaging sheets. Carvacrol (CA) is a natural monoterpenoid present as a main constituent in the essential oils of oregano or thyme [21], [22]. It has proven antimicrobial and antioxidant effects, as reported by many authors [23], [24], [25]. The inclusion of CA in a carrier polymeric matrix could be a useful way to deliver its effects [26]. In this sense, previous studies reported very slow release kinetics of these kinds of compounds from PLA films [27], whereas their encapsulation in more hydrophilic polymers favours the release, providing greater effectiveness as antimicrobial agents [27], [28]. Multilayer assemblies could incorporate the active compound into the polymer layer where the active compound is more effectively delivered in the target food to exert the antimicrobial or antioxidant action.

The aim of this study was to analyse the effect of the aminolization of thermo-processed PLA films on their surface energy (polar and dispersive components) and its impact on the

extensibility of PVA aqueous solutions containing or not CA as active component, and surfactant. The functional properties of the bilayer assemblies as packaging material were also characterized to analyse the aminolization effect on the laminate properties.

2. Materials and methods

2.1. Materials

Poly(lactic acid) (PLA) 4060D (density 1.24 g/cm³; D-isomer content 12 % wt.) was acquired from Natureworks (Minnetonka, MN, USA) in the form of pellets. 1,6-diamino-hexane (for synthesis) was purchased from Merck Millipore Corporation (France), and 2-propanol, hydrochloric acid and dimethyl sulfoxide from PanReac AppliChem (Castellar del Vallès, Barcelona, Spain). Ethyl acetate was acquired from Indukern (El Prat de Llobregat, Barcelona, Spain). Poly(vinyl alcohol) (PVA) (M_w 13,000-23,000; 87-89% hydrolysed), polyoxyethylene sorbitan trioleate Tween 85 (S), carvacrol and phosphorous pentoxide (P₂O₅) were purchased from Sigma-Aldrich (Sigma–Aldrich Chemie, Steinheim, Germany). Ultrapure water (resistivity of 18.2 MΩ cm) was prepared using Milli Q Advantage A10 equipment from Millipore S.A.S., Molsheim, France.

2.2. Mono- and bi- layer preparation

PLA support monolayers

Poly(lactic acid) sheets were obtained by compression moulding. To this end, 4 g of the amorphous PLA pellets were placed on Teflon sheets in a hot plate press (Model LP20, Labtech Engineering, Thailand) and preheated for 4 min at 160 °C. Compression was applied for 4 min at 100 bar and 160 °C, followed by a cooling cycle of 3 min. The films thus obtained were kept in a desiccator with SiO₂ until used.

PLA /aminolization

Surface aminolization of PLA was carried out as described by [5]. Briefly, the PLA films were immersed in ethanol-water (1:1 v/v) solution for 2 h at room temperature to remove possible fatty residues adhered during manipulation. Afterwards, they were washed with abundant deionized water and dried in a vacuum oven at 30 °C for 24 h, until constant weight. The sheets were then immersed for different times (1, 3, 5, 10, 15 and 30 min) at 50 °C in 0.25

mol·L⁻¹ 1,6-hexanediamine solution in 2-propanol. A control sample immersed only in 2-propanol at 50 °C for the different times was also prepared. The treated surfaces were thoroughly rinsed with deionized water for 24 h at room temperature to remove traces of the unreacted diamine and dried in a vacuum oven (30 °C for 24 h). Similarly to [18], the aminolized sheets were then immersed in a 0.1 mol·L⁻¹ hydrochloric acid solution for 3 h at room temperature, in order to positively charge the amino moieties grafted onto the surface. Then, the films were washed with abundant deionized water and dried again under vacuum at 30 °C for 24 h. The weight and thickness (measured by a Palmer digital micrometre from Comecta, Barcelona, Spain) of the dried materials were recorded. All the dried PLA films (treated and activated) were then stored in desiccators with SiO₂ until their use.

PVA /incorporation of actives

PVA film-forming dispersions (FFDs) were prepared by dissolving the polymer (15 wt. %) in ultrapure water, under heating at 80 °C and constant magnetic stirring for one hour. Carvacrol (CA) was added at 15 wt. % with respect to the PVA content. These aqueous formulations were prepared with and without Tween 85 surfactant (S), using three different S:CA weight ratios: 0.3:100, 0.4:100 and 0.5:100. The first ratio value was considered based on an expected CA droplet diameter of 10 µm [29] and a surfactant excess surface concentration of 5 mg/m², in the range of the previously reported values [30]. This initial ratio was increased in order to determine possible benefits of an excess of surfactant on the wettability of PVA solutions. Afterwards, the dispersions were homogenized at 12,000 rpm for 3 min using an Ultra Turrax rotor–stator homogenizer (Model T25D, IKA Germany). CA-free FFD containing only PVA were also prepared as control. The FFDs were degassed under vacuum and allowed to rest at room temperature for 24 h to check their stability.

Bilayer assembly

The bilayer assemblies were obtained by coating the support PLA sheet (aminolized or not) with the selected PVA solutions. For this purpose, the aqueous solution, equivalent to 1.5 g of PVA polymer, was applied onto each PLA sheet by means of a spiral bar coater (100 µm, Elcometer, UK). This implied a PVA/PLA wt. ratio of about 0.35 in the bilayer. The bilayers were allowed to dry at 21 °C and 55-60 % relative humidity (RH). Then, the dry materials were conditioned at 25 °C in desiccators with saturated solutions of Mg(NO₃)₂ ensuring 53 % RH, until their characterization. The weights of the films were carefully recorded before

and after the coating application to check the polymer wt. ratio. The prepared bilayers were labelled based on the untreated (PLA) or aminolized (am-PLA) support, and the applied PVA coating, carrying or not active (C) and/or surfactant (S) (e.g. am-PLA-PVA-C/S describes the bilayer obtained with PLA aminolized support and PVA layer containing both CA and S).

2.3. Analyses of surface properties

Surface free energy of PLA films

The surface free energy of the PLA sheets was assessed pre- and post-aminolization using the sessile drop method [31] by means of a contact angle meter (OCA 20 Dataphysics, Filderstadt, Germany). This involved measurement of the contact angle θ between the analysed surface and different standard liquids of different polarities and known surface tensions. Dimethylsulfoxide (DMSO), ultrapure water, and ethyl acetate were used for this purpose. Their surface tension and dispersive and polar components are, respectively, 44.0, 36.0 and 8.0 mN·m⁻¹ for DMSO, 72.8, 22.1 and 50.7 mN·m⁻¹ for water, and 23.9, 23.9 and 0.0 mN·m⁻¹ for ethyl acetate [32]. According to [33], the surface free energy of the solid (γ_S) can be expressed by Young's equation (equation 1):

$$\gamma_S = \gamma_{SL} + \gamma_L \cdot \cos \theta \quad (\text{eq. 1})$$

where:

- γ_{SL} is interfacial tension solid-liquid;

- γ_L is the surface tension of the liquid, and

- θ is the contact angle formed between the liquid-air interface and the solid surface.

If the polar and dispersive components acting at the interfacial tension are considered, this surface interaction can be described by equation 2. Then, from the values of the contact angle of pure solvents, with known dispersive (γ_L^d) and polar (γ_L^p) components, on a determined surface, the plot of the variables according to equation 2 permits the estimation of dispersive (γ_S^d) (from the intercept of linear plot) and polar (γ_S^p) (from the slope of linear

plot) components of the surface free energy [15]. Solvent drops of 2 μL were placed on the PLA surface and the contact angle was determined at contact times of 0, 30 and 60 s. Ten replicates of the angle measurements were carried out at room temperature (21 ± 1 $^{\circ}\text{C}$) for each film sample and solvent.

$$\frac{1+\cos\theta}{2} \cdot \frac{\gamma_L}{\sqrt{\gamma_L^d}} = \sqrt{\gamma_S^p} \cdot \sqrt{\frac{\gamma_L^p}{\gamma_L^d}} + \sqrt{\gamma_S^d} \quad (\text{eq. 2})$$

Surface tension of PVA solutions

All PVA solutions were characterized in terms of their liquid-vapour surface tension (γ_{LV}) using the same equipment as described for contact angle measurement. The surface tension was estimated by applying the pendant drop method, using the Laplace-Young approximation, as described by [34] and [35]. Briefly, 10-12 μL drops of the PVA solutions were suspended at the flat end of a vertical needle and with the equipment's image processing software the γ_{LV} was determined. At least thirty measurements at room temperature (21 ± 1 $^{\circ}\text{C}$) were taken for each solution.

Wettability of PVA solutions on PLA surface

Wettability of the different PVA solutions (containing or not CA and S) was determined on the PLA film surface (aminolized or not). Wettability is assessed by calculating the spreading coefficient (W_s) (equation 3) that represents the balance of the adhesion (W_a) and cohesion (W_c) works, as a function of the surface tension of the different PVA solutions and their contact angle on the PLA films (equation 4) [15]. This parameter only yields a negative or zero value. The closer the value of W_s is to zero, the better that surface will be coated.

$$W_s = W_a - W_c \quad (\text{eq. 3})$$

$$W_s = \gamma_L(\cos\theta - 1) \quad (\text{eq. 4})$$

To this end, the measurement of the contact angle between PVA solutions and PLA films was taken, by using the sessile method described above. Ten measurements were carried out for each solution.

2.4. Surface microstructure

The surface morphology of control and treated PLA was analysed by Field Emission Scanning Electron Microscopy (FESEM Ultra 55, Zeiss, Oxford Instruments, UK). For this purpose, samples were mounted with carbon tape on stubs, and after sputtering with platinum in an EM MED020 (Leica Microsystems, Germany), were observed under an accelerating voltage of 1 kV.

2.5. Analysis of functional properties of bilayer films

Water vapour and oxygen permeability

Water vapour permeability (WVP) of bilayers was assessed at 25 °C and 53-100 % RH gradient, using ASTM E96-95 gravimetric method [36], and considering the modification proposed by [37]. Briefly, previously conditioned samples were fitted onto Payne aluminium cups (diameter of 3.5 cm) (Elcometer SPRL, Hermelle/s Argenteau, Belgium) containing 5 mL of deionized water and were placed in desiccators with saturated $\text{Mg}(\text{NO}_3)_2$ aqueous solution. A small fan was placed on top of each cup to favour the water vapour transport. The cups were weighed periodically with an analytical balance (± 0.00001 g) and weight loss vs. time was plotted to obtain the water vapour transmission rate (WVTR). Then, the WVP was calculated as described by [38]. Measurements were carried out in triplicate.

The oxygen permeability (**OP**) of conditioned samples was determined at 25 °C and 53 % RH, following the guidance of Standard Method D3985-05 [39]. The equipment OXTRAN (Mocon Lippke, Neuwied, Germany) was used to determine the oxygen transmission rate (OTR). Film samples (area of 50 cm^2) were exposed to pure oxygen flow on one side and pure nitrogen flow on the opposite side. The oxygen transmission values were registered every 10 min until equilibrium was reached. Then the OP was determined as described by [40], taking into account the samples' thickness. At least two replicates per formulation were considered.

Mechanical properties

The tensile properties of the materials were assessed with a universal test machine (TA.XT plus model, Stable Micro Systems, Haslemere, England) following the guidelines of ASTM standard method D882 [41], as previously described by [42]. Conditioned samples (25x100 mm) were fixed in the machine's extension grips (positioned 50 mm apart) and stretched at 50 mm·min⁻¹ until break. Tensile strength at break (TS), Young modulus (YM) and elongation at break ($\epsilon\%$) were obtained from the stress-strain curves. A minimum of eight measurements per sample were taken.

Optical properties

The samples were analysed in terms of their transparency, by means of internal transmittance (T_i) assessed by applying the Kubelka-Munk theory for multiple scattering [43], as previously reported by [42]. A spectrophotometer CM-3600d (Minolta Co., Tokyo, Japan) was used to determine the surface reflectance spectra (wavelength range 400-700 nm) against black and white backgrounds. The value of T_i at 460 nm was selected as the benchmark value for sample comparison.

2.6. Thermogravimetric analysis (TGA) and differential scanning calorimetry (DSC)

Previously P_2O_5 conditioned films were submitted to thermal analyses. Their thermal degradation (TGA) was analysed with a thermo-gravimetric analyser (TGA/SDTA 851e, Mettler Toledo, Schwarzenbach, Switzerland). To this end, approximately 10 mg of samples were placed into alumina crucibles (capacity 70 μ L) and heated from 25 to 600 °C at a rate of 10 K/min, under nitrogen flow (20 mL/min). The thermal weight loss curves (TA) and their derivatives (DTA) were obtained and the onset, peak and endset temperatures for each degradation peak were extracted by using the STARe Evaluation Software (Mettler-Toledo, Inc., Switzerland). For the DSC analyses, a triple step thermal scan was applied using DSC equipment (1 StarE System, Mettler-Toledo, Inc., Switzerland). Samples were cooled and kept at -25 °C for 5 min and then heated at 10 K/min from -25 to 200 °C, where they were maintained for 2 min. Then, samples were cooled from 200 to -25 °C at 10 K/min, maintained at -25 °C for 5 min and afterwards heated from -25 to 250 °C, at 10 K/min. As reference, an empty aluminium pan was used. All thermal analyses were done in duplicate.

2.7. Statistical analysis

The analysis of the data was performed through variance analysis (ANOVA) using the Statgraphics Centurion XVII.64 software. The Fisher Least Significant Difference (LSD) was used to determine significant differences ($p < 0.05$) between samples.

3. Results and Discussion

3.1. Changes in the PLA surface induced by aminolization

The aminolization process of the PLA surface was followed through the changes in the surface energy (SE) of the films (polar and dispersive components) and microstructural observations of the film surface by FESEM. Contact angles of the different solvents on the PLA surface were constant with time for all pure solvents, except for ethyl acetate where changes occurred mainly due to the solvent volatility. Thus, only the contact angle values for 0 seconds contact time were considered. From the contact angle measurements, and taking into account the values of the dispersive and polar components of the surface tension for the different pure solvents, the values of dispersive and polar components of the surface energy of PLA films were obtained. To this end, the linear fitting of eq. 2, according to the variable combinations shown in the equation, was carried out. These obtained values are shown in Table 1 for the surfaces aminolized for different times. The total surface energy (sum of both components) was also determined at each aminolization time.

A notable increase (of almost 100 %) in the polar component value was observed at the shortest treatment times (1 and 3 min). The film submitted to the 5 min treatment did not show a similar trend, having values of the SE components that were more similar to the untreated sample. The changes (% relative to the initial value) in mass and thickness of treated samples are also shown in Table 1. Both parameters increased with treatment time, probably due to solvent adsorption and retention in the polymer matrix and its subsequent swelling. In fact, samples immersed only in solvent at the same temperature also gained mass, but in a lower proportion, as shown in Table 1 (values in brackets). In control treatments using only solvent, the mass gain was greater than in the reactive samples for all treatment times and reached a constant value of about 8 % from 5 min immersion onwards. This indicates that in the presence of reactive, mass change also involves other mechanisms related with the reaction, which could imply losses through the polymer solubilisation in the reactant media. In fact, the sample treated for 30 min exhibited a net

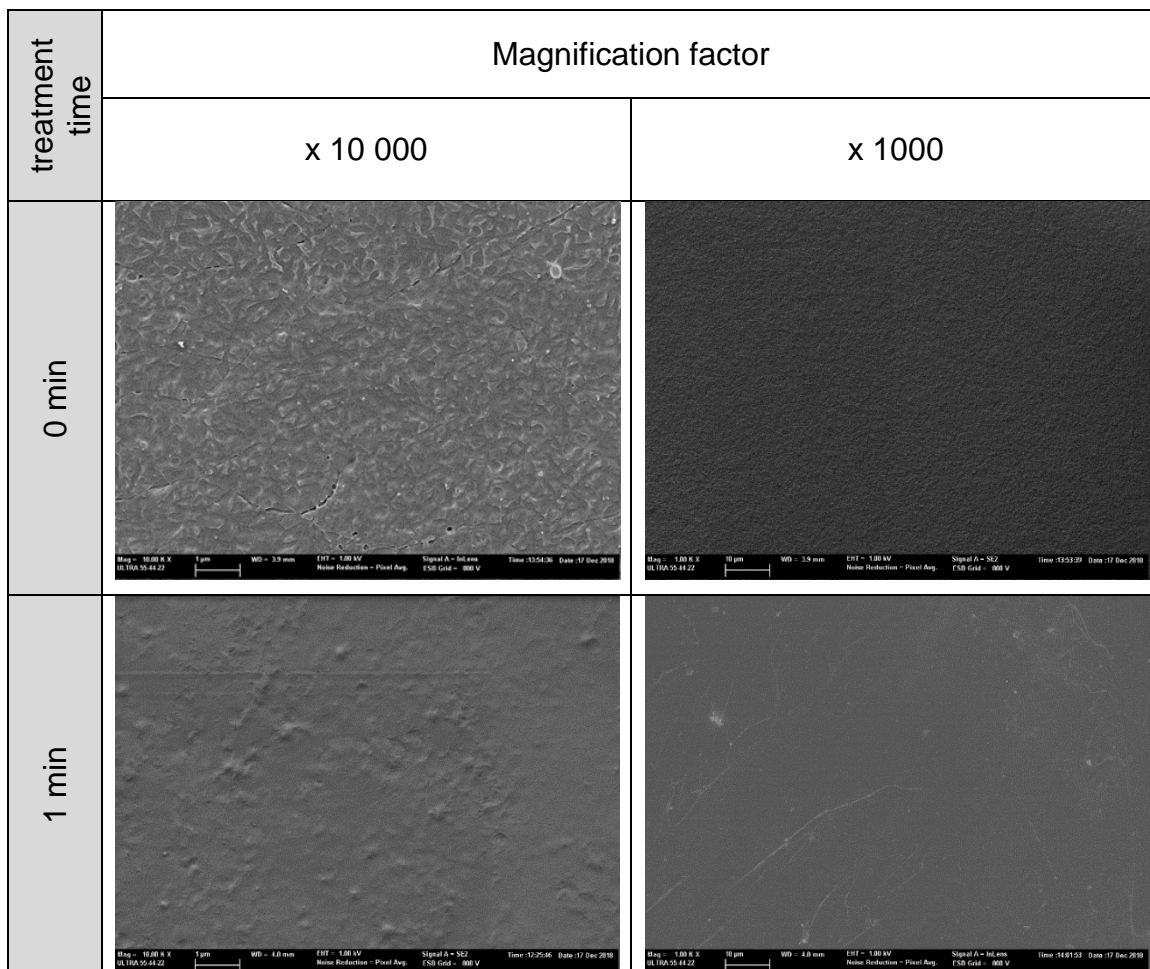
weight loss, while the film thickness greatly increased, thus revealing the effective mass loss of the highly swollen film due to its partial solubilisation in the solvent-reactive system. Then, a prolonged contact with the diamine leads to a high degree of erosion/dissolution of the polylactide. Additionally, beyond the 10 min mark, the post-aminolization samples were visibly brittle. So, they were considered physically unfit for use in the subsequent coating step, as they would provide little mechanical support for the bilayers.

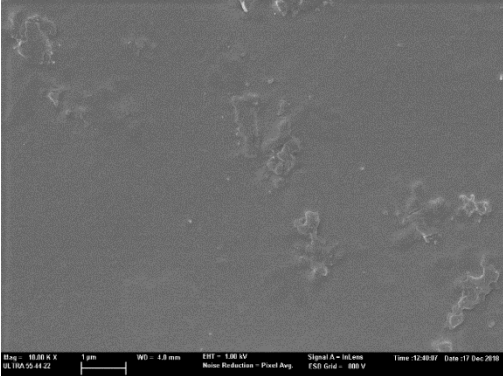
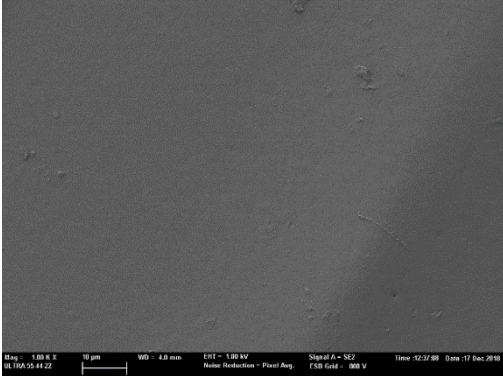
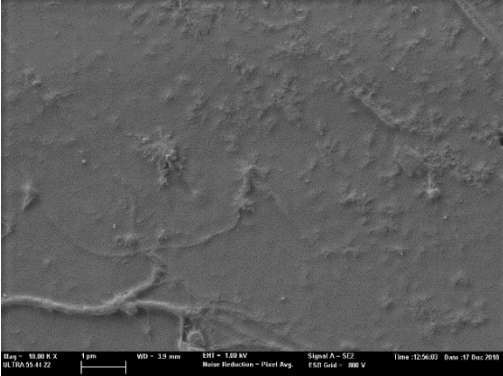
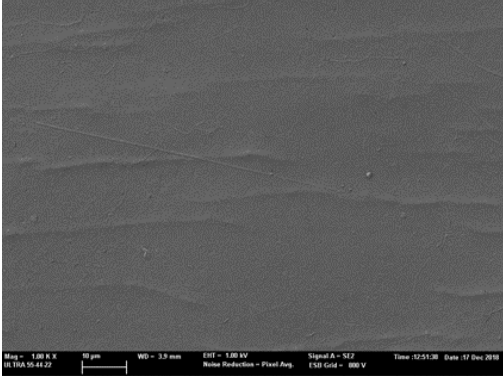
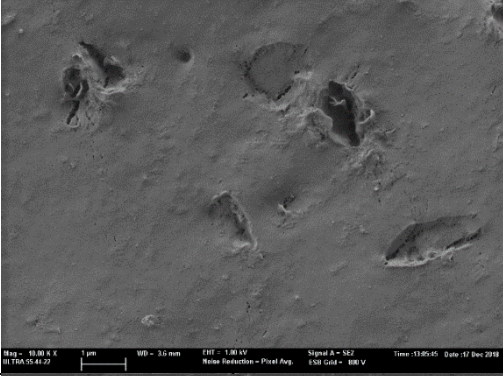
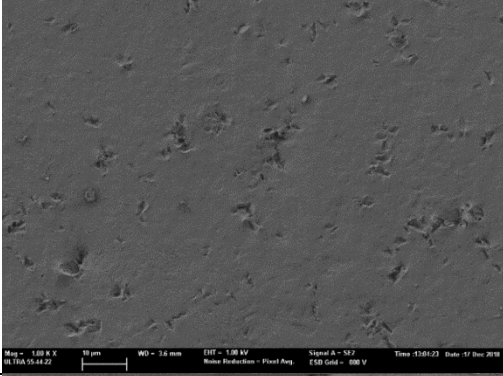
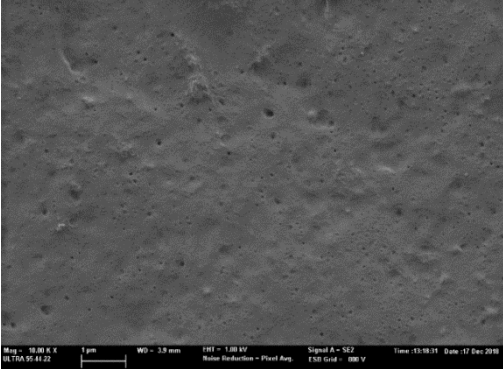
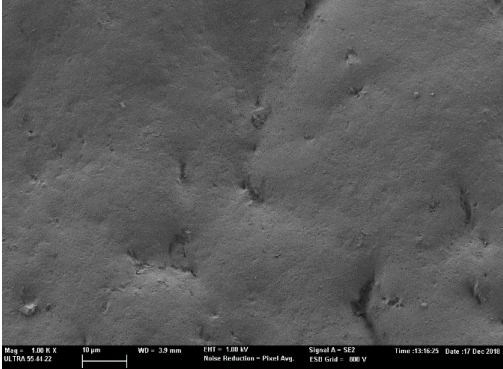
Table 1. Surface energy (SE) and its polar and dispersive components of PLA films submitted to different aminolization times. Relative change (%) with respect to the initial value in mass (Δm) and thickness (Δe) provoked by the process are shown. In brackets, the values of mass gain of films immersed only in solvent.

Aminolization time (min)	PLA surface free energy (mN/m)			Δm (%)	Δe (%)
	SE	Polar component	Dispersive component		
0	29.3	8.8	20.5	n/a	n/a
1	37.0	18.5	18.5	0.5±0.2 (1.2)	7.6
3	37.4	17.6	19.8	0.7±0.2 (5.9)	8.8
5	31.7	9.1	22.6	1.1±0.2 (7.9)	17.2
10	32.3	13.5	18.8	3.2±0.6 (8.4)	21.2
15	n/a	n/a	n/a	4.2±1.2 (7.1)	35.6
30	n/a	n/a	n/a	-5.49 (8.6)	419.2

The FESEM micrographs in Figure 2 show the surface aspect of the PLA films where the changes provoked by the aminolization process at different times can be observed. The initial relatively rough surface of the untreated polylactide films shows a gradual smoothing at short aminolization times (1 and 3 min), as also observed by other authors [19]. This can be attributed to the solubilisation of the more emerging zones of the rough

surface overlapping with the aminolization of the surface chains, as revealed by the increase in the polar component of the film surface energy. However, a more irregular surface was observed at 5 min treatments where the surface tension polar component decreased. This suggests that aminolized chains could prevalently solubilise during treatment, generating an irregular film surface. For the 10 min treatment, visible voids can be observed in the films, confirming the internal action of the 1,6-hexanediamine reactive and partial solubilisation of the film material. The internal diffusion of the reactive and solvent into the films seems to produce a highly porous structure at 15 and 30 min treatments, as revealed by the visible pores in the film microstructure and the great increase in the film thickness. At the end of the latter treatment, the intense erosion of the films structure can be clearly observed in Figure 2, where a high ratio of voids and pores can be seen on the film surface, while the films appeared highly deformed after drying. In fact, the measurements of contact angle were not possible in these distorted films. Film immersion in pure solvent did not provoke a great alteration in the film surface beyond the leaching of the most superficial chains that changed the surface aspect of the films compared with the initial samples (Figure 2).



treatment time	Magnification factor	
	x 10 000	x 1000
3 min		
5 min		
10 min		
15 min		

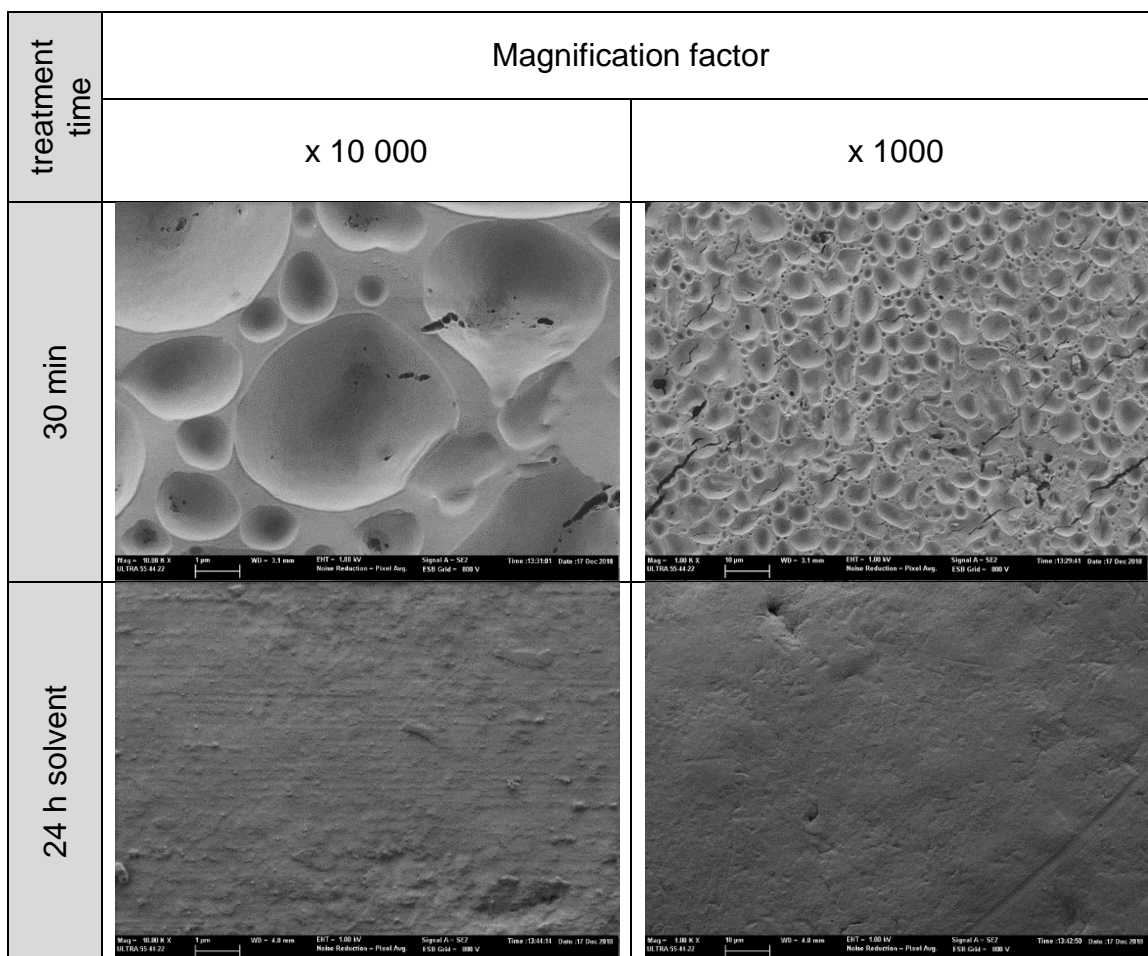


Figure 2. FESEM micrographs of the PLA film surface submitted to the aminolization treatment (different times). Magnification of 10 000 x and 1000 x.

The obtained results indicate that aminolization of PLA films must be carried out for short times (1 or 3 min) where the polar component of the film surface tension increased. Longer treatment times provoked internal damage in the film structure associated with the internal diffusion of reactants and solvent that provoked the swelling of the polymer matrix and the partial solubilisation of the film components.

Wettability of PLA with PVA liquid systems

PLA films treated at 0, 1 and 3 min aminolization (when the polar component of surface energy increased) were submitted to the wettability test with the PVA solutions/emulsions prepared as described in section 2.2, containing or not carvacrol and different ratios of surfactant. Contact angles obtained between PVA liquid systems and the PLA films treated for different times are shown in **Table 2**, as well as the values of surface tension of the different PVA liquid systems. All contact angles were below 90° , indicating that the surface can be wetted by the liquids. The surface tension (γ_L) of the PVA liquid systems was

significantly reduced by carvacrol incorporation, whereas no significant effect of the surfactant was observed at any ratio. The effect of the emulsified carvacrol on the surface tension of PVA solution can be attributed to the presence of small droplets of the compound at the liquid surface that modify the interfacial interaction forces due to its more hydrophobic nature. Likewise, the lack of a significant surfactant effect on the surface tension of the carvacrol emulsions could be due to its prevalent location at the oil-water interface and the main effect of carvacrol droplets at the surface level. This behaviour was also observed by Sapper, Bonet and Chiralt (2019) [44] when thyme essential oil was emulsified in an aqueous solution of cassava starch-gellan with and without surfactant.

As concerns the contact angle, it decreased (from 51 to 33) for pure PVA solutions as the polar component of surface tension increased during aminolization, thus reflecting the greater chemical affinity between the aminolized PLA surface and PVA aqueous solutions. However, for the PVA solution with emulsified carvacrol, the contact angle of non-aminolized PLA was lower (44) and less sensitive to the aminolization time. This agrees with the greater surface affinity of the carvacrol-containing liquid with the initial PLA surface. In fact, the contact angle of this emulsion increased in the case of the 3 min aminolization treatment. The presence of surfactant provoked small changes in the contact angle, which could be attributed to specific interactions of the amphiphilic molecule with the PLA surface that affect the global surface forces at the solid-liquid-air contact. The small ratio of surfactant was more effective at decreasing the contact angle in non-aminolized PLA surfaces than the higher proportions, whereas it was not effective at reducing the contact angle in aminolized PLA surfaces.

The wettability parameter (W_s) values calculated for the different PVA formulations and PLA surfaces are also shown in Table 2. The further from zero the values of W_s are, the less likely it is for that formulation to spread well over the PLA surface. Therefore, the best extensibility was obtained for 3 min treated PLA films with pure PVA solutions, for 1 min treated PLA films with PVA solution with emulsified carvacrol and for 0 min treated PLA support when emulsions contained the lowest ratio of surfactant. Therefore, 1 min aminolized PLA support could be a compromise point to achieve a good extensibility of the different PVA liquid systems while the lowest ratio of surfactant was more adequate to enhance the liquid phase extension. This choice implies an improvement in the extensibility

of the pure PVA solution on PLA films, while a similar extensibility of the three PVA formulations (without and with carvacrol, containing or not surfactant) would be achieved.

Table 2. Surface tension (γ_L) of the PVA solutions (C/S wt. ratios are specified) and contact angles (θ) on PLA layer as a function of the aminolization time. Different superscript letters (a, b, c) and numbers (1, 2, 3) in the same column, and row respectively, indicate significant ($p < 0.05$) differences between samples for the analysed parameter.

	PVA	PVA/C	PVA-C/S (0.3:100)	PVA-C/S (0.4:100)	PVA- C/S (0.5:100)
γ_L (mN/m)	45.4±0.5 ²	36.0±0.3 ¹	36.1±0.4 ¹	36.0±0.2 ¹	36.5±0.2 ¹
Aminolization time (min)	Contact angles (θ)				
0	51±1 ^{c,4}	44±2 ^{a,23}	38±2 ^{a,1}	41±2 ^{a,2}	44±3 ^{ab,3}
1	44±3 ^{b,1}	42±1 ^{a,1}	45±7 ^{b,1}	44±7 ^{ab,1}	46±5 ^{bc,1}
3	33±3 ^{a,1}	47±6 ^{a,3}	49±3 ^{b,3}	48±4 ^{b,3}	42±3 ^{a,2}
	Wettability parameter (W_s)				
0	-17.0±1.0 ^{a1}	-10.0±1.0 ^{a23}	-7.5±1.0 ^{b4}	-9.0±0.7 ^{b3}	-10.5±1.0 ^{ab2}
1	-13.0±2.0 ^{b1}	-9.5±1.0 ^{a2}	-11.0±3.0 ^{a12}	-11.0±3.0 ^{ab12}	-11.0±2.2 ^{a12}
3	-7.0±2.0 ^{c3}	-12.0±3.0 ^{a1}	-12.0±1.3 ^{a1}	-12.0±2.0 ^{a1}	-9.4±1.2 ^{b2}

Thus, from this study, the aminolization time selected for the subsequent application was 1 min, and the PLA films treated for 1 min were coated with PVA, PVA/C and PVA/C-S (0.3:100) formulations to obtain bilayer films whose functional properties were characterized.

3.2. Functional properties of PLA-PVA bilayer films

The obtained bilayer films exhibited a thickness of 230-250 μm from which approximately 22 % corresponded to the PVA layer (56±21 μm average value) and the rest to the PLA sheet (195±11 μm average value). These values are coherent with the mass ratio of each polymer in the laminate (approximately 0.27 for PVA). However, at microscopic level a higher heterogeneity in the PVA thickness was detected, depending on the film sample. Figure 3 shows FESEM micrographs of some bilayer films where differences in the overall thickness of the PVA sheet can be seen, as well as differences in the thickness along a determined film, depending on the roughness of the PLA surface.

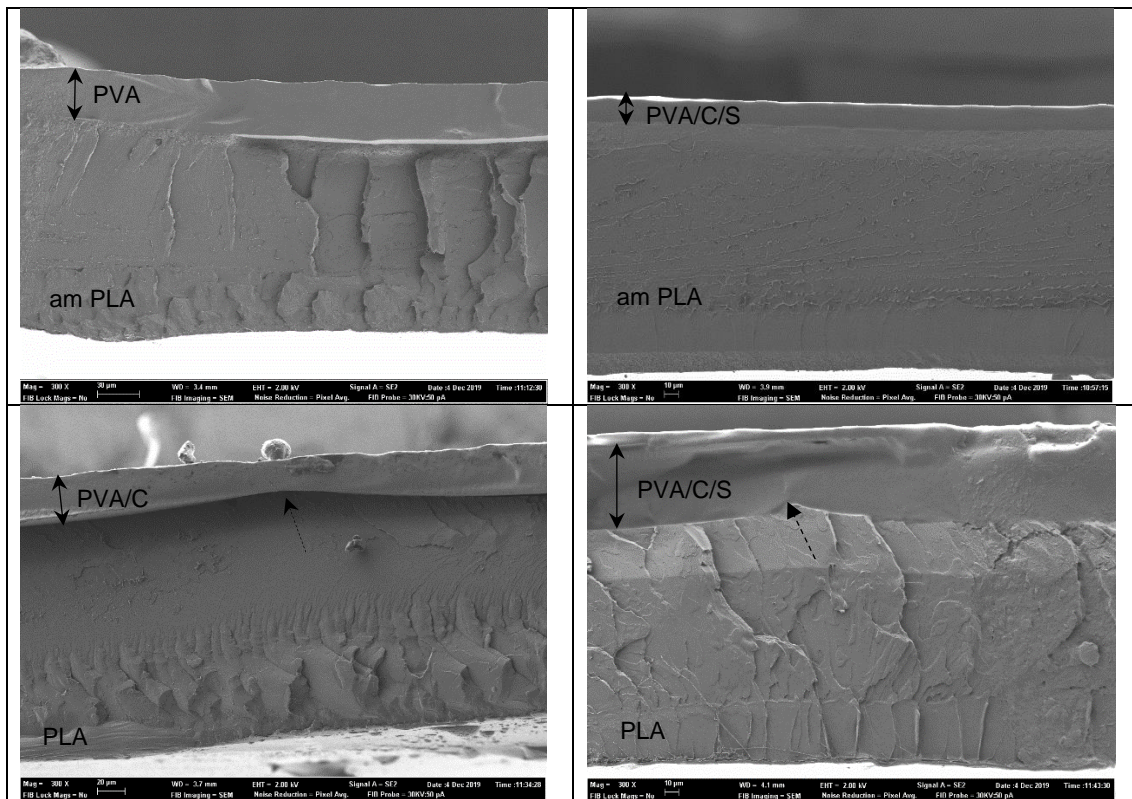


Figure 3. Micrographs of several bilayer cross-sections. Top row: aminolized PLA with PVA (left) and PVA/C/S (right) coatings. Bottom row: untreated PLA with PVA/C (left) and PVA/C/S (right) coatings. Dotted arrows indicate protuberances at PLA surface.

When a small protuberance appeared in the PLA surface (dotted arrows, Figure 3), the PVA layer was thinner, which can be critical when the coating was very thin. This aspect could compromise the barrier capacity provided by the PVA layer in the zones where its thickness was extremely thin (about 10 μm). Then, in the laminates obtained by casting PVA solutions on PLA surface the more hydrophobic PLA layer was thicker, whereas the cast hydrophilic layer of PVA was thinner with great variability in thickness, which could influence its effectiveness at controlling its barrier capacity [45].

Given that most deteriorative processes in foods are caused by water or oxygen exchanges, food packaging materials require a good barrier capacity against moisture and oxygen to extend foodstuff shelf life [46]. The WVP and OP of the obtained bilayers are shown in Table 3, together with the corresponding values of each monolayer. According to the Ideal Laminate Theory [47], the polymer layer with lower permeability usually determines the barrier capacity of laminates for water vapour or gases. As such, the WVP values of bilayers were expected to be around those of the PLA sheet that exhibited the lowest WVP. Indeed, the WVP of bilayers present similar values to those of the PLA monolayer with small

differences between the different samples. Laminates with aminolized PLA exhibited a wider WVP range, the bilayer with the pure PVA sheet being the one with the lowest value.

However, the values of oxygen permeability were not in the range of that of the PVA sheet that should be the limiting layer for oxygen transmission. Both the aminolized bilayers and those non-aminolized with pure PVA showed similar OP values to those of the PLA monolayer. In contrast, non-aminolized laminates containing carvacrol (with and without surfactant) exhibited lower OP values. This could be attributed to the oxygen-blocking effect exerted by the antioxidant CA, but this was not observed in bilayers with aminolized PLA. The lack of effectiveness of PVA sheets in reducing the OP of laminates could be due to the heterogeneous coating at microscopic level that should generate regions in the films with very thin hydrophilic coating. Thus, oxygen transfer would take place, mainly limited by the PLA sheet.

Table 3. Barrier and mechanical properties of bilayer PVA-PLA films. Film thickness and transparency (T_i) are also shown. Different superscript letters in the same column indicate significant differences ($p < 0.05$) between samples.

Multilayer components		WVP x 10 ¹⁰ (g/Pa·s·m)	OP x 10 ¹² (cm ³ /m·s·Pa)	Young Modulus (MPa)	Tensile Strength (MPa)	ε (%)	Thickness (mm)	T _i at 460 nm (%)
am PLA	PVA	0.28±0.03 ^a	4.45±0.47 ^b	1300±200 ^{bc}	53±8 ^b	4.9±0.5 ^a	0.251±0.060 ^a	56±13 ^a
	PVA-C	0.36±0.05 ^{ab}	5.02±0.32 ^{bc}	1140±150 ^{ab}	40±7 ^a	5.4±0.4 ^{ab}	0.231±0.019 ^a	69±10 ^b
	PVA-C/S	0.40±0.09 ^b	5.89±1.07 ^c	1100±300 ^a	41±5 ^a	6.7±2.5 ^{bc}	0.236±0.013 ^a	60±5 ^a
PLA	PVA	0.37±0.05 ^{ab}	4.07±0.16 ^b	1400±50 ^c	49±3 ^b	5.8±0.9 ^{ab}	0.230±0.018 ^a	86.2±0.3 ^c
	PVA-C	0.33±0.01 ^{ab}	0.15±0.02 ^a	1100±120 ^{ab}	42±5 ^a	7.9±2.1 ^{cd}	0.247±0.022 ^a	86±1 ^c
	PVA-C/S	0.36±0.02 ^{ab}	0.20±0.06 ^a	1150±110 ^{ab}	41±4 ^a	8.9±1.0 ^d	0.240±0.010 ^a	85±4 ^c
Monolayers								
	PVA	8.05±0.06	0.0015±0.02	54±5	46±6	97±6	0.065±0.002	86±1
	PLA	0.44±0.03	4.66±0.03	1370±34	53±2	4.3±0.2	0.22±0.01	87.7±0.2

The tensile properties (Young modulus (YM), tensile strength (TS) and elongation (ϵ at break) of bilayers are also presented in Table 3. The bilayers exhibited tensile property values in the range of the stiffest PLA sheet, which also represents the thickest layer of the assembly. The films containing CA with and without surfactant had the lowest values of YM, regardless of the aminolization of the PLA sheet. This could be explained by the partial carvacrol migration into the PLA sheet, weakening the inter-chain forces of the PLA matrix. This effect was also appreciated in the values of the bilayer's resistance to break (TS), which were higher when neither CA nor T85 were present, showing values similar to those of the PLA monolayer. All materials had elongation at break values of under 10 %, denoting a quite brittle behaviour, in the order of PLA films. However, a slight increase in the film extensibility could be appreciated for the CA-carrying laminates, in line with the plasticising effect of the CA that potentially migrated into the PLA sheets.

The internal transmittance (T_i), also presented in Table 3, is directly related to the film transparency. All of the aminolized sheets presented a cloudiness (photos not shown) as result of the aminolization step. This explains the decrease in the T_i parameter for these treated materials. However, this acquired opacity could be considered positive for certain food packaging applications where a reduction in light-induced oxidative reactions is required.

The results indicate that bilayer PLA-PVA films obtained by casting PVA aqueous solutions onto the PLA surface did not provide additional benefits to the PLA monolayers. The expected, the barrier capacity against oxygen potentially imparted by the PVA sheet was not effective, while the PVA did not contribute to the mechanical reinforcement of the PLA layer. Despite PLA aminolization enhancing the polar nature of the PLA surface and thus the chemical affinity with the PVA aqueous solutions to be extended, the obtained PVA coatings were heterogeneous in thickness and the thinner regions seem to limit the barrier capacity of the coating against oxygen.

3.3. Thermal behaviour as affected by the aminolization treatment

A thermal analysis of the obtained materials was carried out in order to discover the effect of aminolization and lamination on the physical state of polymers, which, in turn, affects their functional properties. Table 4 summarizes the degradation temperatures of the different samples, as obtained by thermogravimetric analysis. TGA thermographs (Figure 4) show an

overlapping of the degradation steps of both polymers due to the proximity of its degradation temperature range.

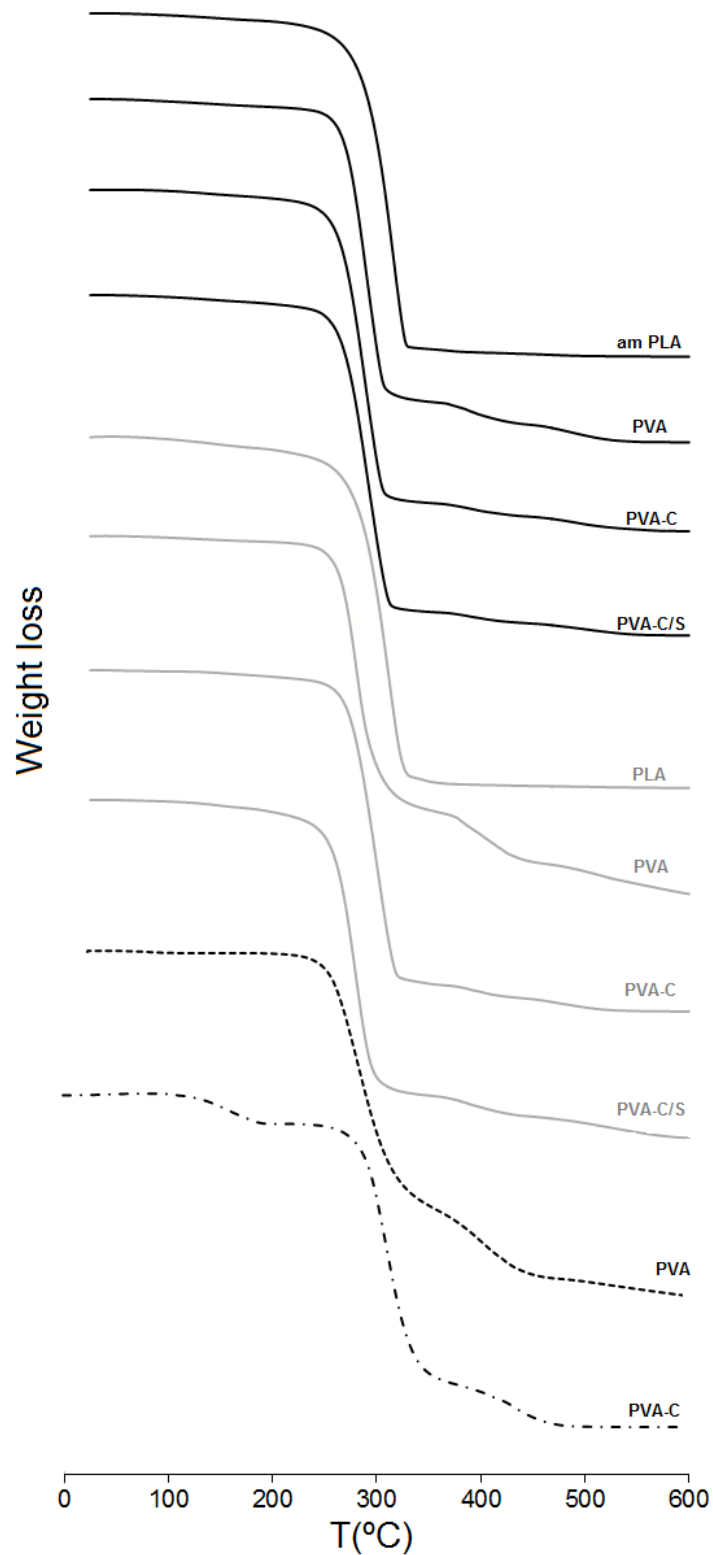


Figure 4. TGA curves of multilayer assemblies with PLA, aminolized (black curves) or not (grey curves), and PVA, containing or not carvacrol (C) and surfactant (S).

The aminolization process did not modify the degradation temperature of PLA, the peak being at 310 °C. PVA starts its degradation and exhibits the peak at a lower temperature (192/288 °C) than the PLA. Thus, bilayers showed notable T_{onset} values in the range of 240-255 °C, lower than that of pure PLA (269 °C). A second and third small degradation peak appeared in bilayers at about 390 and 500 °C, which could be attributed to the PVA degradation in subsequent steps as described by other authors [48], [49]. No significant differences were observed between the degradation behaviour of the different bilayers. No thermo-release of carvacrol from the corresponding bilayers was detected, probably due to the very small mass fraction of the compound in the laminate: about 11 g/g PVA, according to previous studies [29].

Table 4 also shows the glass transition temperature (T_g) for the different materials obtained in the first and second heating scans. In the first heating step, two distinct T_g can be observed, corresponding to the two polymers present in bilayers. For samples without carvacrol, the first one, at a slightly lower temperature, corresponds to the PLA, while the second one must be attributed to the PVA. For laminates without carvacrol, both transitions practically overlap, but these are more decoupled for bilayers with carvacrol due to the plasticizing effect of the compound that shifts the transition of the PVA sheet to a lower temperature, below the T_g of PLA. The DSC thermograms (Figure 5) also revealed the typical relaxation of PLA after T_g in the first heating step, associated with polymer ageing [50]. However, as the thermal history of the materials is erased and they become melt blended in the first step, only a single T_g was observed in the second heating, without relaxation enthalpy. This T_g value was lower for laminates with carvacrol, thus indicating the plasticizing effect of the compound on the melt blended polymer matrix.

Likewise, PVA crystallizes in the laminate and the melting temperature and enthalpies are shown in Table 4. Polymer melting was observed from about 160 °C, with a peak at about 185°C, in agreement with other studies [29]. However, a high degree of variability was observed in the melting enthalpy of PVA when expressed per g of polymer, in both the first and second (values not shown) heating steps, assuming a constant mass fraction of PVA in the bilayer film. Nevertheless, the variable thickness observed in the layers could imply notable differences in the PVA ratio in the DSC analysed samples. This could explain the variability in the melting enthalpy and corroborate the heterogeneous coating in the bilayer obtained by casting. .

Table 4. Thermal parameters of polymers in the multilayer assemblies. Values of pure, non-treated polymers are also included. Different superscript letters in the same column indicate significant differences ($p < 0.05$) between specimens.

Bilayer/ monolayer		TGA*				DSC				
						1 st heating				2 nd heating
		T _{onset 1} (°C)	T _{peak 1} (°C)	T _{peak 2} (°C)	T _{peak 3} (°C)	T _g PLA (°C)	T _g PVA (°C)	T _{peak} (°C)	ΔH (J/g PVA)	T _g (°C)
am PLA	PVA	248±2 ^{cd}	286±3 ^{ab}	392±2 ^{ab}	511±27 ^a	56±1 ^b	68.4±1.0 ^d	185±1 ^{ab}	34±4 ^a	52±3 ^c
	PVA-C	244.9±0.3 ^{bcd}	286±1 ^{ab}	391±1 ^a	496±6 ^a	56.2±0.4 ^b	43.8±0.3 ^a	187±1 ^b	17±2 ^a	44±1 ^a
	PVA-C/S	246±1 ^{bcd}	289±1 ^b	393±0 ^{ab}	508±1 ^a	57.6±0.0 ^c	45.2±0.2 ^b	188±1 ^b	33±28 ^a	49±2 ^{bc}
PLA	PVA	244±1 ^{bc}	280±1 ^a	398±2 ^b	508±2 ^a	56.0±1.0 ^b	68.9±0.1 ^d	189±2 ^b	84±43 ^b	53±2 ^c
	PVA-C	251±4 ^d	292±7 ^b	396±1 ^{ab}	504±28 ^a	57.8±0.7 ^c	44.3±0.7 ^{ab}	183±1 ^a	25±7 ^a	47±2 ^{ab}
	PVA-C/S	241±2 ^b	279±2 ^a	392±1 ^{ab}	530±12 ^a	58.2±0.0 ^c	44.6±0.3 ^{ab}	186±1 ^{ab}	23±8 ^a	45±1 ^{ab}
am PLA		268±1 ^e	310±1 ^c	-	-	55±1 ^{ab}	-	-	-	51.9±0.1 ^c
PLA		269±5 ^e	310±4 ^c	-	-	54.4±0.2 ^a	-	-	-	53±2 ^c
PVA		192±1 ^a	288±4 ^b	398±6 ^b	-	-	55.0±0.3 ^c	-	50±3 ^{ab}	63±3 ^d

* no residue was observed at 600 °C.

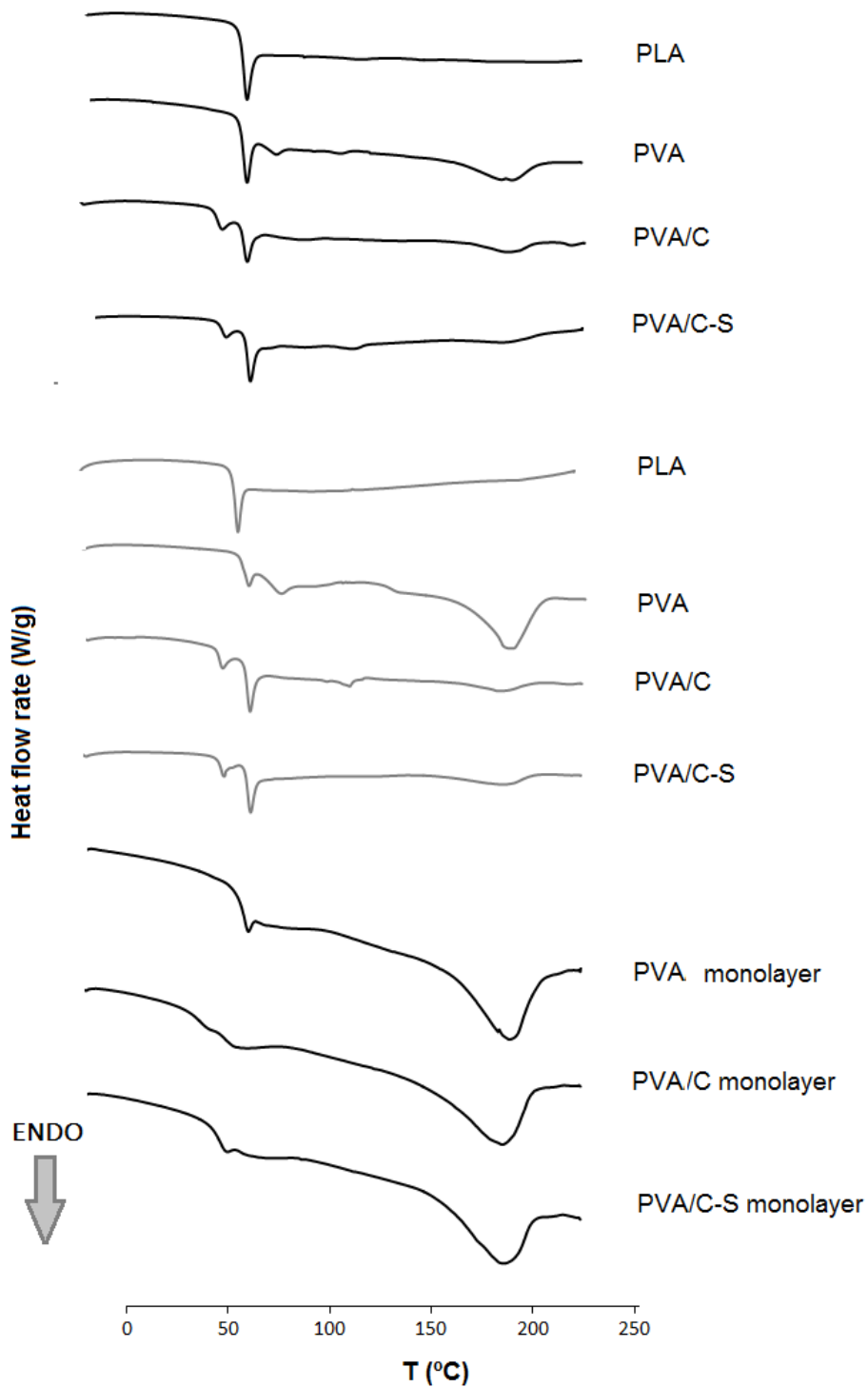


Figure 5. DSC curves of multilayer assemblies with PLA, aminolized (black curves) or not (grey curves), and PVA, containing or not carvacrol (C) and surfactant (S). Monolayers of aminolized PLA (solid black curve), untreated PLA (solid grey curve) and PVA also included. Therefore, DSC analyses revealed the amorphous state of PLA and the semicrystalline nature of PVA in the laminates, without any appreciable effect of the PLA aminolization. However, the variability in the PVA melting enthalpy points to the heterogeneity of the

coating on the laminate obtained by casting, even in the case of aminolized PLA, where wettability was enhanced.

4. Conclusions

The aminolization technique yields PLA surfaces with a greater polar component of the surface free energy, thus enhancing wettability with polar solutions of PVA. When PVA carried carvacrol, this effect did not improve the extensibility of the liquid phase on PLA. The prolonged (>3 min) exposure to 1,6-hexanediamine has negative effects on the polar component and microstructure of the PLA films. The aminolization of the PLA surface did not notably affect the mechanical and barrier properties of PLA-PVA bilayers containing, or not, carvacrol. These properties were very close to those of the major PLA monolayer, while the PVA sheet did not provide the expected oxygen barrier capacity to the laminate. Carvacrol promoted the bilayer stretchability due to its plasticising effect on both PVA and PLA sheets. Based on the results, coating PLA (aminolized or not) with PVA solutions is not recommended for the purposes of obtaining laminates for food packaging applications, since neither the barrier nor the mechanical properties were an improvement on those of PLA films, mainly due to the heterogeneous thickness of the PVA coating.

5. Acknowledgements

The authors thank the Ministerio de Economía y Competitividad (MINECO) of Spain, for the financial support for this study as part of the project AGL2016-76699-R. The author A. Tampau also thanks MINECO for the pre-doctoral research grant #BES-2014-068100.

6. References

- [1] K. Petersen, P. Væggemose Nielsen, G. Bertelsen, M. Lawther, M.B. Olsen, N.H. Nilsson, G. Mortensen, Potential of biobased materials for food packaging, *Trends Food Sci. Technol.* 10 (1999) 52–68. doi:10.1016/S0924-2244(99)00019-9.
- [2] J. Muller, C. González-Martínez, A. Chiralt, Poly(lactic) acid (PLA) and starch bilayer films, containing cinnamaldehyde, obtained by compression moulding, *Eur. Polym. J.* 95 (2017) 56–70. doi:10.1016/j.eurpolymj.2017.07.019.

- [3] D.W. Farrington, J. Lunt, S. Davies, R.S. Blackburn, Poly(lactic acid) fibers, in: R.S.B.T.-B. and S.F. Blackburn (Ed.), *Biodegrad. Sustain. Fibres*, Elsevier, 2005: pp. 191–220. doi:10.1533/9781845690991.191.
- [4] L. Xiao, B. Wang, G. Yang, M. Gauthier, Poly(Lactic Acid)-Based Biomaterials: Synthesis, Modification and Applications, in: *Biomed. Sci. Eng. Technol.*, InTech, 2012. doi:10.5772/23927.
- [5] Y. Zhu, C. Gao, X. Liu, T. He, J. Shen, Immobilization of Biomacromolecules onto Aminolyzed Poly(L-lactic acid) toward Acceleration of Endothelium Regeneration, *Tissue Eng.* 10 (2004) 53–61. doi:10.1089/107632704322791691.
- [6] J. Bonilla, E. Fortunati, M. Vargas, A. Chiralt, J.M. Kenny, Effects of chitosan on the physicochemical and antimicrobial properties of PLA films, *J. Food Eng.* 119 (2013) 236–243. doi:10.1016/j.jfoodeng.2013.05.026.
- [7] S. Collazo-Bigliardi, R. Ortega-Toro, A. Chiralt, Properties of micro- and nano-reinforced biopolymers for food applications, in: T.J. Gutiérrez (Ed.), *Polym. Food Appl.*, Springer International Publishing, Cham, 2018: pp. 61–99. doi:10.1007/978-3-319-94625-2_4.
- [8] <http://polymerdatabase.com/Films/Multilayer%20Films.html> (page accessed in October 2019)
- [9] J.C.-H. Hsu, A.C. Guckenberger, EP0175451A2, 1985.
<https://patents.google.com/patent/EP0175451A2/ru>. (page accessed in September 2019)
- [10] R. Requena, M. Vargas, A. Chiralt, Obtaining antimicrobial bilayer starch and polyester-blend films with carvacrol, *Food Hydrocoll.* 83 (2018) 118–133. doi:10.1016/j.foodhyd.2018.04.045.
- [11] J.F. Martucci, R.A. Ruseckaite, Three-layer sheets based on gelatin and poly(lactic acid), part 1: Preparation and properties, *J. Appl. Polym. Sci.* 118 (2010) 3102–3110. doi:10.1002/app.32751.

- [12] J.W. Rhim, K.A. Mohanty, S.P. Singh, P.K.W. Ng, Preparation and properties of biodegradable multilayer films based on soy protein isolate and poly(lactide), *Ind. Eng. Chem. Res.* 45 (2006) 3059–3066. doi:10.1021/ie051207+.
- [13] A. Cano, E. Fortunati, M. Cháfer, J.M. Kenny, A. Chiralt, C. González-Martínez, Properties and ageing behaviour of pea starch films as affected by blend with poly(vinyl alcohol), *Food Hydrocoll.* 48 (2015) 84–93. doi:10.1016/j.foodhyd.2015.01.008.
- [14] C.C. DeMerlis, D.R. Schoneker, Review of the oral toxicity of polyvinyl alcohol (PVA), *Food Chem. Toxicol.* 41 (2003) 319–326. doi:10.1016/S0278-6915(02)00258-2.
- [15] M. Sapper, A. Chiralt, Starch-based coatings for preservation of fruits and vegetables, *Coatings.* 8 (2018) 152. doi:10.3390/coatings8050152.
- [16] Y. Zhu, C. Gao, X. Liu, J. Shen, Surface modification of polycaprolactone membrane via aminolysis and biomacromolecule immobilization for promoting cytocompatibility of human endothelial cells, *Biomacromolecules.* 3 (2002) 1312–1319. doi:10.1021/bm020074y.
- [17] M.G. Carneiro-da-Cunha, M.A. Cerqueira, B.W.S. Souza, S. Carvalho, M.A.C. Quintas, J.A. Teixeira, A.A. Vicente, Physical and thermal properties of a chitosan/alginate nanolayered PET film, *Carbohydr. Polym.* 82 (2010) 153–159. doi:10.1016/j.carbpol.2010.04.043.
- [18] A.C. Pinheiro, A.I. Bourbon, M.A.C. Quintas, M.A. Coimbra, A.A. Vicente, K-Carrageenan/Chitosan Nanolayered Coating for Controlled Release of a Model Bioactive Compound, *Innov. Food Sci. Emerg. Technol.* 16 (2012) 227–232. doi:10.1016/j.ifset.2012.06.004.
- [19] M. Drobot, Z. Persin, L.F. Zemljic, T. Mohan, K. Stana-Kleinschek, A. Doliska, M. Bracic, V. Ribitsch, V. Harabagiu, S. Coseri, Chemical modification and characterization of poly(ethylene terephthalate) surfaces for collagen immobilization, *Cent. Eur. J. Chem.* 11 (2013) 1786–1798. doi:10.2478/s11532-013-0319-z.
- [20] S. Noel, B. Liberelle, A. Yogi, M.J. Moreno, M.N. Bureau, L. Robitaille, G. De Crescenzo, A non-damaging chemical amination protocol for poly(ethylene terephthalate)-

application to the design of functionalized compliant vascular grafts, *J. Mater. Chem. B.* 1 (2013) 230–238. doi:10.1039/c2tb00082b.

- [21] S. Burt, Essential oils: Their antibacterial properties and potential applications in foods - A review, *Int. J. Food Microbiol.* 94 (2004) 223–253. doi:10.1016/j.ijfoodmicro.2004.03.022.
- [22] K. Can Baser, Biological and Pharmacological Activities of Carvacrol and Carvacrol Bearing Essential Oils, *Curr. Pharm. Des.* 14 (2008) 3106–3119. doi:10.2174/138161208786404227.
- [23] J.A. Kamimura, E.H. Santos, L.E. Hill, C.L. Gomes, Antimicrobial and antioxidant activities of carvacrol microencapsulated in hydroxypropyl-beta-cyclodextrin, *LWT - Food Sci. Technol.* 57 (2014) 701–709. doi:10.1016/j.lwt.2014.02.014.
- [24] E. Mascheroni, V. Guillard, E. Gastaldi, N. Gontard, P. Chalier, Anti-microbial effectiveness of relative humidity-controlled carvacrol release from wheat gluten/montmorillonite coated papers, *Food Control.* 22 (2011) 1582–1591. doi:10.1016/j.foodcont.2011.03.014.
- [25] M. Ramos, A. Beltrán, M. Peltzer, A.J.M. Valente, M. del C. Garrigós, Release and antioxidant activity of carvacrol and thymol from polypropylene active packaging films, *LWT - Food Sci. Technol.* 58 (2014) 470–477. doi:10.1016/j.lwt.2014.04.019.
- [26] C. Turek, F.C. Stintzing, Stability of essential oils: A review, *Compr. Rev. Food Sci. Food Saf.* 12 (2013) 40–53. doi:10.1111/1541-4337.12006.
- [27] J. Muller, A. Casado Quesada, C. González-Martínez, A. Chiralt, Antimicrobial properties and release of cinnamaldehyde in bilayer films based on polylactic acid (PLA) and starch, *Eur. Polym. J.* 96 (2017) 316–325. doi:10.1016/j.eurpolymj.2017.09.009.
- [28] A. Tampau, C. González-Martínez, A. Chiralt, Release kinetics and antimicrobial properties of carvacrol encapsulated in electrospun poly-(ϵ -caprolactone) nanofibres. Application in starch multilayer films, *Food Hydrocoll.* 79 (2018) 158–169. doi:10.1016/j.foodhyd.2017.12.021.

- [29] A. Tampau, C. González-Martínez, A. Chiralt, Polyvinyl alcohol-based materials encapsulating carvacrol obtained by solvent casting and electrospinning. *React. Funct. Polym.* (2020, in press)
- [30] R.K. Owusu Apenten, Q.H. Zhu, Interfacial parameters for selected Spans and Tweens at the hydrocarbon-water interface, *Food Hydrocoll.* 10 (1996) 27–30. doi:10.1016/S0268-005X(96)80050-6.
- [31] D.Y. Kwok, A.W. Neumann, Contact angle measurement and contact angle interpretation, 1999. doi:10.1016/S0001-8686(98)00087-6.
- [32] www.accudynetest.com/surface_tension_table.html (page accessed in October 2018)
- [33] F. Hejda, P. Solař, J. Kousal, Surface Free Energy Determination by Contact Angle Measurements – A Comparison of Various Approaches, *WDS'10 Proc. Contrib. Pap.* (2010) 25–30. <https://pdfs.semanticscholar.org/e5a0/e7dc916cf7f0b4a3e24027cf7421d5d5e0.pdf>
- [34] C. Ribeiro, A.A. Vicente, J.A. Teixeira, C. Miranda, Optimization of edible coating composition to retard strawberry fruit senescence, *Postharvest Biol. Technol.* 44 (2007) 63–70. doi:10.1016/j.postharvbio.2006.11.015.
- [35] M.G. Carneiro-da-Cunha, M.A. Cerqueira, B.W.S. Souza, M.P. Souza, J.A. Teixeira, A.A. Vicente, Physical properties of edible coatings and films made with a polysaccharide from *Anacardium occidentale* L., *J. Food Eng.* 95 (2009) 379–385. doi:10.1016/j.jfoodeng.2009.05.020.
- [36] Standard test methods for Water Vapor Transmission of materials. Standard designations: E96-95. *Annual book of ASTM standards*, Philadelphia, PA: American Society for Testing and Materials (1995) 406–413.
- [37] A. Gennadios, C. L. Weller, C. H. Gooding (1994). Measurement errors in water vapour permeability of highly permeable, hydrophilic edible films. *J. Food Eng.* 21(1994) 395-409. [https://doi.org/10.1016/0260-8774\(94\)90062-0](https://doi.org/10.1016/0260-8774(94)90062-0).

- [38] Á. Perdonés, A. Chiralt, M. Vargas, Properties of film-forming dispersions and films based on chitosan containing basil or thyme essential oil, *Food Hydrocoll.* 57 (2016) 271–279. doi:10.1016/j.foodhyd.2016.02.006.
- [39] Standard test method for oxygen gas transmission rate through plastic film and sheeting using a coulometric sensor. Standard designations: 3985-05. Annual book of ASTM standards. West Conshohocken, PA: American Society for Testing and Materials. (2005)
- [40] A. Cano, A. Jiménez, M. Cháfer, C. González, A. Chiralt, Effect of amylose:amylopectin ratio and rice bran addition on starch films properties, *Carbohydr. Polym.* 111 (2014) 543–555. doi:10.1016/j.carbpol.2014.04.075.
- [41] Standard test method for tensile properties of thin plastic sheeting. Standard D882. Annual book of American standard testing methods. Philadelphia, PA: American Society for Testing and Materials (2001) 162–170,
- [42] R. Ortega-Toro, J. Contreras, P. Talens, A. Chiralt., Physical and structural properties and thermal behaviour of starch-poly(ϵ -caprolactone) blend films for food packaging, *Food Packag. Shelf Life.* 5 (2015) 10–20. doi:10.1016/j.fpsl.2015.04.001.
- [43] J. B. Hutchings, Food and colour appearance. Chapman and Hall food science book, 2nd ed., Gaithersburg, Maryland: Aspen Publication. 1999.
- [44] M. Sapper, M. Bonet, A. Chiralt, Wettability of starch-gellan coatings on fruits, as affected by the incorporation of essential oil and/or surfactants, *Lwt.* 116 (2019) 108574. doi:10.1016/j.lwt.2019.108574.
- [45] F. Debeaufort, M. Martin-Polo, A. Voilley, Polarity Homogeneity and Structure Affect Water Vapor Permeability of Model Edible Films, *J. Food Sci.* 58 (1993) 426–429. doi:10.1111/j.1365-2621.1993.tb04290.x.
- [46] M.A. Cerqueira, Á.M. Lima, J.A. Teixeira, R.A. Moreira, A.A. Vicente, Suitability of novel galactomannans as edible coatings for tropical fruits, *J. Food Eng.* 94 (2009) 372–378. doi:10.1016/j.jfoodeng.2009.04.003.

- [47] V. Siracusa, Food packaging permeability behaviour: A report, *Int. J. Polym. Sci.* 2012 (2012) 1–11. doi:10.1155/2012/302029.
- [48] J. Bonilla, E. Fortunati, L. Atarés, A. Chiralt, J.M. Kenny, Physical, structural and antimicrobial properties of poly vinyl alcohol-chitosan biodegradable films, *Food Hydrocoll.* 35 (2014) 463–470. doi:10.1016/j.foodhyd.2013.07.002.
- [49] A.I. Cano, M. Cháfer, A. Chiralt, C. González-Martínez, Biodegradation behavior of starch-PVA films as affected by the incorporation of different antimicrobials, *Polym. Degrad. Stab.* 132 (2016) 11–20. doi:10.1016/j.polymdegradstab.2016.04.014.
- [50] J. Muller, A. Jiménez, C. González-Martínez, A. Chiralt, Influence of plasticizers on thermal properties and crystallization behaviour of poly(lactic acid) films obtained by compression moulding, *Polym. Int.* 65 (2016) 970–978. doi:10.1002/pi.5142.

GENERAL DISCUSSION

Food packaging industries are currently facing a global environmental issue due to their massive reliance on oil-based synthetic plastics. These plastics have a low rate of degradation, while being derived from a non-renewable resource which is being depleted at a rapid pace. These current concerns have steered focus towards development of bioplastics, a group of biodegradable, sustainably obtained materials. The global production of bioplastics is of about 2.11 million tonnes in 2018, of which only 43 % are biodegradable. Among the available materials, starch and biodegradable polyesters — such as PCL and PLA or PVA — represent an actual alternative for developing biodegradable materials. However, the higher cost of these materials and the particular drawbacks of each polymer make necessary the application of different strategies to obtain competitive materials for food packaging applications. The incorporation of active compounds into the polymer matrices to improve their functionality as antimicrobial or antioxidant packaging or the combination of different polymers in laminates to take advantage of their complementary barrier properties or mechanical performance would improve their suitability for food packaging uses. These active laminates could extend food shelf life, minimising the use of synthetic preservatives, while providing adequate barrier and mechanical properties to the packaging material. Particularly, polymers such as starch or PVA are hydrophilic in nature, with high water sensitivity and permeability to water vapour, but with high oxygen barrier capacity. In contrast, hydrophobic polyesters such as PLA or PCL exhibited good water vapour barrier capacity but limited oxygen barrier capacity.

In the present study, the development of laminated materials containing carvacrol as an antimicrobial/antioxidant compound from natural origin has been studied. Carvacrol incorporation has been carried out by electrospinning of the polymeric solution containing the active compound dissolved or emulsified, depending on the solvent used to prepare the polymer solution. In this process the active substance becomes encapsulated in the polymer matrix, thus ensuring its stability, while allowing its controlled release to the target surface. The use of solvent casting to obtain active sheets with carvacrol has also been tested and compared with the electrospun materials in terms of the encapsulation efficiency.

The encapsulation efficiency of carvacrol in different polar (starch and PVA) and non-polar (PCL and PLA) polymers was determined, as detailed in **Chapters I.1, II.1 and II.2**, by using different encapsulation approaches and the adequate solvent for each polymer, considering food contact solvents with different polarity. Table 1 summarizes the values of the encapsulation efficiency (EE) and carvacrol load in the polymer matrices obtained for the

different experimental conditions. **Chapter I.1** analysed the encapsulation potential of polar versus non-polar systems, using the electrospinning method. To this end, electrospun formulations were prepared with corn starch-sodium caseinate (9:1 w/w ratio), at 2, 4 and 6 wt. % in water, or PCL at 5, 10 and 15 wt. % in glacial acetic acid, using different CA ratios (0, 5, 10 and 15 wt. % with respect to the polymer). It is remarkable, that for polar polymers, CA must be emulsified in the aqueous solvent, whereas CA is dissolved, together with the non-polar polymer in the organic solvent. The ES process parameters were optimised for each system. Thus, the applied voltage was in the range 9.5-14.5 kV for the non-polar systems and remarkably higher (12-22 kV) for the polar ones, according to the required higher electric field to overcome their greater surface tension. For the polar systems, the polymer concentration (related with the viscosity of the formulation) determined the feasibility of the ES process. Thus, emulsions with 2 % and 6 % polymer showed poor ES performance, whereas the intermediate polymer concentration (4 %) better fitted the process requirements. Microstructural observations showed significant differences between the two different systems and indicated a better electrospinning ability of the PCL solutions than starch aqueous systems. PCL matrices had a well-defined bead-and-tail morphology, while in the starch based systems, no evidence of CA droplets was observed, thus suggesting that the compound was intimately absorbed in the polymer structure. Using PCL matrices, better carvacrol EE values were obtained (Table 1) compared to the polar ones, where lower values with great variability were obtained. The highest EE (around 80 %) was obtained in the PCL systems with the highest polymer concentration, regardless of the CA-polymer ratio used. The maximum carvacrol load in the electrospun polymer was obtained for the 15 wt. % PCL solution with 15 g CA / 100 g PCL.

In Chapter II.2, the carvacrol encapsulation in PVA matrices — using two different encapsulation methods (solvent casting or electrospinning) — was studied. Aqueous formulations of low molecular weight PVA (15 wt. %) with a CA load of 15 wt. % with respect to the polymer, containing or not Tween 85 at 0.3 g / 100 g carvacrol were submitted to solvent casting and electrospinning. The solutions presented good electrospinning behaviour, generating fibrous mats with spherical beads. The highest encapsulation (83 %) was obtained with the surfactant-free blend, leading to a final CA load of 12 g / 100 g PVA (Table 1). The electrospun mats generated when surfactant was present exhibited EE (75-77 %) similar to that of the materials obtained by casting. Despite the polar nature of PVA and the use of aqueous systems, a high EE of CA was observed in the PVA matrix, in both

electrospun mats and cast films. This was attributed to the specific interactions between the negative charges of partially acetylated PVA chains and the phenolic hydroxyl, forming Lewis adducts, contributing to the CA bonding to the polymer matrix. When surfactant was not present, a strongly bonded, non-thermo-releasable CA fraction was detected. This fraction was up to 40 % of total carvacrol in the ES samples, and only about 18 % in cast films. The addition of Tween 85 led to the formation of CA-entrapping micelles, which limited the carvacrol-polymer interactions, thus promoting its further release during thermal analysis. In electrospun mats, PVA was practically amorphous whereas it was semicrystalline (about 40 % crystallinity) in the cast films. The presence of carvacrol within the PVA matrix promoted plasticization of the amorphous phase. Electrodeposition of carvacrol-loaded PVA onto other non-polar polymer sheet emerged as an interesting strategy for developing active laminates, where PVA layer provides the oxygen barrier capacity and the non-polar polymer provides the barrier capacity to water vapour.

Non-polar, PLA systems were analysed in **Chapter II.2** as to their ability to encapsulate carvacrol by using two different encapsulation methods (solvent casting or electrospinning) and different solvents. PLA (15 wt. %) dissolved in food-contact binary solvent systems (EtAc and DMSO) was used as carvacrol carrier (20 wt. % with respect to PLA). Microscopy analysis showed that the electrospun mats had a predominantly fibrous appearance with few spindle-like structures. The fibre diameter appeared thinner in CA-loaded mats and it increased with the increase of the EtAc ratio in the solvent mixture. The EE and carvacrol load in the polymer matrix depended on the encapsulation method and solvent system. Thus, the study revealed a lower EE in the electrospun samples than the cast films, this being 52-68 % and 76-89 %, respectively (Table 1), depending on the ratio EtAc:DMSO. The increase of EtAc ratio in the solvent mixture contributed to a higher retention of the active in the electrospun mats. This effect was not observed in the cast materials, where the low EtAc ratio led to the highest EE values.

Table 1. Summary of the encapsulation efficiency and polymer load of carvacrol in the different polymer systems studied in the present doctoral thesis, organized by their respective chapters.

Chapter	Nomenclature	Formulation composition (g compound / 100 g liquid system)						Evaporation process	EE	
		solvent	S:NaCas	PCL	PVA	PLA	CA (g/100 g polymer)		%	g CA / 100 g polymer
I.1	P ₂ C ₅	water	2	-	-	-	5	ES	16±2	0.7±0.1
	P ₂ C ₁₀		2	-	-	-	10		38±12	4±1
	P ₂ C ₁₅		2	-	-	-	15		27±2	4±2
	P ₄ C ₅		4	-	-	-	5		24±6	1.2±0.3
	P ₄ C ₁₀		4	-	-	-	10		51±25	5±1
	P ₄ C ₁₅		4	-	-	-	15		47±4	7±1
	P ₆ C ₅		6	-	-	-	5		55±3	3±1
	P ₆ C ₁₀		6	-	-	-	10		65±12	7±5
	P ₆ C ₁₅		6	-	-	-	15		75±4	11±6
	N ₅ C ₅	glacial acetic acid	-	5	-	-	5		68±3	4±2
	N ₅ C ₁₀		-	5	-	-	10		69±2	7±2
	N ₅ C ₁₅		-	5	-	-	15		55±1	8±1
	N ₁₀ C ₅		-	10	-	-	5		84±2	4±1
	N ₁₀ C ₁₀		-	10	-	-	10		83±3	8±4
	N ₁₀ C ₁₅		-	10	-	-	15		78±1	11±2
	N ₁₅ C ₅		-	15	-	-	5		82±1	4.23±0.03
	N ₁₅ C ₁₀		-	15	-	-	10		80.9±0.2	7.94±0.02
	N ₁₅ C ₁₅		-	15	-	-	15		85±2	13±2
II.1	ES-PC	water	-	-	15	-	15	ES	83±9	12±2
	ES-PCS		-	-	15	-	15*		77±7	11±1
	C-PC		-	-	15	-	15	Casting	75±2	10.9±0.3
	C-PCS		-	-	15	-	15*		76±3	11.0±0.4
II.2	PLA-CA ES(0:1)	EtAc: DMSO (0:1)	-	-	-	15	20	ES	52±4	10.3±0.8
	PLA-CA C(0:1)		-	-	-	15	20	Casting	78±4	15.6±0.8
	PLA-CA ES(1:3)	EtAc: DMSO (1:3)	-	-	-	15	20	ES	62±6	12.4±1.3
	PLA-CA C(1:3)		-	-	-	15	20	Casting	89±6	17.7±1.2
	PLA-CA ES(2:3)	EtAc: DMSO (2:3)	-	-	-	15	20	ES	68±2	13.6±0.5
	PLA-CA C(2:3)		-	-	-	15	20	Casting	76±3	15.1±0.5

*contains Tween 85 at a ratio 0.3 g / 100 g

Nevertheless, this led to a CA load in the mats of 10-13 g / 100 g polymer, comparable to the load obtained for electrospun PVA materials. TGA and DSC analysis revealed that CA-free matrices retained more solvent than the samples with CA, this effect being more noticeable in fibres than in cast films. Similarly, only about 40 % of the encapsulated carvacrol became thermo-released from the fibres before the polymer degradation, while in the cast samples the total CA amount was thermo-released. This suggested different interactions forces between polymer-carvacrol in the electrospun mats and cast films. Similarly to the PVA samples, carvacrol also had a plasticizing effect in the PLA matrices.

The next phase within the present thesis consisted of developing active multilayer materials, by assembling polymer layers with complementary properties that also act as carriers of carvacrol. This approach would allow a progressive release of the active compound at the interface of the foodstuff, avoiding its direct application. Multilayers were developed by combining polar (starch or PVA) with non-polar (PCL or PLA) polymer sheets and characterized as to their functional properties.

Thus, starch-PCL laminates (**Chapter I.2**) were developed by electrospinning the PCL solution in glacial acetic acid (GAA) (with or without CA) onto a thermoplastic starch layer, followed by hot compression with another thermoplastic starch sheet. The effects of the electrospun mats on the multilayers' functional properties (barrier, tensile and optical, thermal behaviour, antimicrobial activity and release kinetics) were studied. The inclusion of the PCL mats, greatly reduce of the water vapour permeability of the starch films, with no relevant effect on other functional properties.

The antimicrobial activity of the electrospun mats and the multilayers — tested *in vitro* against *Escherichia coli* and *Listeria innocua* — showed growth inhibition of Gram (-) strain, whereas no antilisterial effect was noticed. This was due to the insufficient carvacrol release to reach the MIC of this bacteria. This response was delayed in time for the multilayers, compared with electrospun mats, due to the thicker layer through which CA must diffuse to reach the target point in the culture medium. The effectiveness of the antimicrobial action of carvacrol was not only dependent on its load in the carrier material, but also on the matrix capacity to release the proper CA amount to the food system, as well as the type of food in contact. The release kinetics of carvacrol from the electrospun mats in food simulants of different polarities was also studied (**Chapter I.2**). The mats showed a faster and higher CA release ability in food simulants of low polarity, where practically the total active amount from the fibres was delivered at equilibrium. In more aqueous systems (similar to the *in vitro*

culture medium) only 60-75% of CA content was delivered at a slower rate, thus explaining the limited antibacterial action observed when the MIC was high. Thus, the application of these active starch based materials in less polar foodstuffs would be recommended to fully benefit from the protective effect of the encapsulated carvacrol.

A second group of laminates was developed with surface-activated PLA films, obtained by compression moulding and subsequent aminolization (**Chapter II.2**). These were combined with CA-loaded PVA, applied as a coating. The aminolization process at low exposure times (1 and 3 min) increased the polar component of the PLA surface free energy, enhancing its wettability by aqueous solutions of PVA, although this effect was poorly noted when the solution carried CA. Despite this outcome, the obtained bilayer assemblies did not exhibit notable improvement in the mechanical and barrier properties, which were very close to those of the untreated PLA monolayer. Despite expectations, the PVA did not improve the oxygen barrier capacity of the multilayer, probably due to the heterogeneous thickness of the coating layer.

Table 2. Summary of multilayer films developed in the present doctoral thesis, arranged by chapters.

Chapter	Notation	Film description	Sample code in the figures
I.2	S-S	Films of TPS with electrospun PCL layer (60=60 min; 90=90 min) containing or not CA	1
	S-PCL60-S		2
	S-PCL(CA)60-S		3
	S-PCL90-S		4
	S-PCL(CA)90-S		5
II.2	amPLA-PVA	Films of aminolized PLA support with PVA coating containing CA and/or surfactant	6
	amPLA-PVA/C		7
	amPLA-PVA/C/S		8
	PLA-PVA	Films of not-treated PLA support with PVA coating containing CA and/or surfactant	9
	PLA-PVA/C		10
	PLA-PVA/C/S		11
	PVA	Pure PVA cast film (monolayer)	12
	PLA	Pure thermo-processed PLA film (monolayer)	13

Table 2 presents briefly the composition of the multilayers analysed in different chapters. From the food packaging point of view, barrier properties and mechanical behaviour were analysed as indicators of the materials' performance. Figures 1 and 2 show the maps of the barrier properties (WVP vs. OP) and tensile parameters (TS, MPa vs. Elongation at break, %) and Figure 3 summarizes the values of Elastic modulus (EM, MPa) of all films described in Table 2.

Food packaging materials have specific requirements in terms of barrier capacity to gases such as oxygen or water vapour to limit the gas exchange between the packaged foodstuff and the environment, thus avoiding degradative processes such as oxidations or moisture induced deterioration. In Figure 1, the location of the different development films in terms of their WVP and OP can be observed. All PLA based formulations showed low WVP, compared to the starch based laminates, which have higher values for this parameter due to their hydrophilic nature. Nevertheless, the inclusion of the PCL mats notably reduced the WVP of the starch laminates. In contrast, all starch multilayers exhibit very low values of OP when compared to those of PLA. Although PVA films also exhibit very low OP values, according to its hydrophilic nature, PVA coating of PLA was not effective at reducing the OP values of PLA-PVA laminates, even with the improved extension capacity of PVA solution induced by PLA aminolization.

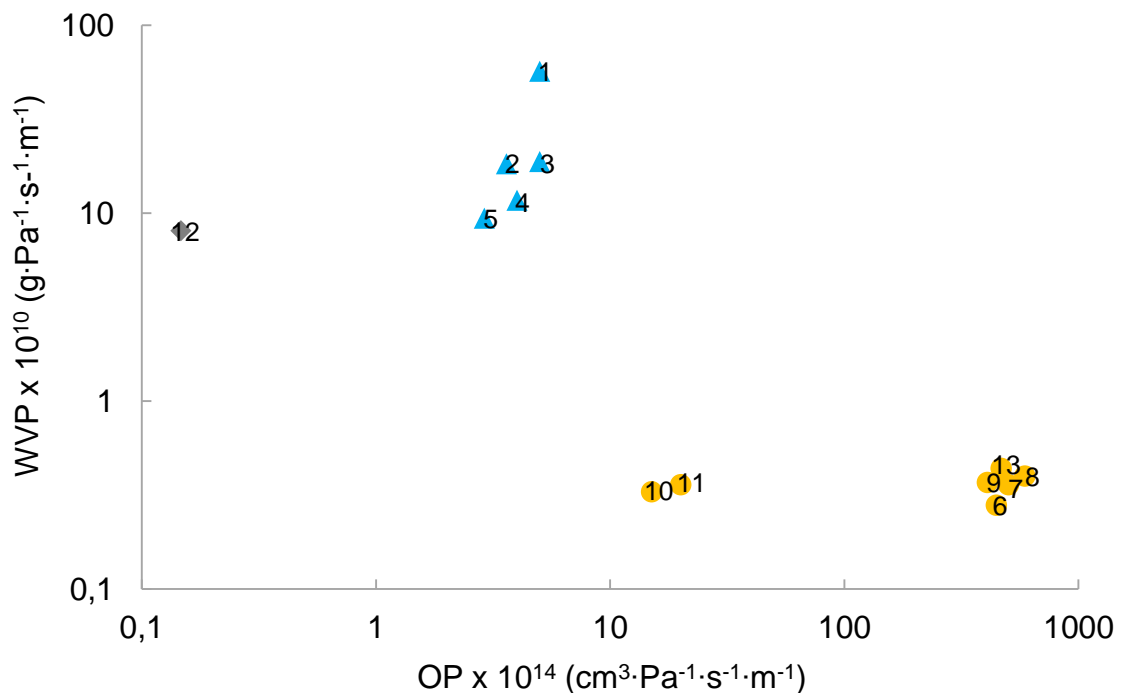


Figure 1. Map of gas barrier properties showing the location of the different films analysed in this doctoral thesis.

In terms of mechanical performance, Figures 2 and 3, the PLA-PVA laminates exhibited higher mechanical resistance and lower extensibility than starch-PCL laminates, according to the mechanical performance of the PLA and starch that are the major components in the respective multilayers. Incorporation of carvacrol slightly reduced the film resistance, in both kind of laminates, according to its plasticising effect in the polymer matrices, but the values remain in the range of the carvacrol-free laminates. Likewise, the stiffness of laminates was also near the values of the major polymer in the multilayer (starch or PLA); the PLA laminates were stiffer than the starch laminates (Figure 3).

Then, the obtained multilayer exhibits properties useful for food packaging purposes, depending on the kind of food. No moist foods, sensitive to oxidation process, could be packaged in starch laminates that provide good protection to oxygen transfer, whereas moist foods, less sensitive to oxidation, could be packaged in PLA laminates. In both cases, the encapsulated carvacrol would provide antimicrobial action to enlarge the food shelf life. However, specific tests for determined food systems are required to validate the effectiveness of the obtained materials at preserving food quality and safety during the required time.

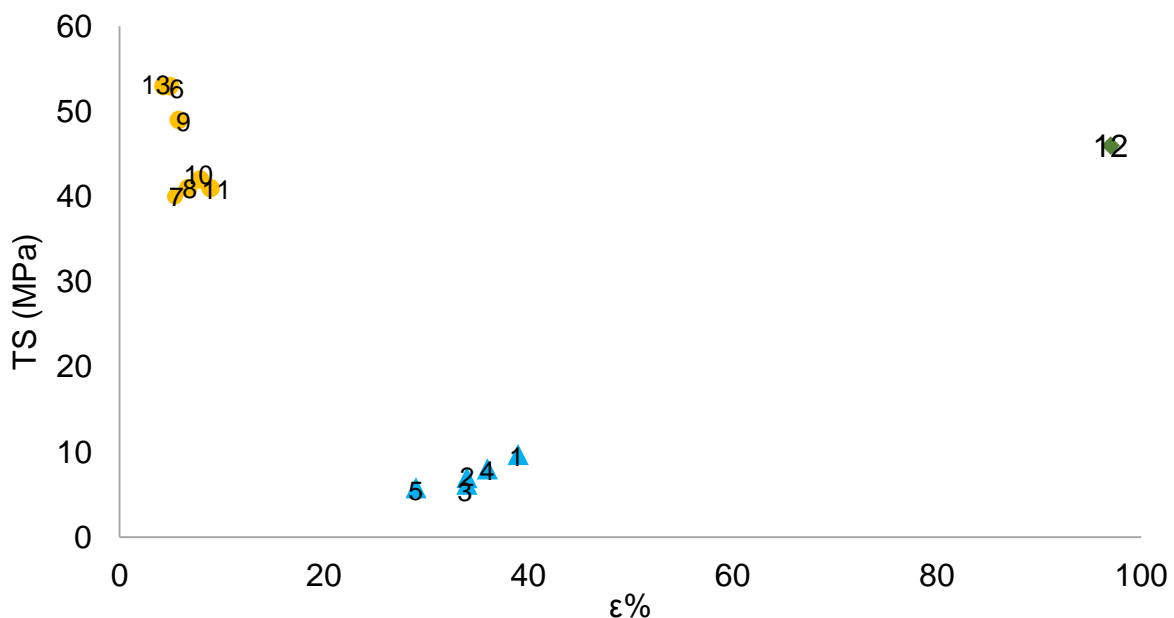


Figure 2. Map of mechanical properties (Tensile Strength vs. Elongation at break) showing the location of the different films.

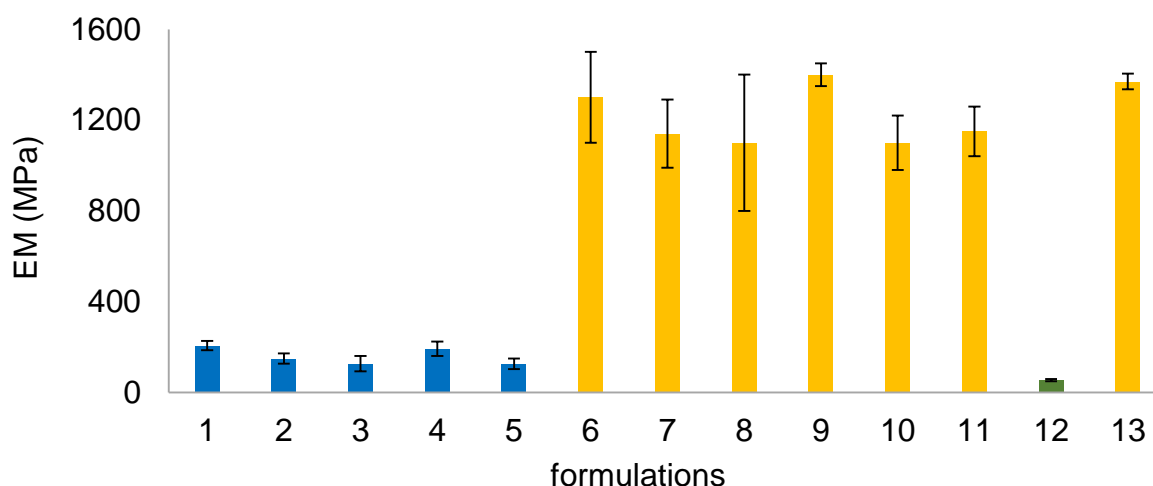


Figure 3. Values of elastic modulus of the different laminate assemblies. PVA (12) and PLA (13) monolayers are included for comparison purposes.

As final characterization of the developed materials, the biodegradation behaviour was studied (**Chapter I.3**) for the starch (TPS) based multilayers with and without carvacrol. The study of disintegration and biodegradation of the TPS containing CA-loaded PCL electrospun mats was carried out under thermophilic composting throughout 84 and 45 days respectively. The disintegration trend was similar in all multilayers reaching values of 75-80% at the end of the assay. The biodegradation test revealed that CA affected the compost inoculum activity, slightly limiting the process, but reaching values very close to that established by the ISO method (90 %).

As a general conclusion, encapsulation of carvacrol in non-polar polymers was more effective than in polar starch matrices. However, partially acetylated polar PVA was also useful to encapsulate carvacrol, without surfactant, due to the development of specific interactions between the negatively charged acetyl groups and the hydroxyl group of carvacrol. The solvent used to dissolve the polymer and carvacrol prior to the encapsulation process (electrospinning or solvent casting) plays an important role in the process effectiveness, both in the encapsulation efficiency and solvent retention in the encapsulating matrix. The latter aspect is of crucial importance for food contact materials where toxic residues compromise product safety. Likewise, it was possible to obtain multilayer starch films with PCL, encapsulating carvacrol by electrospinning, with good performance as active packaging material, useful for non-moist, oxidation sensitive foods. However, PLA laminates with PVA coatings, encapsulating or not carvacrol, did not provide enough barrier capacity

to oxygen - so these could only be useful for products that are not sensitive to the oxidation process.

CONCLUSIONS

1. Greater CA encapsulating efficiency (>80 %), with lower variability, was obtained for the PCL-based systems than for the starch-based ones. This may be explained by different factors: the greater solubility of PCL in GAA, allowing for the use of higher polymer concentrations with adequate viscosity, the greater compatibility of CA and PCL and the linearity of the polymer chain, which permits the chain to unfold in the electric field and its subsequent entanglement to form fibres. This nanostructure presented better cohesiveness and adhesiveness in the electrospun material, which also contribute to the coating performance. The lower variability in the CA retention, associated with the lack of water in the liquid systems, which helps to avoid steam drag effects, also represents an advantage with respect to the aqueous systems. Therefore, in order to obtain tightly adhered electrospun layers with the highest CA load in the matrix, it is recommended that the highest PCL concentration (15 %) and CA ratio (15 %) be used.

2. Electrospun PCL fibre mats encapsulating CA were effective at controlling the growth of *E. coli*, when the surface density of CA loaded fibres was 1.2 and 1.8 mg/cm², the latter being more effective. In both cases, the CA released into the culture medium exceeded the MIC of the bacteria. Nevertheless, these mats were not effective at controlling the growth of *L. innocua*, since a greater release of CA was necessary to achieve the MIC of this bacterium. Not only did the CA load in the fibres determine their antimicrobial effect, but also its release capacity into the aqueous media. In this sense, the fibre showed a faster release and higher release capacity of the active in fatty foodstuffs (simulants D1 and D2), where practically the total amount of CA could be released from the fibres. However, in more aqueous food systems (simulants A and B), such as the bacteria culture medium, a more limited CA delivery (60-75 %) occurred with a slower rate, which reduced the potential effectiveness of the encapsulated active. This meant that the Gram negative bacteria (*E. coli*) could be effectively inhibited, whereas no growth inhibition was observed for Gram positive (*L. innocua*), which would require a greater surface density of the electrospun CA-loaded PCL fibres. This behaviour was reproduced in multilayer starch films containing the CA-loaded electrospun PCL fibres between two starch sheets, although a delayed response was observed for the antimicrobial action. In these multilayer films, a great reduction in the water vapour permeability was also observed with respect to that of starch films, without any notable changes in the other packaging functions. Therefore, active electrospun PCL fibre in multilayer starch films represents an interesting alternative for the purposes of active food packaging.

3. All multilayer films (containing or not CA) exhibited the same trend of disintegration throughout the composting exposure time. The biodegradation process of pure bilayer starch films was retarded, in comparison with starch-PCL multilayer, by the greater effective thickness of the bilayer, due to the highest adhesion forces between the starch sheets. In contrast, starch-PCL multilayers, exhibited an earlier, more extended degradation behaviour with lower peak rate. The biodegradation test revealed that the presence of CA notably affected the compost inoculum activity, thus limiting the biodegradability of the CA-loaded multilayers to a maximum value of around 85 %. Nevertheless, the biodegradation values reached by the CA loaded films were very close to that established by the standard ISO method to be considered as biodegradable material (90 %). Further biodegradation studies under longer composting times are recommended to evaluate the total biodegradation of carvacrol-loaded SPS films.

4. PVA aqueous solutions (15 % w/w) containing CA (15 g/100 g polymer) exhibited good electrospinning behaviour, leading to loaded mats with fibres and spherical beads, that retained up to 83 % of the active, giving rise to matrices with up to 12 g carvacrol/100 g polymer. The greatest encapsulation efficiency occurred in the blend without surfactant (83 %) and the formulations with surfactant exhibited similar encapsulation efficiency to that obtained in the casting process (75-77 %). Two fractions of carvacrol could be distinguished in the encapsulating materials; the more strongly bonded, non-thermo-releasable fraction was higher (40 % of the total) in ES samples without surfactant and lower in those containing surfactant, whereas in cast samples this fraction accounted for about 18 % of total carvacrol. Therefore, the addition of the Tween 85 surfactant limited the retention of CA by the PVA matrix, due to its less stable micelle-encapsulating effect that reduced the amount of carvacrol that was more strongly bonded to the polymer. PVA-CA interactions also promoted the plasticization of the polymer, which was practically amorphous in the ES samples and semi-crystalline (about 40 % crystallinity) in the cast samples. Thus, the use of electrospinning as a delivery system for the purposes of successfully applying carvacrol-loaded PVA fibres in active packaging materials represents an interesting strategy, while the PVA layer would provide oxygen barrier capacity coherent with its polar nature.

5. The carvacrol encapsulation efficiency in PLA matrices was higher for solvent casting (76-89 %) than for electrospinning (52-68 %) and was affected by the ratio EtAc:DMSO in the solvent mixture. Nevertheless, fibers reached a carvacrol-load of 10-13 g per 100 polymer

(against 15-18 in cast samples), from which only about 40 % was thermo-released before the polymer degradation, which indicates its strong retention in the fibers. In contrast, carvacrol was practically thermo-released in total in cast samples, which indicates lower retention forces in the matrix. As far as the solvent, the incorporation of the EtAc to DMSO significantly increased the encapsulating efficiency in the fibers (from 50 to almost 70 %), although in the cast samples a higher efficiency was only observed for the smallest ratio of EtAc. The electrospun material of PLA with or without carvacrol, using EtAc:DMSO mixtures as solvents, exhibited a fiber structure with few beads. Fiber diameter decreased when it contained carvacrol and increased when the proportion of EtAc in the solvent mixture rose. Based on the current study, electrospinning of solutions of PLA and carvacrol (20 wt. % with respect to the polymer) in mixtures of EtAc:DMSO (both valid for food contact) could be used effectively in obtaining active multilayer materials for the packaging of foodstuffs when applied onto a supporting polymer layer.

6. The aminolization technique yields PLA surfaces with a greater polar component of the surface free energy, thus enhancing wettability with polar solutions of PVA. When PVA carried carvacrol, this effect did not improve the extensibility of the liquid phase on PLA. The prolonged (>3 min) exposure to 1,6-hexanediamine has negative effects on the polar component and microstructure of the PLA films. The aminolization of the PLA surface did not notably affect the mechanical and barrier properties of PLA-PVA bilayers containing, or not, carvacrol. These properties were very close to those of the major PLA monolayer, while the PVA sheet did not provide the expected oxygen barrier capacity to the laminate. Carvacrol promoted the bilayer stretchability due to its plasticising effect on both PVA and PLA sheets. Based on the results, coating PLA (aminolized or not) with PVA solutions is not recommended for the purposes of obtaining laminates for food packaging applications, since neither the barrier nor the mechanical properties were an improvement on those of PLA films, mainly due to the heterogeneous thickness of the PVA coating.

As a general conclusion, encapsulation of carvacrol in non-polar polymers was more effective than in polar starch matrices. However, partially acetylated polar PVA was also useful to encapsulate carvacrol, without surfactant, due to the development of specific interactions between the negatively charged acetyl groups and the hydroxyl group of carvacrol. The solvent used to dissolve the polymer and carvacrol prior to the encapsulation process (electrospinning or solvent casting) plays an important role in the process

effectiveness, both in the encapsulation efficiency and solvent retention in the encapsulating matrix. The latter aspect is of crucial importance for food contact materials where toxic residues compromise product safety. Likewise, it was possible to obtain multilayer starch films with PCL, encapsulating carvacrol by electrospinning, with good performance as active packaging material, useful for non-moist, oxidation sensitive foods. However, PLA laminates with PVA coatings, encapsulating or not carvacrol, did not provide enough barrier capacity to oxygen - so these could only be useful for products that are not sensitive to the oxidation process.